

THE DESIGN AND EXPERIMENTAL ANALYSIS
OF A ROTARY SICKLE FOR CUTTING
AND TRAJECTING PLANT STEMS

By

Bobby Lynn Bledsoe
Bachelor of Science
University of Tennessee
Knoxville, Tennessee

1953

Submitted to the Faculty of the
Graduate College
of the Oklahoma State University
in partial fulfillment of the
requirements for the Degree
of
DOCTOR OF PHILOSOPHY
August, 1969

NOV 5 1969

THE DESIGN AND EXPERIMENTAL ANALYSIS
OF A ROTARY SICKLE FOR CUTTING
AND TRAJECTING PLANT STEMS

Thesis Approved:

Jay G. Porterfield

Thesis Adviser

Lawrence O. Roth

Er. Schubert

James R. Partin

B. J. Wilson

D. D. Aurham

Dean of the Graduate College

729863

PREFACE

Financial assistance for this basic design study came from two National Science Foundation Traineeships, a grant by the Oklahoma Wheat Research Foundation, and from research assistantships extended by the Agricultural Engineering Department, all of which are gratefully acknowledged.

To Professor Jay G. Porterfield, my major advisor, I am especially indebted for suggesting an "auger Knife" investigation and for his counsel and encouragement throughout the course of study.

To the other members of the advisory committee: Professor E. W. Schroeder, Head, Dr. Gordon L. Nelson, and Dr. Lawrence O. Roth, of the Agricultural Engineering Department; Dr. Henry R. Sebesta of the Mechanical Engineering Department - I express sincere appreciation for the critical review of the work and the constructive suggestions that each provided.

To others who assisted with this investigation, I express my gratitude, especially to Norvil Cole, Galen McLaughlin, Jesse Hoisington, and Ron Wolf, whose technical skills provided the hardware vital to such a study as this.

For their patience and endurance during the several years of the program of study, I express my thanks to Anne, my wife, and to our children, Belinda and Lynn Andrew.

TABLE OF CONTENTS

Chapter	Page
I. INTRODUCTION AND STATEMENT OF PROBLEM.	1
The Cutting Function of Field Machinery	1
Requirements and Design Goals for Cutting Devices Used on Forage Crops.	2
Design Goals for Cutting Devices Used on Seed Crops.	2
Inadequacies of Conventional Cutting Devices and Schemes to Correct Them	3
Proposed New Rotary Cutting Device.	7
Research Objectives	8
II. REVIEW OF LITERATURE	10
Basic Nature of Cutting	10
Mode of Stem Failure - Two Opposed Element Cutting	13
Mode of Stem Failure - Single Element (Impact) Cutting.	21
Mode of Stem Failure - Sawing	24
Motion of Severed Stems Resulting From Impact Cutting.	28
Variables Affecting Cutting	30
Previous Design of Rotary Cutters With Blades Approximately Helical in Configuration	39
III. DESIGN OF THE CUTTING DEVICE	51
Approach.	51
Model Study	52
General Specifications and Design Details of the Cutter	54
IV. KINEMATIC AND CUTTING FORCE ANALYSIS	71
Kinematic Analysis.	71
Cutting Force Analysis.	77

Chapter	Page
V. DIMENSIONAL ANALYSIS	83
Input Energy and Maximum Torque Responses	83
Motion of Severed Plant Stalks	94
Alternative Response Pi Terms Considered	97
VI. EXPERIMENTAL PLAN AND TEST PLANT MATERIAL	100
Types of Multifactor Experimental Plans	100
Choice of Experimental Plan	104
Randomization Procedure	106
Main Experimental Plans	106
Auxiliary Experiment Plans	114
Plant Material Used in Tests	114
VII. APPARATUS FOR THE EXPERIMENT	125
Rotor Drive System and Instrumentation for Determining Input Energy	128
Plant Stem Carriage, Track, and Drive System	135
Instrumentation to Determine Stem Displacement	143
Apparatus for Plant Physical Property Tests	147
Auxiliary Equipment for High Speed Motion Picture Studies	153
VIII. EXPERIMENTAL PROCEDURE	158
Calibration of Equipment	158
Data Taking Procedure	166
Data Reduction	172
IX. PRESENTATION AND ANALYSIS OF DATA	177
Cutting Effectiveness Tests	177
Classification of Severing Actions	177
Variation in Actual Cutting Height	181
Trajection of Severed Stems	183
Conclusions Regarding Independent Variable Ranges	187
High Speed Motion Picture Studies	187
Cutting Mechanism: Square Edge Blades, Low Speed Level	188
Cutting Mechanism: Square Edge Blades, High Speed Level	200
Cutting Mechanism: Sharp Blades, Low Speed Level	205
Cutting Mechanism: Sharp Blades, High Speed Level	210

Chapter	Page
Further Analysis of Severed Stem	
Trajectory	216
Check on Rotor Speed	218
Main, Screening of Parameter, Tests	221
Analysis of Variance	222
Graphs of Treatment Means and	
Discussion of Results.	225
Comparison of Responses for	
Dull and Sharp Blades.	239
Stem Physical Property Tests.	243
Prediction Equations.	247
X. SUMMARY AND CONCLUSIONS.	253
Summary	253
Conclusions	257
Suggestions for Further Study	259
BIBLIOGRAPHY.	260
APPENDIX A.	264
APPENDIX B.	266
APPENDIX C.	273
APPENDIX D.	292
APPENDIX E.	313

LIST OF TABLES

Table	Page
I. Effect of Variables on Energy Transferred to Severed Stems by Impact Cutting.	31
II. Effect of Knife Design Parameters on Cutting Force & Energy As Reported in the Literature.	33
III. Effect of Knife Operating Parameters on Cutting Force & Energy As Reported in the Literature.	36
IV. Effect of Plant Characteristics on Cutting Force & Energy as Reported in the Literature.	38
V. Maximum Effective Bevel Angles of Blades for Rotor Assemblies Tested	69
VI. Fundamental Quantities for Energy Input Analysis.	87
VII. Structure of Required Experimental Plan	101
VIII. Factor Level Coding As Determined By Randomization Procedure	107
IX. Main Experimental Plan Dull Blade Series. . . .	108
X. Main Experimental Plan Sharp Blade Series	110
XI. Experimental Plan for Preliminary Cutting Effectiveness Tests Dull Blade Series	112
XII. Experimental Plan for High Speed Motion Picture Study Dull Blade Series	113
XIII. Experimental Plan for High Speed Motion Picture Study Sharp Blade Series.	113
XIV. Comparison of Theoretical and Calculated Rotor Speeds.	220
XV. Summary of Results of Analysis of Variance. . . .	223

Table	Page
XVI. Independent Variables Having Significant Effect on the Response Variables at the $\alpha = .15$ and $\alpha = .05$ Levels.	224
XVII. 99 Percent Confidence Limits for Difference in Overall Response Means Between Dull and Sharp Blade Test Series	240
XVIII. Optimum Values of Selected Independent Parameters Based on Main Experiment Data	242
XIX. Summary of Regression Analysis for $\Pi_8 = Se/Be$ <u>Versus</u> Stem Moisture Content . . .	246
XX. Mean Values of Moisture Content <u>Versus</u> Time in Chamber For Various Parts of the Experiment.	249
XXI. Mean Values of Π_8 and Π_{10} for Levels of Nominal Diameter Sharp Blade Series. . . .	249
XXII. Mean Values of Moisture Content, Π_8 , $1/\Pi_8$, and Π_{10} for Levels of Time in Chamber Sharp Blade Series.	249

LIST OF FIGURES

Figure	Page
1. Schematic Diagram of Knife Cutting and Pure Shear Cutting	12
2. Theorized Cutting Action in Material of Fibrous Nature.	14
3. Three-dimensional Bending of a Single Stalk Between Two Knives.	15
4. Comparison of Load Deformation Curves for Plant Stalks and Sheet Iron	16
5. Reaction of a Single Stalk to Knife Force	23
6. Comparison of Lundberg and Conventional Saw Teeth	28
7. Force System on Single Stalk and Resulting Motion.	29
8. Previous Rotary Cutters Approximately Helical in Configuration.	40
9. Graphical Analysis of the Cutting Action of the Elliptical Disk Rotor Designed by Miller	44
10. Inherent Dynamic Unbalance of Elliptical Disk Rotor.	47
11. Rotor of Spinslicer Mowing Machine.	50
12. Model Cylindrical Helical Cutter Used to Study General Design Requirements	53
13. General Design Features Specified for Rotor and Ledger Tube of Cylindrical Helical Cutter	56
14. Test Rotor Assembly and Ledger Tube Features (26 Degree Rotor Assembly Shown)	60
15. Top View of Rotor Drive Shaft and Ledger Tube Without Rotor Assembly in Place.	60

Figure	Page
16. Top View of 36 Degree Rotor Assembly Mounted in Ledger Tube.	61
17. Rear View of 36 Degree Rotor Assembly Mounted in Ledger Tube.	61
18. Perspective View of 36 Degree Rotor Assembly.	62
19. Identification of Component Parts of 36 Degree Rotor Assembly.	62
20. Rotor Segment Fabrication Procedure and Description of Resulting Part	64
21. Cross Sections of Square and Sharp Edge Blades Tested (Section Magnified 10X; 20 Degree Bevel Angle on Sharp Blade)	65
22. Effective Bevel Angles at Start and End of Single Element Cutting For 46 Degree Rotor.	67
23. Test Rotor Assemblies Fitted with Sharp Blades (Left to Right Arrangement: 26, 36, 46, and 56 Degree Rotors)	69
24. Variation in Knife Angle with Lateral Distance Along Blade Edge	70
25. Geometry of Motion of Points on the Cutter Rotor Relative to Uniformly Spaced Plants Along the Row	72
26. Double Cutting Effect and Comparison of Zones of Double Cutting for Different Feed Rates.	75
27. Effect of Ledger Tube Angular Position on Cutting Zone and Double Cutting	76
28. Diagram of Resultant Force on a Plant Stem From a Point on the Rotor Sector Blade Edge	78
29. Two Element Cutting of a Plant Stem Between the Ledger and Rotor Blades	79
30. Area of Plants Cut by Each Rotor Sector Per Revolution (Diagram Shown Is for Feed Rate $L = 3/2 D$).	81
31. Geometric Parameters of Helical Cutter.	85

Figure	Page
32. Typical Load Deflection Curves for (a) Transverse Shear Failure (b) Bending	86
33. Left-handed Coordinate System Established to Define Motion of Severed Plant Stems	94
34. Frequency Histogram of Stem Nominal Diameter	116
35. Gage and Method Used for Determining Stem Nominal Diameter	117
36. Fixture and Method Used for Locating Center of Gravity of Plant Stem	117
37. Comparison of Physical Properties of Stems from 1965 and 1968 Crops	120
38. Conditioning Chamber and Auxiliary Equipment for Changing Moisture Content of Plant Stems	122
39. Interior View of Conditioning Chamber Showing Stems Subjected to Mist of Hot Water from Overhead Nozzle	122
40. Moisture Content of Plant Stems <u>Versus</u> Time in Conditioning Chamber	124
41. Rotor Drive System Layout	130
42. Schematic Diagram of Instrumentation for Monitoring Instantaneous Torque, Rotor Shaft Displacement, and Carriage Velocity	133
43. Rotor Drive System and Associated Instrumentation	134
44. Rotor Drive Speed Controller (In Foreground), Carrier-Amplifier-Recorder, and Dual Beam Oscilloscope and Camera	134
45. Carriage-Dolly-Release Lever System (a) Ready To Be Loaded by Winch (b) In Loaded Position	137
46. (a) Carriage-Dolly System Undergoing Acceleration by Action of 80-Pound Spring Set; (b) Dolly in Home Position	137
47. Rear View of Test Stand Showing Braking Frame Assembly	139
48. Carriage Latched to Braking Frame After Deceleration	139

Figure	Page
49. Details of Carriage Construction.	141
50. Cross Section of Carriage and Track	142
51. Overall View of Test Stand Showing Construction of Center Track Section.	145
52. Front View of Rotor Drive System and Horizontal and Vertical Grid Boards for Determining Stem Displacements.	145
53. Equipment Arrangement for Photographing Vertical Displacement Trace of Severed Stems.	146
54. Photograph of Equipment Used to Record Stem Vertical Displacement	149
55. Stem Testing Machine and Load-Deflection Curve Recording Instruments	149
56. Schematic Drawing of Stem Testing Machine	150
57. Saw and Fixture for Cutting One Inch Lengths from Test Stems	152
58. Stem Cross Sections on Micro Projector Ready for Images To Be Recorded on Photosensitive Paper	152
59. Schematic Diagram of Equipment Arrangement for Filming High Speed Motion Pictures of Cutting Action and Stem Trajectory.	156
60. Camera Location and Equipment Arrangement for Taking the Cutting Action Films	157
61. Equipment Arrangement for Stem Trajectory Filming as Seen from Camera Location.	157
62. Dead Weight Calibration of Torque Pickup and Recorder System	161
63. Torque Pickup Calibration Equipment	164
64. Stem Testing Machine Calibration Equipment.	164
65. Oscillograph Record of Torque Pickup Calibration	165
66. Oscillograph Record of Stem Testing Machine Calibration	165

Figure	Page
67. Typical Cut Ends of Stems Severed in the Dull Blade Test Series.	178
68. Typical Cut Ends of Stems Severed in the Sharp Blade Test Series	178
69. Summary of Cutting Effectiveness Test Results	180
70. Cutting Height Definition	182
71. Severed Stem Displacement Patterns for CED Test Series	184
72. Severed Stem Displacement Patterns for PD and PS Test Series.	186
73. Cutting of Stem by 26 Degree Rotor with Square Edge Blade, 3600 RPM. Numerals Are Frame Numbers (MPF: 4800 Frames/Sec.) Trial PD-3, Stem No. 3.	189
74. Trajection of Stem by 26 Degree Rotor with Sharp Blade, 1800 RPM. Numerals Are Frame Numbers (MPF: 1800 Frames/Sec.) Trial PS-10, Stem No. 1.	190
75. Cutting Mechanism with Square Edge Blades on the 26 Degree Rotor at 1800 RPM and with a Feed Rate of 1 3/4 in./rev. (Stems 1 and 2, Trial PD-1)	191
76. Displacement and Velocity of Selected Points on Stem 1, Trial PD-1 and Stem 3, Trial PD-3.	196
77. Trajection of Stem 3, Trial PD-12 (a); and of Stem 9, Trial PD-10 (b).	198
78. Rotation of Stem 3, Trial PD-1 about its Z Axis Immediately After Being Severed.	199
79. Mechanism of Cutting with Square Edge Blades on the 26 Degree Rotor at 3600 RPM and with a Feed Rate of 5 1/4 in./rev. (Stem 3, Trial PD-3)	201
80. Mechanism of Cutting Stems with Sharp Blades on the 26 Degree Rotor at 1800 RPM and with a Feed Rate of 1 3/4 in./rev. (Stems 5 and 6, Trial PS-1).	206
81. Displacement and Velocity Plots of Point C on Stem 5, Trial PS-1	208

Figure	Page
82. Trajection of Stem 1, Trial PS-11 (a); and of Stem 1, Trial PS-10 (b)	209
83. Mechanism of Severing Stems with Sharp Blades on the 26 Degree Rotor at 3600 RPM and with a Feed Rate of 5 1/4 in./rev. (Stem 3, Trial PS-3)	211
84. Displacement and Velocity of Point D on Stem 3, Trial PS-3 and of Point E on Stem 6, Trial PS-4	212
85. Cutting Mechanism of 56 Degree Rotor with Sharp Blades at 3600 RPM and with a Feed Rate of 5 1/4 in./rev. (Stem 6, Trial PS-4) . . .	214
86. Trajectory of Stem 9, Trial PS-9 (a) and of Stem 1, Trial PS-8 (b)	215
87. Cutting Mechanism for 46 Degree Rotor with Sharp Blades, Rotating at 3600 RPM with a Feed Rate of 3 1/16 in./rev. (Stem 8, Trial PS-6)	217
88. Analysis of Trajectory of Stem Center of Gravity.	219
89. Energy Input Per Stem Cut <u>Versus</u> Independent Variable Parameters (Solid Line = Sharp Blade; Dashed Line = Dull Blade)	226
90. Maximum Torque Per Stem Cut <u>Versus</u> Independent Variable Parameters (Solid Line = Sharp Blade; Dashed Line = Dull Blade).	230
91. Energy Input Index <u>Versus</u> Independent Variable Parameters (Solid Line = Sharp Blade; Dashed Line = Dull Blade).	233
92. Maximum Torque Index <u>Versus</u> Independent Variable Parameters (Solid Line = Sharp Blade; Dashed Line = Dull Blade).	234
93. X Displacement Index <u>Versus</u> Independent Variable Parameters	236
94. Y Displacement Index <u>Versus</u> Independent Variable Parameters	237
95. Z Displacement Index <u>Versus</u> Independent Variable Parameters	238

Figure	Page
96. $\Pi_8 = \text{Se/Be}$ <u>Versus</u> Percent Moisture: (a) 13/64 Diameter Stems; (b) 17/64 Diameter Stems.	244
97. $\Pi_8 = \text{Se/Be}$ <u>Versus</u> Percent Moisture: (a) 21/64 Diameter Stems; (b) 25/64 Diameter Stems.	245
98. Graphs of Percent Moisture Content <u>Versus</u> Time in Chamber, Π_{10} <u>Versus</u> Nominal Diameter, and $1/\Pi_8$ <u>Versus</u> Time in Chamber . . .	250

CHAPTER I

INTRODUCTION AND STATEMENT OF PROBLEM

The Cutting Function of Field Machinery

Cutting is the first step of many field operations. Conventional forage harvesting involves cutting the plant stalks; and many seed crops are harvested by combines which first cut off the entire stalk, or that portion of it to which the seeds are attached, then remove the seed in subsequent operations.

Forage crops may be chopped or cut with a flail-type mower but usually are mowed with knives attached to a reciprocating sickle bar. This same method is generally used on combines to cut seed bearing crops. In mowing forage crops, high knife speed is required to attain adequate capacities in acres mowed per hour. Slower knife speeds are feasible in cutting seed crops. On a combine, typical speed of the sickle drive flywheel is from 400 to 450 rpm, resulting in 800 to 900 cutting strokes per minute. Practical sickle drive speeds for tractor mowers without a reciprocating counter balance range from 800 to 1000 rpm (1600 to 2000 cutting strokes per minute) (1).

Requirements and Design Goals for Cutting Devices Used on Forage Crops

To reduce irregular stubble length caused by excessive stalk deflection before cutting and for minimum power requirements, Kepner (2) recommends a mower cutting action of high velocity extending over a large part of the cutting cycle. Further, he recommends that unbalanced forces be kept to a minimum, that the included angle between the cutting edges should be kept small enough so that stalks will be cut before being expelled forward, and that desired cutting action and mechanical durability be maintained at forward speeds up to 10 miles per hour.

Design Goals for Cutting Devices Used on Seed Crops

The design objectives specified for forage cutting devices also apply to the cutting mechanisms of combines. But here a further requirement is made in that the cutting of seed bearing plants should be done with minimum disturbance of the stalks to avoid shattering and losing a portion of the seed. Also the reel and other devices used to guide plants into the cutter bar and move the cut stalks from the sickle onto the combine header pan should not unduly shake the plants. In a five year study of soybean harvesting practices, Lamp, Johnson, and Harkness (3) found that harvest losses varied from 8.8 to 19.3 percent, with the average loss exceeding 10 percent. Over 80 percent of the harvesting losses were gathering losses, almost all of which resulted

from knife and reel agitation of the plants. Even greater gathering losses occurred in the first attempts to harvest castor beans with a combine. About 50 percent of the seed shattered to the ground at normal combine forward speeds, according to Arms (4). Many seed shattered when the reel engaged the plant. Additional seed were jarred loose from the plant and fell to the ground when the knife cut the stalk.

Inadequacies of Conventional Cutting Devices and Schemes to Correct Them

The speed of the cutting knives of a conventional mower is limited by the high, unbalanced inertia forces induced by the mass of the reciprocating sickle bar. These unbalanced forces vary as the square of the speed of the driving crank and produce high, cyclic loads on the drive members and supporting frame. The loading must be kept below levels that unduly shorten the useful life of the drive and frame parts, hence the limit on maximum operating speed.

A portion of the input energy is dissipated in work to overcome the opposition to reciprocating motion imposed by the inertia of the unbalanced mass. Also friction forces, which oppose the sliding action of the cutter bar, waste input energy and cause rapid wear.

Several design schemes to overcome the speed limitations of the conventional mower have been investigated. Elfes (5) lists the different approaches as: (1) balancing out a major

portion of the inertia forces generated by the single reciprocating sickle bar through the addition of a practical counterbalancing device or by the use of two oppositely travelling reciprocating sickles, each balancing the inertia force of the other; (2) replacing the reciprocating sickle with an endless chain or band fitted with suitably spaced knives; (3) using a high-speed, single-element, impact-cutting blade rotating in a horizontal plane; (4) using a reel type mower similar to the common lawn mower. Each of these approaches proved to have limitations. With double reciprocating sickle mowers, suitable guards to protect the knives without interfering with the cutting action have been a problem. High energy losses due to friction plague both counterbalanced, single-sickle mowers and the double-sickle mowers. The endless band type mower has proved subject to plugging in cutting fine, tough grasses, possibly because of the constant direction of motion. The single-element, impact-type, rotary mower makes multiple cuts on each stalk and thus requires more power than a device which cuts each stalk only once. An excessively large diameter reel-type mower is required to cut tall grasses satisfactorily.

In regard to cutting with minimum disturbance of the plant, one approach that met with some success was the substitution of a high speed circular saw for the reciprocating sickle blades on a castorbean harvester (6). A saw, 12 inches in diameter, was driven at 2500 rpm in a horizontal plane. The saw cut the castor stalks easily, without

vibration, and with no shaking off of the seed capsules. There was no positive means to move the plants, once cut-off, back away from the saw, however. As a result, plants accumulated at the saw feed opening and obstructed the proper flow of plants to the saw.

The power requirement for cutting with a single reciprocating sickle bar was estimated by Kepner (2) to be 60 percent of the energy input to the mower. In evaluating a newly designed high speed mower, Elfes (5) determined that cutting required an average of only 33 percent of the input energy. Peak energy requirement for cutting was only 12 percent of the total peak energy input. Chancellor (7) measured the energy required to cut individual stalks of forage and from these determinations calculated the power requirement for cutting a 7 foot swath of 2 feet tall timothy hay, yielding 2 tons of 20 percent moisture hay per acre. At a forward speed of 7 miles per hour, the average cutting power was computed to be 0.22 horsepower. Assuming an average total input power of 2.5 horsepower, the 0.22 horsepower for cutting represents only 9 percent of the input power to the mower. Prince, Wheeler, and Fisher (8) determined the cutting energy for individual forage stalks and for mowing masses of stalks with a reciprocating sickle bar. They found a wide difference in the actual energy required to mow the masses of stalks and that theoretically required based on values measured for cutting individual stalks. The increase is attributed to bending of stalks to the ledger.

plate, the cutting of one stalk against another, and cutting with the knife edge at other than a 90 degree angle to the stalk.

Harbage and Morr (9) in developing a high-capacity, ten-foot mower, found that peak cutting loads on the mower drive pitman were less than the peak inertia loads when using a sharp knife. With a dull knife, however, peak cutting loads exceeded peak inertia loads by a factor of two when mowing bluegrass. This finding would indicate cutting energy requirements depend on degree of knife sharpness; hence, previously listed estimates are with the assumption of a sharp knife.

A further estimate of cutting energy requirements that corroborates the findings of Elfes and Chancellor is that made by Richey (10). He reported test results for cylinder and flywheel type forage choppers which indicate cutting energy makes up from 13 to 32 percent of the input energy. The remainder of the input energy was attributed to air and bearing friction, kinetic energy imparted to the chopped material, and to the frictional resistance encountered by the chopped material in passing through the housing.

In view of the findings of various investigators, an acceptable estimate of the maximum required cutting energy for a mower, assuming a sharp blade, is about one third of the total input energy. Thus the mechanical efficiency of a mower is less than 33 percent, rather low.

Proposed New Rotary Cutting Device

An investigation of a different type cutting device appears warranted, especially for use in harvesting seed bearing crops. Such a device should be simple in design, easy to adjust and repair, and capable of cutting either forage or seed bearing crops, the cutting action should impart little disturbance to shatter the seed from the stalk. If the device could fulfill the additional function of moving the severed stalks away from the cutting zone, still with minimum disturbance of the plants, it would be a significant improvement - one simple machine component, capable of cutting and trajecting plant stems while imparting minimum disturbance to the stems, and operating at high speeds with high mechanical efficiency.

The use of cutting elements arranged spirally about a horizontal, rotating shaft possibly can provide the objectives sought. Direction of rotation would be such that the cutting edges move forward and up in engaging the plants. With proper balancing, there would be no restriction on speed. Since speed would be constant and cutting continuous, there would be no power surges or cutting force peaks, hence little vibration imparted to drive or frame members. Motion would be imparted to the cut-off plant by energy transfer during impact of the cutting elements with the plant. Velocity components up, forward, and to one side would result. Because of the forward motion of the mower relative to the plant, the plant would already have a rearward component of

velocity relative to the cutting elements. Hence, the resultant velocity of the cut-off plant could be such as to deliver it to a receiving platform behind the cutting member.

Research Objectives

1. Design and fabricate a balanced, rotary cutting device having blades approximately helical in configuration. Provide a method of attaching blades to the rotor structure that allows replacement of the blades.
2. Evaluate the proposed cutter experimentally, using a typical edible seed crop (soybeans), to accomplish the following purposes:
 - A. Test the hypothesis that such a device can both cut and traject plant stems effectively in one operation.
 - B. Determine the mechanism of cutting utilized by the device with square edge (dull) and with sharp edge blades through high speed motion picture photography.
 - C. Screen the principal design and operating parameters of the cutter that might possibly affect the responses of input energy per stem cut, maximum torque developed per stem cut, and resulting displacements of the severed stem to determine those factors that do have a non-trivial effect and the desirable levels of those factors. Perform

the screening-of-parameter tests for both square edge and sharp edge rotor blades using a statistically designed orthogonal main-effect experimental plan.

- D. Compare results for the square edge and sharp edge blades to test the hypothesis of no difference in effectiveness of the blade types. If one is more effective, develop dimensionally correct functional relationships between the important response variables and the pertinent design, operating, and plant physical property parameters for the cutter fitted with the more effective blade type - within the limits provided by the screening-of-parameter data collected.

CHAPTER II

REVIEW OF LITERATURE

Several aspects of cutting plant stalks have been investigated and reported in the literature. Topics included are the basic nature of cutting, differences in means of cutting, and the effect of plant and knife variables on the requirements for cutting.

Basic Nature of Cutting

Stroppel (11) examined several methods of cutting solid, homogeneous materials like metals. He proposed an explanation of the cutting action and extended the theory to include non-rigid, fibrous materials such as plant stalks. His definition of cutting as quoted by Feller (12) is:

a mechanical separation process on a solid body by the use of a cutting tool whose wedge-formed cutting parts are under pressure and overcome the cohesion of the material due to the higher specific normal and thrust forces along the cutting edge.

He classified cutting tools into: (1) those employing a single element; (2) those employing two opposed elements; and (3) those using multiple, miniature single elements (saws). Either single element or two opposed element tools

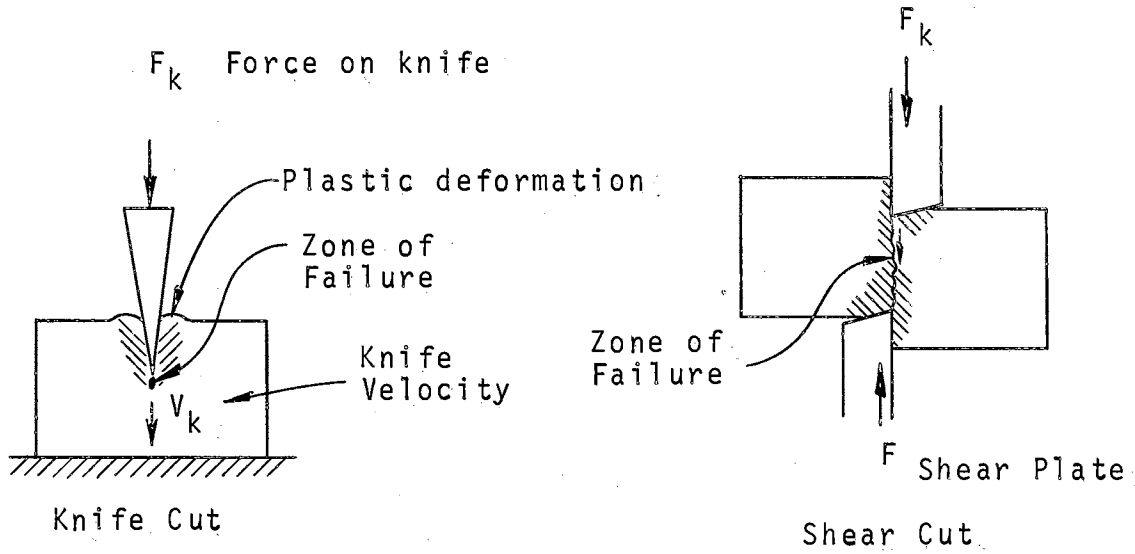
can produce a "knife cut" or a "shear cut", depending on the design of the cutting blades.

In knife cutting, the zone of failure precedes the cutting edge through the body. Severance of the material is attributed to the concentrated force along the knife edge and not to the components of force perpendicular to the wedge surfaces which intersect to form the edge. In other words, knife cutting differs from splitting. Motion of the knife can be normal to the cutting edge (a pressing cut), in the same direction as the edge (a slicing cut), or both simultaneously. The effectiveness of a slicing type of cut with a smooth blade is related to the microscopic notches along the edge resulting from grinding irregularities. These minute notches are said to produce a fine sawing effect.

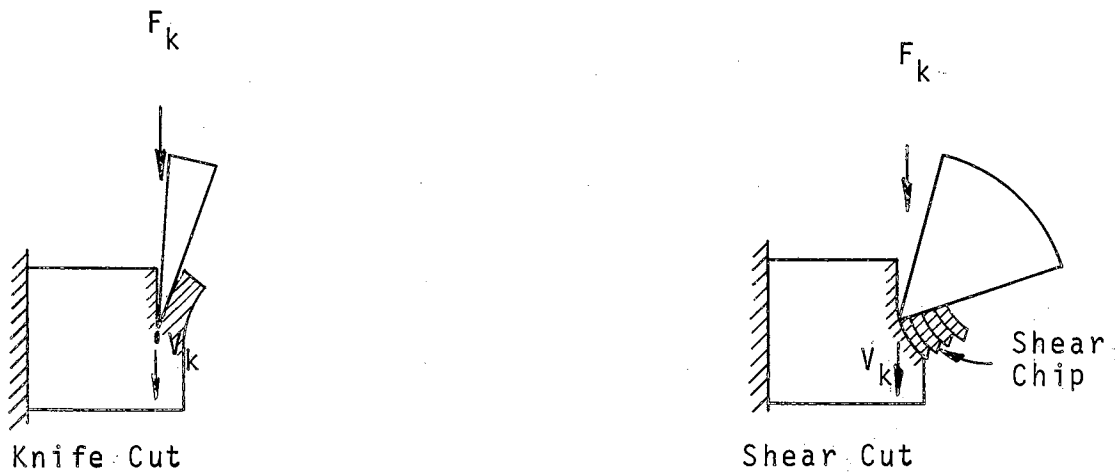
In "pure shear" cutting, forces applied to the cutting tool cause failure along a shear plane. The tool edge does not penetrate through the material being cut in the manner of knife cutting.

Sawing combines the actions of knife cutting and pure shear cutting. The multiple teeth making up the cutting edge penetrate the material from pressure on the blade normal to the direction of motion. Then each tooth shears and removes a small particle of material as a result of motion along the blade edge.

Knife cutting and pure shear cutting for single element and two opposed element tools are described schematically as shown in Figure 1.



Two Element Cutting



Single Element Cutting

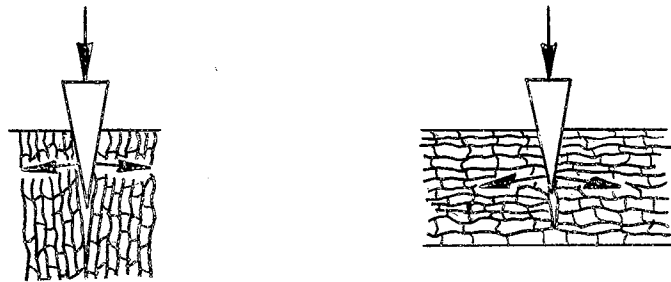
Figure 1. Schematic Diagram of Knife Cutting and Pure Shear Cutting

It is implied that for single element cutting, the support of, or the inertia of, the body reacts to the cutting tool pressure to permit cutting without accelerating the body.

Mode of Stem Failure - Two Opposed Element Cutting

Since small plant stems are not rigidly supported and are of relatively low mass, it is common to cut them between two opposed edges forced together. The resulting cutting action on the heterogeneous, fibrous plant stems differs from that of shearing homogeneous, crystalline substances like metals, as Koniger (13) emphasizes. He states that metals are cut between two opposing edges by inducing failure along a shear plane without appreciable penetration of the cutting tool (the "pure shear" cut defined by Stroppel). A more detailed description of this action is given by Svahn and Lundstrom (14) who state that a normal metal shearing operation is characterized by the following sequence of actions: (a) elastic deformation, (b) plastic deformation, (c) cutting action, and (d) shearing fracture. In contrast, fibrous materials, according to Koniger, are cut by the knife acting as a wedge to cause separation of the cell structure. The components of force perpendicular to the wedge surfaces are depicted as being of prime importance in causing the cutting action. Thus he disagrees with Stroppel's theory that fibrous materials are severed by concentrated forces along the knife edge and not by splitting. Figure 2

illustrates his theory of cutting fibrous materials between two opposed elements.



Along the Fiber Transverse to the Fiber

Figure 2. Theorized Cutting Action in Material of Fibrous Nature

Fisher, Kolega, and Wheeler (15) conducted tests in which individual stems of forage plants were cut between two opposed elements and proposed an explanation of the mode of failure based on the experimental evidence. Because of the stem structure of common forage plants, "an outer annular ring of rather tough fiber with either a hollow center or soft core," they theorized that the first action of opposed, beveled knives acting on a stem would be:

...one of compression in which the normal nearly circular cross section is deformed into an oval shape. Bending of the outer fibers also occurs along the longitudinal axis of the stem, making this a three-dimensional bending problem...

This concept is illustrated by Figure 3.

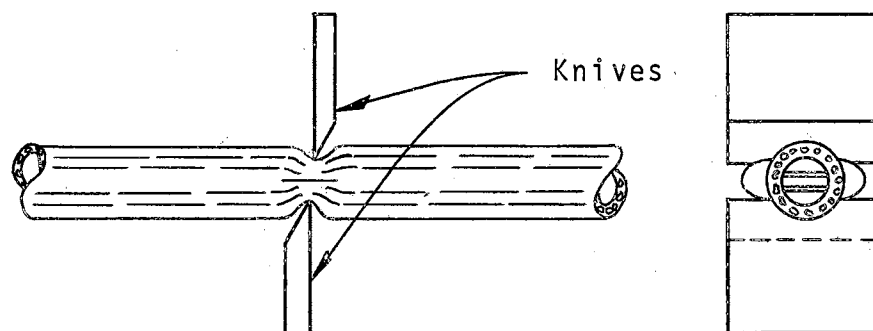


Figure 3. Three-dimensional Bending of a Single Stalk Between Two Knives

It was further theorized that after the compression phase, cutting of the outer fibers began "due to either the shearing action of the knives, failure of these fibers due to excessive bending, or both." Because of extreme compression along the line-like cutting edge of the knives, it was thought that some wedging action might occur due to the sharpness angle of the knife, as hypothesized by Koniger. This action might elongate the fibers along their longitudinal axes, causing them to fail in tension. With further compression of the bunched fibers, it was thought the knife force increased markedly to shear the uncut mass of fibers then suddenly drop off to zero.

An apparatus was made in which the force on the moving knife was incremented slowly by the addition of hanging weights. The distance between the knife edges was continuously measured. Thus a load-deflection curve for a single stem of alfalfa was plotted. Figure 4 illustrates the

result. It shows the failure of the stem did proceed in two distinct steps as hypothesized. Also shown in Figure 4, for comparison, is a load-deflection curve resulting from shearing sheet iron between two edges. The scale is reduced so that the shape may be more directly compared to the shape of the stem load-deflection curve. The sheet iron curve was plotted by Krabbe as discussed by Svahn and Lundstrom (14).

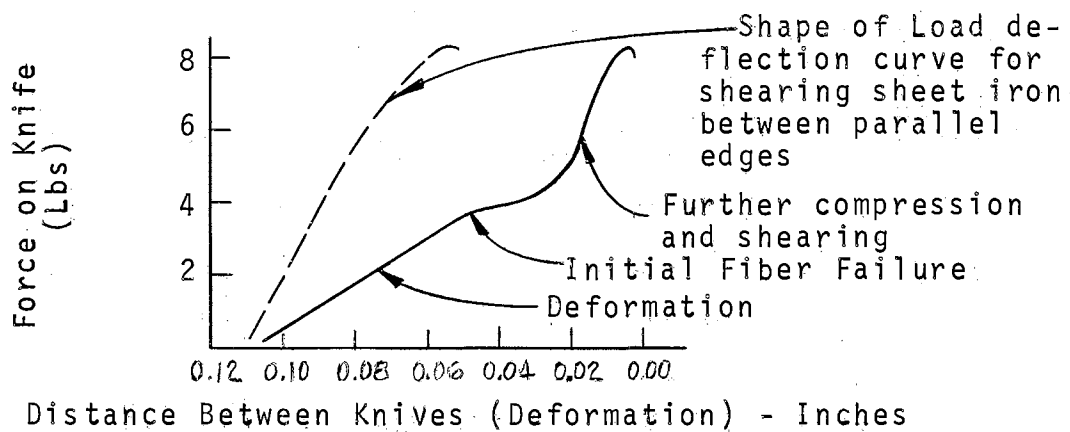


Figure 4. Comparison of Load Deformation Curves for Plant Stalks and Sheet Iron.

By measuring the energy required to cut different size stems with sharp and dull knives, it was found that the effect of dullness was more pronounced for small stems. Thus it was reasoned that the nature of the cutting action changed with increase in stem size. Since the bevel angle of the knife cutting edge would produce more of a wedging effect on larger stems, it was hypothesized that dull blades

cause small stems to fail in shear, while with larger stems, tensile failure of the fibers might occur from the wedging effect.

Chancellor (16) used 30-power laboratory binoculars to observe slow cutting of single stalks of forage plants. He determined that initial flattening of the stem was accompanied by cracking along its length produced by failure of the transverse bonding of the fiber groups to each other. This cracking allows flattening of the stem for an extensive distance each side of the area in direct contact with the cutting edges. Thus initial longitudinal bending is less pronounced than shown by Figure 3. The initial flattening produced, in effect, two sheets of fibers, one above the other between the cutting edges. The top fiber sheet (the one in contact with moving cutting edge) failed first, followed by increased forces previous to failure of the second sheet of fibers. This is the pattern of failure predicted by Fisher, Kolega, and Wheeler (15). Failure of the fiber sheets was along a plane inclined roughly 45 degrees to the longitudinal axis of the stem.

Chancellor proposed that each of the two sheets of fiber fails as a result of bending and transverse compressive stresses imposed by the blade edge. He reasoned that these stresses combine to produce a shear stress of greatest intensity along a plane inclined approximately 45 degrees to the longitudinal axis of the stem. He concluded that failure took place on the plane of maximum shear stress, but he

thought that failure of the individual cells of the fibers might be of a tensile nature.

In consideration of the effects of plant physical properties on cutting, McClelland and Spielrein (17) designed a static grass tester to determine the ultimate bending strength of forage stems. They found a linear relationship between bending force causing failure and the linear density (weight per unit length) for ryegrass, lucerne, oats, and wheat. Their conclusion was that the stems, although of biological character, "obeyed a readily established law of mechanical behavior." Different species of plants and different varieties within a species exhibited different inherent mechanical characteristics. But it was stated that once the mechanical constants of a particular variety of plant were determined, a prediction of bending strength could be made by measuring the linear density.

In a similar investigation, Prince (18) designed special testing machines to determine the ultimate bending and torsional strengths of forage stalks. He also determined the relationship between stalk diameter and linear density. His findings corroborate those of McClelland and Sprilrein with respect to bending strength; that is, the force required to cause failure of a stalk in bending varies linearly with the weight per unit length (linear density) of the stalk. However, Prince found that moisture content of the stalk affected the bending strength. Thus knowledge of the moisture content, linear density, species, and

variety of a plant is required to predict the ultimate bending strength of the stalk.

The ultimate torsional strength of alfalfa stalks was found to vary linearly with the weight per unit length of the stalk. Also, as with ultimate bending strength, the slope of the straight line graph of the relationship was steeper for stalks of lower moisture content.

To gain further insight into the mode of failure of forage stalks when subjected to the action of two opposed knife elements, a comparison of the ultimate tensile strength and ultimate shear strength of the stalk is in order. One of the equations for ultimate bending strength determined by Prince (18) applies to 38 day old alfalfa of 71% moisture content (wet basis). One of the equations for ultimate torsional strength applies to 41 day old alfalfa of 68% moisture content. If these stalks are assumed equivalent and a linear density of 0.05 grams per centimeter is selected as typical, the computed ultimate bending force, by Prince's equation, is:

$$F = -144.85 + 3572.83 (.05) = 63.79 \text{ gms.}$$

This force acted at a distance of 5.8 centimeters from the stalk support to produce a moment of $(5.8) (63.79) = 369.98$ gm-cm. when the stalk failed. The ultimate torque on the same stem when torsional failure occurs is:

$$T = 67.38 + 1085.83 (.05) = 121.67 \text{ gm-cm.}$$

From Figure 4, it is apparent that for a plant stem cut between two opposed edges, the load-deflection curve for

each of the two sheets of fibers of the flattened stem is similar in shape to the curve for sheet iron sheared between two opposed edges. Therefore, assume for comparison purposes that the heterogeneous stalks fail similarly to homogeneous metal rods subjected to the same type of loading. Fictitious maximum tensile and shear strengths, computed for the equivalent metal rod, should provide a reasonably accurate estimate of the actual ultimate tensile strength to shear strength ratio. Then if

S_{fu} = ultimate flexural stress,

S_{su} = ultimate torsional stress,

M = applied bending moment; T = applied torque,

c = distance from neutral axis to the extreme fiber,

I = moment of inertia of the cross section,

J = polar moment of inertia of the cross section,

r = radius of the rod,

$$\frac{S_{fu}}{S_{su}} = \frac{Mc/I}{Tr/J}$$

But $r = c$, and $J = 2I$ for a circular cross section.

$$\text{then } \frac{\frac{Mc}{I}}{\frac{Tc}{2I}} = \frac{2M}{T} = \frac{2(369.98)}{121.67} = 6.08$$

This estimate shows that forage stalks are about six times stronger in tensile strength than in shear strength. If this is so, then it is most probable that failure of the stem occurs by shearing along the plane of maximum shear stress. The maximum shear stress results from the combined

localized bending and transverse shear loads imparted by the two opposed edges acting on the stalk. With the assumed loading, there seems to be little logic in supposing that failure of the individual fibers is in tension. Nor does it appear likely that tensile failure of stem fibers, resulting from the wedging action of the knife, occurs when large stems are cut with a dull knife (as opposed to pure shear cutting of smaller stems by the same knife). Rather the dull knife can effect concentrated localized bending stress on the coarse fibers of the large, stiff stems to increase the combined shear stress on the failure plane of the fibers. Thus, less force is required than for failure by transverse shear loading alone. The same dull edge is relatively wide with respect to the fibers of small stems; thus transverse shear loading, with little localized bending, results and requires higher forces to produce failure.

Mode of Stem Failure - Single Element (Impact) Cutting

Chancellor (16) studied impact cutting by photographing the plant stem at the instant of cut with a high speed camera. He found that the stems deflected little during impact cutting and only in the vicinity of the knife. After the cut, the severed stem underwent additional deflection because of energy, in excess of that required to sever the stem, imparted by impulse during the cutting process. He theorized that the mechanism of failure was basically the same as that of a stem cut between two elements. In this

case, the inertia of the plant acts as the second element. The cutting force is reacted by the attempted instantaneous acceleration of the stem fibers. Because of the high velocity of the blade, the force acting on the stem is large enough to cut individual fibers before their movement relative to other fibers results in compression of the stem into two flat sheets. Thus impact cutting is characterized by continuous severing of the stem fibers rather than first compressing them into two flat sheets and then cutting the sheets individually as occurs when shearing between two elements.

Johnston (19), in studying the behavior of crops during mowing by the use of high speed motion picture photography, observed the nature of the impact force developed between a single plant stem and the advancing knife. In this instance, the knife velocity was considerably below that commonly used for impact cutting. Still, the results are similar, and he gives a clear explanation of the action.

Impact is considered to last while the section of straw at the point of contact is being accelerated to knife speed. The mass of the length of straw near the knife edge will be more important over this small interval of time because bending will rapidly reduce the acceleration experienced by higher or lower parts. As the bending deflection increases, the force due to the rigidity of the straw will become important. Thus the force between the straw and the knife edge will, apart from impact, depend on the deflection of the straw, that is, on the distance the knife has moved.

His film showed that when the knife contacted a single straw, considerable bending occurred in the portion of the straw in front of the knife, while the top of the straw

moved very little. A drawing (Figure 5) showing superimposed frames of the high speed photographs is used to illustrate this action.

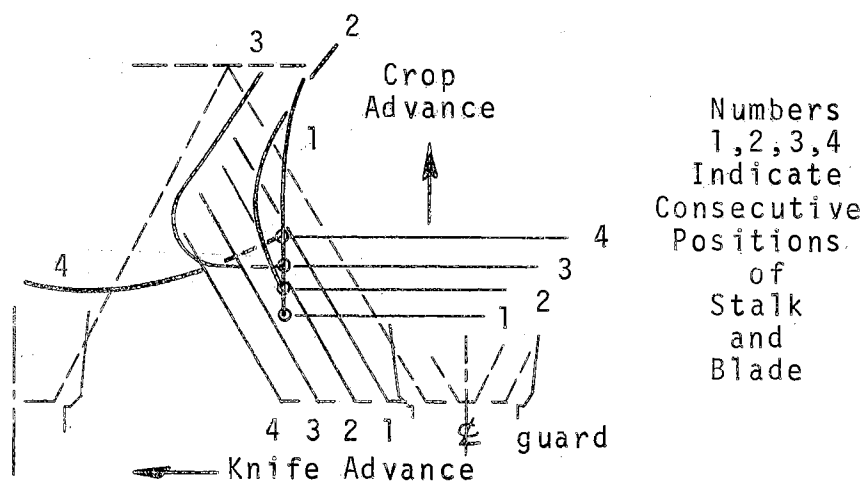


Figure 5. Reaction of a Single Stalk to Knife Force.

He concluded that "the straw resisted the knife motion as a propped cantilever [beam], the inertia of the top of the straw being in effect the prop." This conclusion is corroborated by a high speed moving picture study conducted by Feller (12) of the cutting action of a single element impact blade. He found that with a cutting velocity of 25.8 feet per second, "When the knife hit the stalks they were pushed about 1 inch before being cut while the top part did not move."

The assumption of the stalk reacting to the knife motion like a propped cantilever beam appears to confirm Chancellor's conclusion that impact cutting produces the same type of stem failure as cutting between two elements. Transverse shear and bending loads combine to produce a stress exceeding the shear strength of the stem fibers and cause separation along the plane of maximum shear.

Mode of Stem Failure - Sawing

One key difference in cutting between two opposed elements and by a single high speed blade is noted in considering a slicing or sawing cut. Motion of the stem along the knife edge, as it is penetrated and severed by the knife, is a defining characteristic of a slicing cut. Johnston's high speed motion picture films of the cutting action of two opposed knives (angle between cutting edge and direction of motion approximately 60 degrees) showed no slip of the stalk along the edge in transport to the opposing ledger plate or during cutting (19). Thus cutting between two elements is a pure pressing type of cut. In contrast, Feller's film of single element cutting showed extensive slip or sliding of the stalk along the blade to give a combination pressing-slicing type of cut (12).

To better explain the kind of cutting action investigated, Chancellor (16) defined a chopping (pure pressing) cut as one in which the normal force between the blade and

the stalk assumes whatever value necessary to cause uniform motion of the blade through the stalk with no motion along the blade.

A pure slicing or sawing cut is one in which the force perpendicular to the blade edge remains constant, and the stalk moves along the blade the required distance for cutting.

Both Feller (12) and Chancellor (16) refer to V. P. Goryachkins's equation for a slicing type of cut as given by Bosoi (20):

$$P^3 S = K$$

where

P = the normal pressure of the blade on the stalk

S = the distance the stalk moves along the blade before being completely severed

K = a constant

Goryachkin stated that a slicing type cut required less power than a pure pressing type of cut. Chancellor's experiments refuted this claim. He found the energy required for a pure slicing cut to be approximately twice that required for chopping - with smooth, serrated, or saw tooth blades. Smooth blades required the most energy, serrated next, and the saw tooth blade required the least of the three for cutting. However, an increase in the normal pressure on smooth or serrated blades reduced the cutting energy requirements to the point of approaching, but still not equaling, the energy required for chopping.

Feller (12), on the other hand, found that a combined pressing-slicing type of cut required less energy for single element cutting than a pure pressing cut alone. He determined that a knife angle (angle between the blade edge and the direction of motion) of 60 degrees required minimum cutting energy. By introducing Goryachkin's equation in the formula for work done (energy expended), i.e., work is proportional to $P \times S = P \times \frac{K}{p^3} = \frac{K}{p^2}$, he claimed to verify Goryachkin's finding for knife angles up to 60 degrees, since P increases with larger knife angles. Above this value, the relationship does not hold.

The increased energy required for small knife angles (producing pure slicing) is explained by Feller as resulting from the high friction force caused by the blade wedging into the stalk. Energy is dissipated by this friction force acting over the distance the stalk slides along the blade during cutting.

Chancellor (16) gave a somewhat different explanation for increased energy required for slicing. He theorized that the individual fibers were engaged by the blade in small groups and bent and stretched in the direction of motion in a manner similar to a taut horizontal cord fixed at both ends with a weight hung at the center. He suggested that a smooth blade engaged the fiber bundles by friction; thus it would catch and release the bundles several times before causing failure. A serrated blade is more positive in

engaging the fibers and carrying them to failure. A saw blade is the most positive of all. The tensile nature of the failure plus multiple engagement and release of the fiber bundles by smooth and serrated blades require more energy to cause failure.

After studying the nature of sawing wood, Harris (21) described the mode of failure of individual fibers as a shearing action. But whether failure is by shearing, by tension and flexure, or by a combination of the three, the distinguishing feature of sawing with a toothed blade is the formation of a kerf (notch) with accompanying sawdust. This results from successive teeth being "set" (deformed slightly) to opposite sides of the blade. Thus cutting takes place in two parallel planes, producing, as Chancellor (16) points out, "twice as many cuts as necessary."

To reduce the high energy required by cutting in two parallel planes when sawing, Alex Lundberg of Sweden designed a saw with modified teeth. The Lundberg saw teeth have the high point in the center instead of on the outside like conventional teeth, Figure 6. With this design, a finer set is permissible, producing less of a kerf and a smaller amount of saw dust. A coarser pitch (larger teeth and fewer of them) is feasible, and power requirements are reportedly reduced (22).

An approach similar to that of Lundberg's design might well reduce the energy required for sawing small stems.

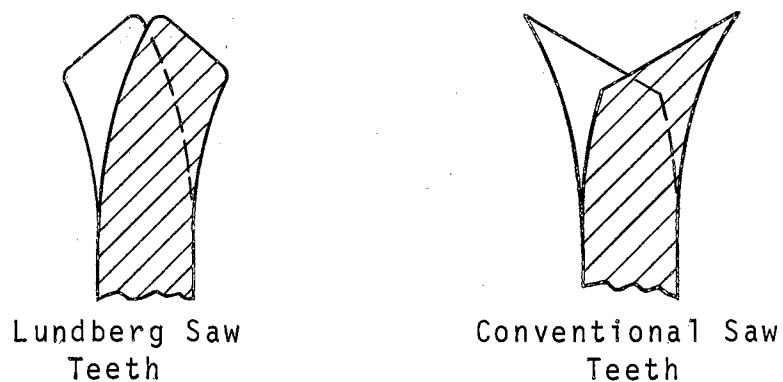


Figure 6. Comparison of Lundberg and Conventional Saw Teeth

Motion of Severed Stems Resulting From Impact Cutting

A plant stem, being flexible, acquires some velocity before being severed by a single, high velocity blade. Thus energy in excess of that required for cutting is transferred to the stem, as evidenced by its gain in momentum. This acquired kinetic energy produces motion of the severed stem after the knife has passed.

An indication of the extent of energy transfer to the severed plant is shown by high speed motion pictures of impact cutting taken by Feller (12). Alfalfa stalks, 18 inches tall and 1/8 inch in diameter at the base, were thrown a distance of 15 feet when cut 3 inches above the base by a sharp knife traveling 31.8 feet per second with the knife edge perpendicular to the direction of travel. The film showed that after the stem was cut, the lower part

of it moved faster than the upper part such that the stem approached a horizontal position in flight.

Considering the separated stem as a rigid free body and assuming that a constant force acts at the cut end for a short time to give an impulse equivalent to that causing the gain in momentum during cutting leads to anticipation of the plane motion shown by the film. The horizontal force acting at the cutting zone can be replaced by an equivalent horizontal force and a couple acting at the center of gravity of the stalk. This force system would produce combined translation and rotation of the stalk. Figure 7.

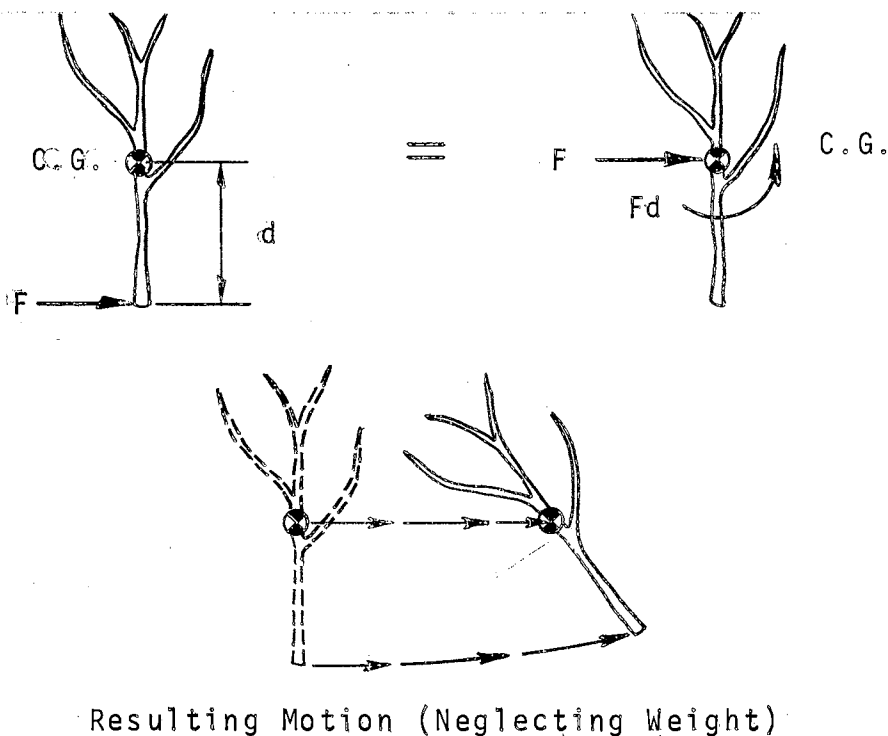


Figure 7. Force System on Single Stalk and Resulting Motion

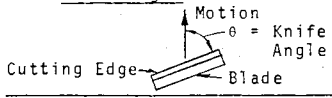
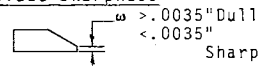
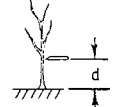
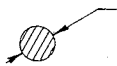
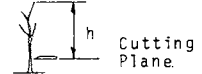
The amount of energy transferred to the severed stem depends on a number of variables. Feller (12) determined that knife angle, knife velocity, plant height, and plant species influenced the energy transfer. Chancellor (16) investigated the effects of knife velocity, stem size, blade sharpness, and distance between the cut and the point of stem support on the energy transfer. He clamped 8 1/2 inch long stems of timothy plants at one end and photographed the deflection of the free end when cut by an impact knife (blade edge perpendicular to the direction of travel). By considering the clamped stem as a cantilever beam, he calculated the energy transfer necessary to cause the given deflection. Results of these two investigations are summarized in table I.

Variables Affecting Cutting

Variables influencing the ability of a cutting mechanism to sever plant stalks and affecting the force level and energy input required to accomplish this cutting may be grouped into three broad categories: knife design parameters, knife operating parameters, and plant characteristics.

An important design parameter is the angle between the knife edge and the direction of motion of the knife (for impact cutting) or between the two opposed cutting elements (for two element shearing). Both of these angles are described as the knife angle. Other important design parameters include the bevel angle of the knife edge and the

TABLE I
EFFECT OF VARIABLES ON ENERGY TRANSFERRED
TO SEVERED STEMS BY IMPACT CUTTING

VARIABLE	INVESTIGATOR	RESULTS
<p>1. <u>Knife Angle</u></p>  <p>Motion θ = Knife Angle Cutting Edge Blade</p>	Feller (12)	<p>With a sharp knife, maximum energy transferred with $\theta = 90^\circ$. Very small transfer with $\theta = 30^\circ$.</p>
<p>2. <u>Knife Velocity</u></p>	<p>Feller (12)</p> <p>Chancellor (16)</p>	<p>With a sharp knife, energy imparted was <u>greater</u> for <u>higher</u> velocities when cutting 18 inch tall alfalfa plants (1/8 dia. stems). Velocity range: 9.52 to 27.3 ft. per sec. Knife angle: 60 to 90 degrees.</p> <p>Velocity had <u>no effect</u> when cutting 18 inch tall sudan grass (1/4 dia.) under the same conditions.</p> <p>Small increase of deflection with velocity in range of 136, 205, & 237 ft. per sec. when cutting 8 1/2 inch long timothy stems 4 inches from support with a sharp knife & 90 degree knife angle.</p>
<p>3. <u>Blade Sharpness</u></p>  <p>$\omega > .0035$" Dull $< .0035$" Sharp</p>	Chancellor (16)	Greater energy transferred by dull knife (90 degree knife angle) for small stems. Difference between dull and sharp blades less pronounced for large stems.
<p>4. <u>Distance of Cut From Point of Stem Support</u></p>  <p>d</p>	Chancellor (16)	Greater energy transfer with increased distance between cut and point of stem support. (Cuts 2, 4, & 6 inches from support; 8 1/2 inch long stems)
<p>5. <u>Stem Size</u></p>  <p>Diameter or Weight Per Unit Length</p>	Chancellor (16)	Greater energy transfer to heavier stems (.015 gms. per cm. vs .035 gms. per cm.)
<p>6. <u>Plant Height</u></p>  <p>h Cutting Plane</p>	Feller (12)	Increased energy transfer with increased velocity for 18 inch tall alfalfa plants; no increase of energy transfer with increased velocity for 5 1/4 inch tall alfalfa plants. (Sharp knife, 45 degree knife angle; cut 1/4 inch above base of plants.)
<p>7. <u>Plant Species</u></p>	Feller (12)	Marked difference in amount of energy transferred to alfalfa and sudan grass stems at higher velocities. Difference possibly related to stiffness of the stems.

degree of sharpness of the edge as defined by the thickness at the point of the bevel. The clearance between two opposed shearing elements affects cutting force and energy requirements. Its effect depends on the degree of knife sharpness, however, being more pronounced with a dull knife than with a sharp one. Still other design parameters are the type of blade (smooth, serrated, or notched) and the width of blade contact with the material to be cut. The latter is determined by the knife section dimensions and the spacing of the sections along the cutter bar.

Knife velocity, in the direction of motion of the blade edge, is an operating parameter of prime importance. Further, the relationship of the knife velocity to the forward motion of the knife carriage determines the feed rate, or the forward advance of the carriage per cutting stroke. The feed rate in turn determines the area of plant stalks cut per stroke, the height of cut above the base of the plant for a given cutter bar height adjustment, and the orientation of plant stalks relative to the knife edge when cut. All these variables have been found to affect cutting force and energy, as have the cutter bar height setting and the normal force on the blade (in sawing).

Plant characteristics which affect cutting force and energy requirements are species and maturity of the plant, stalk diameter, plant height, and moisture content.

TABLE II

EFFECT OF KNIFE DESIGN PARAMETERS ON CUTTING FORCE & ENERGY
AS REPORTED IN THE LITERATURE

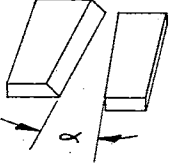
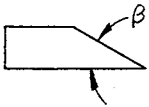
VARIABLE	CUTTING ACTION	INVESTIGATOR	RESULTS
1. <u>Knife Angle</u>	Two Element Shearing	Chancellor (16)	Less energy required for knife angles between 0 & 20 degrees. Force required decreases with increased knife angles (angles tested: 0, 15, 30, & 45 degrees).
		McClelland & Spielrein (23)	For smooth, sharp, beveled knife and ledger plate blades (19° bevel angle), minimum energy required for knife angle between 17 & 25°. Angles tested: 0, 17, 25, & 35 degrees.
	Single Element Impact	Feller (12)	With a sharp knife (15° bevel angle), minimum energy required for knife angle of 60° when cutting plants 3 inches above point of support; and $\alpha = 45^\circ$ when cutting plants 1/4 inch above point of support. Angles tested: 7, 15, 30, 45, 60, 75, & 90 degrees. With dull knife (15° bevel; 1/32 radius at point), best performance with $\alpha = 90^\circ$.
2. <u>Bevel Angle</u>	Two Element Shearing	Chancellor (16)	Slight increase in energy & force required with increase of β from 20° to 30°. Rapid increase for β above 30°. (Range tested: 20° - 80°)
		Fisher-Schlemn (Cited by McClelland & Spielrein (23)	Optimum energy & force requirements with minimum wear when $\beta = 24^\circ$. (Range tested: 14° - 30°)
		McClelland & Spielrein (23)	Compared angles of 19° & 90° (square). From 2.5 to 3.5 times more energy required for $\beta = 90^\circ$.

TABLE II (Continued)

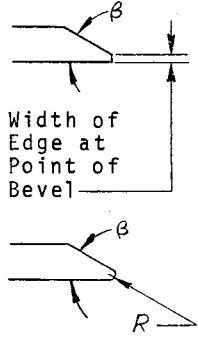
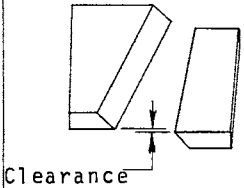
VARIABLE	CUTTING ACTION	INVESTIGATOR	RESULTS
<p>3. <u>Knife Sharpness</u></p> 	Two Element Shearing	Chancellor (16)	With edge width below .0035 inch, little effect on force or energy; above .0035 inch width, force & energy increase with increased width of flat ($\beta = 25^\circ$).
		Liljedahl et al. (24)	Sharp knife required less energy and was little affected by knife to ledger plate clearance or plant moisture content. With $\beta = 30^\circ$, I = sharp (no radius at point); II = .003 inch radius; III = .006 inch R.; IV = .012 inch R., then at zero clearance, ratio of energy requirements was: I:II:III:IV = 1:1.2:2.2:3.1. At .016 inch clearance, I:II:III:IV = 1:2.7:4.9:6.
		Prince & Wheeler (25)	Using a knife blade with $\beta = 25^\circ$ and a square ledger plate, energy requirement doubled when a 1/32 inch radius was put on edge of ledger plate.
	Single Element Impact	Chancellor (16)	Increase of force and energy requirements for a dull knife with response similar to cutting between two elements.
		Feller (12)	Energy requirements doubled by putting 1/32 inch radius on edge of blade. ($\beta = 15^\circ$).
<p>4. <u>Clearance</u></p> 	Two Element Shearing	Chancellor (16)	With sharp knife, clearance below .025 inch has little effect. Energy & force increase with increased clearance above .025 inch. Range tested: .005, .015, & .025 inch.
		Liljedahl et al. (24)	Little effect with sharp knife. Rapid increase in energy requirements with increase of clearance with dull knife. Range tested: 0 to .016 inch in increments of .002 inch.
		McClelland & Spielrein (23)	Slight increase in energy requirements for .026 cm. clearance over .005 cm. clearance with sharp, beveled blade. Ratio of 1.2 to 1. For square blades, ratio was 2.2 to 1.

TABLE II (Continued)

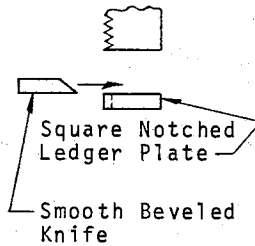
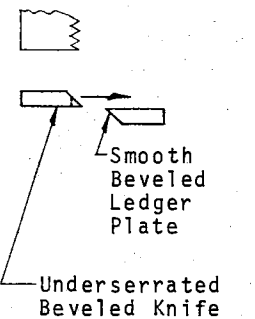
VARIABLE	CUTTING ACTION	INVESTIGATOR	RESULTS
5. <u>Type of Blade</u>	Two Element Shearing	Chancellor (16)	Three combinations tested: I---underserrated, beveled blade with a square shear plate II--smooth, beveled blade with a square shear plate III-smooth, beveled blade with a smooth, beveled shear plate Ratio of energy requirements: I:II:III = 1.6:1.2:1. (Avg.)
	 Square Notched Ledger Plate Smooth Beveled Knife	Liljedahl et al. (24)	Three combinations tested: I---smooth, beveled blade/square shear plate II--smooth, beveled blade/beveled shear plate III-smooth, beveled blade/square shear plate including relief angle No advantage to III. Lowest energy required by II. With dull blade, ratio of energy required was I:II = 2:1.
	 Smooth Beveled Ledger Plate Underserrated Beveled Knife	McClelland & Spielrein (23)	Three combinations tested: I---square, notched blade/square, notched shear plate II--square, smooth blade/square, notched shear plate III-beveled smooth blade/square, notched shear plate Ratio of energy required in cutting oats; I:II:III = 5:3:1.
		Prince & Wheeler (25)	Four combinations tested: I---smooth, beveled blade/beveled shear plate II--smooth, beveled blade/square shear plate III-smooth, square blade/beveled shear plate IV--smooth, square blade/square shear plate Ratio of energy requirements (.14" dia. alfalfa stems): I:II:III:IV = 1:1.5:1.8:3.5
	Pure Slicing or Sawing	Chancellor (16)	Three types of saw blades tested: I---smooth; II--serrated; III-saw toothed (32 teeth/inch) Average energy requirement ratio: I:II:III = 2.8:1.1:1

TABLE III
EFFECT OF KNIFE OPERATING PARAMETERS ON CUTTING FORCE & ENERGY
AS REPORTED IN THE LITERATURE

VARIABLE	CUTTING ACTION	INVESTIGATOR	RESULTS
1. <u>Knife Velocity</u> (in direction of motion of blade edge)	Two Element Shearing	Chancellor (16)	Change of velocity in range of 5.75 to 17 ft. per sec. had little effect on either force or energy requirements; slight increase in energy, slight decrease in force with increasing velocity. (Sharp knife)
		McClelland & Spielrein (23)	Slight increase in energy requirements with increase in velocity in range of 1.88 to 4.05 ft. per sec. (Sharp knife)
	Single Element Impact	Chancellor (16)	Change of velocity in range of 140 to 280 ft. per sec. had little effect on energy requirement. Minimum velocity recommended: 150 ft/sec. (Sharp knife)
		Feller (12)	With sharp knife, velocity increase in range of 9.57 to 31.8 ft./sec. did not affect cutting energy. Min. vel. to cut 1/8 dia. alfalfa: 8.4 ft./sec. Min. vel. to cut 1/4 dia. sudan grass: 21.6 ft./sec.
2. <u>Feed Rate</u> (forward travel of knife carriage per cutting stroke) F, feed rate, in./stroke V, forward velocity, in./min. S, strokes/min. h, throat depth of knife, in. I, cutting index	Two Element Shearing $F=V/S=h/I$ $I=hS/V=h/F$	Kepner (2)	Feed rate recommended: 2/3 relative motion of two cutting elements per stroke. For fixed ledger plate, & cutter bar movement of 3 inches per stroke, $F=2/3 \times 3 = 2$ in./stroke For knife throat depth of 1 3/4 in., $I=h/F=1.75/2 = .88$
		Lamp, Johnson, & Harkness (3)	Minimum cutting index recommended: .45 $F=h/I=1.75/.45=3.89$ in./stroke
	Single Element Impact	Chancellor (16)	Feed rate recommended: that which allows cutting one stem at a time

TABLE III (Continued)

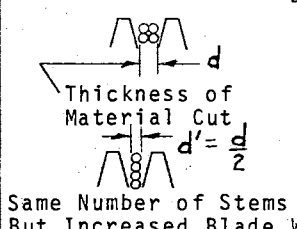
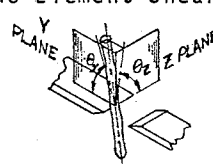
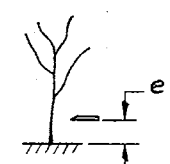
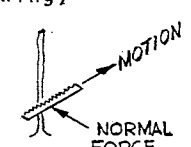
VARIABLE	CUTTING ACTION	INVESTIGATOR	RESULTS
3. <u>Thickness of Material Cut per Knife Stroke</u>	 <p>Thickness of Material Cut d</p> <p>$d' = \frac{d}{2}$</p> <p>Same Number of Stems But Increased Blade Width</p>	Chancellor (16)	For a given number of stems to be cut, force & energy increase with the thickness of material cut.
		Liljedahl et al. (24)	For a given number of stems to be cut, doubling the thickness increased energy required by 25%.
		Prince & Wheeler (25)	Increased energy required for increased thickness of cut.
4. <u>Orientation of Stalk Relative to Knife When Cut</u>	<p>Two Element Shearing</p> 	Prince & Wheeler (25)	Energy required with plant oriented such that $\theta_x = \theta_y = 90^\circ$ is greater than that for another orientation. The particular best orientation depends on the plant species and the type of knife & shear plate used. (i.e., for alfalfa, and knife & ledger plate with 25° bevel angles, θ_y had no effect; $\theta_z = 75^\circ$ required 14% less energy than $\theta_z = 90^\circ$)
5. <u>Height of Cut Above Base of Plant</u>	<p>Single Element Impact</p> 	Chancellor (16)	Increased energy required with increased distance of cut from point of support (8 1/2 in. timothy stems cut 2, 4, & 6 inches from support).
		Feller (12)	With all other conditions constant, changing cutting height from 3 to .25 inches above support decreased cutting energy by 50%.
6. <u>Normal Force on Blade</u>	<p>Pure Slicing (Sawing)</p> 	Chancellor (16)	Increased normal force decreased cutting energy proportionally, for smooth blade. Less effect on energy for serrated blade; only slight effect for saw-toothed blade.

TABLE IV
EFFECT OF PLANT CHARACTERISTICS ON CUTTING FORCE & ENERGY
AS REPORTED IN THE LITERATURE

VARIABLE	CUTTING ACTION	INVESTIGATOR	RESULTS
1. <u>Plant Species</u>	Two Element Shearing & Impact	McClelland & Spielrein (17)	Ultimate bending strength varies with species, affecting both force & energy required for cutting.
	Single Element Impact	Prince (18)	Ultimate bending & ultimate torsional strengths vary with species, affecting both force & energy required for cutting.
	Pure Slicing or Sawing	Chancellor (16)	Difference in ultimate tensile strength of stem fibers of various species has some effect on cutting energy. There was little effect on cutting force.
2. <u>Maturity of Plants</u>	Two Element Shearing	Prince & Wheeler (25)	Younger plants require less energy. (i.e. alfalfa at 55 days required twice the cutting energy as alfalfa at 28 days with the same diameter stalk. Moisture content of the two samples were within 10% of each other)
3. <u>Moisture Content</u>	Two Element Shearing	Chancellor (16)	Higher energy requirements but lower forces at higher moisture contents. Maximum force required at 35% moisture content (wet basis).
		Liljedahl et al (24)	Maximum energy requirement at about 30% moisture content (wet basis). With a sharp blade, moisture content had little effect on energy requirement; with a dull blade, effect more pronounced.
		Prince & Wheeler (25)	Energy requirement increased by 40% as moisture content decreased from 74% to 48% (w.b.). Further drying to 20% moisture had no effect on energy.
4. <u>Diameter of Stalk</u>	Two Element Shearing	McClelland & Spielrein (17)	Linear relationship between bending force for failure and mass per unit length of stalk. Thus force & energy to cause failure are proportional to stalk diameter.
		Prince (18)	Ultimate bending & torsional strengths of plant stems are proportional to linear density of stem. Linear density is proportional to stem diameter. Thus force & energy requirements for cutting increase with stem size.
	Single Element Impact	Chancellor (16)	Force & energy requirements increase as stem size increases.
5. <u>Height of Plant</u>	Single Element Impact	Chancellor (16)	No effect on force or energy requirement for 8.5 inch tall timothy stems extending 2.5, 4.5, & 6.5 inches above cutting plane.
		Feller (12)	Slight increase in energy requirement for taller plants (i.e., .47 ft-lb per stalk for 1/4 dia. sudan grass stems 8 inches tall compared to .59 ft-lb per stalk for the same diameter stem 18 inches tall. All other conditions constant.)

Results of previous investigations of the effect of the different variables on cutting force and energy are listed in Tables II through IV.

Previous Design of Rotary Cutters with Blades
Approximately Helical in Configuration

The idea of a "rotary sickle" to replace the reciprocating cutter bar of mowing machines was considered during the period between 1885 and 1900. Beekman (26) (27) was granted United States patents on at least two devices using rotary knives on a horizontal shaft. In his patent claims, he refers to "a rotating cutter provided with a helical cutting edge lying in the surface of a cone." His concept was one of hooked knives rotating on a horizontal shaft with downward motion during the cutting cycle. The spiral outer surface of the knives would feed the grass or grain laterally into the sharp inner hook surface of the adjacent knife where cutting would take place.

The use of a helical shaped cutting edge was proposed for lawn mower designs during the period from 1940 to 1950. The helical edge was approximated by elliptical shaped disks equally spaced along a horizontal shaft and positioned at an angle to the shaft center line such that the peripheral surface of the disks was cylindrical. Newton (28) received a patent on such a device in 1942. Figure 8 (A) illustrates his design. Positioned beneath the rotor disk assembly (shaded on the drawing) was a stationary cutter bar having V-shaped sections. The disks rotated downward on the

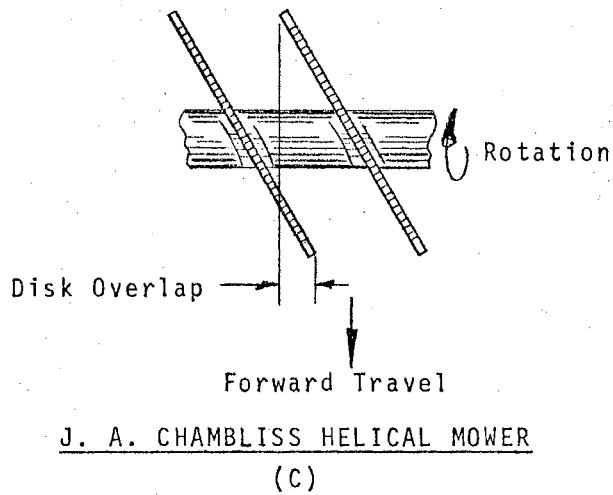
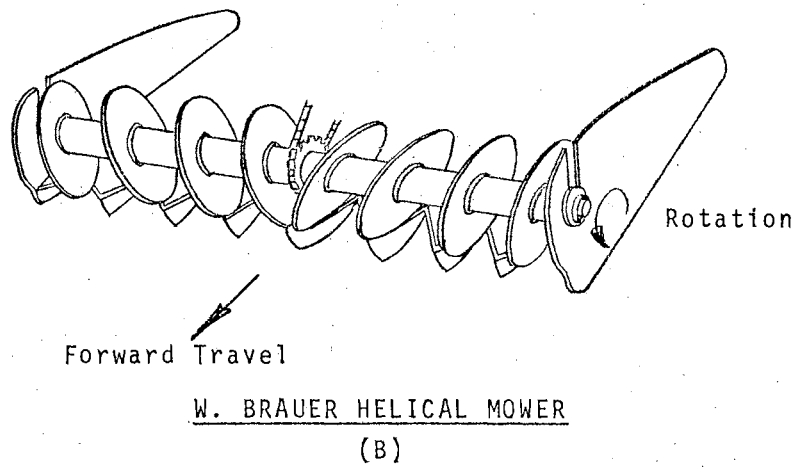
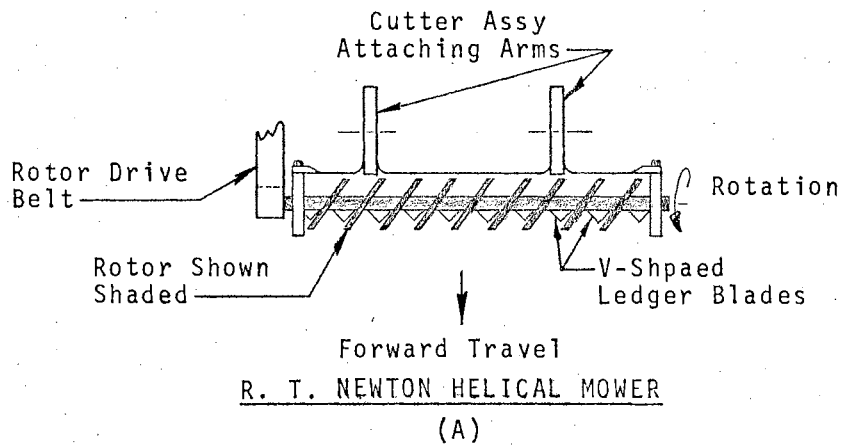


Figure 8. Previous Rotary Cutters Approximately Helical in Configuration

cutting stroke to separate the grass, grain, or other material into bunches and cut them by a shearing action between the fixed ledger blades and the rotating disk edges. Because of its inclined position on the shaft, each disk deflected the material to be cut first to one side then to the other in one complete revolution.

Another design, patented by Brauer (29) in 1946, incorporates a rotor with fixed ledger blades beneath it very similar to the Newton design. The principal difference is that half the disks are inclined on the rotor shaft in one direction and half in the opposite direction as illustrated by Figure 8 (B). Direction of rotation is downward during the cutting cycle.

Chambliss (30) proposed a mower design that eliminated the stationary ledger bar beneath the rotor. Cutting was to be accomplished by the scything action of the flat inclined disks of the rotor assembly alone. In his design, granted a United States patent in 1958, he proposed square or rectangular shaped disks with serrated edges. The dimensions of the disks and the spacing of them along the rotor axis was such that the cutting swath of each disk overlapped that of the adjacent one. Figure 8 (C) illustrates the arrangement. Direction of rotation of the disk edges was specified to be upward on the cutting stroke rather than downward like that of previous designs. By specifying that cutting was to be effected by the rotor disk edges alone, it was implied that the effective diameter of the disks and the

rotational speed would be great enough to give peripheral velocities in the range of 150 feet per second, that required for single element impact cutting with square knife edges.

Apparently without prior knowledge of the patented mower designs using horizontal rotors with cutting edges approximately helical in configuration, Miller (31) conceived and built a stalk cutter based on these same principles in 1965. The rotor assembly of his design consists of elliptical shaped disks arranged at an angle to the rotor shaft like that of the Newton design. A key difference exists in the configuration of the fixed ledger blades in Miller's design, however. He used curved ledger blades to be concentric with the peripheral surface of the rotor disks for an arc of approximately 90 degrees.

In evaluation tests of the stalk cutter, Miller found that the cutting action was effective. A moderate stand of alfalfa stems and weeds with stems up to 3/8 inch in diameter were cut easily and without winding of stems about the rotor or clogging of the feed openings. Upward rotation of the rotor disks during the cutting cycle produced better results than downward rotation. With upward rotation, the severed stems fell to the rear of the cutter assembly. Rotor speeds of 3380, 3600, 5650, and 6750 revolutions per minute were tried with no excessive vibration noted. Feeding the plant stalks into the cutter at a rapid rate proved to be a problem. And small stems had a tendency to bend over and slip between the rotor and ledger blade edges

without being cut. Close clearance between the rotor cutter edges and the concentric ledger blades was required for a good shearing action.

A graphical analysis of one cutting cycle of the cutter designed by Miller should give some insight to the cutting action of the helical cutters described thus far, since the rotors of the Newton, Brauer, and Chambliss machines are very similar to Miller's design. Figure 9 presents the analysis. Part (A) of the illustration shows a rotor disk just after it has completed deflecting plants to the ledger blade on the right side and is about to begin sweeping the next group of plants fed into the feed opening to the left-side ledger blade. Note that the knife angle at point 1 on the disk is 16 degrees. Also note that the upper portion of the disk virtually closes off the V-shaped feed opening between the ledger blades to the right and left of the disk. Section E - E through point 1 on the disk and in the plane of rotation of the disk shows the effective bevel angle of the disk cutting edge at point 1 to be 145 degrees.

Portion (B) of the illustration shows the rotor disk after it has rotated to the position where point 2 is at bottom dead center. The V-shaped feed opening still is largely blocked by the upper portion of the disk. The knife angle has changed to 25 degrees, and the effective bevel angle at point 2 is 119 degrees.

Portion (C) of the illustration depicts the disk after it has further rotated until point 3 is at bottom dead

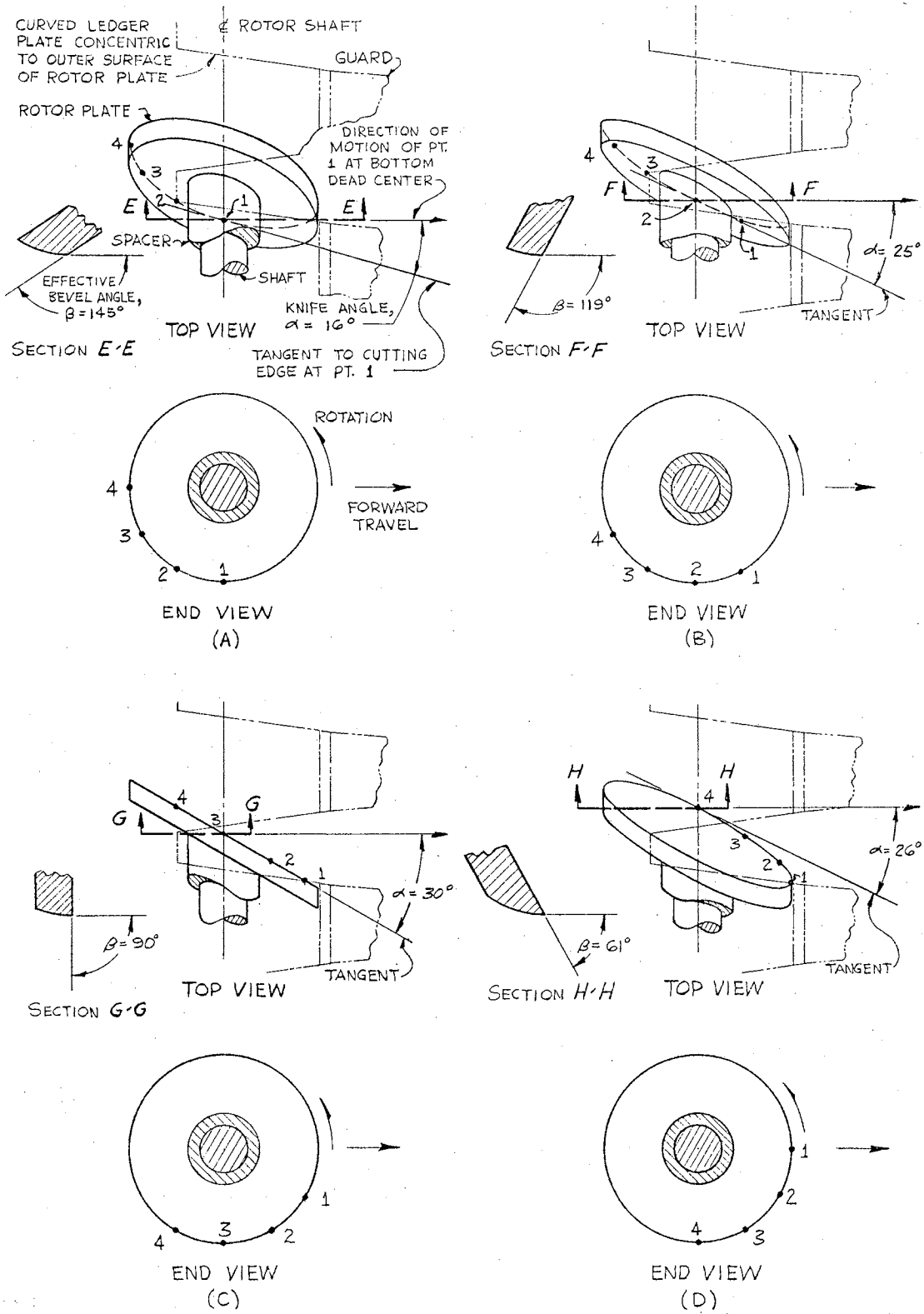


Figure 9. Graphical Analysis of the Cutting Action of the Elliptical Disk Rotor Designed by Miller

center. Here its position is such that its face plane is viewed as a line and the knife angle is 30 degrees, the nominal or design knife angle of the cutter. The effective bevel angle at point 3 is 90 degrees.

Further rotation of the disk brings point 4 to bottom dead center, the situation shown by portion (D) of the illustration. Here the knife angle has decreased to 26 degrees, and the effective bevel angle at point 4 is 61 degrees.

It is seen that points 1 and 4 are shrouded by the ledger blades. Therefore all contact of the disk edge with plant stalks in moving them to the left ledger blade occurs between points 1 and 4. Assuming two element shearing of the stalks between the disk edge and the concentric ledger edge, the shearing occurs along that portion of the disk edge between points 3 and 4. The effective bevel angle of the disk edge where actual cutting takes place is then greater than 61 degrees but less than 90 degrees. In effect it is a dull cutting edge. Since the curved ledger blades were made by forming standard mower ledger blades, the angle between the ledger edge and the direction of motion of points on the rotor is approximately 8 degrees. The knife angle for two element shearing thus varies from about 36 to 38 degrees.

The peripheral speeds of points along the disk edge during the tests conducted by Miller were: at 3380 rpm, 29.5 ft. per sec.; at 3600 rpm, 31.4 ft. per sec.; at 5650 rpm, 49.3 ft. per sec.; and at 6750 rpm, 58.9 ft. per sec. The maximum peripheral velocity tested was only about one

third the recommended 150 ft. per sec. velocity for single element impact cutting with a dull edge. As a result, it is correct to assume that cutting took place by two element shearing between the effectively "dull" rotor edge and the ledger blade edge. The dull rotor edge explains the close clearance between the rotor and ledger blades found necessary for cutting small stems. It is a requirement predicted by the work of other researchers on the effects of knife design parameters on cutting. See Table II.

Another characteristic of helical cutters employing the elliptical disk type rotor can be understood by referring to Figure 10. End and top views of the rotor designed by Miller are shown with the disk in a position such that its face plane is normal to the plane of the paper. Consider two equal and diametrically opposite particles of mass making up the rotor disk, particles P and P' in the illustration. When the rotor is stationary (part (A) of Figure 10), the moment about the rotor center, O, due to the weight of particle P is equal and opposite to that due to the weight of particle P'. The same is true for every two diametrically opposite mass particles, and the rotor is thus statically balanced.

When the rotor assembly rotates about its axis, however, a different situation arises, as is shown by part (B) of Figure 10. Since the particles P and P' have equal mass and have equal angular velocity due to rotation of the disk, the centrifugal force produced by each is equal. But since the

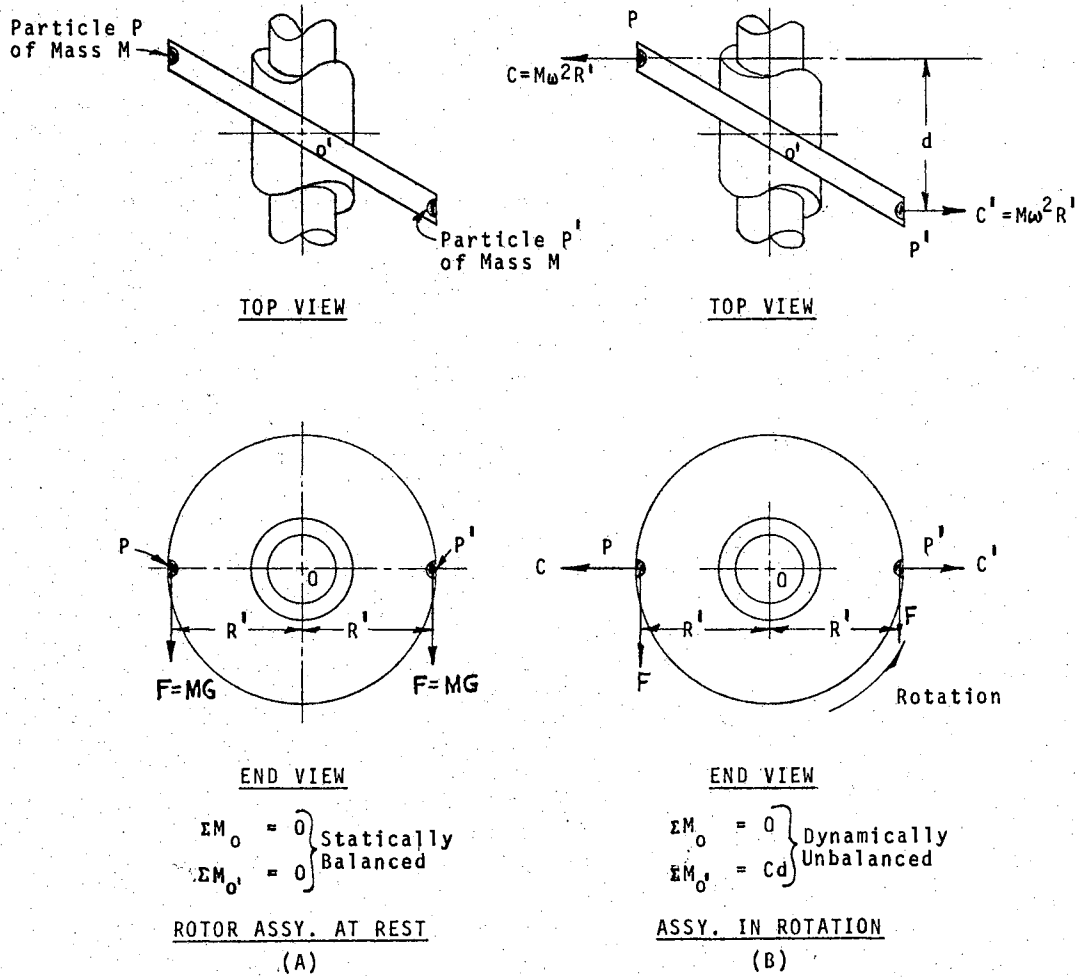


Figure 10. Inherent Dynamic Unbalance of Elliptical Disk Rotor

forces C and C' are not collinear, a couple, $T=Cd$, is produced. The total effect produced by the mass of the entire disk being non-symmetrically disposed along the shaft axis is a larger couple which produces unequal bearing forces and induces vibration of the assembly.

From the preceding discussion, the characteristics of helical cutters utilizing the elliptical disk type of rotor construction can be summarized as:

1. The knife angle varies from point to point along the cutting edge, since the disk edge only approximates a true cylindrical helical line. The nominal or "design" knife angle can be defined as the angle between the plane of the rotor disk when it is viewed as a line and the plane of rotation of the disk. Then the knife angle at points along the edge of the disk to either side of the point where the disk plane appears as a line will be progressively less than the nominal knife angle. The knife angle at any point remains unchanged as the point rotates about the shaft axis, however.

2. The effective bevel angle of the disk edge varies from an obtuse to an acute angle when sections are taken in the plane of rotation but at different points along the shaft axis. In general, the bevel angle is well above the 30 degree maximum angle recommended for sharp edge cutting and thus presents an effectively "square" or dull cutting edge to the plant stems.

3. An inherent dynamic unbalance exists in the rotor design.

4. Plant stalks are partially blocked from entering the cutting zone of the disk edge during the early part of each cutting cycle. The upper part of the disk occupies the available space and prevents the plants from entering the zone.

A mower based on the Chambliss (30) patent was introduced to the agricultural equipment market during the year 1968 by the Spinslicer Company (32). The rotor of this machine is constructed with a ten inch diameter base cylinder to which are welded protrusions for attaching four longitudinal rows of inclined and curved edge cutter blades. The four rows of blades are equally spaced about the periphery of the base cylinder, and adjacent rows of blades are inclined in opposite directions. Each blade is attached to its supporting base protrusion by three bolts. The blades and mounting protrusions are positioned obliquely to the base cylinder axis. In other words, there is no point about the periphery of the base cylinder when viewed in the plane of rotation, perpendicular to the cylinder axis, at which a blade surface appears as a line. This construction reduces the effective bevel angle of the blades. This feature, along with a chamfer on the trailing edge of each blade, provides for a "sharp edge" type of cutting action. The radial distance from a point on the cutter edge to the rotor center line is approximately seven inches. Rotor speed is

approximately 2000 rpm. Thus the peripheral velocity of points along the cutting edges is about 122 ft. per sec., almost high enough for single element impact cutting even with a square edge or dull type of blade. Figure 11 illustrates the general construction features of the Spinslicer machine rotor.

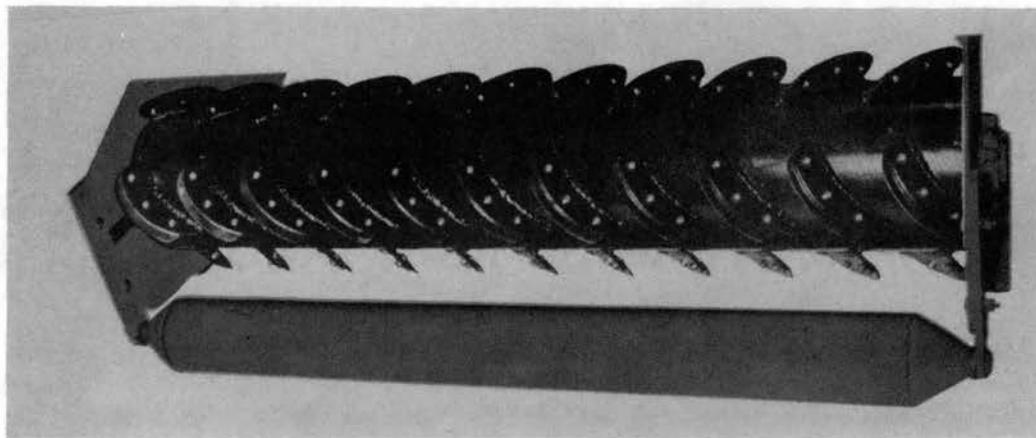


Figure 11. Rotor of Spinslicer Mowing Machine

CHAPTER III

DESIGN OF THE CUTTING DEVICE

When the cutting device for this study was designed, during the months of May through July, 1966, the previous work on cylindrical helical cutters was unknown to the author. As a consequence, the expedient design guides that might have been drawn from the information presented in the last section of Chapter II were not available.

Approach

The general cutting principles developed by other researchers as recorded in Tables I through IV of Chapter II were utilized in deciding overall design specifications. For example, from the tables the optimum knife angle for two element shearing is within the range of 15 to 25 degrees. The optimum knife angle for single element impact cutting is within the range of 45 to 90 degrees, depending on whether the blade is sharp or dull. Feller (12) reported an optimum angle of 60 degrees for a sharp blade. Since the mechanism of cutting with a cylindrical helical blade was not known, it was desired to span the range of 15 to 60 degree knife angles in the device to be designed and tested. Another example pertains to the bevel angle of a

sharp blade. From the tables, it should be less than 30 degrees, preferably around 25 degrees.

Being concerned with both effective cutting and the trajectory of the severed stems made design requirements more strict than would be the case if cutting effectiveness alone comprised the objective. The twofold purpose required that compromises be made in desired specifications. Rotational speed and the size of the cutter diameter is a case in point. A large cutting edge diameter allows high peripheral velocities at lower rotational speed than a small diameter cutter. But a large diameter cutter makes necessary a larger energy transfer to the severed stem in order to trajectory the cut end high enough to clear the cutter. High peripheral velocity to insure impact cutting is desired, but rotational speed should not be so high as to require unrealistic feed rates (forward travel per cutter revolution) of a harvesting machine that might utilize a helical cutter. Thus a sacrifice in peripheral velocity to keep a reasonable size cutter diameter and feed rates was thought necessary.

Model Study

To gain a better understanding of design alternatives available and thus to keep a rational footing in deciding on the cutter specifications, a model cylindrical helical cutter was built, Figure 12. A portion of a three inch diameter conveyor auger formed the rotors. Conventional square edge flighting comprised one rotor; a modified

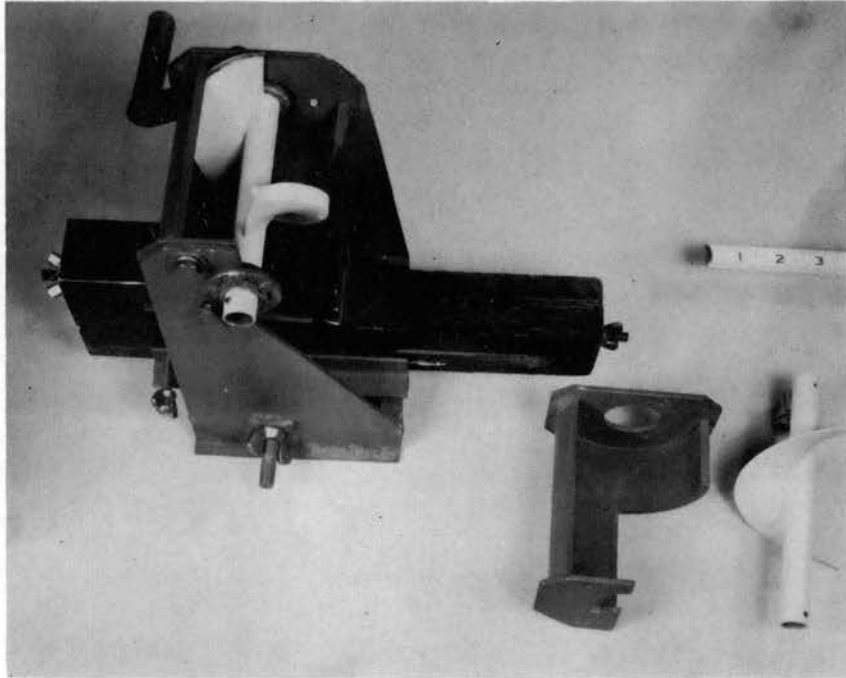


Figure 12. Model Cylindrical Helical Cutter
Used to Study General Design
Requirements

flighting, the conventional square edge type with a ledge welded to the outer periphery to provide a sharper edge, comprised another. Square edge and beveled edge ledger tubes were made. A plant holding block was designed and located beneath the rotor-ledger tube assembly of the model. The plant holding block had guide rails for lateral and transverse positioning relative to the rotor axis.

Qualitative cutting tests using the model provided valuable insights into desirable cutter specifications. It was clear that the rotor having a sharp edge provided by the ledge on its outer periphery cut more effectively than the square edge rotor. Also tests emphasized the fact that all

points along the rotor edge have radial motion only; lateral motion of plant stems derives from sliding of the stems along the edge. To prevent stems from being expelled forward out of the cutting zone in two element shearing between the rotor and ledger tube edges, it appeared a reverse slope ledger blade angle (opposite to the slope of the rotor blade angle) would be desirable. Further, it appeared that a cutting zone large enough to accept and allow severing plant stems at least 1/2 inch in diameter should have a minimum width of 1 1/2 inches. The importance of not blocking the cutting zone with the inactive blades if multiple blades were used about the rotor periphery was demonstrated.

General Specifications and Design

Details of the Cutter

Following the model study, extensive graphic analyses of possible geometric configurations for a cylindrical helical cutter were made. A cutter diameter of 3 1/2 inches was chosen as a workable compromise to fulfill the objectives of a desirable peripheral speed and minimum space requirements. At 3600 rpm the peripheral velocity is 55 feet per second, which is about 1/3 the velocity required for single element impact cutting with a dull blade but almost double the 32 feet per second velocity at which Feller observed impact cutting with a sharp blade. An attempt to approximate a 20 degree double helix for a suitable cutter configuration failed to meet space

requirements. A 26 degree nominal blade or knife angle turned out to be the minimum obtainable within the space requirements set.

The geometric configuration selected as best for fabrication and test is one that might be classified as a modified elliptical disk design, since only portions of complete elliptical disks are used. Figure 13 illustrates the design. Two identical sectors, which appear v-shaped in the top view of Figure 13, are positioned diametrically opposite on the rotor shaft to provide a structure with inherent static and dynamic balance. The two diametrically opposed v-shaped sectors comprise one rotor knife section. Each "leg" of the v-shaped sectors consists of a portion of a flat elliptical disk set at an angle to the rotor shaft such that its periphery lies in the surface of a right circular cylinder with an axis identical to that of the rotor shaft. The disk edges, which lie in the cylindrical surface, then approximate cylindrical helices with a helix angle equal to the angle between the plane of the disk and the plane of rotation. At the periphery of each disk, on its "outside" face, a ledge is extended transverse to the disk face. The outer edge of the ledge, which lies in the cylindrical surface and is approximately parallel to the disk edge, also forms an approximation to a cylindrical helix. The ledge has a bevel angle of 30 degrees, measured parallel to the rotor axis, at every point along its edge. This edge forms one of the two cutting edges of each v-shaped sector.

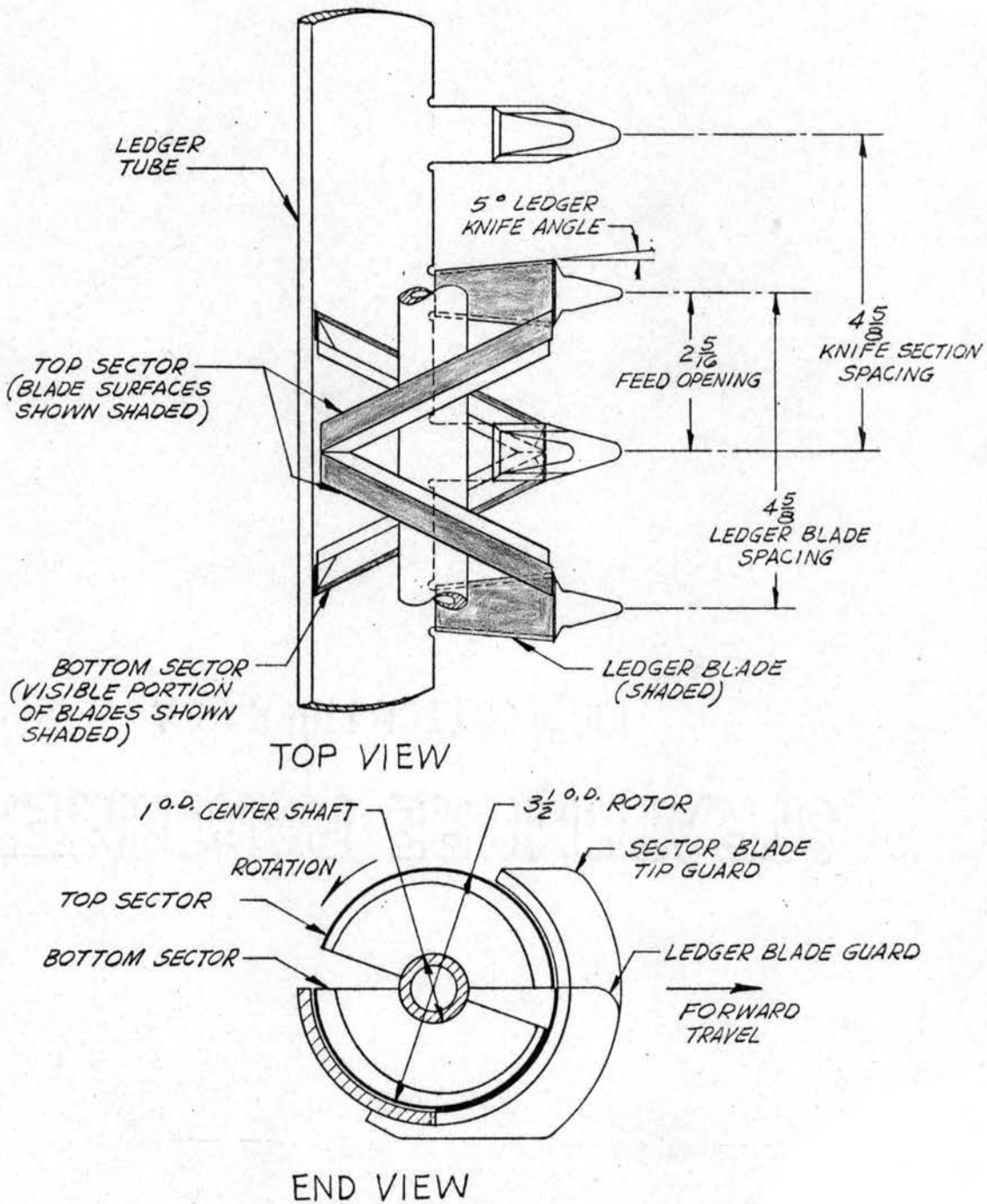


Figure 13. General Design Features Specified for Rotor and Ledger Tube of Cylindrical Helical Cutter

assembly. Thus the effective bevel angle of the cutting edge, measured in the plane of rotation, will be less than 30 degrees at every point. The periphery of the ledge extends the periphery of the disk sector to form a wide surface for attaching blades. This feature fulfills the design objective of detachable blades to allow trial of both square edge and sharp edge blades - and to allow blade replacement instead of sharpening on production rotor assemblies of this type.

Each v-shaped sector assembly is symmetric about the plane of rotation through the center of the "vee." Thus the left side of the sector approximates a right hand cylindrical helix and will deflect plant stems to the left while the right side of the sector approximates a left hand cylindrical helix and will deflect plant stems to the right. Each of the two identical sector assemblies diametrically opposed on the rotor shaft will deflect plant stems in the same manner. The alternate direction deflecting action characteristic of the complete elliptical disk or wobble plate design is not present. However, since plant stems are deflected toward a ledger blade along a lateral distance that is at most only 1 1/2 inches, and since there is no lateral motion of the rotor blade relative to the fixed ledger blade to cause jamming of plant fibers in the clearance space between them in the first place (this is true of the complete elliptical disk or

wobble plate design also), there appears to be little advantage in the two-way deflection action.

Since each sector assembly is symmetric about the plane of rotation through its center, and the cutting edge action of the sector on either side of the plane of symmetry is judged to be identical except for lateral deflection of the plant stems in opposite directions, just the left half of the rotor sector geometry was fabricated for test. A cylindrical plate was included at the plane of symmetry to improve the rigidity of the structure and to provide for drilled holes to correct the unbalance due to constructional inaccuracies. To adequately span the desired range of knife angles, rotors with 26, 36, 46, and 56 degree knife angles were constructed. To provide for quick interchange of the four rotor assemblies, a mounting shaft with snug fitting contacting surfaces at each end of the rotor mounting section and with one attaching bolt at the outer end was designed. Figure 14 shows these features.

The ledger tube configuration was arbitrarily determined. The ledger blade angle is five degrees, with a slope opposite to that of the rotor blade angle. It was intended that the replaceable ledger blade be concentric with the rotor peripheral surface. However constructional inaccuracies made the surfaces eccentric. When the ledger blade touched the rotor periphery in line-to-line contact

at either end of its 90 degree arc of extent, the center of the blade cleared the rotor surface by approximately 0.010 inch. The ledger tube was designed such that it could be rotated about the rotor axis and be clamped at different positions to change the location of the start of the cutting zone. Start of the cutting zone is defined to be where the ledger tube shielding of the rotor blade ends. The ledger tube-rotor assembly arrangement, shown by a line drawing in Figure 14, is further illustrated by Figures 15, 16, and 17. Figure 15 is a photograph of the rotor mounting shaft and ledger tube without a rotor assembly in place. Figure 16 presents the same view but with the 36 degree rotor assembly mounted on the shaft. Figure 17 depicts the 36 degree rotor and the ledger assembly as viewed from the rear. The two capscrews clamping the ledger assembly to the main frame - through slotted holes to allow changing the angular orientation of the ledger tube - are seen in this view. The black tape covering parts of the ledger assembly was used to reduce the fluorescent light emitted by these surfaces during ultraviolet light photographic studies of severed plant stem motion. In these illustrations, the 36 degree rotor is fitted with square edge (dull) blades.

A detailed description of the test rotor assembly construction will be given with reference to the 36 degree rotor. The photograph comprising Figure 18 gives a perspective view of this rotor assembly. Figure 19 is a

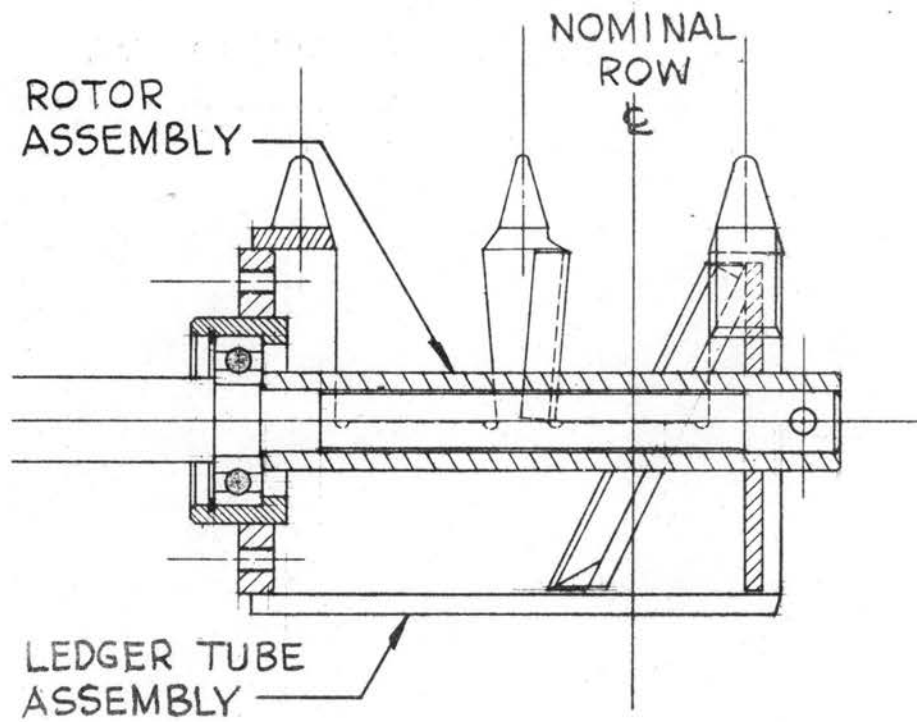


Figure 14. Test Rotor Assembly and Ledger Tube Features (26 Degree Rotor Assembly Shown)

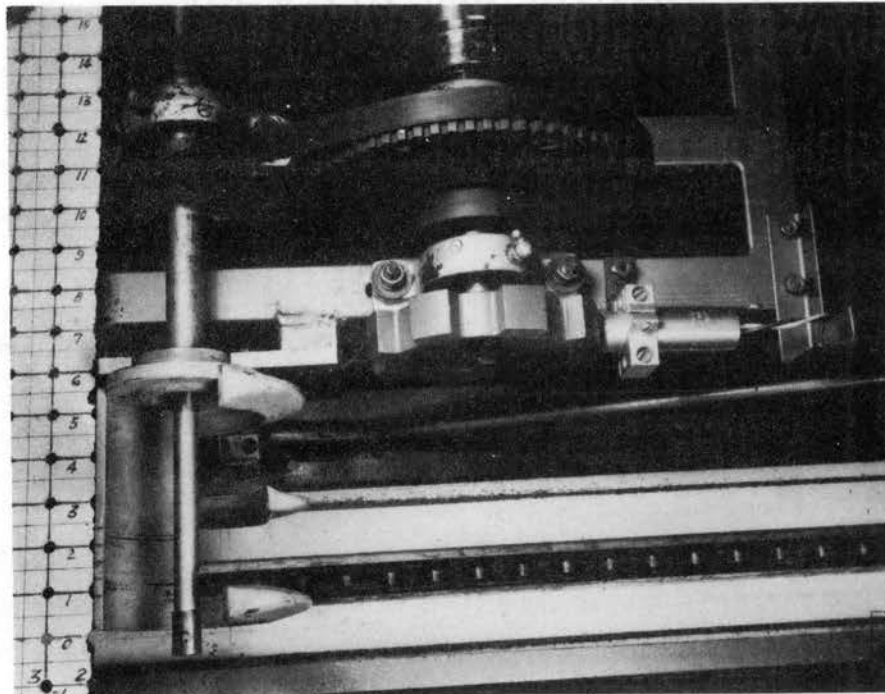


Figure 15. Top View of Rotor Drive Shaft and Ledger Tube Without Rotor Assembly in Place

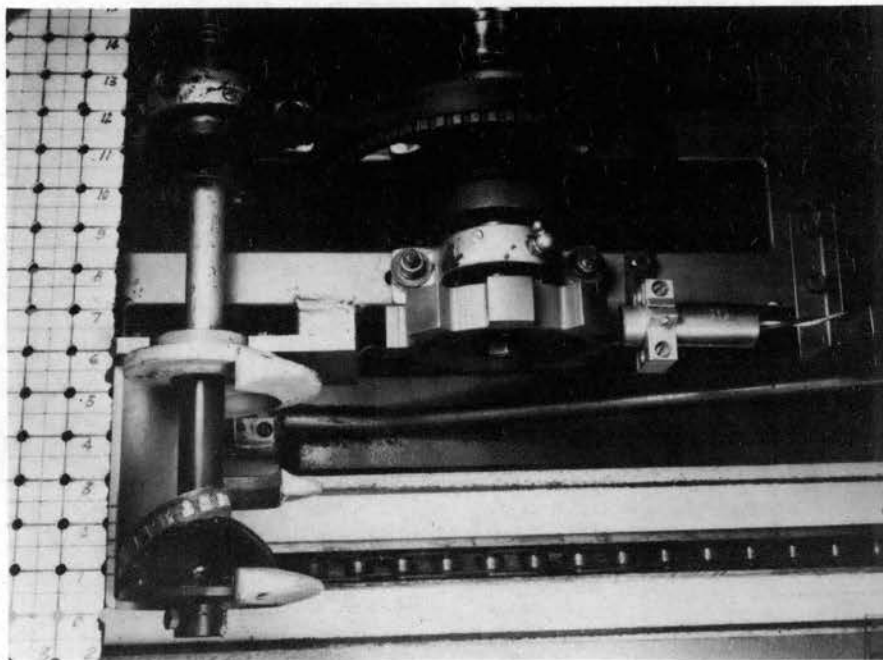


Figure 16. Top View of 36 Degree Rotor
Assembly Mounted in Ledger
Tube

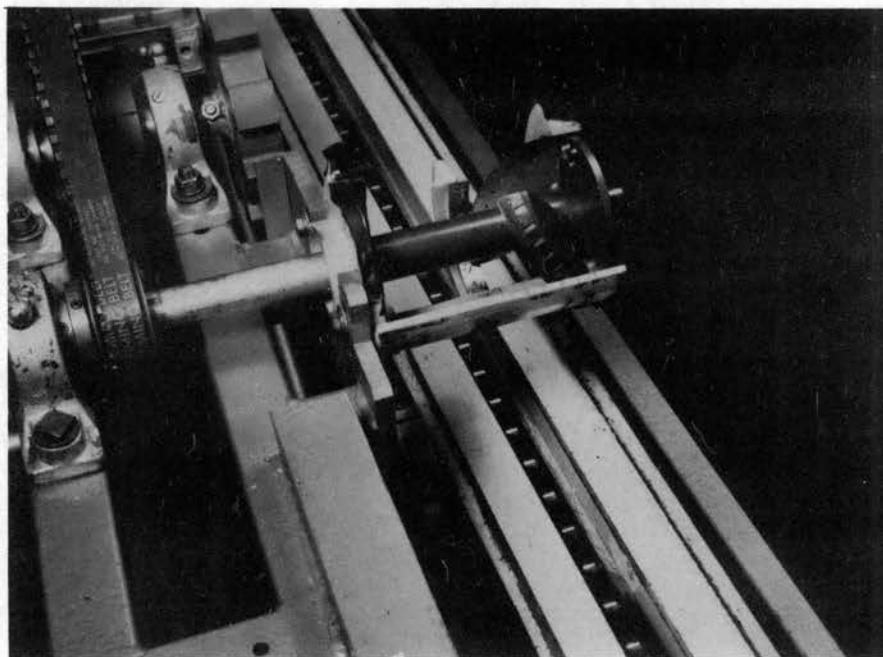


Figure 17. Rear View of 36 Degree Rotor
Assembly Mounted in Ledger
Tube

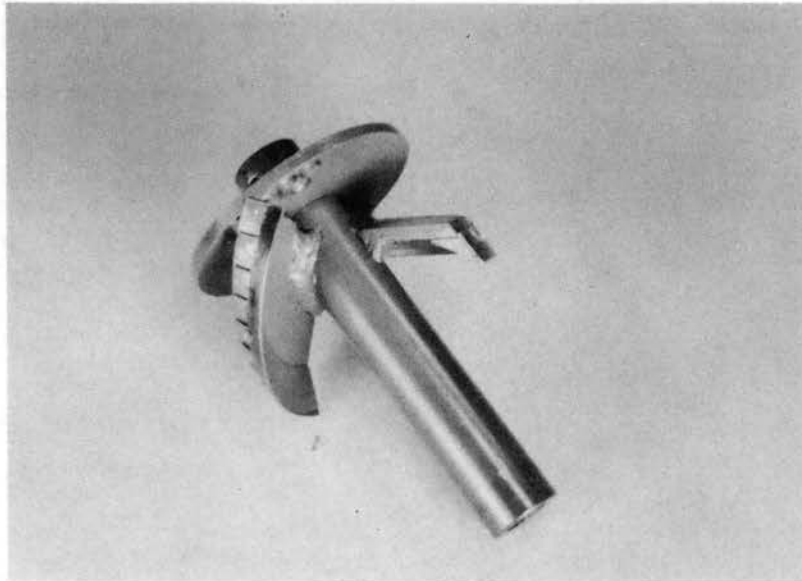


Figure 18. Perspective View of 36 Degree Rotor Assembly

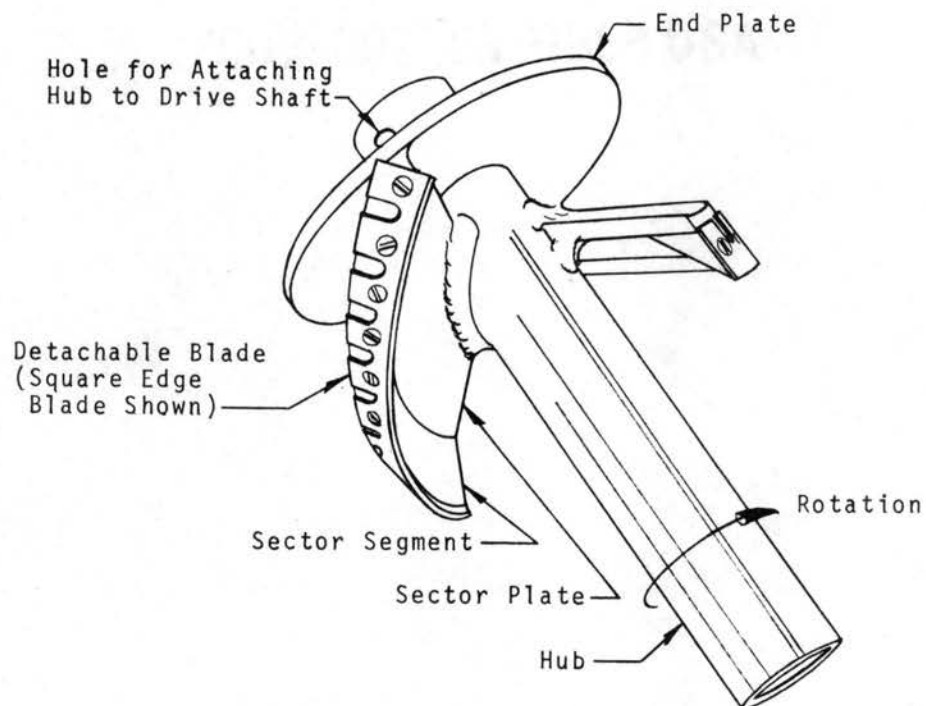


Figure 19. Identification of Component Parts of 36 Degree Rotor Assembly

line drawing of the perspective view with the component parts of the assembly labeled.

The hub is machined from 1" O.D. x 7/32 wall cold drawn seamless steel tubing (AISI C1015). Slots for accurately positioning the sector plates at the correct knife angle orientation were machined in the hub. The sector plates, geometrically portions of an elliptical disk, were machined from #7 Ga. (.1793" thick) cold rolled sheet steel. The sector segments are attached to the plates by #3-56UNF stainless steel flat head machine screws. After being tightened in place the heads and ends of the machine screws were tack welded to prevent loosening. The sector segments, which provide the bevel angle required for sharp edge blade cutting, are fairly complex parts. The segments were machined from 3 1/2" O.D. x 5/16 wall cold drawn seamless steel tubing (AISI C1015). Figure 20 shows the fabrication procedure and gives a clear picture of the configuration of the segments. As noted in the illustration, the plane surface of the segment that abuts against the elliptical shaped sector plate in assembly is bounded by two elliptical curves and approximates a right helicoid. The outer elliptical curve matches that of the sector plate. The periphery of the segment is a portion of the 3 1/2 inch diameter cylindrical surface of the tube from which it is machined. The surface which provides the bevel angle for the cutter structure is seen to be a portion of the surface of a truncated right circular cone with a 30

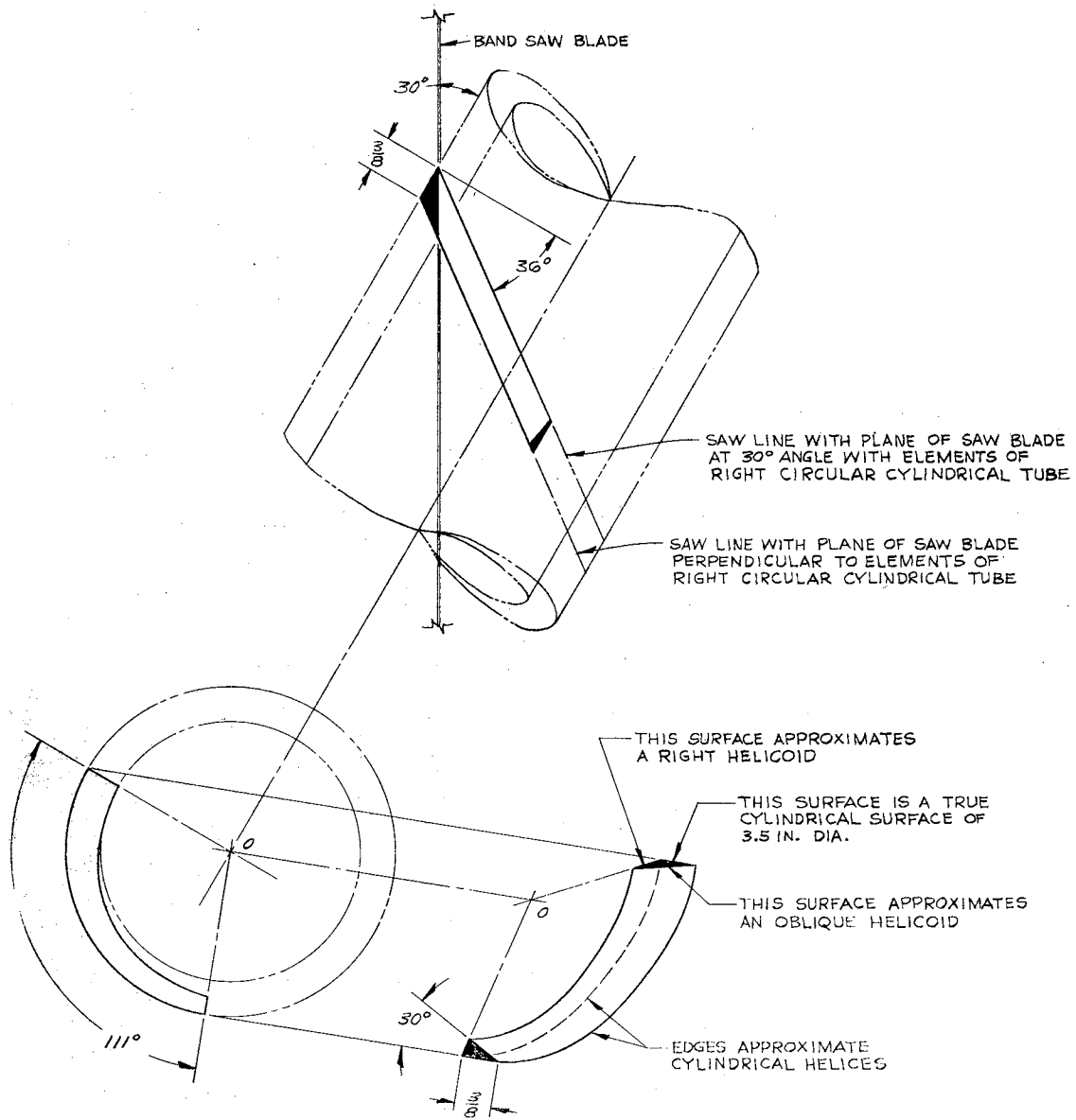


Figure 20. Rotor Segment Fabrication Procedure and Description of Resulting Part.

degree angle between its axis and elements. The base and truncating plane of the cone are oblique to the cone axis such that the conical surface of the segment approximates an oblique helicoid. After the segment was attached to the plate for each sector, the sector assemblies were welded to the rotor hub and end plate. The cylindrical peripheral surfaces were then turned and ground in a lathe to a diameter of 3.440/3.436 inch. Holes for attaching the blades were located, drilled and tapped, and the blades were attached to complete the rotor assemblies. The assembly then was balanced at 3600 rpm on a dynamic balancing machine.

Cross sections of the two types of blades tested on the rotors are shown by Figure 21.

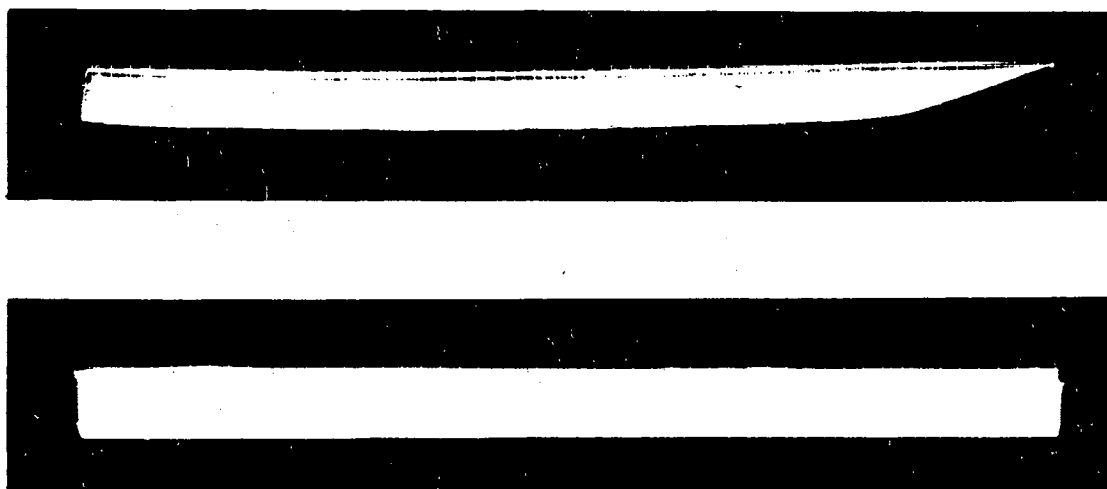


Figure 21. Cross Sections of Square and Sharp Edge Blades Tested (Section Magnified 10X; 20 Degree Bevel Angle on Sharp Blade)

In the photograph, the blade cross section are magnified ten times by an optical comparator. The square edge blade does indeed present a square edge, 90 degree angle, to the plant stems to be cut. It was fabricated from 1/32 inch thick steel Milford precision flat stock which was in an annealed state. The sharp edge blade has a 20 degree bevel angle and was fabricated from 0.028 inch thick Milford 3808K1 band knife stock (used on band saws). The blade material had to be stretched to seat properly on the rotor sector surfaces, and this operation required heating the band knife stock. The temper of the metal in the cutting edge was not appreciably altered in the process, however, as it retained its shape and sharpness and was not damaged by subsequent cutting of plant stems. Had the blades been fabricated from a 3 1/2 inch tube of blade stock, the cylindrical surface required could have been obtained without stretching the material. The blades were attached to the rotor sectors with #3-56UNF flat head stainless steel machine screws. The heads were recessed in countersunk holes in the blade material. After attaching the blades, the rotor assembly was mounted in a lathe and the cylindrical outer surfaces of the blades subjected to a light grind operation to true them. With the sharp blades, the space above the attaching screw heads in the recessed blade holes was filled with solder before the final grind operation.

The effective bevel angle of the blade rotor sector assembly is illustrated by Figure 22 for the square edge

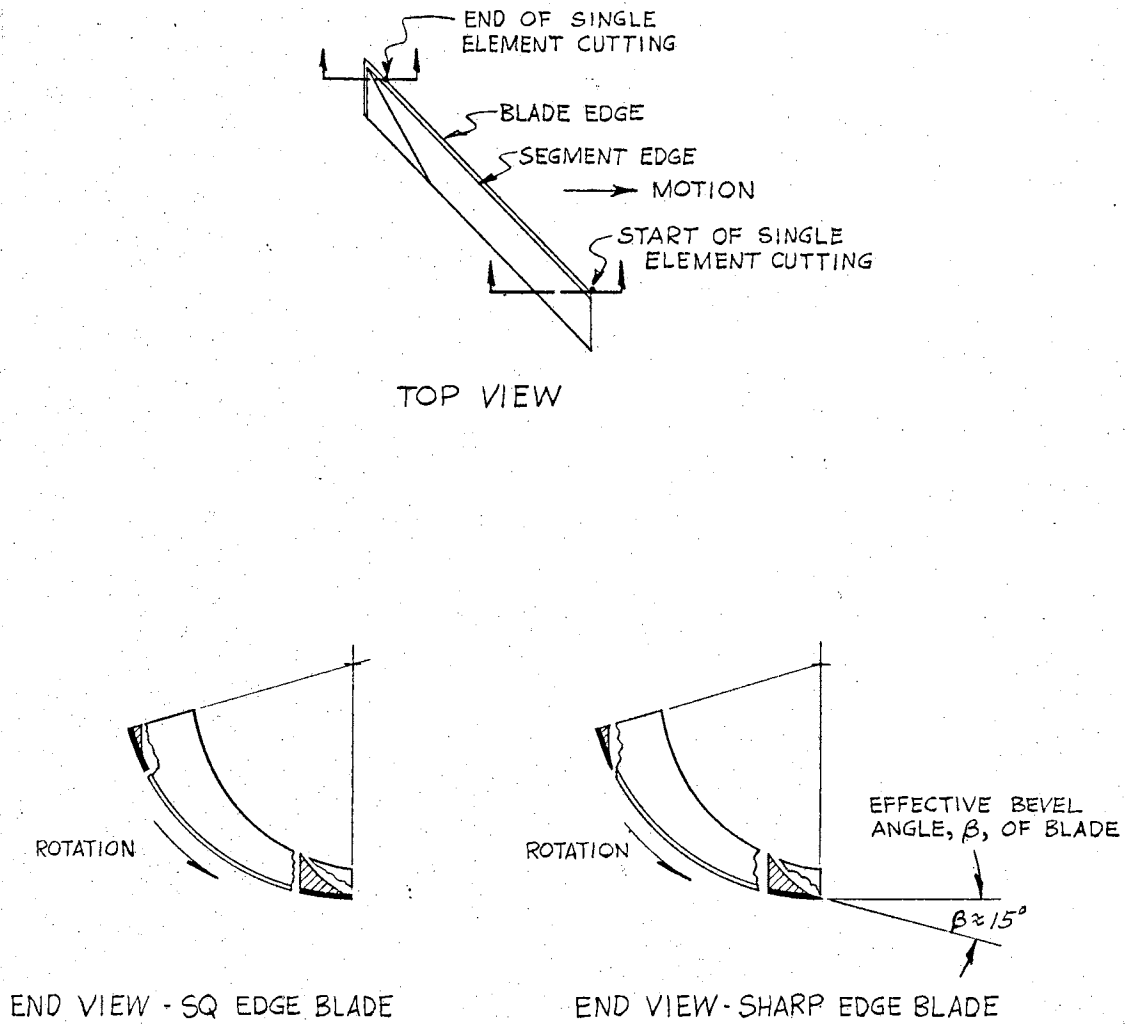


Figure 22. Effective Bevel Angles at Start and End of Single Element Cutting for 46 Degree Rotor

and sharp edge blades attached to the 46 degree rotor. For the sharp edge blade, the transition between the blade bevel angle and the sector segment bevel angle is seen to be a smooth one. The square edge blade presented a cutting edge similar to the elliptical disk rotors discussed in the last section of Chapter II. At the point along the blade edge where the knife angle is equal to the nominal knife angle of the rotor sector, the effective bevel angle of the blade can be calculated from the equation

$$\beta' = \arctan (\tan \beta \sin \alpha) \quad (3-1)$$

where

β' is the effective bevel angle (in the plane of rotation)

β is the blade bevel angle

α is the knife angle

Since the nominal knife angle is the maximum knife angle of a rotor assembly, the above relation gives the maximum effective bevel angle of the rotor assembly. Table V lists these maximum effective bevel angles for the rotor assemblies tested. The acute effective bevel angles give decisively sharp cutting edges for the rotor sectors.

A comparison of the four test rotor assemblies fitted with sharp blades is presented by Figure 23.

The variation in knife angle from the nominal value with lateral distance along the blade edge is charted for each rotor in Figure 24.

TABLE V
MAXIMUM EFFECTIVE BEVEL ANGLES OF BLADES
FOR ROTOR ASSEMBLIES TESTED

ROTOR ASSEMBLY	MAX EFFECTIVE BEVEL ANGLE OF BLADE
26 DEGREE	9° 4'
36 DEGREE	12° 5'
46 DEGREE	14° 40'
56 DEGREE	17° 15'

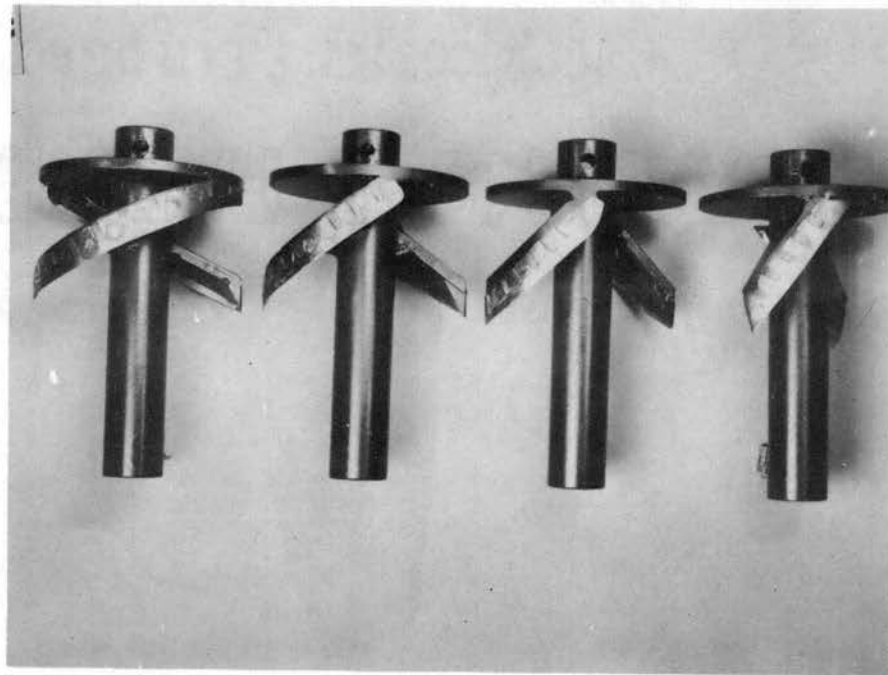


Figure 23. Test Rotor Assemblies Fitted with Sharp Blades (Left to Right Arrangement: 26, 36, 46, and 56 Degree Rotors)

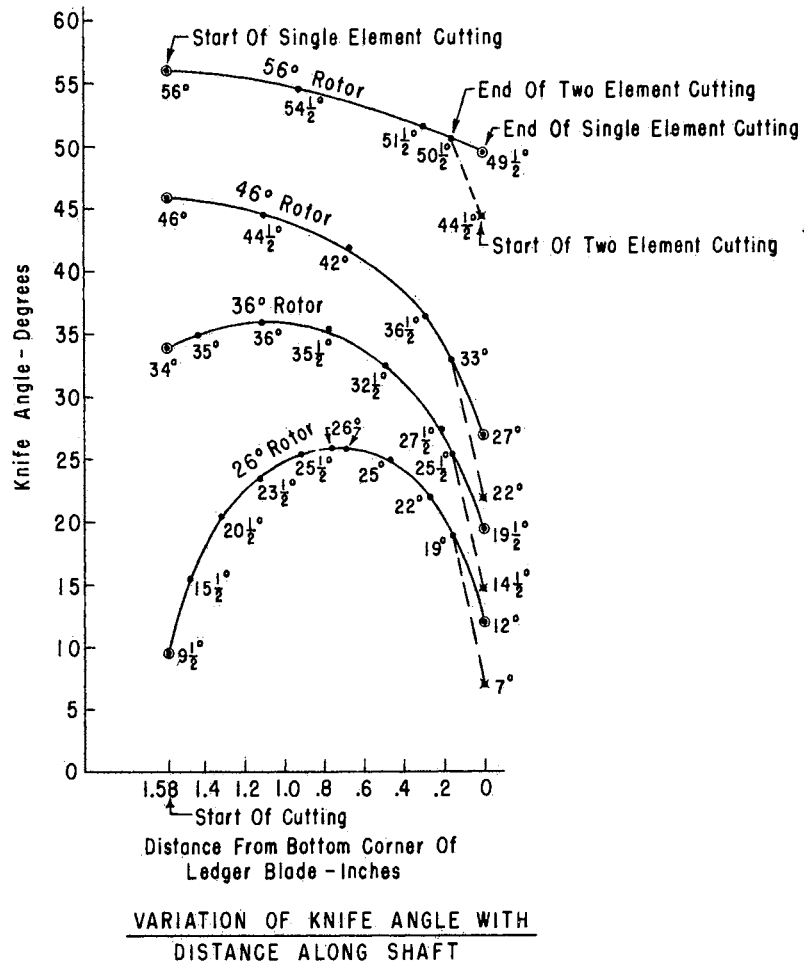
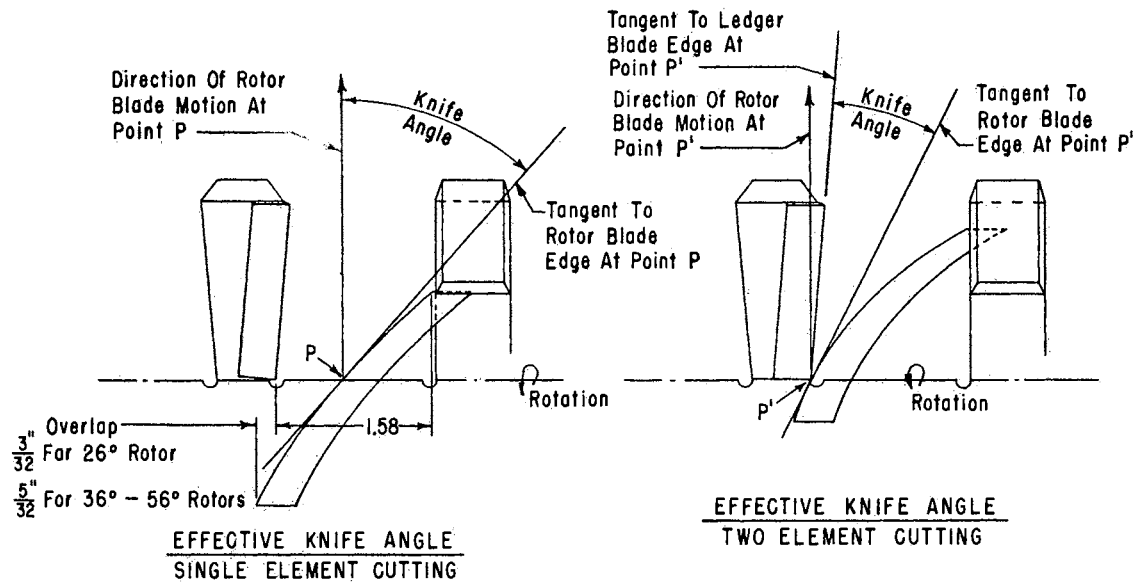


Figure 24. Variation in Knife Angle with Lateral Distance Along Blade Edge

CHAPTER IV

KINEMATIC AND CUTTING FORCE ANALYSIS

Kinematic Analysis

The trace on a vertical plane of a point on the cutting edge of the helical blade rotor is one of a family of curves that may be described as inverted looped trochoids. The particular curve traced will depend on the angular velocity of the rotor and the linear velocity of the center of the rotor relative to the plants to be cut - or ground. For a rotor of diameter D , if for example the linear velocity, V , of the rotor center, is such that the center moves forward (translates) a distance $3/2 D$ for each revolution of the rotor, a point on the rotor periphery will trace the curve shown in Figure 25. The solid line represents a point on the outer circumference of one of the two identical diametrically opposed sectors of the rotor. The phantom line (solid line interrupted periodically with two short dashes) represents a point on the other sector exactly opposite the first point.

Assume a point along the edge of the rotor sector blade will cut into a plant stem any time the point is moving forward (where forward is defined as the direction of the velocity, V , of the rotor center relative to the earth).

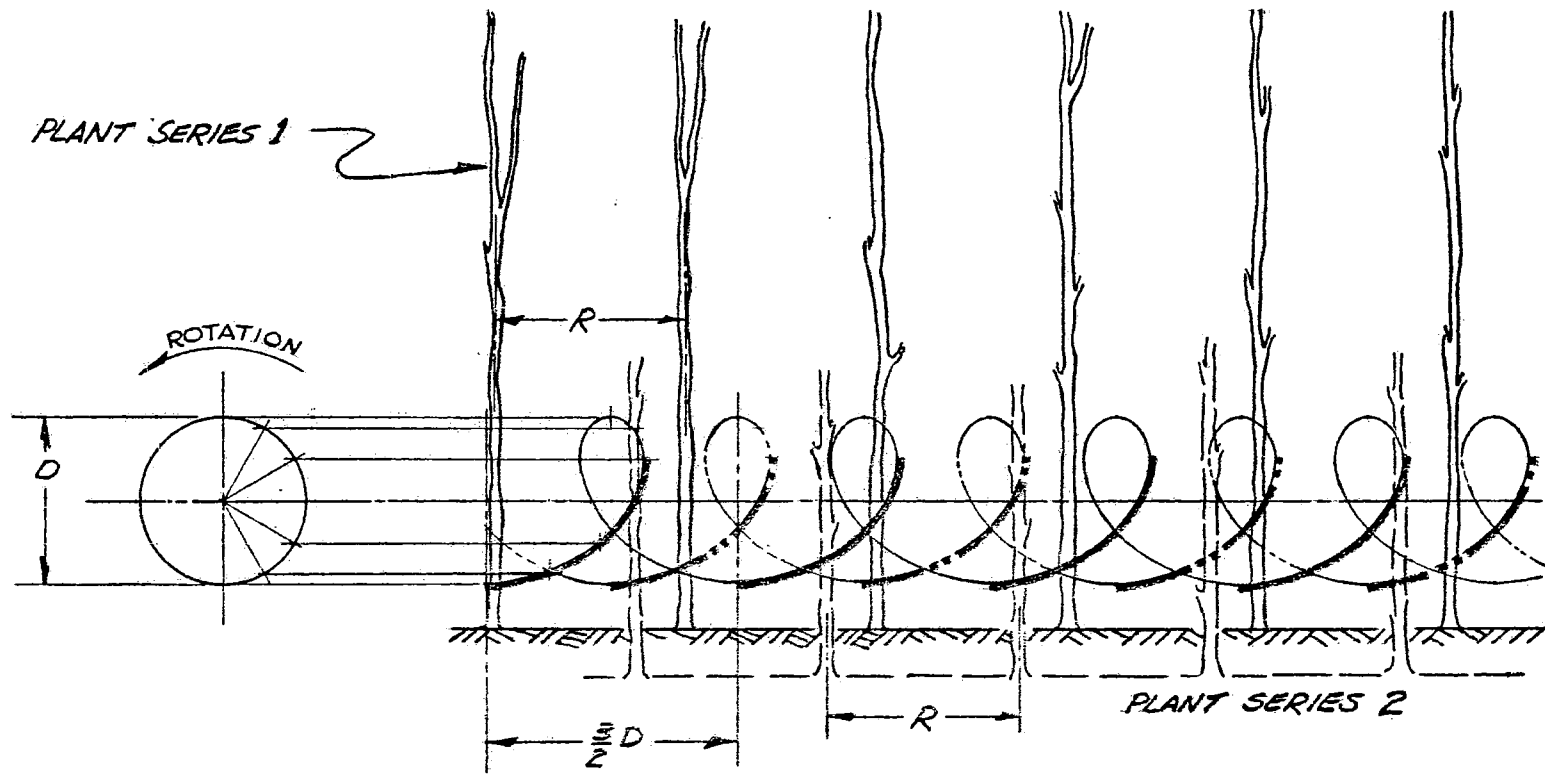


Figure 25. Geometry of Motion of Points on the Cutter Rotor Relative to Uniformly Spaced Plants Along the Row

With this assumption, the active cutting zones of two opposite points on the rotor periphery are as shown by the heavy shading along the curves in Figure 25. The cutting zone of any point on a sector blade edge begins at bottom dead center of the rotor since the shielding portion of the ledger tube ends there.

If the plants to be cut are uniformly spaced a distance R apart along the row, successive plants will engage a point on the sector blade at different positions along its zone of action as shown by Figure 25. For each plant to be engaged at an identical position in the zone, the plant spacing, R , would have to equal the rotor center advance per revolution, or some integral multiple thereof. The position in the cutting zone of the first plant in a series of equally spaced plants is entirely random. It might be engaged by a point on the sector just after bottom dead center or just before exit of the point from its active cutting zone. Compare plant series 1 and 2 on Figure 25. Hence the extent of rotation of a point on the blade past bottom dead center when it first engages the plant to be cut is a random value. Evaluated over a long enough period of cutting, this value should be a normally distributed function, of which the arithmetic mean could be considered the nominal value of the function.

Examination of the cutting zones of two opposite points on the rotor diagramed in Figure 25 reveals that if a plant should be cut in the upper end of the cutting zone of one

sector, the remaining stubble will be cut again by the opposite sector. This possibility of "double cutting" is illustrated in further detail by Figure 26. As shown by Figure 26, the zone of double cutting is greater in length for lower values of advance of the rotor center per revolution (feed rate). Thus the probability of double cutting for a feed rate of $L = D/2$ is about three times that for a feed rate of $L = 2D$.

However another parameter affects the extent of the zone of double cutting - as well as the extent of the cutting zone itself. This parameter is the angular position of the stationary ledger tube. The normal position of the tube may be considered that which exposes a point on the rotor blade for active cutting at bottom dead center of the rotor, Figure 27a. Rotation of the ledger tube in a clockwise direction from the normal position exposes the blade to the plant before bottom dead center is reached. This lengthens the cutting zone and increases the zone of double cutting, Figure 27b. Counterclockwise rotation of the ledger tube prevents exposure of the blade to the plant until after bottom dead center is passed, which shortens the cutting zone. The shorter cutting zone may completely eliminate the double cutting zone and introduce a zone of "drag cutting" in its place, Figure 27c. Plant stems in the drag cutting zone will be untouched by the first rotor sector, then contacted by the edge of the ledger tube and deflected or "dragged" forward slightly before the second

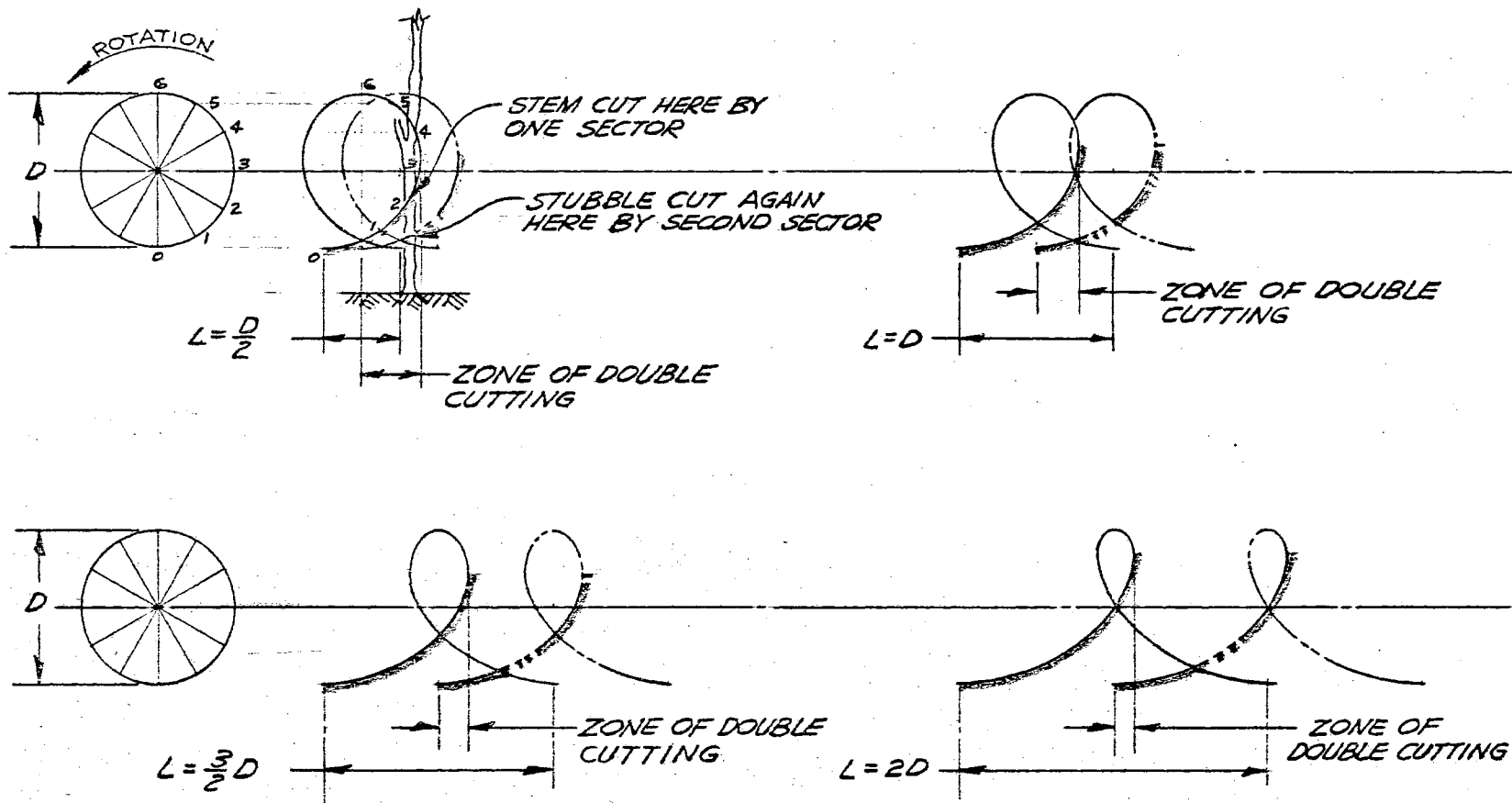
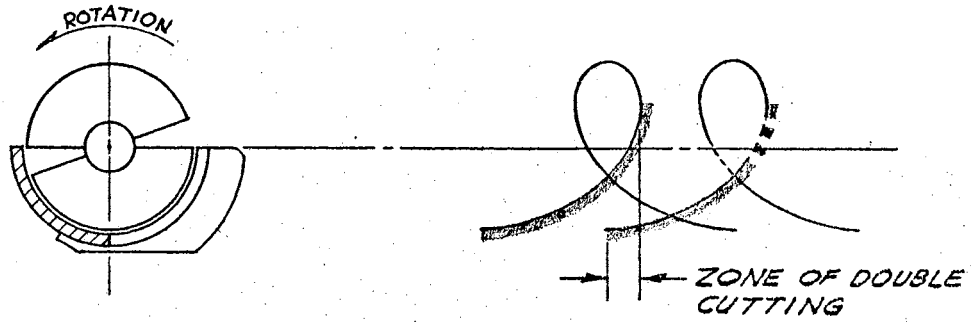
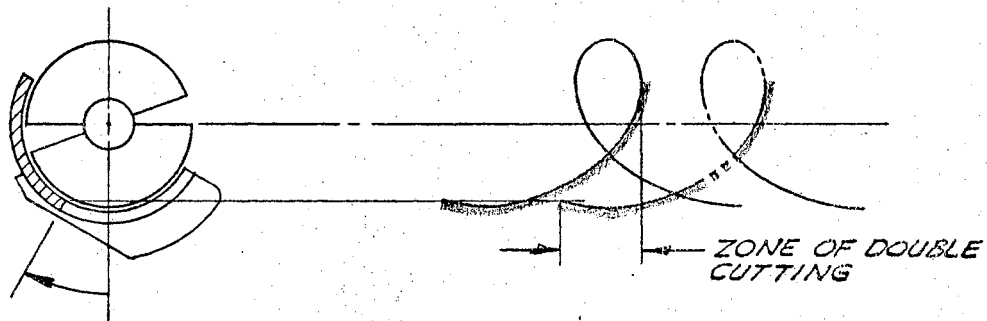


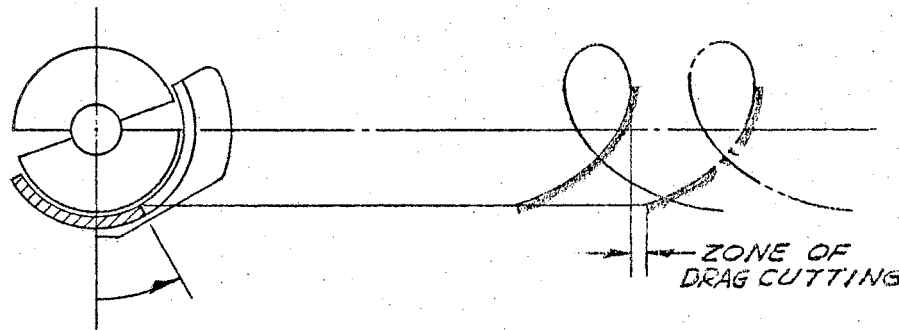
Figure 26. Double Cutting Effect and Comparison of Zones of Double Cutting for Different Feed Rates



a. Normal Position - Blade Exposed at Bottom Dead Center



b. Position for Lengthened Cutting Zone - Greater Double Cutting Zone



c. Position for Shorter Cutting Zone - Elimination of Double Cutting Zone

Figure 27. Effect of Ledger Tube Angular Position on Cutting Zone and Double Cutting

sector blade engages and cuts them. Thus the angular position of the rotor shield portion of the ledger tube relative to bottom dead center of the rotor is a parameter which must be considered in evaluating the cutting device - from either an energy input or plant motion standpoint.

Cutting Force Analysis

The resultant force of a rotor sector blade on a plant stem when motion of the stem along the blade edge is impending is diagrammed in Figure 28. The point of contact of the blade edge with the plant stem is point P. The angular position of this point from bottom dead center of the rotor is denoted angle ρ . This angle, the knife angle, α , and the friction angle between the plant and the blade, ψ , all affect the line of action of the resultant force F. Since the blade configuration is an approximation to a cylindrical helical edge, the knife angle, α , varies with change in axial location of the cutting point along the blade edge. (For a true cylindrical helical edge, the knife angle would be constant with respect to axial location of the cutting point.) However, for any point on the blade, the knife angle, α , is unchanged with rotation of the point about the rotor center. And for a given plant species and blade material, the friction angle, ψ , would be expected to remain constant. Thus change in angular position of the blade point about the rotor center, angle ρ , is the principal cause of a constantly changing line of

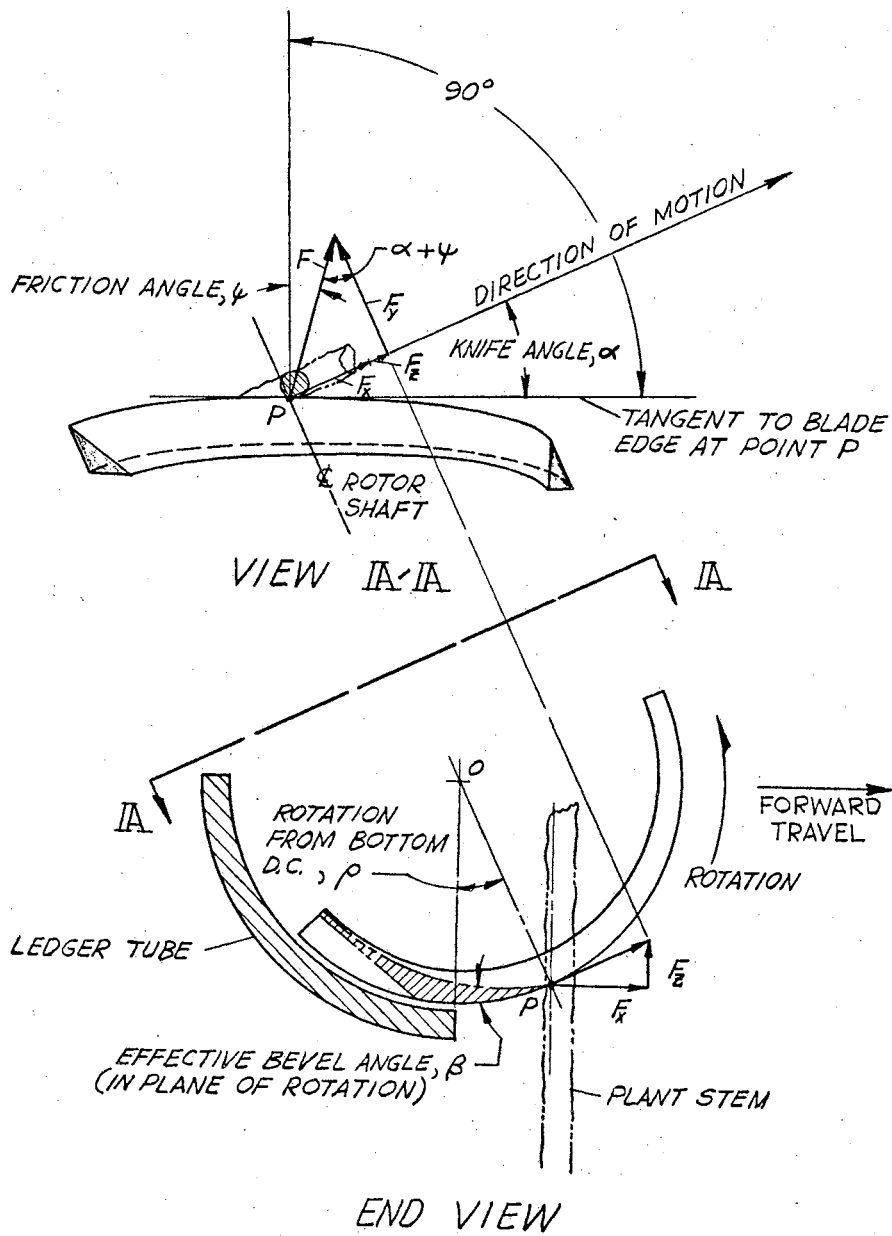


Figure 28. Diagram of Resultant Force on a Plant Stem from a Point on the Rotor Sector Blade Edge

action of the resultant force. (The stiffness of the plant stem in bending is assumed to be the same in any direction transverse to the stem.)

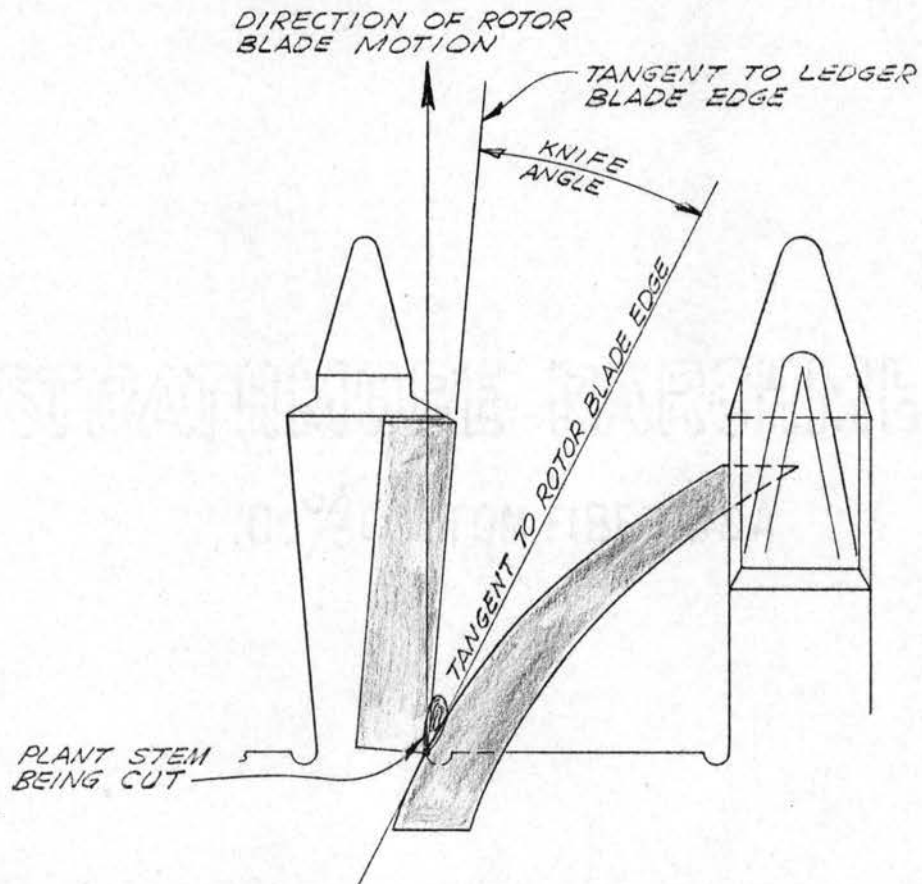


Figure 29. Two Element Cutting of a Plant Stem
Between the Ledger and Rotor Blades

The discussion so far assumes the rotor blade cuts into a plant stem on contact to give single element impact cutting. Should the force system not produce this type of cut, and certainly it will not with a square edged or dull blade at low velocities, then the plant stem will slide

along the blade edge into a position to be cut between the ledger tube fixed blade and the moving rotor blade. Figure 29 illustrates the resulting two-element type of cut.

The force diagram of Figure 28 applies to either single element impact cutting of the plant stem or to deflection of the stem along the blade. If the resultant force, F , is resolved into components along the rotor axis, F_y ; parallel to a vertical centerline of the rotor, F_z ; and perpendicular to a vertical centerline of the rotor, F_x ; the component forces are defined by

$$F_y = F \cos (\alpha + \psi) \quad (4-1)$$

$$F_x = F \sin (\alpha + \psi) \cos \rho \quad (4-2)$$

$$F_z = F \sin (\alpha + \psi) \sin \rho \quad (4-3)$$

The axial or "side" component of force, F_y , depends only on F , α , and ψ , while the vertical component and the horizontal component in a vertical plane depend on F , α , ψ , and ρ . The axial force component, F_y , is the one which moves the plant stem along the rotor blade into contact with the ledger tube blade for two-element cutting between the two blades. And it is independent of angular position of the point on the blade about the rotor center. Therefore a plant stem will be deflected toward the ledger blade by a point on the rotor blade at all times during contact of the blade and the stem. The ground area encompassing plants whose stems will be deflected by each sector of the rotor per revolution can be determined graphically by plotting the

forward motion of successive points along the rotor blade edge. This is done in Figure 30.

To trajectory the severed stems onto a catching platform of a harvesting machine, it would seem desirable to have

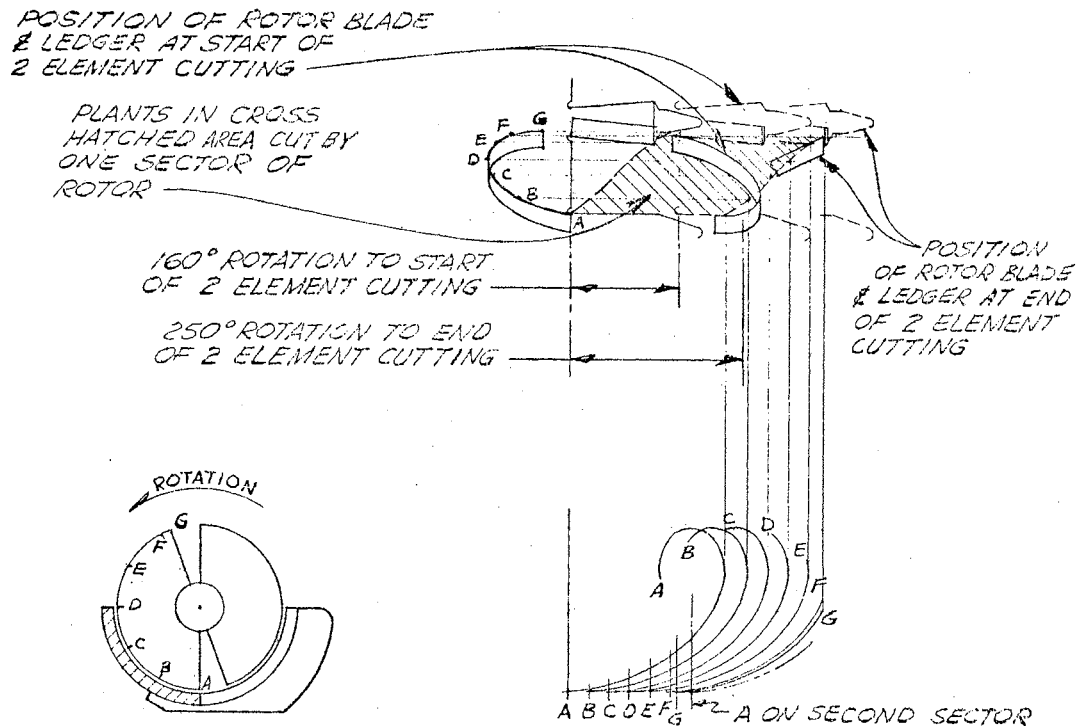


Figure 30. Area of Plants Cut by Each Rotor Sector Per Revolution (Diagram Shown Is for Feed Rate $L = 3/2 D$)

minimum acceleration of the stem in the direction of forward travel of the machine. Further, upward acceleration of the whole stem, or at least a pronounced upward rotation of the cut end is desirable to allow the platform to "run under" the severed stem before it falls downward due to the earth's

gravity field. The cutting action to accomplish these purposes should be one with a minimum F_x force component. In the equation for F_x , the friction angle ψ is assumed constant. For a given resultant cutting force F , then, to obtain a minimum F_x component, the knife angle α should be small and the angle ρ should be large. This implies the 26 degree rotor with the ledger tube oriented counterclockwise from its normal position should give the best stem trajectory results.

CHAPTER V

DIMENSIONAL ANALYSIS

One of the objectives of this study is to relate the response variables of interest to the independent, controllable parameters that have a non-trivial effect on them. The response variables to be considered are the input energy per stem cut, maximum torque developed per stem cut, and the displacement of the stem center of gravity and cut end in three orthogonal directions after cutting. Dimensional analysis affords a means of reducing the number of variables to be considered in an experiment and of reporting results in a general, dimensionally correct form.

Energy Input and Maximum Torque Responses

Consider now the pertinent quantities or fundamental parameters involved in the energy input to cut and impart motion to plant stems, using the helical cutter. Knife angle, whether for single element or two-element cutting is an important parameter. For the approximate cylindrical helical configuration of the cutting edge of the design proposed, however, the knife angle and the rate of change of knife angle with axial distance depend on the angle between the plane of the rotor sector plate and the rotor

axis (angle α of Figure 31), the axial distance from the intersection of the plane and the axis to the point where contact with the plant stem is made (distance l' of Figure 31), and the rotor diameter (dimension D on Figure 31). Since the rotor is fixed axially with respect to the ledger tube, the axial distance from the intersection of the rotor plane and axis (l') can be defined in terms of the axial distance from a reference point (bottom corner) of the fixed ledger blade to the point of contact. On Figure 31, $l'=l-g$.

It will be assumed that the rotor shaft diameter (dimension d in Figure 31) will be kept small enough such as not to interfere with plants entering the cutting zone of the rotor blades. Thus it will not be a pertinent variable in the cutting and trajectory analysis.

It is known that input energy and force required to cut plant stems depend on the plant species, maturity, moisture content, and stem diameter (16, 17, 18). But this group of mixed parameters - some qualitative, some quantitative - should be replaced with pertinent, controllable, quantitative ones if possible. For cutting and trajectory of plant stems, parameters giving some measure of the shear strength and stiffness in bending of the stems seem logical choices. Figure 32 shows typical load-deflection curves resulting from transverse shear failure tests and bending tests (one inch or greater deflection) of the soybean plant material used in this study. The load - deflection curves for both types of test are highly

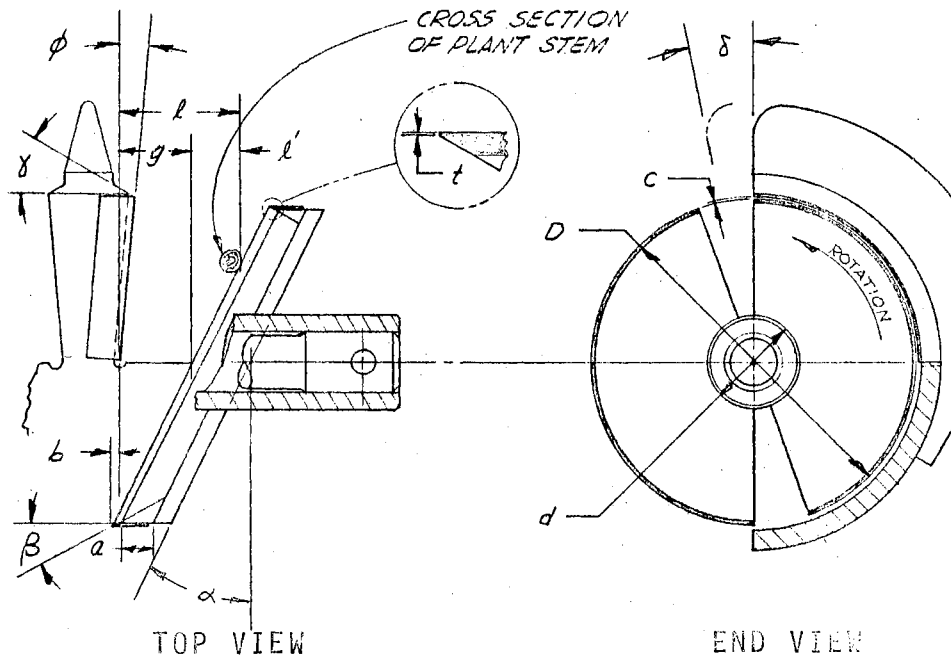
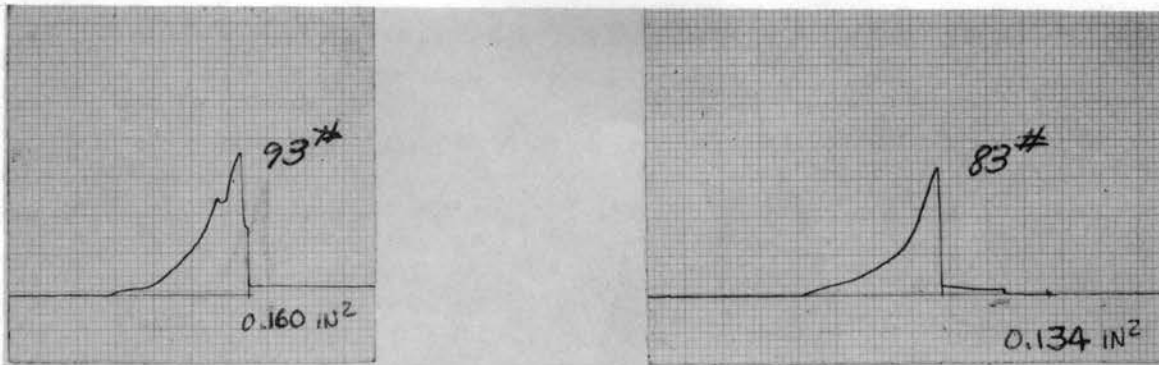


Figure 31. Geometric Parameters of Helical Cutter

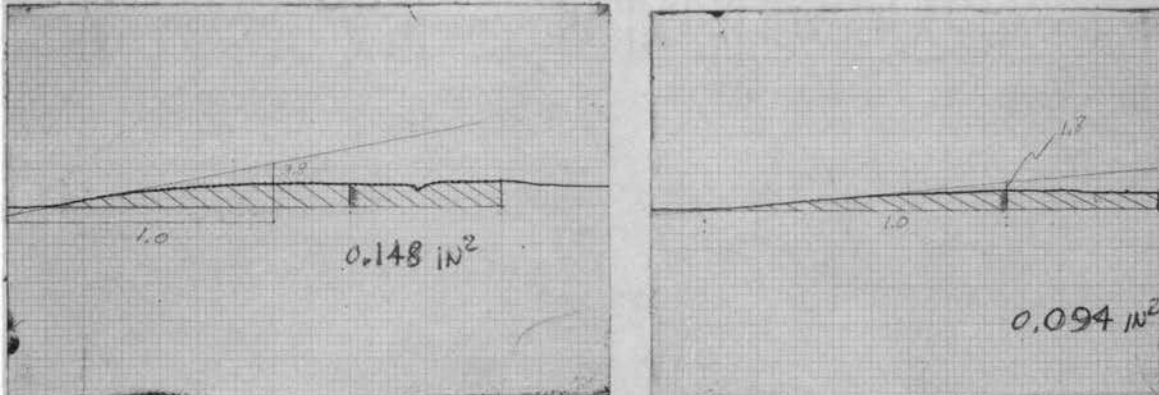
non-linear and subject to wide variation from stem to stem. Ultimate shear force and maximum bending force for a one inch deflection might be adopted as the variables indicative of shear strength and stiffness in bending of a given plant stem at a given cutting height. However, it appears less variation in test values would result if some sort of mean ultimate shear and mean bending load were used.



Test D-46
 Applied Load: 3 3/8"
 above base
 Wet Linear Density:
 0.2700 Gm/In
 Dry Linear Density:
 0.2051 Gm/In

Test D-50
 Applied Load: 3 1/2"
 above base
 Wet Linear Density:
 0.1804 Gm/In
 Dry Linear Density:
 0.1380 Gm/In

- (a) Shear failure curves for 17/64 dia. soybean stems conditioned 4 hrs. Moisture content: 31% dry basis. Avg. dia. of stems at failure cross sections: 0.19 in. Vertical scale: 50 lb. per cm.; Hori. scale: 0.16 in/cm.



Test D-46
 Applied Load: 3 3/8"
 above base

Test D-50
 Applied Load: 3 1/2"
 above base

- (b) Cantilever bending load-deflection curves for 17/64 dia. soybean stems described in (a) above

Figure 32. Typical Load Deflection Curves for (a) Transverse Shear Failure (b) Bending

Thus the variables chosen are input energy ($\text{in} - \text{lb}_f$) per unit stem average diameter to shear the stem at a given height, and input energy ($\text{in} - \text{lb}_f$) per unit deflection to deflect the stem one inch at the given height.

In light of the above considerations, the pertinent quantities relating to the response of energy input per stem cut are judged to be as listed in Table VI. Symbols are in reference to Figure 31.

TABLE VI
FUNDAMENTAL QUANTITIES FOR ENERGY INPUT ANALYSIS

No.	Symbol	Description of Quantity, Units	Dimensions
<u>Pertaining to Cutter Geometry</u>			
1	D	Diameter of rotor, in.	L
2	n	Number of cutting elements about periphery of rotor	-
3	α	Angle between plane of rotor sector plate and plane of rotation, rad.	-
4	l	Axial distance from ledger blade bottom corner to point of contact with plant stem, in.	L
5	β	Bevel angle of rotor blade ledge, rad.	-
6	a	Width of rotor blade ledge, in.	L
7	t	Thickness of point of bevel of rotor blade (knife sharpness), in.	L
8	ϕ	Ledger edge angle, rad.	-

TABLE VI (Continued)

No.	Symbol	Description of Quantity, Units	Dimensions
9	γ	Bevel angle of ledger blade edge, rad.	-
10	b	Overlap of rotor and ledger blade edges, in.	L
11	c	Clearance between rotor and ledger blades, in.	L
12	ρ	Angular displacement of stem contacting point on rotor, rad.	-
<u>Pertaining to Operating Characteristics</u>			
13	ω	Rotor angular velocity, rad./sec.	T^{-1}
14	V	Velocity of rotor center, in./sec.	LT^{-1}
15	e	Height of cut above base of plant, in.	L
16	δ	Angular position of bottom corner of ledger tube blade relative to bottom center of rotor, rad.	-
17	U	Input energy to cut and impart motion to plant stem, in-lb _f .	LF
<u>Pertaining to Plant</u>			
18	m	Wet linear density of stalk in vicinity of point of cut, lb _m /in.	ML^{-1}
19	h	Height of stalk center of gravity above ground line, in.	L
20	Se	Energy per unit average diameter to shear stem at point of cut, in-lb _f /in.	LF/L=F
21	Be	Energy per unit deflection to deflect stem one inch at point of cut, in-lb _f /in.	LF/L=F

TABLE VI (Continued)

No.	Symbol	Description of Quantity, Units	Dimensions
22	ψ	Friction angle between plant stem and blade edge, rad.	-
<u>Other</u>			
23	Ne	Newton's second law coefficient, lb_f/lb_m in/sec ²	$FM^{-1}L^{-1}T^2$
24	G	Strength of earth's gravity field, lb_f/lb_m	FM^{-1}

With 24 fundamental quantities and with a dimensional matrix rank of 4, Buckingham's Pi Theorem defines $24-4=20$ pi terms (33, 34, 35). By inspection these pi terms are determined to be:

$$\Pi_1 = \frac{U}{Gmh^2}$$

Energy input index; index of ratio of total input energy to the potential energy of the stem in the earth's gravity field due to a measure of its wet mass and the height of its center of gravity. This potential energy is a function of the size of the plant, therefore Π_1 may be thought of as an index of total input energy per unit "size" of plant.

$\Pi_2 = \frac{V}{\omega D}$ Feed rate index; index of ratio of rotor center velocity relative to plant to the rotor peripheral velocity.

$\Pi_3 = \frac{\omega^2 NeD}{G}$ Rotor speed index; index of ratio of centrifugal force at rotor blade edge to gravity force.

$\Pi_4 = \alpha$ Rotor angle index; rotor sector plate angle.

$\Pi_5 = \frac{l}{D}$ Lateral position index; index of ratio of lateral position of plant relative to bottom corner of ledger tube to rotor diameter.

$\Pi_6 = \delta$ Ledger orientation index; angular orientation of ledger tube relative to rotor bottom dead center.

$\Pi_7 = \frac{e}{D}$ Cutting height index; index of ratio of cutting height to rotor diameter.

$\Pi_8 = \frac{Se}{Be}$ Shear force to bending force index; index of ratio of mean shear force to mean bending force for one inch deflection at point of cut.

$$\Pi_9 = \frac{h}{D}$$

Plant center of gravity height index;
index of ratio of height of plant center of gravity to rotor diameter.

$$\Pi_{10} = \frac{Se}{Gmh}$$

Shear force to gravity force index;
index of ratio of mean shear force of stem at point of cut to gravity force on the stem. Since the gravity force is a function of the wet mass per unit length of the stem and the height of its center of gravity, quantities relating to size of the stem, Π_{10} may be considered an index of the mean shear force per unit "size" of stem.

$$\Pi_{11} = \frac{t}{D}$$

Knife sharpness index.

$$\Pi_{12} = \frac{a}{D}$$

Rotor ledge width index.

$$\Pi_{13} = \frac{b}{D}$$

Blade overlap index.

$$\Pi_{14} = \frac{c}{D}$$

Blade clearance index.

$$\Pi_{15} = \beta$$

Rotor cutting edge bevel angle.

$$\Pi_{16} = \phi$$

Ledger edge angle.

$$\Pi_{17} = \gamma$$

Ledger blade edge bevel angle.

$$\Pi_{18} = n$$

Number of cutting elements about periphery.

$\Pi_{19} = \psi$ Friction angle between plant and knife blade.

$\Pi_{20} = \rho$ Angular displacement of the stem contacting point on the rotor blade from bottom dead center of the rotor.

The first pi term, Π_1 , is the response dimensionless quantity, and it may be written as some function of Π_2 through Π_{20} . Thus

$$\Pi_1 = F(\Pi_2, \Pi_3, \dots, \Pi_{20}) \quad (5-1)$$

But Π_{12} through Π_{18} are to be held constant through fixed geometry of the cutter as follows:

$$\Pi_{12}, \text{ rotor ledge width index, } = \frac{a}{D} = \frac{0.375}{3.5} = 0.107$$

$$\Pi_{13}, \text{ blade overlap index, } = \frac{b}{D} = \frac{0.157}{3.5} = 0.045$$

$$\Pi_{14}, \text{ blade clearance index, } = \frac{c}{D} = \frac{0.005}{3.5} (\text{avg.}) = 0.0015$$

$$\Pi_{15}, \text{ rotor cutting edge bevel angle, } = \beta = 30^\circ \text{ or } 0.524 \text{ rad.}$$

$$\Pi_{16}, \text{ ledger edge angle, } = \phi = 5^\circ \text{ or } 0.087 \text{ rad.}$$

$$\Pi_{17}, \text{ ledger blade edge bevel angle, } = \gamma = 30^\circ \text{ or } 0.524 \text{ rad.}$$

$$\Pi_{18}, \text{ number of cutting elements about periphery, } = n = 2 \text{ sectors.}$$

Also, as previously discussed, $\Pi_{19} = \psi$, the friction angle between the plant stem and the blade edge, will be assumed constant for a given species of plant and for a given blade material. And $\Pi_{20} = \rho$, angular displacement of the

contact point on the rotor blade from bottom dead center of the rotor will be assumed equal to a mean value. Then Π_1 , may be written as a new function of Π_2 through Π_{11} .

$$\Pi_1 = F' (\Pi_2, \Pi_3, \dots, \Pi_{11}) \quad (5-2)$$

or

$$\frac{U}{Gmh^2} = F' \left(\frac{V}{\omega D}, \frac{\omega^2 NeD}{G}, \alpha, \frac{l}{D}, \delta, \frac{e}{D}, \frac{Se}{Be}, \frac{h}{D}, \frac{Se}{Gmh}, \frac{t}{D} \right) \quad (5-3)$$

The maximum torque developed in cutting a plant stem is influenced by the same set of fundamental quantities - variables and dimensional constants - that relate to input energy per stem cut. Therefore, let a new dimensionless response variable (dependent pi term) including the maximum torque developed in cutting, T_{mx} , be defined:

$$\Pi_1' = \frac{T_{mx}}{Gmh^2}, \quad \text{Maximum torque index; index of the ratio or maximum torque developed in cutting and trajecting a plant stem to potential torque developable at a unit radius due to the plant stem linear mass and height of its center of mass in the earth's gravity field.}$$

Then in a different functional relationship, the maximum torque index, Π_1' , can be related to the same set of dimensionless quantities (pi terms) as the input energy index. Thus

$$\Pi_1' = f(\Pi_2, \Pi_3, \dots, \Pi_{11}) \quad (5-4)$$

or

$$\frac{Tmx_2}{Gmh} = f\left(\frac{V}{\omega D}, \frac{\omega^2 NeD}{G}, \alpha, \frac{l}{D}, \delta, \frac{e}{D}, \frac{Se}{Be}, \frac{h}{D}, \frac{Se}{Gmh}, \frac{t}{D}\right) \quad (5-5)$$

Motion of Severed Plant Stalks

With reference to Figure 33, the severed plant is seen to be an unconstrained rigid body in space with six degrees of freedom; i.e., six independent spatial coordinates are required to define the spatial motion of the body with respect to chosen reference axes. Thus translation in the x, y, and z directions and rotations in the xy, xz, and yz planes must be considered. Rotation of the plant in the xz plane is certain to occur, and possibly in the xy and yz planes also. These rotations will be checked by high speed motion picture photography, particularly with reference to shock that could cause seed shattering. But attempts to correlate resulting motion with independent parameters will be restricted to the maximum horizontal displacements of the plant center of gravity and of its

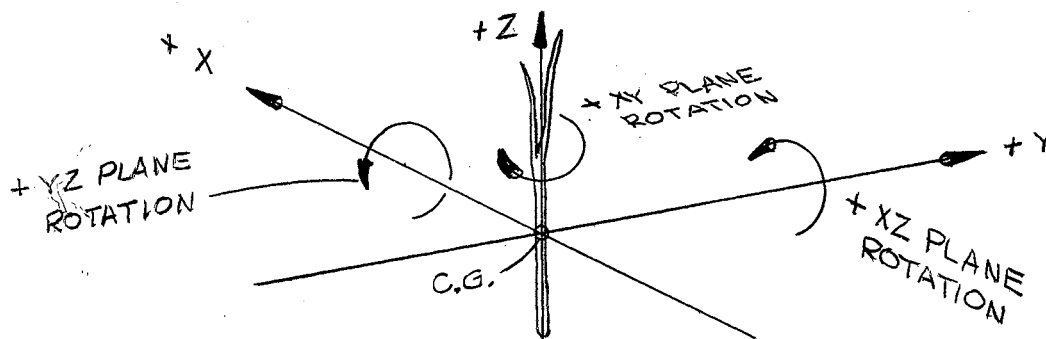


Figure 33. Left-handed Coordinate System Established to Define Motion of Severed Plant Stems

cut end in the x and y directions on a reference grid board and to the maximum upward vertical displacement of the center of gravity and the cut end (in the positive z direction).

The left-handed coordinate system chosen to define the stem motion is assumed fixed to the cutter. The Y-axis coincides with the centerline of the rotor shaft, and the X-axis coincides with the centerline of the row of plants to be cut.

Since force and displacement are vector quantities (having both magnitude and direction), it is allowable and convenient to resolve the quantities into their components in the x, y, and z directions and to consider each motion component, and the force system causing it, independently.

A preliminary high speed motion picture study of the cutting action of the 26 degree rotor fitted with a square edge or dull blade showed that the stem cut end left contact with the cutting surface of the rotor immediately after being severed. The kinetic energy imparted to the stem to affect its path of trajectory was transferred by impact while the stem was being deflected to the fixed ledger blade by the rotor and when being cut between the ledger and rotor blades. No two stage - cut then trajectory force system exists. For this cutting mechanism, and if air resistance (drag forces) are assumed of second order significance or negligible, exactly the same set of fundamental quantities apply to the responses of stem

displacement as to energy input and maximum torque developed.

It appears logical to make the above assumptions for this study and to assert that all the response pi terms to be considered are different functions of the same set of independent pi terms. Hence if

$\Pi_1'' (1) = \frac{X_{C.G.}}{D},$ C. G. X-displacement index; index of ratio of resultant displacement of the severed stem center of gravity in the X direction to the rotor diameter.

$\Pi_1'' (2) = \frac{X_{END}}{D},$ end X-displacement index; index of ratio of resultant displacement of the severed stem cut end in the X direction to the rotor diameter.

$\Pi_1'' (3) = \frac{Y_{C.G.}}{D},$ C. G. Y-displacement index, index of ratio of resultant displacement of the severed stem center of gravity in the Y direction to the rotor diameter.

$\Pi_1'' (4) = \frac{Y_{END}}{D},$ end Y-displacement index; index of ratio of resultant displacement of the severed stem cut end in the Y direction to the rotor diameter.

$\Pi_1'' (5) = \frac{Z_{C.G.}}{D}$, C. G. Z-displacement index, index of ratio of resultant positive displacement of the severed stem center of gravity in the Z direction to the rotor diameter.

$\Pi_1'' (6) = \frac{Z_{END}}{D}$, end Z-displacement index, index of ratio of resultant positive displacement of the severed stem cut end in the Z direction to rotor diameter.

Then

$$\Pi_1'' (1) = F' (1) (\Pi_2, \Pi_3, \dots, \Pi_{11}) \quad (5-6)$$

$$\Pi_1'' (2) = F' (2) (\Pi_2, \Pi_3, \dots, \Pi_{11}) \quad (5-7)$$

$$\Pi_1'' (3) = F' (3) (\Pi_2, \Pi_3, \dots, \Pi_{11}) \quad (5-8)$$

$$\Pi_1'' (4) = F' (4) (\Pi_2, \Pi_3, \dots, \Pi_{11}) \quad (5-9)$$

$$\Pi_1'' (5) = F' (5) (\Pi_2, \Pi_3, \dots, \Pi_{11}) \quad (5-10)$$

$$\Pi_1'' (6) = F' (6) (\Pi_2, \Pi_3, \dots, \Pi_{11}) \quad (5-11)$$

Alternative Response Pi Terms Considered

There is no unique set of pi terms relating the fundamental quantities pertaining to a given physical system. Several solutions may satisfy Buckingham's Pi Theorem correctly, but the group of solution pi terms may not all be equally useful (35). No "standard" dimensionless groups seemed applicable to the analysis of the helical cutter. The dimensionless groups specified hopefully have a rational and direct relationship to this particular problem, but there is no guarantee that such is the case. The description of each pi term following its definition attempts to convey the logic behind its selection.

To be easily understood, it is desirable that the energy input index and maximum torque index have nearly a one to one correspondence with the dimensioned response variables of energy input per stem cut and maximum torque developed per stem cut. That is, if the energy input per stem cut increases with increase of an independent variable pi term, rotor speed index, for example, then the input energy index should likewise increase - and in relatively the same proportion. At the same time, it is desirable to remove the effects of stem size from the response, that is, put all energy input values on a "per unit stem size" basis. The dimensionless groups of variables listed for

the energy input and maximum torque indices at least tend to accomplish these goals.

Another dimensionless group of variables was first chosen as the energy input index. This group, $\frac{U}{NeMV^2h}$, was considered an index of the ratio of total input energy per stem cut to the kinetic energy of the plant relative to the rotor center. Preliminary analysis of test results using this response pi term revealed that it did not follow the response pattern of the dimensioned variable energy input per stem cut. The velocity of the plant relative to the rotor center distorted the response pattern. Thus this pi term was discarded in favor of the one listed.

CHAPTER VI

EXPERIMENTAL PLAN AND TEST PLANT MATERIAL

As indicated in Chapter V, at least ten independent variables may influence each of the response π_i terms to be considered in an experimental analysis of the proposed helical cutter. However, one of the independent variable π_i terms, π_{11} , the knife sharpness index, will be fixed at two discrete values: that for a square edge or dull blade with $\frac{t}{D} = \frac{.031}{3.5} = 8.85 \times 10^{-3}$; and that for a sharp, beveled edge blade with $\frac{t}{D} = \frac{.001}{3.5} = 0.28 \times 10^{-3}$. Consequently, the structure of the required experimental plan must be that of two series of tests, one series with use of the dull blade and another with use of the sharp blade, as diagrammed in Table VII. As Table VII indicates, each of the two series of tests required is a multifactor experiment with eight response variables and nine independent variables or factors.

Types of Multifactor Experimental Plans

Two basic types of experimental plans are used for multifactor experiments, the classical plan and the factorial plan (35). In the classical approach, all independent variables except one are held constant while this one is

TABLE VII
STRUCTURE OF REQUIRED EXPERIMENTAL PLAN

Dull Blade Series ($\pi_{11} = \frac{t}{D} = 8.85 \times 10^{-3}$)		Sharp Blade Series ($\pi_{11} = \frac{t}{D} = 0.28 \times 10^{-3}$)	
R Response Variable	Proposed Functional Relationship	R Response Variable	Proposed Functional Relationship
π_1 π_1' π_1'' (1) \cdot \cdot π_1'' (6)	$R = f(\pi_2, \pi_3, \dots, \pi_{10})$	π_1 π_1' π_1'' (1) \cdot \cdot π_1'' (6)	$R = f'(\pi_2, \pi_3, \dots, \pi_{10})$

changed through its range of values and the effect on the response variable noted. This procedure is repeated for each of the independent variables. In the factorial approach, all the independent variables are changed for each test run as specified by some predesigned statistical scheme. For an equal number of trials, the factorial plan gives results much greater in precision than the classical plan; that is, the experimental error will be lower in the factorial plan, since each effect is based on all trials in the experiment whereas each effect in the classical

plan is based on just the trials over the range of one factor, assuming no replication of runs. However the factorial plan is restricted to response functions that are sums of functions of the independent variables or ones that are products of functions of the independent variables.

One form of the classical plan recommended by Murphy (33) for determining prediction equations in engineering experiments is termed the component equation method. With its use, the multifactor experiment is converted into a series of single factor experiments in which all the independent variables but one are held at some mid-range value. The results from each series of experiments are used to relate the response variable to one independent variable by a component equation. The component equations then are combined to determine the multifactor prediction equation. This method is valid only when no interactions exist between the independent variables. That is, the resultant prediction equation must be either an additive or multiplicative mathematical expression and not a mixed one. If an additive expression relates the response variable to the independent variables, then it must have no terms involving products of two or more independent variables. If a multiplicative expression fits the results, it must have no terms that has one independent variable as an exponent of another. If interaction exists, the component equation method, being simply a limited classical plan, offers the advantage of ready transformation into a more complete classical plan.

simply by including additional experimental trials. To unravel interaction relationships, each independent variable must be changed through its range in additional test sequences, with the other independent variables held at different values in each sequence.

Where no interaction between independent variables is a justified assumption, the orthogonal main-effect experimental plans designed by Addelman and Kempthorne (36) are applicable and give more precise results with a fewer number of trials than the classical, component equation method. The plans are based on asymmetrical, fractional, factorial experiment designs and provide unbiased estimates of the main effects of all included factors when no interactions are present. If interactions between factors are present, estimates of the main effects will deviate from their true values by other than experimental error. The effect of a factor is measured by the change in response produced by a change in the level of the factor. When the levels of a factor (independent variable) are equally spaced over the range of values to be tested, the nature of the polynomial regression function that best describes the factor effect on the response variable can be readily determined by either regression or analysis of variance techniques utilizing orthogonal polynomial coefficients (37). Thus polynomial component equations are defined by this method.

Choice of Experimental Plan

With highly variable soybean stems comprising the experimental units for the proposed investigation, imprecise results were anticipated, and a factorial type experimental plan was the logical choice. Nine independent pi terms, Π_2 through Π_{10} , were to be screened to determine which ones had non-trivial effects on each of the response variables. Of these nine independent pi terms, however, the two relating to plant physical properties could not be accurately controlled. To overcome this difficulty, a statistical approach that disregards dimensions and sets response variables as equal to a function of dimensioned quantities was adopted. Plant stem nominal diameter at the base (ground) line is controllable and was selected to replace $\Pi_{10} = \frac{Se}{Gmh}$ as one independent variable. Time of treatment in a moisture conditioning chamber is precisely controllable and was selected to replace $\Pi_8 = \frac{Se}{Be}$ as an independent variable. The remaining seven independent pi terms can be controlled within close limits.

To allow conversion back to all dimensionless factors in determining prediction equations for selected response pi terms, it was decided to "pair" the test plant stems; that is, to select two nearly identical stems for each experimental trial. Then for each stem subjected to a cutting test, a nearly identical stem would be subjected to physical tests to determine its stiffness in bending and its

transverse shear strength at the height above ground that the first stem was cut. The average diameter of the physical test stem would be determined near the test cross section, and the moisture content and linear density of both stems would be measured. These measurements would be made on portions of the stem adjacent to the cut section.

Three levels of Π_3 , feed rate index, and of Π_7 , cutting height index, were judged sufficient to allow determining the effect on the response variables and to allow spanning a realistic range of operating values. Four levels were specified for each of the other factors. The levels for all factors were to be equally spaced to allow determining the type of polynomial response function that best fit the effect of each factor. These requirements call for a basic $4^7 \times 3^2$ (seven factors with four levels; two factors with three levels) orthogonal main-effect plan. Of the plans listed by Addelman and Kempthorne (36), basic plan 13 with 32 trials was the one selected for use.

To provide a more accurate basis for computing experimental error, two replications of each treatment combination were specified (three replications were specified at first, but the sizeable time period required for each experimental run forced a reduction to two.) Thus each of the two main multifactor experiment series was enlarged to 64 trials.

Randomization Procedure

The randomization procedure prescribed by Addelman and Kempthorne was followed. This procedure is:

1. Choose the appropriate plan.
2. Randomly assign the factors to the columns of the chosen plan.
3. Randomly assign the levels of each factor to the numbers 0,1,2,3 representing the levels of factors in the listed experimental plan.
4. Randomly assign the treatments to the experimental units.

In carrying out step 4, all the plant stem experimental units were necessarily pre-sized according to four levels of nominal diameter and according to four levels of height of center of gravity within each diameter classification. Also to facilitate execution of the experiment, the order of treatment combinations was arranged to allow all trials involving a given level of the factor "time of treatment in moisture chamber" to be run consecutively.

Main Experimental Plans

Table VIII lists the factors in each of the main test series and the code assigned to each factor level according to the randomization procedure. Tables IX and X present the experimental plans for the dull blade and sharp blade test series respectively. As previously noted, the dull blade test series was begun with a plan that called for three replications of each treatment combination. After 30 runs, this plan was revised to the two replication plan.

TABLE VIII
 FACTOR LEVEL CODING AS DETERMINED BY RANDOMIZATION PROCEDURE

Factor	Factor Levels	Dull Blade Series		Sharp Blade Series	
		Test Plan Column Randomly Assigned to Factor	Code Assigned to Factor Levels	Test Plan Column Randomly Assigned to Factor	Code Assigned to Factor Levels
Nominal Diameter	13/64 in.	3	3	4	0
	17/64 in.		0		2
	21/64 in.		2		1
	25/64 in.		1		3
Time in Chamber	2 hr.	4	2	1	1
	4 hr.		3		2
	6 hr.		0		0
	8 hr.		1		3
Π_2 Rotor Speed Index	322 (1800 rpm)	7	1	3	0
	644 (2546 rpm)		2		3
	966 (3118 rpm)		0		2
	1288 (3600 rpm)		3		1
Π_3 Feed Rate Index	0.08 (1.75 in/rev)	8	1	8	2
	0.14 (3.06 in/rev)		0		1
	0.20 (4.38 in/rev)		2		0
Π_4 Rotor Angle Index	0.454 (26°)	2	2	7	1
	0.628 (36°)		1		3
	0.802 (46°)		0		0
	0.976 (56°)		3		2
Π_5 Lateral Position Index	0.107 (0.38 in)	6	0	6	2
	0.214 (0.75 in)		1		0
	0.321 (1.12 in)		2		1
	0.428 (1.50 in)		3		3
Π_6 Ledger Orientation Index	-0.0873 (-5°)		0		0
	0.0000 (0°)		1		3
	0.0873 (+5°)		2		1
	0.1746 (+10°)		3		2
Π_7 Cutting Height Index	0.286 (1.00 in)	9	1	9	2
	0.500 (1.75 in)		0		0
	0.714 (2.50 in)		2		1
Π_9 C.G. Height Index	2.25 (7.88 in)	1	2	2	3
	2.75 (9.62 in)		1		2
	3.25 (11.38 in)		3		0
	3.75 (13.12 in)		0		1

TABLE IX

MAIN EXPERIMENTAL PLAN
DULL BLADE SERIES

Plan Col. No.	1	2	3	4	5	6	7	8	9
Factor	π_9	π_4	Nom. Dia.	Time in Chamber	π_6	π_5	π_2	π_3	π_7
Trial No.	Coded Value of Factor Levels								
1	3	1	0	0	3	3	2	1	2
2	0	3	1	0	1	3	1	2	0
3	3	2	1	0	2	0	3	1	2
4	1	3	2	0	3	2	3	0	1
5	0	0	0	0	0	0	0	0	0
6	3	2	1	0	2	0	3	1	2
7	0	3	1	0	1	3	1	2	0
8	0	0	0	0	0	0	0	0	0
9	2	1	3	0	1	2	0	1	1
10	1	0	3	0	2	1	2	2	1
11	3	1	0	0	3	3	2	1	2
12	1	3	2	0	3	2	3	0	1
13	2	1	3	0	1	2	0	1	1
14	2	2	2	0	0	1	1	1	1
15	2	2	2	0	0	1	1	1	1
16	1	0	3	0	2	1	2	2	1
17	1	1	2	2	1	0	3	1	0
18	2	0	2	2	2	3	1	0	2
19	0	2	0	2	2	2	0	1	1
20	3	3	0	2	1	1	2	0	1
21	3	0	1	2	0	2	3	2	1
22	1	2	3	2	0	3	2	1	0
23	2	3	3	2	3	0	0	2	2
24	0	2	0	2	2	2	0	1	1
25	1	2	3	2	0	3	2	1	0
26	2	0	2	2	2	3	1	0	2
27	0	1	1	2	3	1	1	1	1
28	3	0	1	2	0	2	3	2	1
29	0	1	1	2	3	1	1	1	1
30	3	3	0	2	1	1	2	0	1
31	2	3	3	2	3	0	0	2	2
32	1	1	2	2	1	0	3	1	0

TABLE IX (Continued)

Plan Col. No.	1	2	3	4	5	6	7	8	9
Factor	Π_9	Π_4	Nom. Dia.	Time in Chamber	Π_6	Π_5	Π_2	Π_3	Π_7
Trial No.	Coded Value of Factor Levels								
33	3	3	2	3	2	1	0	1	0
34	0	1	3	3	0	1	3	0	2
35	1	1	0	3	2	0	1	2	1
36	1	2	1	3	3	3	0	0	1
37	2	0	0	3	1	3	3	1	1
38	0	1	3	3	0	1	3	0	2
39	0	2	2	3	1	2	2	2	2
40	1	1	0	3	2	0	1	2	1
41	2	0	0	3	1	3	3	1	1
42	3	0	3	3	3	2	1	1	0
43	1	2	1	3	3	3	0	0	1
44	0	2	2	3	1	2	2	2	2
45	3	3	2	3	2	1	0	1	0
46	2	3	1	3	0	0	2	1	1
47	2	3	1	3	0	0	2	1	1
48	3	0	3	3	3	2	1	1	0
49	1	0	1	1	1	1	0	1	2
50	2	1	1	1	2	2	2	0	0
51	3	1	2	1	0	3	0	2	1
52	1	0	1	1	1	1	0	1	2
53	0	0	2	1	3	0	2	1	1
54	2	1	1	1	2	2	2	0	0
55	3	2	3	1	1	0	1	0	1
56	3	1	2	1	0	3	0	2	1
57	0	3	3	1	2	3	3	1	1
58	2	2	0	1	3	1	3	2	0
59	1	3	0	1	0	2	1	1	2
60	2	2	0	1	3	1	3	2	0
61	3	2	3	1	1	0	1	0	1
62	1	3	0	1	0	2	1	1	2
63	0	3	3	1	2	3	3	1	1
64	0	0	2	1	3	0	2	1	1

TABLE X
 MAIN EXPERIMENTAL PLAN
 SHARP BLADE SERIES

Plan Col. No.	1	2	3	4	5	6	7	8	9
Factor	Time in Chamber	π_9	π_2	Nom. Dia.	π_6	π_5	π_4	π_3	π_7
Trial No.	Coded Value of Factor Levels								
1	0	3	1	0	1	3	1	2	0
2	0	0	0	0	0	0	0	0	0
3	0	2	2	3	1	2	2	2	2
4	0	3	3	1	2	3	3	1	1
5	0	1	3	3	0	1	3	0	2
6	0	1	1	2	3	1	1	1	1
7	0	0	2	1	3	0	2	1	1
8	0	2	0	2	2	2	0	1	1
9	0	3	3	1	2	3	3	1	1
10	0	2	2	3	1	2	2	2	2
11	0	0	2	1	3	0	2	1	1
12	0	1	3	3	0	1	3	0	2
13	0	0	0	0	0	0	0	0	0
14	0	2	0	2	2	2	0	1	1
15	0	1	1	2	3	1	1	1	1
16	0	3	1	0	1	3	1	2	0
17	1	3	0	1	0	2	1	1	2
18	1	1	0	3	2	0	1	2	1
19	1	1	2	2	1	0	3	1	0
20	1	3	2	0	3	2	3	0	1
21	1	1	0	3	2	0	1	2	1
22	1	2	3	2	0	3	2	1	0
23	1	0	3	0	2	1	2	2	1
24	1	0	1	1	1	1	0	1	2
25	1	2	1	3	3	3	0	0	1
26	1	2	3	2	0	3	2	1	0
27	1	1	2	2	1	0	3	1	0
28	1	0	3	0	2	1	2	2	1
29	1	0	1	1	1	1	0	1	2
30	1	3	0	1	0	2	1	1	2
31	1	2	1	3	3	3	0	0	1
32	1	3	2	0	3	2	3	0	1

TABLE X (Continued)

Plan Col. No.	1	2	3	4	5	6	7	8	9
Factor	Time in Chamber	Π_9	Π_2	Nom. Dia.	Π_6	Π_5	Π_4	Π_3	Π_7
Trial No.	Coded Value of Factor Levels								
33	3	2	3	1	1	0	1	0	1
34	3	0	3	3	3	2	1	1	0
35	3	2	1	0	2	0	3	1	2
36	3	0	1	2	0	2	3	2	1
37	3	2	3	1	1	0	1	0	1
38	3	1	2	1	0	3	0	2	1
39	3	1	0	0	3	3	2	1	2
40	3	3	0	2	1	1	2	0	1
41	3	3	2	3	2	1	0	1	0
42	3	0	3	3	3	2	1	1	0
43	3	2	1	0	2	0	3	1	2
44	3	1	2	1	0	3	0	2	1
45	3	3	0	2	1	1	2	0	1
46	3	0	1	2	0	2	3	2	1
47	3	1	0	0	3	3	2	1	2
48	3	3	2	3	2	1	0	1	0
49	2	3	1	3	0	0	2	1	1
50	2	1	3	0	1	2	0	1	1
51	2	0	2	2	2	3	1	0	2
52	2	3	3	2	3	0	0	2	2
53	2	2	2	0	0	1	1	1	1
54	2	2	0	1	3	1	3	2	0
55	2	0	2	2	2	3	1	0	2
56	2	2	0	1	3	1	3	2	0
57	2	1	3	0	1	2	0	1	1
58	2	1	1	1	2	2	2	0	0
59	2	3	3	2	3	0	0	2	2
60	2	2	2	0	0	1	1	1	1
61	2	0	0	3	1	3	3	1	1
62	2	1	1	1	2	2	2	0	0
63	2	0	0	3	1	3	3	1	1
64	2	3	1	3	0	0	2	1	1

TABLE XI
 EXPERIMENTAL PLAN FOR PRELIMINARY
 CUTTING EFFECTIVENESS TESTS
 DULL BLADE SERIES

Test No	No Trials in Test	Conditions				
		Rotor Angle (Degrees)	Rotor Speed (RPM)	Feed Rate (In/Rev)	Plant Stems (1965 Crop)	
					Nom. Dia. (In.)	Time in Conditioning Chamber (Hrs)
CED-1	10	26	1800	1.75	17/64	0
CED-2	10	26	1800	5.25	17/64	0
CED-3	10	26	3600	1.75	17/64	0
CED-4	10	26	3600	5.25	17/64	0
CED-5	10	56	1800	1.75	17/64	0
CED-6	10	56	1800	5.25	17/64	0
CED-7	10	56	3600	1.75	21/64	0
CED-8	10	56	3600	5.25	21/64	0
CED-9	10	56	3600	5.25	21/64	8
CED-10	10	56	3600	1.75	21/64	8
CED-11	10	56	1800	5.25	21/64	8
CED-12	10	56	1800	1.75	21/64	8
CED-13	10	26	1800	1.75	17/64	8
CED-14	10	26	1800	5.25	17/64	8
CED-15	10	26	3600	5.25	17/64	8
CED-16	10	26	3600	1.75	17/64	8

Note: 1 Stem per Trial

Responses to be Observed: Type of Cut
 Actual Cutting Height
 X & Y Displacements of
 Stem Cut End & C. G.

TABLE XII
EXPERIMENTAL PLAN FOR HIGH SPEED MOTION PICTURE STUDY
DULL BLADE SERIES

Test No. For Photographing		Conditions					
		Rotor Angle (Degrees)	Rotor Speed (RPM)	Feed Rate (In./Rev)	Description of Plant Stems		
Cutting Action	Stem Trajectory				Nom Dia (In)	Crop Year	Time in Conditioning Chamber (Hrs.)
PD-1	PD-12	26	1800	1.75	17/64	1965	2
PD-2	PD-11	26	3600	1.75	17/64	1965	2
PD-3	PD-10	26	3600	5.25	17/64	1965	2
PD-4	PD-7	56	1800	1.75	17/64	1965	2
PD-5	PD-8	56	3600	1.75	17/64	1965	2
PD-6	PD-9	56	3600	5.25	17/64	1965	2

TABLE XIII
EXPERIMENTAL PLAN FOR HIGH SPEED MOTION PICTURE STUDY
SHARP BLADE SERIES

Test No. For Photographing		Conditions					
		Rotor Angle (Degrees)	Rotor Speed (RPM)	Feed Rate (In./Rev)	Description of Plant Stems		
Cutting Action	Stem Trajectory				Nom Dia (In)	Year Crop	Time in Conditioning Chamber (Hrs.)
PS-1	PS-11	26	1800	1.75	17/64	1965	2
PS-2	PS-10	26	1800	1.75	17/64	1968	2
PS-3	PS-9	26	3600	5.25	17/64	1968	2
PS-4	PS-8	56	3600	5.25	17/64	1968	2
PS-5	PS-12	56	1800	1.75	17/64	1968	2
PS-6	PS-7	46	3600	3.06	21/64	1968	2

shown. For those treatment combinations where three replications were run, one of the three was eliminated by procedures explained in Chapter IX before the results were analyzed.

Auxiliary Experiment Plans

A preliminary series of tests was planned to check the suitability of the range of levels chosen for some of the independent variables and to give an indication of cutting effectiveness of rotors equipped with square edge blades. Table XI diagrams the experimental plan for this test series.

Cutting effectiveness tests were also run in connection with the high speed motion picture studies to determine the mechanism of cutting with dull and sharp blades. Tables XII and XIII indicate the experimental plans for these tests.

Plant Material Used In Tests

The stems of soybean (Glacine Max) plants of the Hill variety comprised the experimental units for all the cutter evaluation tests. Approximately 4000 plants were gathered, part of them on September 25 and the remainder on October 1, 1965, at the Perkins Experiment Station of Oklahoma State University. The planting date was May 25, 1965, and the seedlings emerged May 27. Thus the plants were gathered 120 and 127 days after emergence. Yield of the crop was 26.2 bushels per acre. The plants were pulled from the ground -

roots and all - and tied into bundles of from about 30 to 80 plants each. These bundles were hung from racks - tops down - in an indoor storage area until used for test.

To determine the size range of the plant stems, a random sample was taken from the lot and analyzed. The roots were cut off at the ground line. Then the average diameter of the stem at the ground line was measured with calipers and recorded. Figure 34 presents the histogram of the results. The average diameter of the lot is seen to be about $1/4$ inch, with the range extending from $5/64$ to $29/64$ inch.

The four levels of nominal diameter at the base of the stems to be used for the cutting tests were chosen as $13/64$, $17/64$, $21/64$, and $25/64$ inch respectively. The plants were measured for nominal diameter by a gage made for this purpose as illustrated by Figure 35.

The height of the center of gravity above the base of a plant was determined by balancing the stem on a horizontal pin and marking it. Figure 36 shows the fixture used for this purpose. Since the location of the center of gravity changed with change of moisture content of the plant stem, this quantity was not determined until just previous to running a test. However a preliminary investigation of variation of height of center of gravity within the diameter classifications was made to learn what a representative range of values for this factor would be. Distance from the base end of the stems to the center of gravity varied from 10 to 19 inches, the average being about 15 inches. A

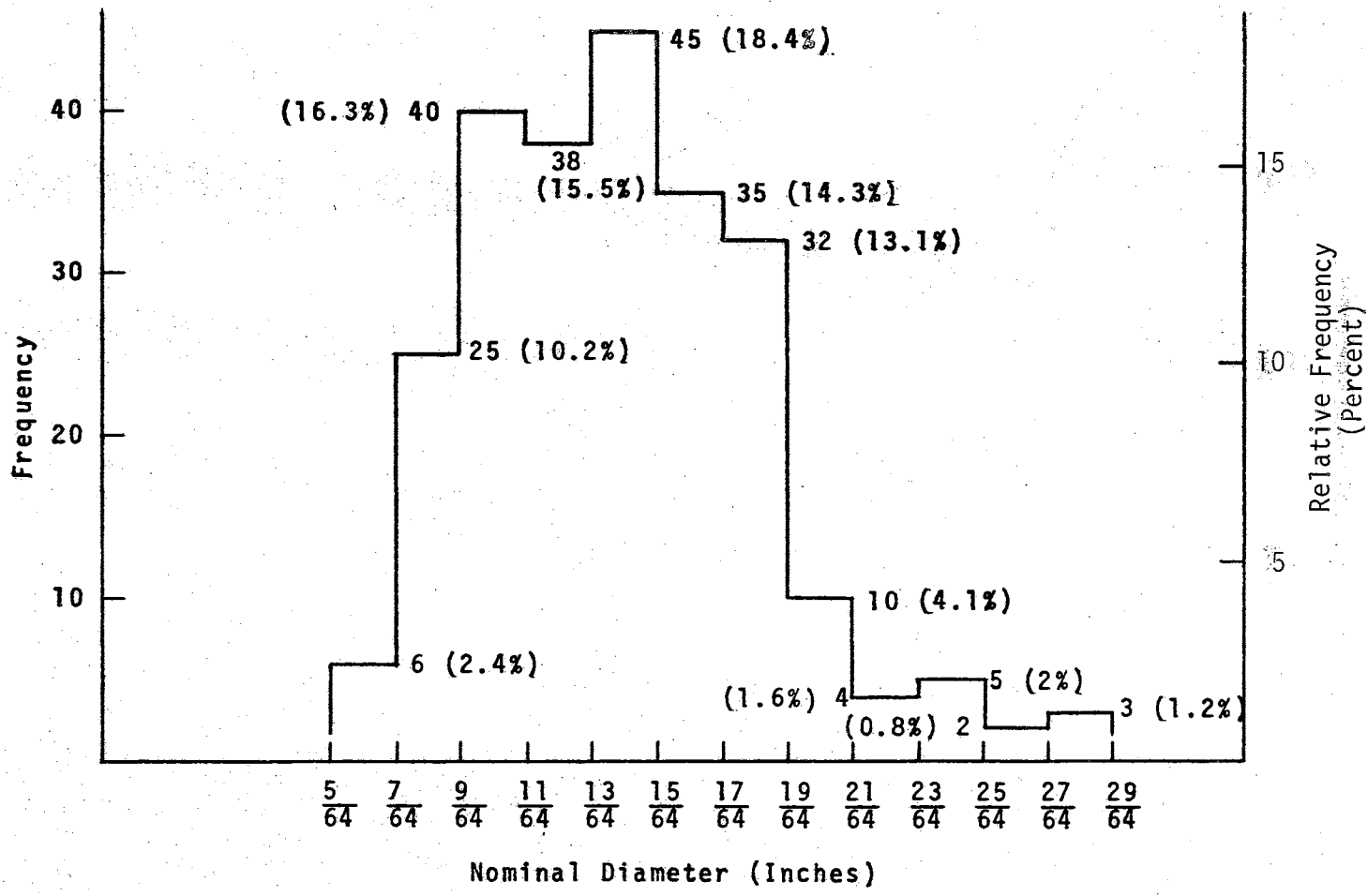


Figure 34. Frequency Histogram of Stem Nominal Diameter

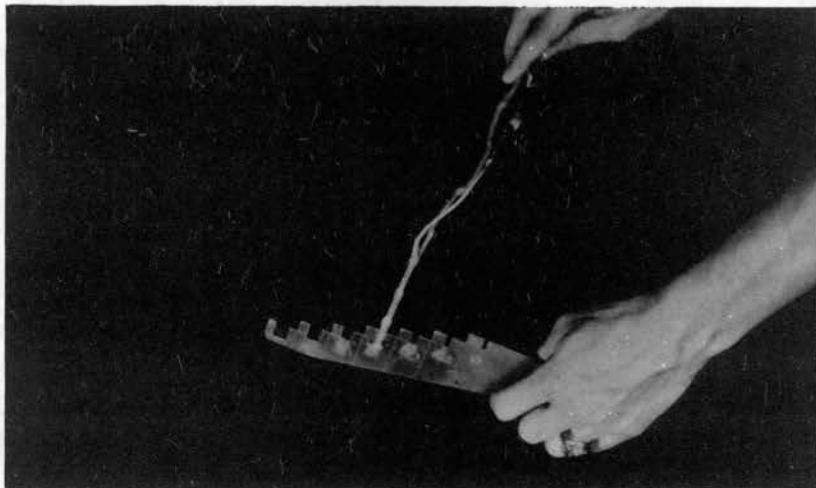


Figure 35. Gage and Method Used for Determining Stem Nominal Diameter

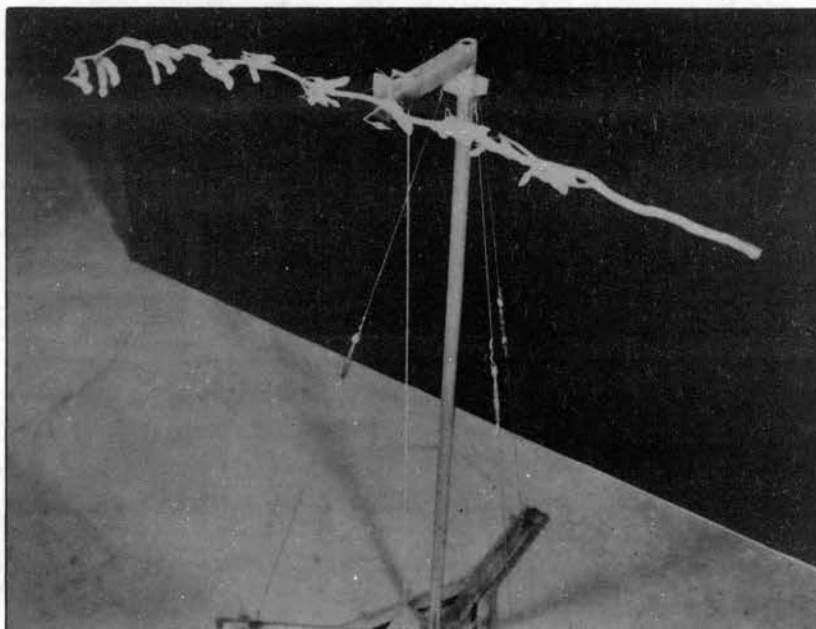


Figure 36. Fixture and Method Used for Locating Center of Gravity of Plant Stem

distance of 1 1/2 inch was allowed for securing the bottom end of a stem in a holding clamp for cutting tests. If the base (ground) line is then assumed to be the top of the clamp or 1 1/2 inch above the stem end, the distance from the base line to the center of gravity varied from 8 1/2 to 17 1/2 inches. This distance is "h" in the pi term $\frac{h}{D} = \Pi g$. The four levels first selected for Πg were 2.75, 3.25, 3.75 and 4.25.

Of course the position of the center of gravity of the stems shifted toward the base when seed shattered from the pods, most of which were located on the upper portions of the plants. As the plants dried during the long indoor storage period, a large portion of the seed pods opened and let the seeds fall out. After this change, a new range of values had to be chosen for Πg . The new levels were 2.25, 2.75, 3.25, and 3.75.

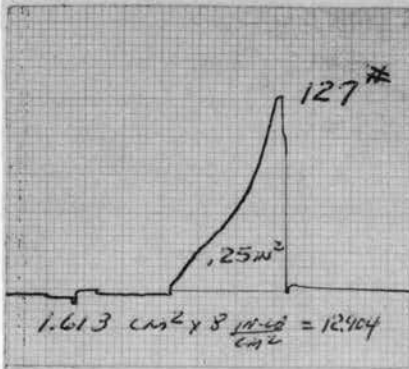
The change in the center of gravity due to seed loss was undesirable for two reasons: (1) the new center of gravity location nearer the base end of a stem was not typical of stems with a full complement of seed; (2) the loss of the seed previous to the cutting tests prevented full evaluation of the seed shattering effect of the different cutting treatment combinations. Although undesirable, this change caused stem trajectory results to be on the conservative side, for a stem with all its seed pods intact would have more of its mass concentrated near the top. This would tend to decrease the extent of motion of the top in the direction

of the cutter bar forward travel and increase the relative motion between the top and the machine catching platform.

The 2 1/2 to 3 year storage period was not anticipated when the plants were gathered. The time required to design and fabricate the cutter and test stand and to procure the necessary instrumentation to run the tests turned out to be much greater than expected. Except for the loss of seed, the stems did not deteriorate in storage, however. There was no visible evidence of decay whatsoever.

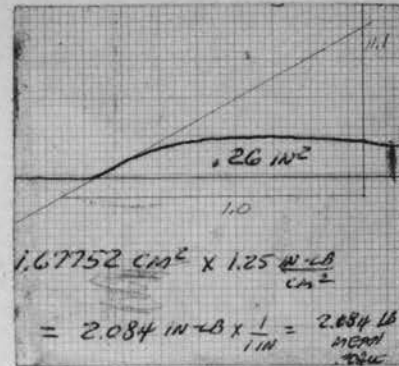
To check further against change in physical characteristics of the stems, a number of plants for the 1968 crop of Hill variety soybeans grown at the Perkins Experiment Station were gathered for comparison with the 1965 crop stems. Planted May 12, 1968, the seedlings emerged seven days later on May 19. The stems were gathered October 21, 1968, 155 days after emergence. Yield of the plot was 25.6 bushels per acre. Physical tests were run to determine shear strength and stiffness in bending of these stalks, which appeared less sound than those gathered in 1965. Figure 37 gives a qualitative comparison of results of tests on the 1965 and 1968 crop stems.

Another comparison of stalks from the two crop years was provided by using groups of stems from both in the high speed motion picture test series for the rotors fitted with sharp blades. This test series also gave limited data on seed shattering effects, since the 1968 crop plants had numerous well filled seed pods intact.



Shear Failure Curve

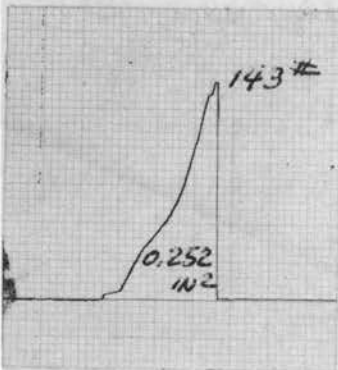
Vert. Scale: 5 lb/mm
 Hori. Scale: 0.016 in
 Load Point: 2.5 in above base



Bending Load-Defl. Curve

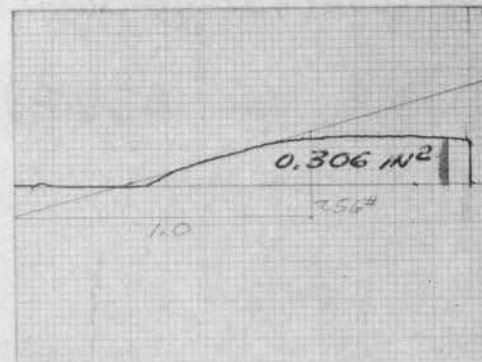
Vert. Scale: 0.5 lb/mm
 Hori. Scale: 0.025 in/mm
 Load Point: 2.5 in from base

Typical 1965 Crop Stem: 18.65% moisture (Dry Basis);
 0.2450 gms/in dry linear density, 0.208 in. avg. dia
 2 1/2 in. from base



Shear Failure Curve

Vert. Scale: 5 lb/mm
 Hori. Scale: 0.016 in./mm
 Load Point: 2.38 in above base



Bending Load-Defl. Curve

Vert. Scale: 0.5 lb/mm
 Hori. Scale: 0.025 in./mm
 Load Point: 2.38 in above base

Typical 1968 Crop Stem: 19.62% moisture (Dry Basis);
 0.2508 gms/in linear density; 0.238 in avg. dia. 2 3/8
 in. from base

Figure 37. Comparison of Physical Properties of Stems from 1965 and 1968 Crops

After 2 1/2 to 3 years in storage, the plant stems dried to a very low moisture level - about 7 to 9 percent (dry basis). It was thus necessary to reconstitute the stems and moisture in some way to learn how physical properties influenced by moisture content affected the cutting and trajectory responses.

A small environment control chamber equipped with an air conditioner and water spray inlet and with a drain outlet in the bottom was used for this purpose. A series of tests was run with the chamber to determine a way to increase moisture content of the plants in a predictable manner. The treatment found best was that of spraying a mist of preheated water (180°F) above the plant stems suspended tops down in a holding rack. The moisture content increased roughly in proportion to the period of time the stems were so treated. The nozzle used was a Delavan WDA 1.00 90°A hollow cone type. The air conditioner fan only - no refrigeration of air was involved - was used to circulate air in the chamber and thus prevent the interior walls from being saturated with water to cause structural damage. Figure 38 is an exterior view of the conditioning chamber. In the foreground is the water heater with thermostat set for 180°F water temperature. Water from the heater flows to the nozzle inside the chamber through the hose leading to the chamber top. The air conditioner unit is seen mounted in one side of the chamber. Figure 39 shows plant stems being treated inside the chamber.

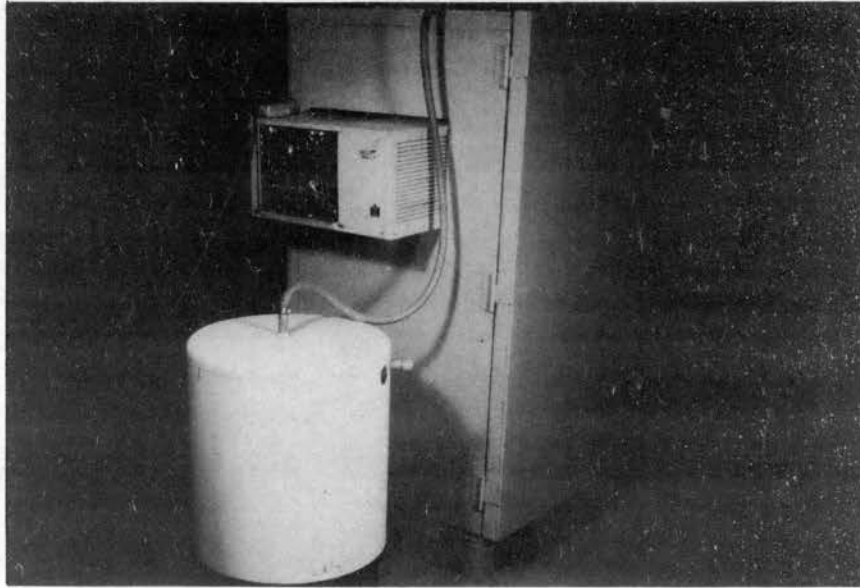


Figure 38. Conditioning Chamber and Auxiliary Equipment for Changing Moisture Content of Plant Stems

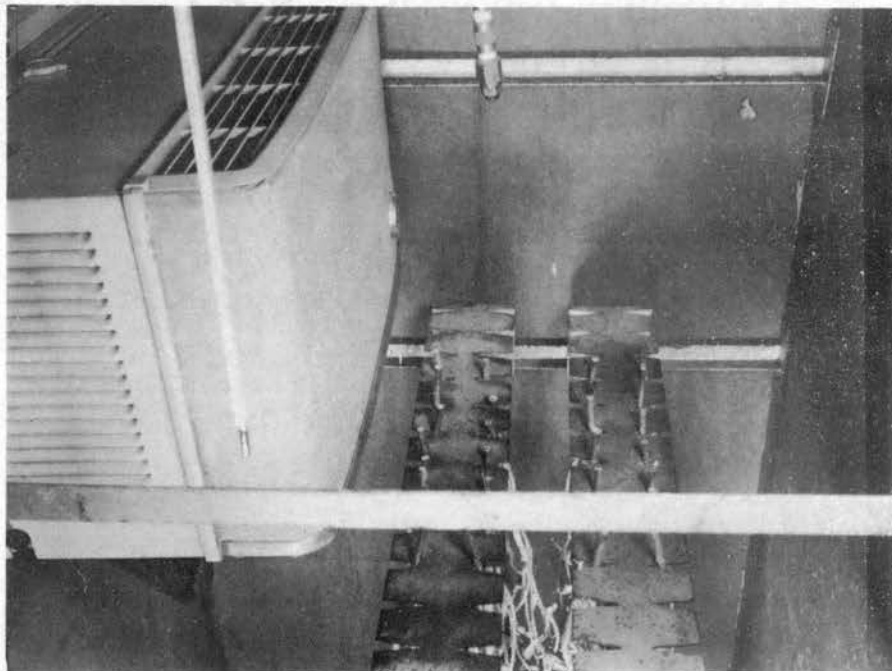


Figure 39. Interior View of Conditioning Chamber Showing Stems Subjected to Mist of Hot Water from Overhead Nozzle.

The desirable response of stem moisture content as a linear function of time of conditioning in the chamber was only partially realized, as Figure 40 (a) illustrates. The graphs show that the response varied with stem nominal diameter. Averaged over stem diameter, however, the response has a more desirable form. Figure 40(b). With a correlation coefficient of only .90 and a standard deviation of 16.27% moisture content, the results are a far cry from the optimum, but were considered the best obtainable with the equipment available. Thus, time of treating stems in the chamber was adopted as one of the controllable independent variables in place of the more pertinent variable "moisture content," which in turn would be in place of the most pertinent variable: a dimensionless combination of stem physical properties affected by moisture content.

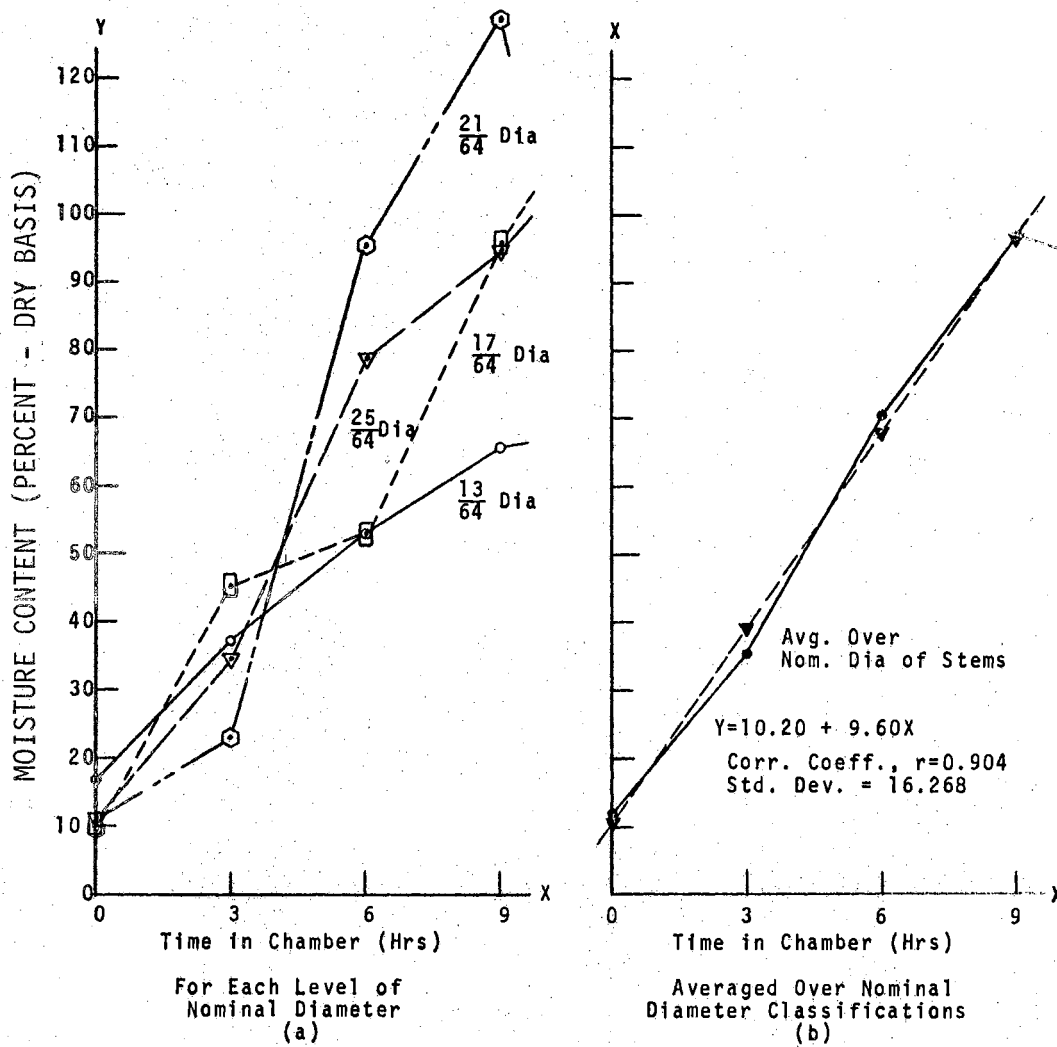


Figure 40. Moisture Content of Plant Stems versus Time in Conditioning Chamber

CHAPTER VII

APPARATUS FOR THE EXPERIMENT

The equipment needed to carry out a planned experiment is that necessary to measure the response terms, or those variables from which the response terms can be calculated, and that necessary to adjust the independent factors to the desired levels and to accurately keep them at those levels.

The response variables of interest in this study are input energy per stem cut, the maximum torque developed per stem cut, and the resultant displacement along three orthogonal reference axes of the center of gravity and cut end of the severed stem. A self contained torque transducer mounted in the rotor drive system would give a continuous readout of instantaneous torque developed. This response variable in conjunction with a readout of instantaneous angular displacement of the rotor shaft provides information for a torque - displacement plot from which both input energy per stem cut and maximum torque developed per stem cut can be obtained. Therefore a torque pickup and a rotor shaft angular displacement sensor were selected as two of the over-all specifications for the apparatus. The severed stem displacements with respect to the reference axes chosen

and illustrated in Chapter V pose additional measurement problems. The x and y displacements - in a horizontal plane - are easy enough to determine by use of a simple horizontal grid board. But the positive vertical displacement (z displacement) must be obtained while the trajected stem is in flight. For a permanent record of this response, photographic techniques prove the most direct measuring method, and their use was specified as another over-all requirement of the apparatus.

Of the ten independent factors to be screened in this investigation, three relate to the cutter design. These are rotor angle index, knife sharpness index, and ledger orientation index. As discussed in Chapter III, four rotor assemblies were built to provide the four desired levels of rotor angle index. The two desired levels of knife sharpness index were provided by the detachable blade feature of the rotors. The four desired levels of ledger tube orientation were provided by the method of attaching the ledger tube assembly to the main frame.

An additional three independent factors of the ten to be screened pertain to plant stem physical properties and were discussed in Chapter VI. These are nominal diameter of the stem, time of treatment in the moisture conditioning chamber, and height of the stem center of gravity. However, additional auxiliary equipment to measure and plot the load deflection data for shear failure and cantilever bending tests of the stems, and to determine the stem linear density,

moisture content, and average diameter at the cut section had to be designed and built as a part of the over-all apparatus requirements.

The four remaining independent factors of the ten to be investigated may be considered operating parameters. The four are rotor speed index, feed rate index, lateral position index, and cutting height index. Attaining and controlling the desired rotor speeds must be included in the requirements of the rotor drive system. Feed rate, lateral position of the plant stem relative to the ledger blade when contacted by the rotor blade, and cutting height pertain to another system, that of the mobile machine relative to the fixed plant row - in terms of prototype harvesting equipment. Considering the response variables again, the resultant displacements of the severed stem are to be measured in relation to a set of reference axes fixed to the mobile harvesting machine. Since relative motion between the plant row and the mobile machine is involved, for test purposes, this system can be designed in either of two ways: (1) keep the plant stems stationary and move the cutter assembly along a simulated row of plants or (2) keep the cutter assembly stationary and move the row of plants relative to it. Considering the equipment components available for use in this study, it was decided that better control over the independent factors could be maintained by keeping the cutter assembly stationary.

With the over-all specifications of the test apparatus determined, component parts were designed and fabricated or procured, and the components were assembled into the final test unit. Description of the resulting make-up of the apparatus falls logically under four headings: (1) The Rotor Drive System and Instrumentation for Determining Input Energy, (2) Plant Stem Carriage, Track, and Drive System, (3) Instrumentation to Determine Stem Displacement, and (4) Apparatus for Plant Physical Property Tests. For the high speed motion picture studies, additional equipment was required and will be described under the heading of Auxiliary Equipment for High Speed Motion Picture Studies.

Rotor Drive System and Instrumentation for Determining Input Energy

The rotor drive system was designed to use the speed control components and the torque pickup unit available in the Agricultural Engineering Department equipment inventory. A Master Electric Div. type DM 1/2 HP shunt wound direct current electric motor comprised the power source. A Minarik Electric Co. Model SH56EFB speed control unit supplied direct current to the armature and field windings of the motor. The controller unit has full wave silicon rectifiers for AC to DC conversion and has provision for motor speed adjustment by means of a variable autotransformer that supplies voltage to the armature rectifiers. A high degree of speed regulation is provided by a transistorized feedback

control circuit. A BLH Electronics Type A-05 torque pickup having a capacity of 500 in-lb_f was the torque sensor used.

Slip ring noise can cause errors if a torque pickup is used to measure torques below ten percent of its capacity (38). It was estimated that torque requirements to sever soybean plant stems with the helical cutter would be about 10 to 50 inch-pounds, depending on the diameter of the stem. Thus in order to use the A-05 torque pickup according to recommended practice, it was necessary to "multiply" the cutting torque before applying it to the sensor unit. To make this provision, a countershaft mounting arrangement for the sensor was designed in which the cutting torque was stepped-up by a factor of four before application to the torque pickup shaft.

The layout of the rotor drive system is shown by Figure 41. The full-load torque of the 1/2 HP electric motor was not sufficient to meet the estimated cutting torque requirements of the rotor assembly. Consequently, it was necessary to incorporate a flywheel in the drive system. And to protect the torque pickup against possible overloads, a shear bolt arrangement was included in the flywheel to torque unit drive line. The design provided for the bolt to fail at 550 in-lb_f torque. Calculations for the flywheel and shear bolt designs are recorded in Appendix A.

The torque pickup was mounted in the countershaft assembly as a floating shaft sensor with flexible couplings at each end, and it was carefully aligned such that total

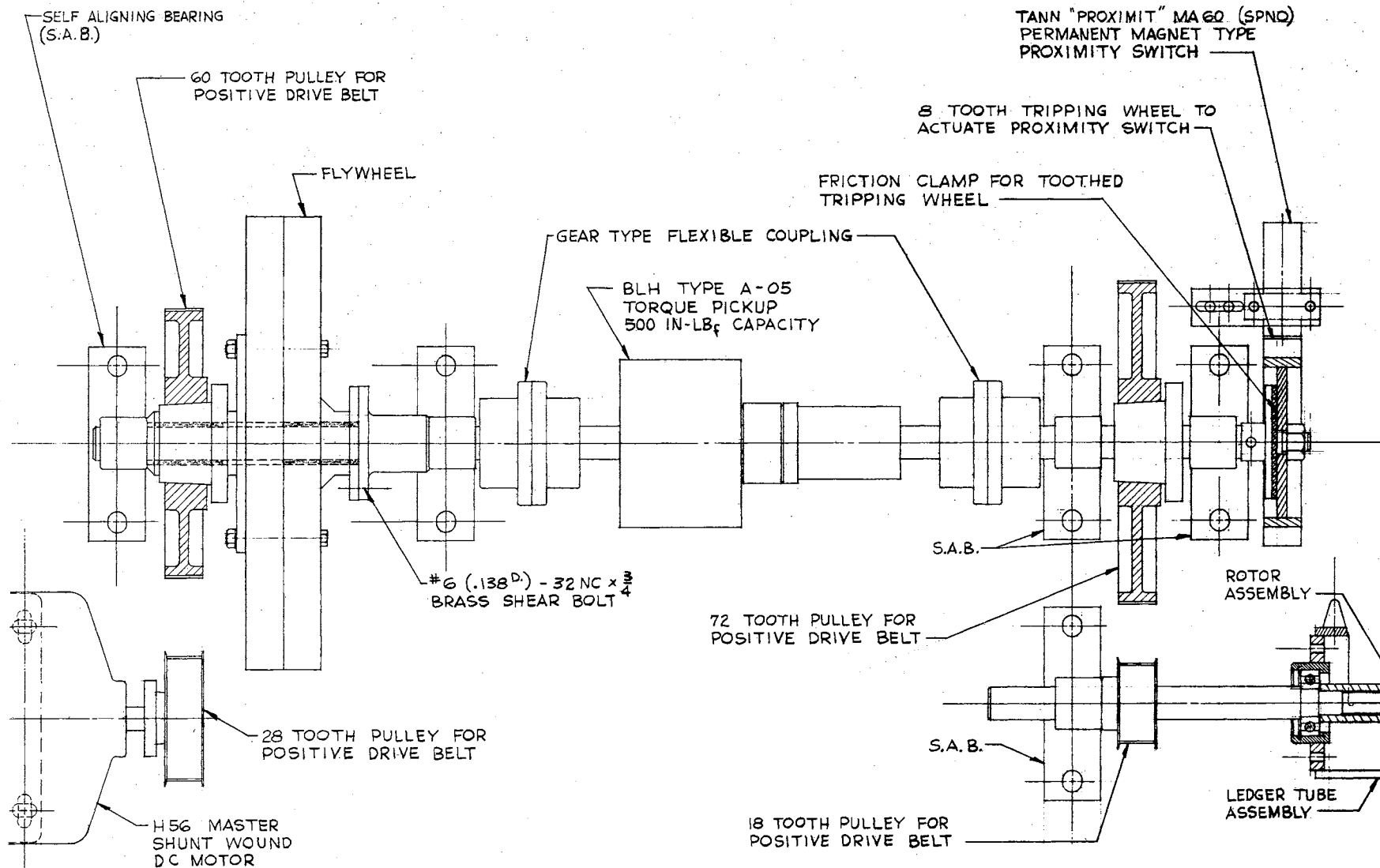


Figure 41. Rotor Drive System Layout

runout of the torque unit shaft - measured with a dial indicator on the coupling periphery - was below 0.002 inch. Worthington, 3/8 inch pitch, positive drive belts were used to transmit power from the motor to the countershaft and from the countershaft to the rotor drive shaft.

Instrumentation to measure the energy input per stem cut centered about a Sanborn Model 321 Carrier - Amplifier - Recorder. The torque pickup served as one full (four arm) resistance bridge transducer to one channel of the recorder. The second channel was used in a half (two arm) resistance bridge circuit to record rotor shaft angular position. The sensor in this circuit was a Tann Controls Co. Model MA 60 Proximit single pole, normally open, permanent magnet, proximity switch. Response time of the switch from open to close or close to open condition is less than one millisecond. A toothed wheel was used to activate the switch at each one half revolution of the rotor shaft. As shown by Figure 41, a friction clamp held the toothed wheel in position on the countershaft assembly. Thus it could be set to "trip" the switch at any position of the rotor shaft. The marker circuit of the recorder was used in conjunction with a second Tann Model MA 60 Proximit switch to monitor the velocity of the stem holding carriage as it passed below the cutter. Three lugs, spaced 18 inches apart and extending to the right of the carriage, "tripped" this switch.

The response of the recorder galvanometer writing arms was too slow to give accurate indication of instantaneous torque during the short cutting periods at high rotor speeds - 1800 to 3600 rpm. To overcome this difficulty, the monitor output signals from the two channels of the recorder were fed to the two channels of a Tektronix Inc. Type 502 A Dual Beam Oscilloscope. The single sweep feature of this oscilloscope was used to give one display of cutting torque and rotor shaft displacement during cutting. A DC signal, taken as an AC signal through an inductive coupling with the carriage velocity monitoring circuit, then rectified by a diode bridge, triggered the single sweep of the dual beams of the oscilloscope. Thus the oscilloscope was triggered when the proximity switch tripping lug at the front of the carriage passed under the rotor and cutting was imminent. A Hewlett-Packard Model 197 A Oscilloscope Camera with a Polaroid Land Camera back was used to record the traces of a single sweep of the oscilloscope dual beams.

Figure 42 presents a schematic diagram of the instrumentation system. Figure 43 is a photograph of the rotor drive system showing the torque, shaft angular displacement, and the carriage velocity transducers. Figure 44 shows the rotor drive speed controller (in foreground), the carrier-amplifier-recorder, and the dual-beam oscilloscope with the camera attached.

The no load torque signal from the torque pickup showed cyclic variation of the same frequency as the countershaft

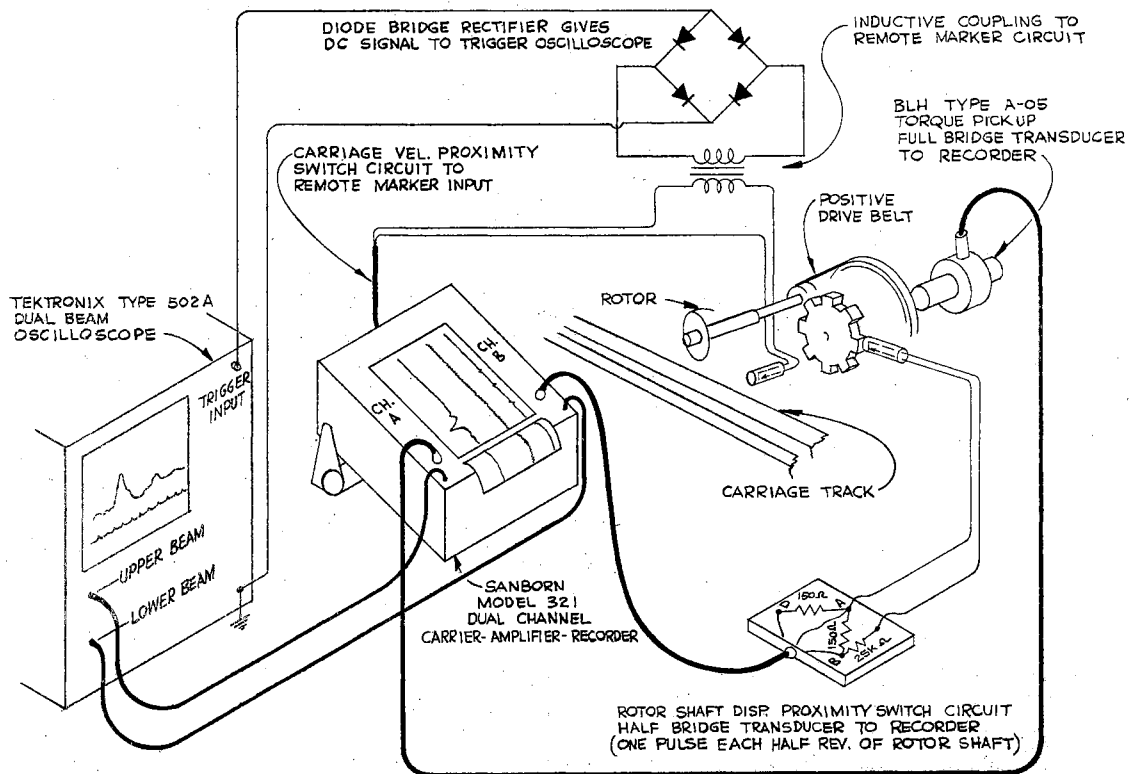


Figure 42. Schematic Diagram of Instrumentation for Monitoring Instantaneous Torque, Rotor Shaft Displacement, and Carriage Velocity

rotational speed. The magnitude of this cyclic variation went as high as 2 in-lb_f peak to peak at some rotational speeds. Extensive experimentation was carried out in an attempt to "smooth out" these effects. First the rotational torque of each of the six bearings (other than the motor bearings) in the drive assembly was checked and those indicating the highest torque were replaced. Then recordings of the cyclic effect were made over a speed range from 500

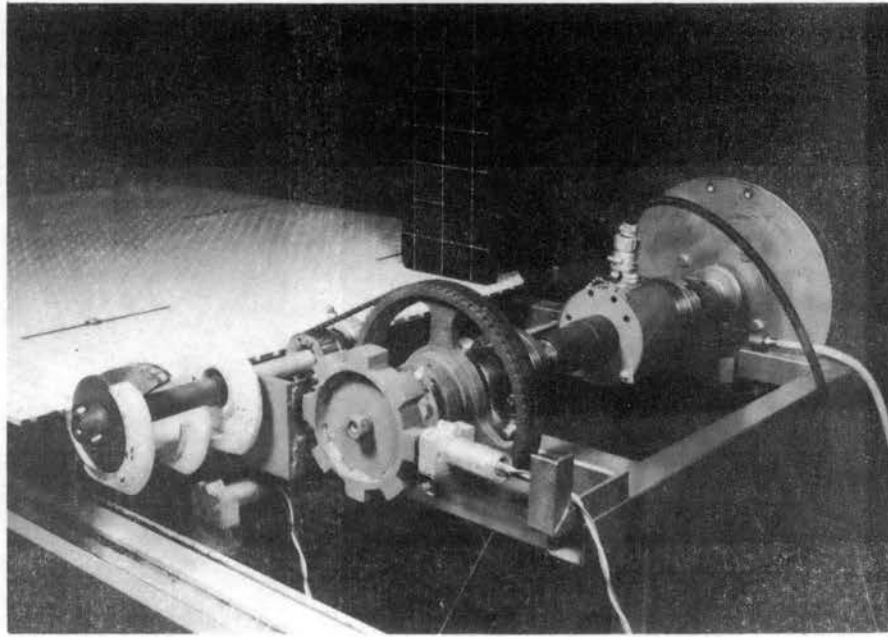


Figure 43. Rotor Drive System and Associated Instrumentation

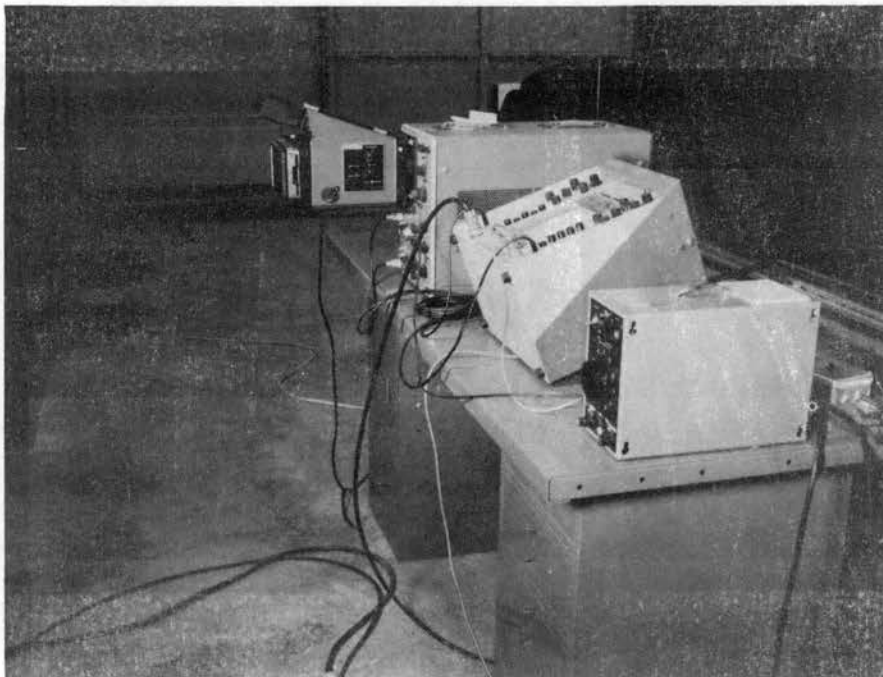


Figure 44. Rotor Drive Speed Controller (In Foreground), Carrier-Amplifier-Recorder, and Dual Beam Oscilloscope and Camera

to 3600 rpm. The cyclic variations were attributed to torsional vibration of the rotational system and thus would be related to the natural frequencies of the system. It appeared that the variation was greatest when the cutter rotational speeds were 900, 2700, and 3600 rpm. To lessen the variation, the first rotor speed range selected for test, 900 through 3600 rpm, was revised to a new range of from 1800 to 3600 rpm.

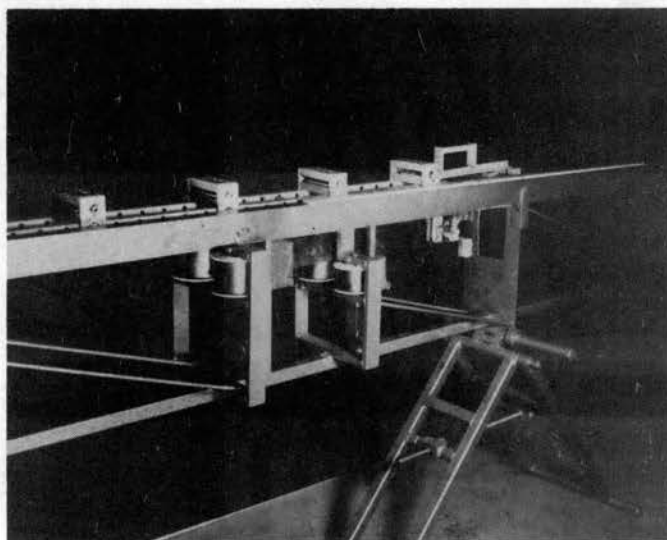
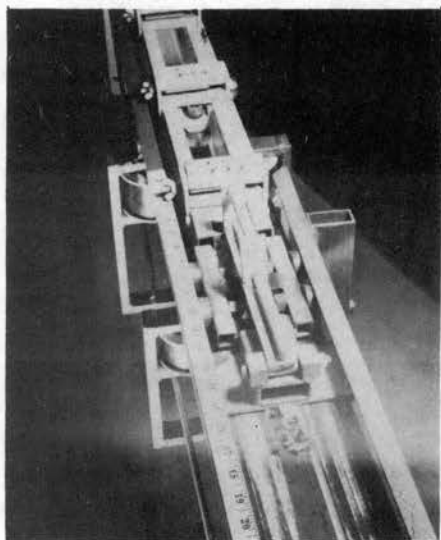
Plant Stem Carriage, Track, and Drive System

To accurately control the velocity of plant stems as they were moved through the cutting zone (simulating the forward velocity of a harvesting machine moving through the field), it was decided to isolate accelerating loads from the carriage drive system and to use flywheel effects to smooth out any speed variations due to cutting loads transmitted by the plant stems before they were completely severed. Thus the carriage drive system was designed in three parts: acceleration section, constant velocity section, and deceleration or braking section. In the acceleration section, Hunter Spring "Neg'ator" constant force springs were used to provide the carriage accelerating energy. Two sets of springs were used, and the spring attaching arm of the accelerating dolly was designed to allow coupling to either set individually or to both sets simultaneously. Constant forces of approximately 48, 80, and 128 pounds

thus were available to act on the dolly and carriage. With an accelerating distance of up to 39 inches, in increments of approximately 1/4 inch, the carriage could be brought to any desired velocity up to 20 mph. A winch, release handle, and ratchet lock were used to "load" the dolly-carriage system. Kinetic energy of the dolly was absorbed by having it impact against thick rubber bumpers faced with metal plates. Arriving at a suitable bumper design required much trial and effort.

Figure 45(a) shows the carriage, dolly, release lever arrangement when the system is ready to be "loaded" by the winch. Figure 45(b) shows the system with both sets of springs attached to the dolly arm and extended to a "loaded" position. Figure 46(a) is an action shot of the carriage and plant stems being accelerated by the 80 pound spring set. Figure 46(b) illustrates the dolly in "home position" after the carriage has traveled on down the track.

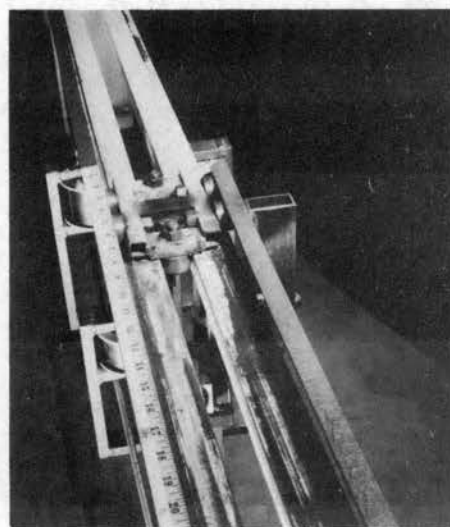
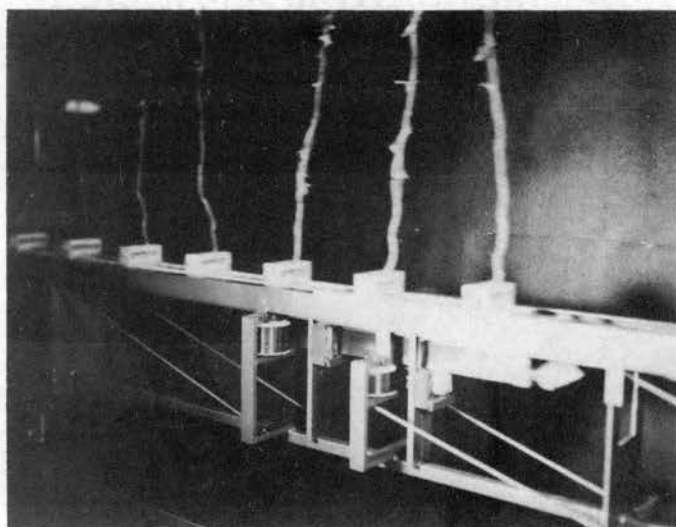
The constant velocity portion of the carriage drive system had as its chief component a 236 pitch length of Rex C-2059, 1 1/4 inch, double pitch, hollow pin, carrier roller conveyor chain. Extended over two 20 tooth 7.991 inch pitch diameter sprockets spaced 135 inches apart, the chain rollers were supported on a frame member. Hardwood block guides were added on each side of the chain - for both its top and bottom lengths - to restrain its side movement and confine each roller to a straight line path.



(a)

(b)

Figure 45. Carriage-Dolly-Release Lever System (a) Ready To Be Loaded by Winch (b) In Loaded Position



(a)

(b)

Figure 46. (a) Carriage-Dolly System Undergoing Acceleration by Action of 80-Pound Spring Set; (b) Dolly in Home Position

Two spring loaded pawls, one at each end of the carriage, engaged the chain rollers to drive the carriage at chain velocity. The pawls were designed to override the chain rollers if the carriage were traveling at a higher velocity than the chain.

Energy input to the chain drive was provided by a 1/2 HP. AC electric motor through a Graham Variable Speed Transmission. Output from the Graham unit was infinitely variable from 0 to 230 rpm. A radius arm arrangement (to allow raising and lowering the track without disturbing the drive) of 84 pitches of No. 40 (1/2 inch pitch) roller chain connected the Graham variable speed output to the carriage drive chain input. A speed step-up ratio of 4.286 was employed. The carriage drive input shaft was equipped with two 8 1/2 inch diameter by 1 inch thick steel flywheels symmetrically placed on either side of the main drive sprocket.

The deceleration section of the carriage drive system consisted of a braking frame which latched to the front of the carriage when impacted by it and which was free to move rearward with the carriage except for the opposing force of two 16.5 pound constant force springs. Figure 47 presents a rear view of the test stand which shows in the foreground the braking frame assembly and the constant force springs which provide the braking force. Figure 48 shows the carriage latched to the braking frame after deceleration.

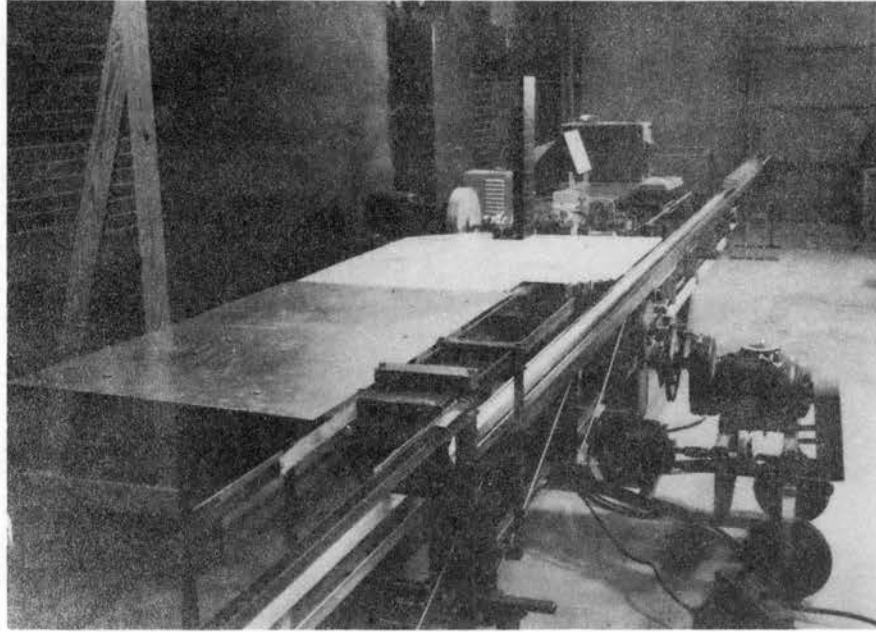


Figure 47. Rear View of Test Stand Showing Braking Frame Assembly

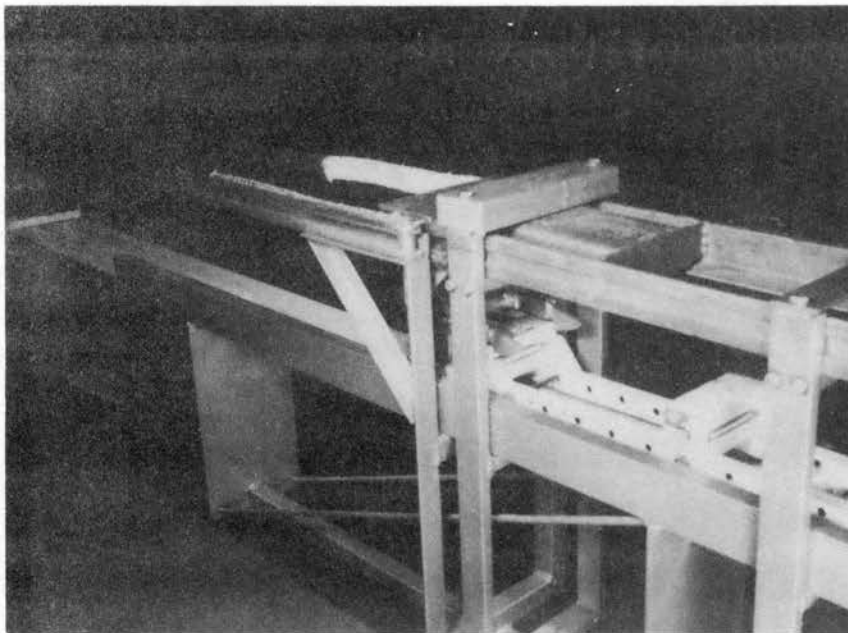


Figure 48. Carriage Latched to Braking Frame After Deceleration

The carriage proper consisted of a structure, six feet in length, made principally of 3/4 inch square steel tubing. Attaching holes were provided for locating stem clamping blocks at 1 1/2 inch intervals along its length. Four 1 1/4 inch diameter cam follower rollers were the wheels of the carriage. Two additional cam follower rollers of the same size but mounted vertically constrained the carriage laterally in the guiding track. Three proximity switch tripping lugs extended from the right side of the carriage. These were mounted 1.5 ft. apart. Figure 49 shows the carriage construction. Figure 50 is a cross section of the carriage and its guiding track. This illustration also shows the method employed to clamp plant stems in the carriage blocks.

To provide adjustment to the desired levels of cutting height index and lateral position index, the entire carriage track assembly was made adjustable vertically and laterally with respect to the cutter rotor. The track was designed in three sections: front (accelerating section), center (constant velocity section), and rear (decelerating section). The center section was the main section, and lateral and vertical adjustment were built into it. Each end section had auxiliary supports with vertical adjustment only. For lateral adjustment, the vertical supports were slid across the floor. The center track section was attached to the main frame by a track support beam assembly. The beam assembly moved up and down on two circular columns of the main frame by means of linear bearings. A screw and

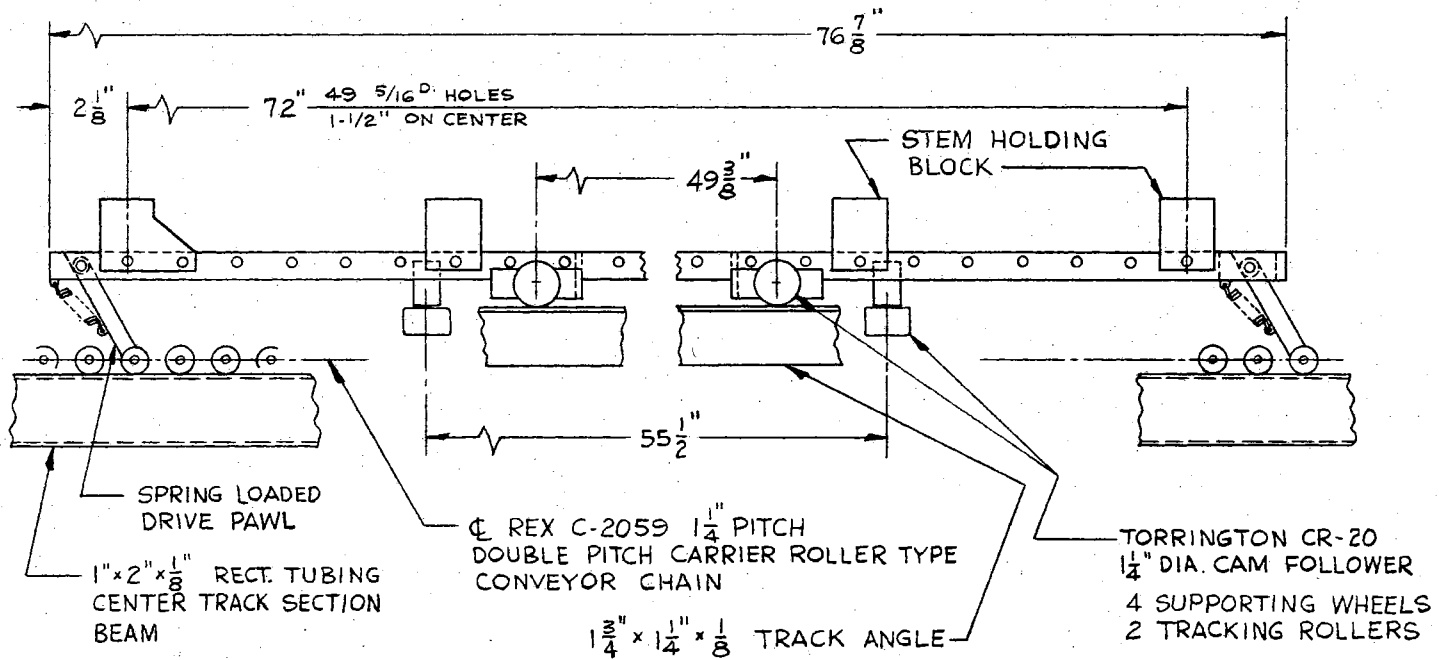


Figure 49. Details of Carriage Construction

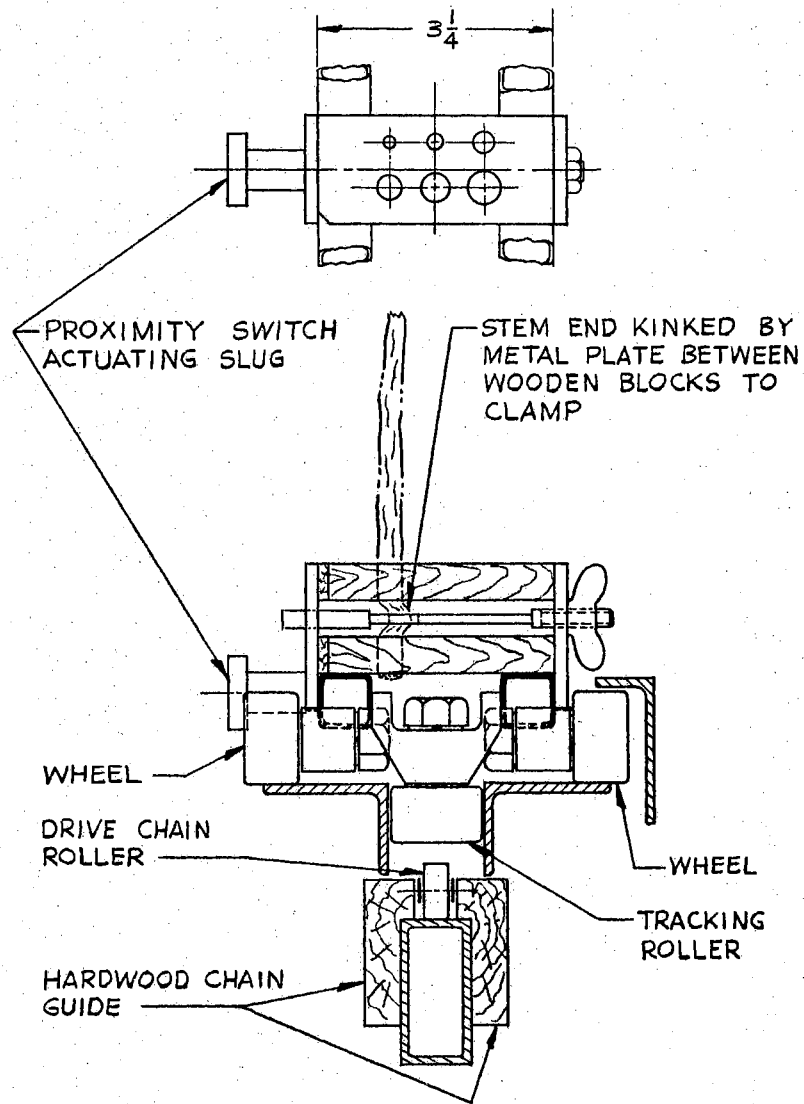


Figure 50. Cross Section of Carriage and Track

adjusting handle, centered between the two support columns raised and lowered the beam. The beam assembly had three equally spaced pins, each two inches in diameter, on which sleeves of the center track section mounted. A screw and handle assembly through the center pin provided lateral adjustment of the track section on the pins. Set screws were used to clamp the two end sleeves on the pins at desired lateral locations. Figure 51, an overall view of the center track section, shows the construction.

Instrumentation to Determine Stem Displacement

With respect to the reference axes chosen (Figure 33, Chapter V), the X and Y displacements of the center of gravity and the cut end of a severed stem were read from a grid board. A horizontal plane through the rotor shaft center line contained the top surface of the grid board. It was approximately 3 ft. wide by 4 ft. long and was made from a perforated, wood composition panel 1/4 inch thick. The perforations were one inch on center. These holes were used as guides in scribing the grid lines on the board, the grid lines being 1/2 inch apart in both the X and Y directions. The grid board was attached to the main frame of the test stand through slotted holes. This attaching method provided for adjusting the same base or "zero" reference line to the simulated plant row center when the lateral position of the row with respect to the ledger blade was

changed as called for by the experimental plan. At the higher rotor speeds and feed rates, the severed stems were often trajected past the original grid board. Consequently, a sheet metal table "extension" was constructed to increase the area of the board. Figure 52 illustrates the original grid board and the extension to it, also the vertical grid board used.

The vertical grid board, with a height of 24 inches and a width of 6 inches, had graduations 2 inches apart. The grid lines were scribed and filled in with white ink mixed with a fluorescent powder. A Graflex Inc. Graphic View II camera with a Polaroid Land Model 500 4 x 5 inch film holder back was positioned to the front of the vertical grid board as shown by Figure 53. The camera had a 135 mm f/1.4 lens which was fitted with a Kodak 2B filter. This filter would pass only fluoresced ultraviolet light; reflected ultraviolet light was blocked. A Black Light Eastman Corp. Model B-100 Spectroline long wave ultraviolet lamp with a spot bulb and filter was used to incite fluorescence of the 2 inch spaced grids of the vertical grid board and of the center of gravity and lower ends of the plant stems, these areas of the stem having been coated previous to each test with a slurry made from fluorescent powder and water. The tests were run in a darkened room, and a time exposure of the stem trajectory made on the film due to the fluorescence of the slurry coated areas when activated by the ultraviolet light beam. The lamp used a high pressure mercury vapor

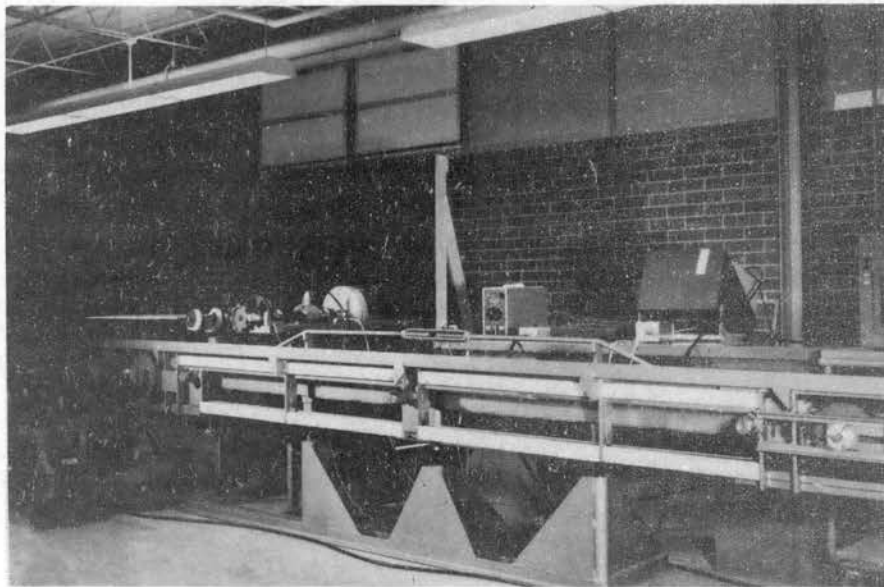


Figure 51. Overall View of Test Stand Showing Construction of Center Track Section

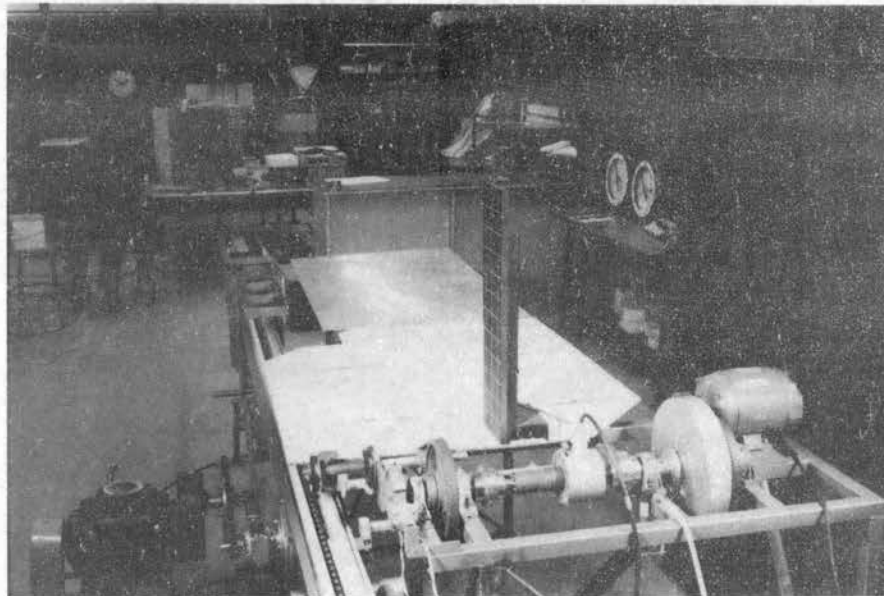


Figure 52. Front View of Rotor Drive System and Horizontal and Vertical Grid Boards for Determining Stem Displacements

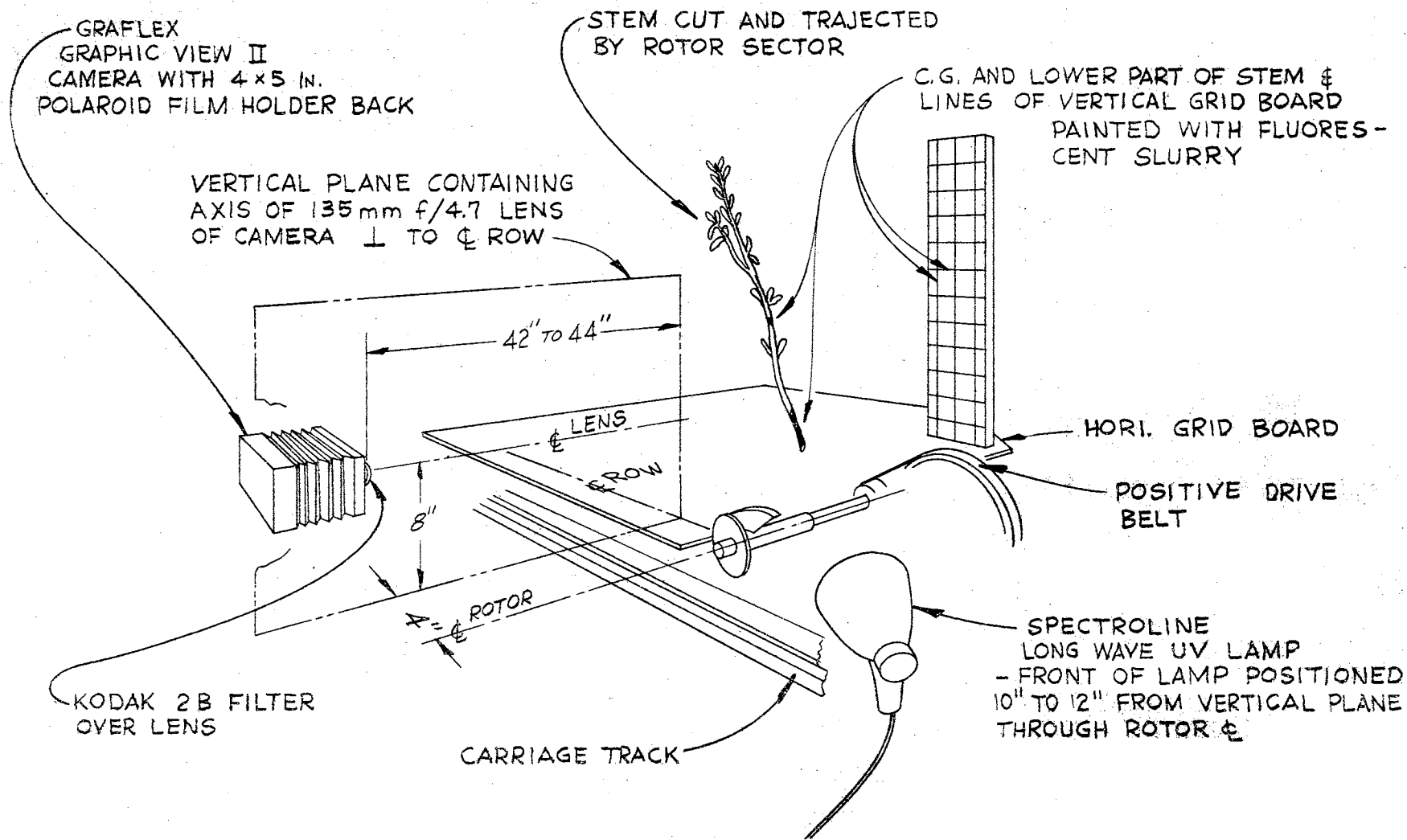


Figure 53. Equipment Arrangement for Photographing Vertical Displacement Trace of Severed Stems

bulb rated at 100 watts and operated on 115 volt, 60 cycle, AC power. Figure 54 is a photograph of the equipment setup.

Apparatus for Plant Physical Property Tests

A stem testing machine utilizing the cross feeds and precise way alignment of a 16 inch engine lathe was built to determine the shear failure and cantilever bending load-deflection curves of the plant stems. The frame of the testing machine was made of aluminum to avoid marring the lathe ways on which it was aligned and clamped. The load was applied to the stems by means of a ram attached to the compound rest cross slide of the lathe. Since the velocity of the cross slide was constant regardless of the applied load, deflection measurement was determined by the cross slide and recorder chart velocities. Suggs and Splinter (39) measured deflection for load-deflection tests of tobacco plant stems in a similar manner. An axial load cell was fabricated by machining a steel strap to a thin cross section and attaching two etched-foil, paper backed BLH Corp. strain gages. An identical part with two of the same strain gages attached served as a dummy gage assembly for temperature compensation. The four gages were wired in a 4 leg resistance bridge circuit such that bending loads on the load cell had cancelling effects, and only axial loads were measured. This transducer circuit coupled to a Sanborn Model 321 Carrier-Amplifier-Recorder produced the load-deflection curves of interest.

Figure 55 is a photograph of the testing machine, recorder, and an oscilloscope with camera that provided for greater resolution of the curves for smaller stems. It was found that the oscilloscope and camera were not needed for the tests of this study, however. Figure 56 provides a schematic diagram of the testing machine.

The lathe had 3 spindle speeds and 48 lead screw feeds such that 144 cross slide constant velocities were available to drive the testing machine ram. A computer program was written to calculate and print out each of these available velocities.

A wide range of loading rates have been employed by other investigators studying physical properties of plant stems. McClelland and Spielrein (17) used a rate of 9.45 inches per minute in applying bending loads to stems of alfalfa, ryegrass, wheat, and oat plants. Prince (18) employed a loading rate of 1.5 inches per minute in bending alfalfa, timothy, and oat stems. Suggs and Splinter (39) loaded tobacco stems in bending at a rate of 0.2 inches per minute. Halyk and Hurlbut (40) used a loading rate of 1 inch per minute in bending and shear tests of alfalfa stalks. This rate was adopted for the tests "because it approximated the ASTM standard breaking time for textile yarns."

The cross slide velocity that came closest to a one inch per minute loading rate, that of 0.9694 inches per minute, was selected for use in the shear failure tests. For the cantilever bending tests, a cross slide velocity of

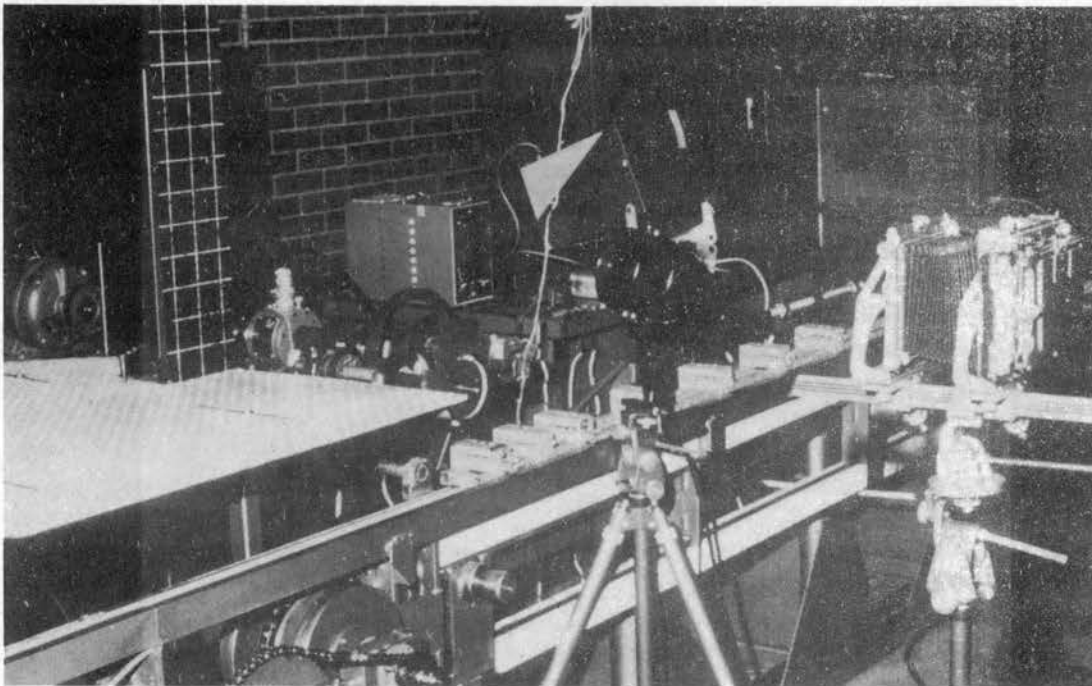


Figure 54. Photograph of Equipment Used to Record Stem Vertical Displacement

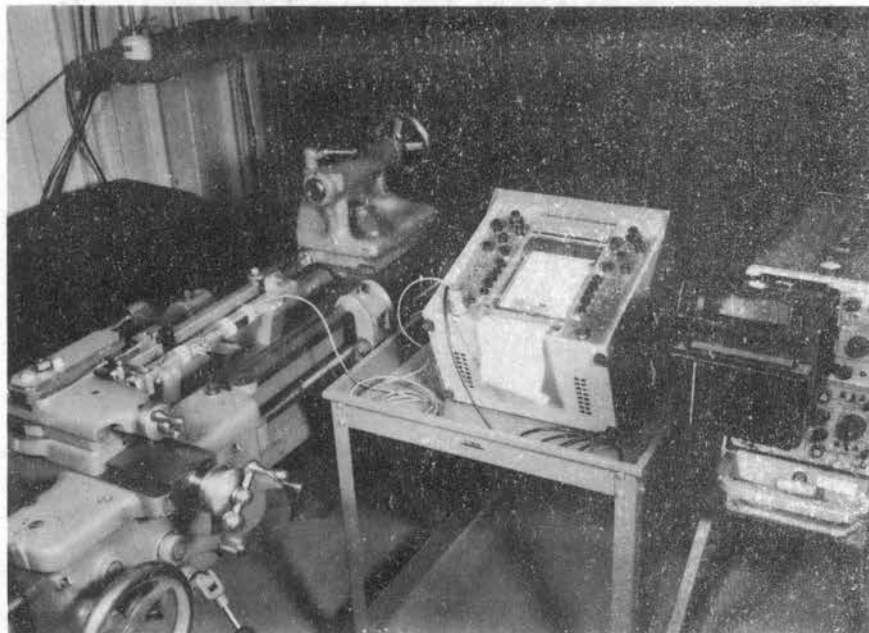


Figure 55. Stem Testing Machine and Load-Deflection Curve Recording Instruments

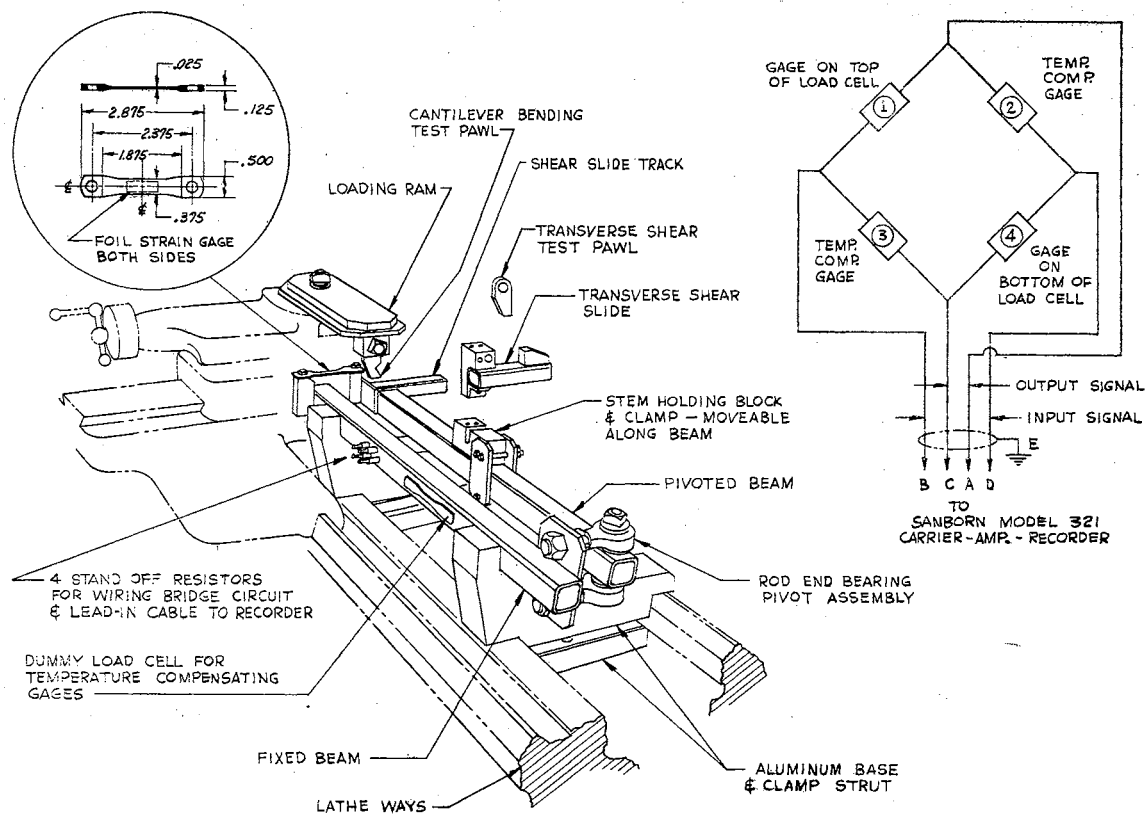


Figure 56. Schematic Drawing of Stem Testing Machine

7.4419 inches per minute was selected because its use, along with the use of a 5 millimeter per second recorder chart speed, gave a convenient chart deflection scale: 1/4 inch deflection per centimeter graduation on the chart.

To determine linear density and moisture content of the stems tested, it was necessary to accurately cut a specified length from the stem for weighing, drying, and reweighing. This was accomplished by using a 60 tooth saw, 1 1/2 inches in diameter and 0.023 inch thick, manufactured by the Chicago Wheel Co. and driving it at 10,000 rpm by a

1/4 HP Dumore Inc. universal electric motor. The saw and its drive assembly were included in a test fixture which also had a stem holding clamp and locating collars to allow sawing exactly one inch lengths from a plant stem. This fixture was patterned after one designed by Bartok and Prince (41). Figure 57 shows the stem specimen sawing apparatus.

The one inch stem specimen were weighed on a Mettler Model H6 Analytical Balance and were dried in a controlled temperature oven manufactured by Precision Scientific Co.

The method used to determine the average diameter of a stem cross section was to cut out a disk of the stem about 1/8 inch thick near the section of interest using the stem specimen sawing apparatus previously described. The bark was sanded from the disk and the pith removed from the center of the disk. The disk shaped cross section then was placed in the viewing field of a Wilder Optical Co. Model AF Micro Projector. The image projected on the viewing screen was magnified by ten. Kodak Kodabromide F5 photographic paper was exposed to the image (in a darkened room) for three seconds. The exposed photographic paper was placed in a light tight box and taken to a film processor for developing. Figure 58 shows three stem cross sections with identifying symbols in the viewing field of the micro projector.

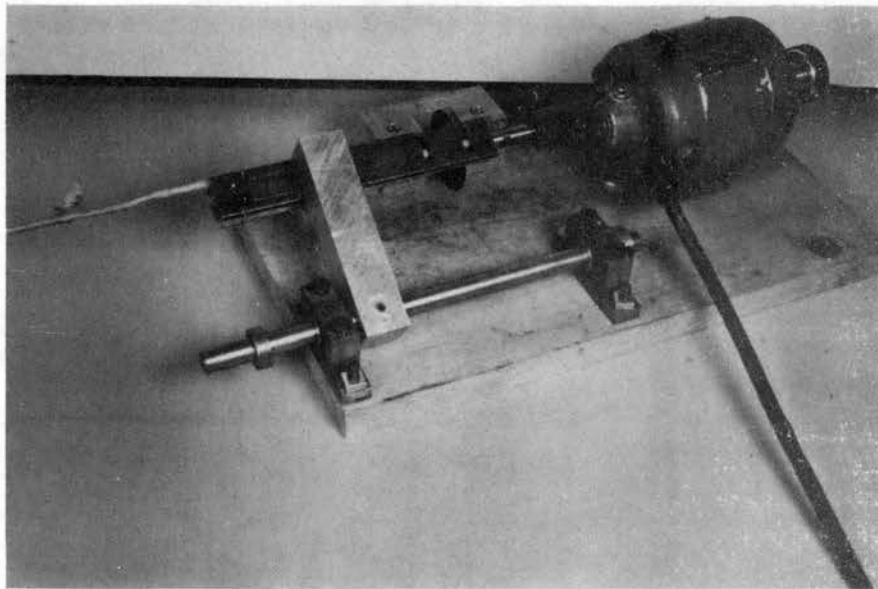


Figure 57. Saw and Fixture for Cutting One Inch Lengths from Test Stems

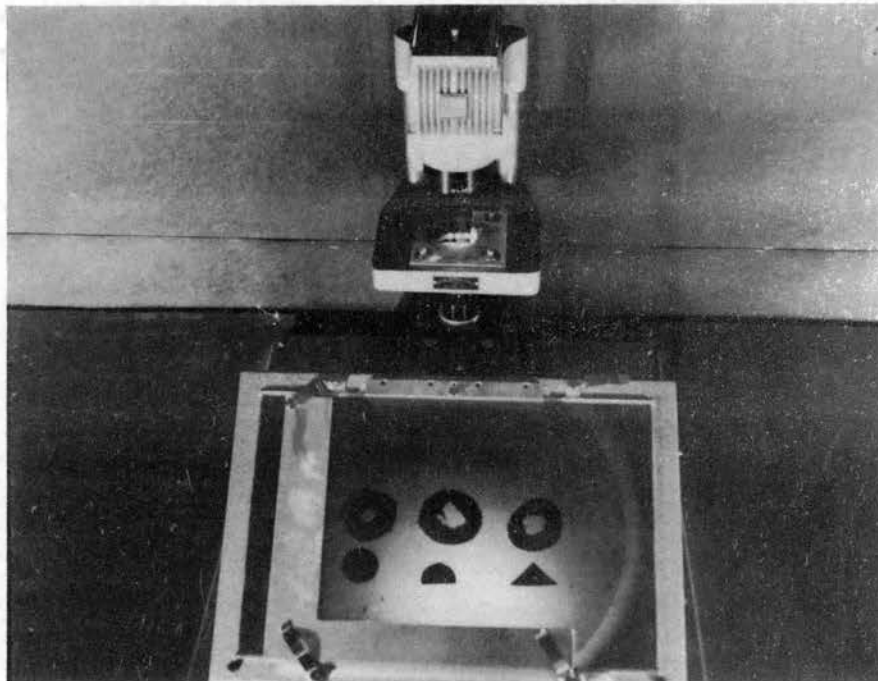


Figure 58. Stem Cross Sections on Micro Projector Ready for Images To Be Recorded on Photosensitive Paper

Auxiliary Equipment for High Speed Motion Picture Studies

A Fastax camera, Category I - WF 3 model, manufactured by Revere-Wollensak Division of the 3M Company, comprised the chief item of equipment for the high speed motion picture filming. This camera used 100 foot rolls of 16-mm film. A superior Electric Co. Powerstat variable transformer, model 116B, provided the input voltage to drive the camera. Maximum output of the transformer was 140 volts AC, which gave a maximum mean picture frequency:

("Mean picture frequency refers to the picture frequency at the midpoint of the usable film strip, or about 60 feet from the beginning of the film." (42))

of about 4800 frames per second. The camera was equipped with two neon lamps for placing timing and event marks on the outboard and inboard sides respectively of the film. A model 3106A Wollensak Pulse Generator was used with the outboard neon lamp to place a timing mark on the film each millisecond. Every tenth pulse from this unit had a duration of 100 microseconds compared to 30 microsecond duration for the other pulses. This feature resulted in every tenth timing mark on the film being wider in extent and assisted greatly during micromotion analysis of the film. A circuit including the rotor shaft position indicating proximity switch and toothed "tripping" wheel was designed to supply the inboard neon lamp with a signal for each half revolution of the rotor shaft. These resulting marks on the film,

in conjunction with the timing marks, were used to check rotational speed of the cutter.

A switching circuit was devised to automatically turn on the camera at the proper time so that it was up to speed by the time cutting of the plant stems began. A maintained contact, single pole, double throw, snap action switch with a roller leaf actuator was operated by a cam fixed to the carriage to close the contacts of a switching relay. The heavy duty contacts of the relay closed the circuit on the secondary or output side of the variable transformer to provide operating voltage to the camera. The snap action switch operated by the carriage was clamped to the track and thus could be positioned at different distances from the cutter rotor. With this arrangement, the start-up time for the camera could be held to desired values regardless of the carriage velocity - which changed with changes in rotor speed and feed rate indices.

Two different lens assemblies were used in the Fastax camera for the motion picture studies. To photograph the cutting action, a 152 mm f/2.7 lens was the objective lens; to photograph the severed stem trajectory, a 35 mm f/2.0 lens was the objective lens.

The minimum subject to camera focal plane distance for the 155 mm lens is about 72 inches. To obtain this distance in filming the rotor cutting action, and still retain the object framing desired, a camera tripod mounting stand was built. For filming the severed stem trajectory, a background screen, constructed of tar paper (15 lb. weight black felt paper) was used as recommended by Hyzer (43).

A flat mirror, set at a 45 degree angle with the plant row center line was included in the field of view of the camera lens when filming the stem trajectories. This provided a view of the motion of the stems transverse to the row center line which otherwise would not have appeared, since the lens axis was perpendicular to the row center line. The mirror was not mounted in line with the camera lens axis, however; so that the view was not a true one - distances appeared foreshortened.

Two Wollensak WF 323 high intensity incandescent lamps, made especially for high speed motion picture filming, provided the principle lighting source for taking the motion pictures. Additional No. 2 Superflood EBV incandescent lamps were used to increase the available light; but their effect was minimal, especially in the trajectory filming sequences, where there was a severe need for additional illumination.

Figure 59 shows a schematic diagram of the equipment setup for the high speed movie filming. Figure 60 is a photograph of the setup for filming the cutting action; Figure 61 is a view from the camera position of the arrangement for filming the stem trajectories.

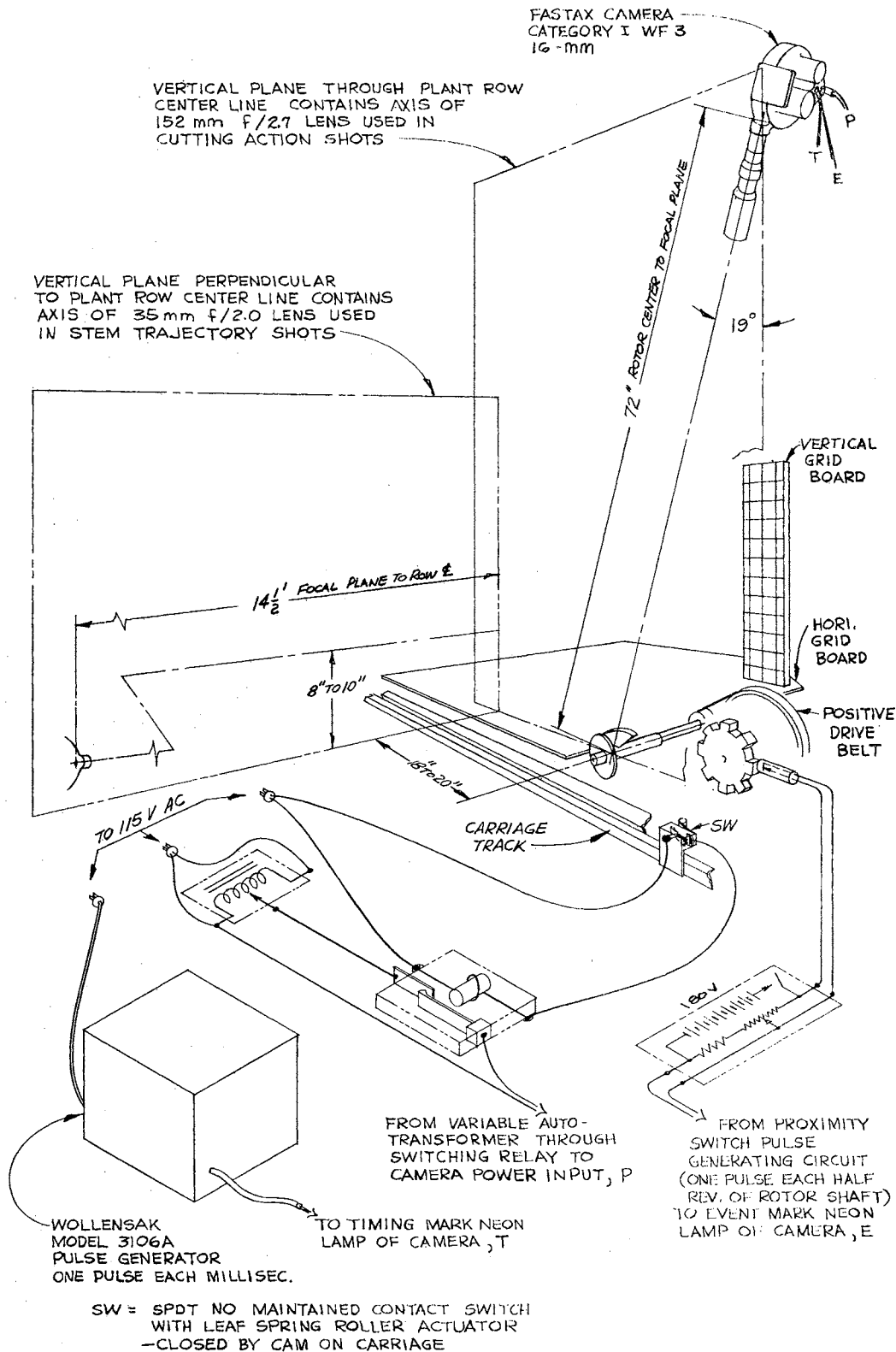


Figure 59. Schematic Diagram of Equipment Arrangement for Filming High Speed Motion Pictures of Cutting Action and Stem Trajectory.

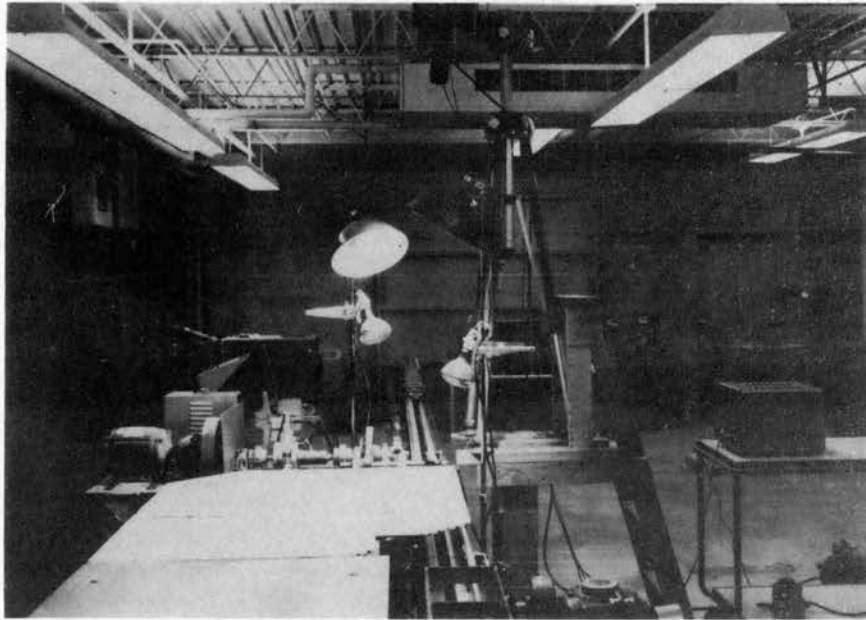


Figure 60. Camera Location and Equipment Arrangement for Taking the Cutting Action Films

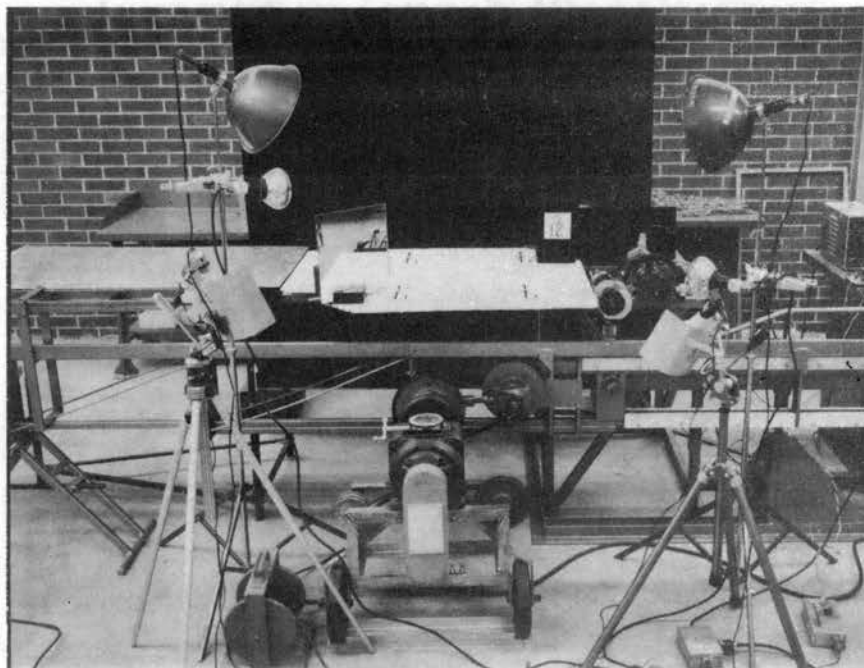


Figure 61. Equipment Arrangement for Stem Trajectory Filming as Seen from Camera Location

CHAPTER VIII

EXPERIMENTAL PROCEDURE

For this investigation, experimental procedures relate to calibration of the equipment, to data taking, and to reduction of the raw data to a form suitable for analysis.

Calibration of Equipment

Speed of the cutter rotor and of the carriage propelling chain drive sprocket were adjusted to desired levels by use of a General Radio Co. type 1531-A "Strobotac" electronic stroboscope. Before each check of speed adjustment, the stroboscope was calibrated to line frequency at the high and low dial settings recommended by the manufacturer. The accuracy of the instrument is supposed to be $\pm 1\%$ of the dial reading after calibration. Consequently, the rotor and carriage velocities are believed to have been maintained at least within $\pm 2\%$ of nominal values.

The velocity of the carriage resulting from acceleration by the constant force spring assembly was synchronized to the velocity of the carriage propelling chain by a preliminary series of trials. A computer program was written to calculate the theoretical velocity of the carriage at the end of the acceleration action by the 48, 80, and 128 lb_f.

spring combinations for one inch increments of spring deflection up to 42 inches total deflection. The work-energy method of analysis was used in making the calculations. By accurately weighing component parts of the carriage and typical plant stems, the mass of the carriage with stems in place was estimated to be 25 lbs_m. This value was used in the calculations. The print out of the computations provided initial settings for trial. The carriage velocity monitoring instrumentation, described in Chapter VII, was used to check the carriage velocity just before it engaged the propelling chain for the constant velocity portion of its travel. Adjustments were made in the spring deflection distance until the velocity of the carriage at the end of its accelerating period just matched the propelling chain velocity specified in the experimental plan. The required spring deflection distances were marked along the top surface of the side guide angle of the track assembly to complete the calibration. An index mark on the carriage was brought in alignment with the correct calibration mark for a given carriage velocity by means of the loading winch. When released at this position, the accelerating dolly attached to the constant force springs acted on the carriage to bring it up to the chain velocity. Engagement of the carriage pawls with the propelling chain rollers was a very smooth action, as a result.

For a given velocity, the lowest spring force (and, conversely, the longest deflection distance) that could

accelerate the carriage up to speed within the total accelerating distance provided was selected for use. This kept the magnitude of the acceleration at a minimum to avoid inducing motion of the plant stems mounted in the carriage blocks. The highest carriage velocity used in the tests, 26.25 ft. per sec. for a feed rate of 5.25 inches per revolution at 3600 rpm rotor speed, was attained in an accelerating distance of just under 3 1/2 ft. by use of the 128 pound spring combination. The resulting acceleration magnitude was approximately 100 ft./sec.² or just over 3 g's. This acceleration induced no vibratory motion of the plant stems, judging from the high speed motion picture films showing the stems as they approached the cutting zone.

A summary of the various rotor and carriage velocities used in the experiment and of the spring size-deflection combinations required to accelerate the carriage to propelling chain velocity are recorded in tabular form in Appendix B.

To calibrate the recorder and oscilloscope response deflections to torque pickup output, a static or "dead weight" calibration procedure was adopted. A balanced, symmetric lever was constructed to attach to the rotor drive shaft. The lever was designed with a support beam for mounting standard slotted kilogram weights, like those used in soils testing laboratories, at a distance of 2.835 inches from the shaft center. See Figure 62. A one kilogram weight mounted

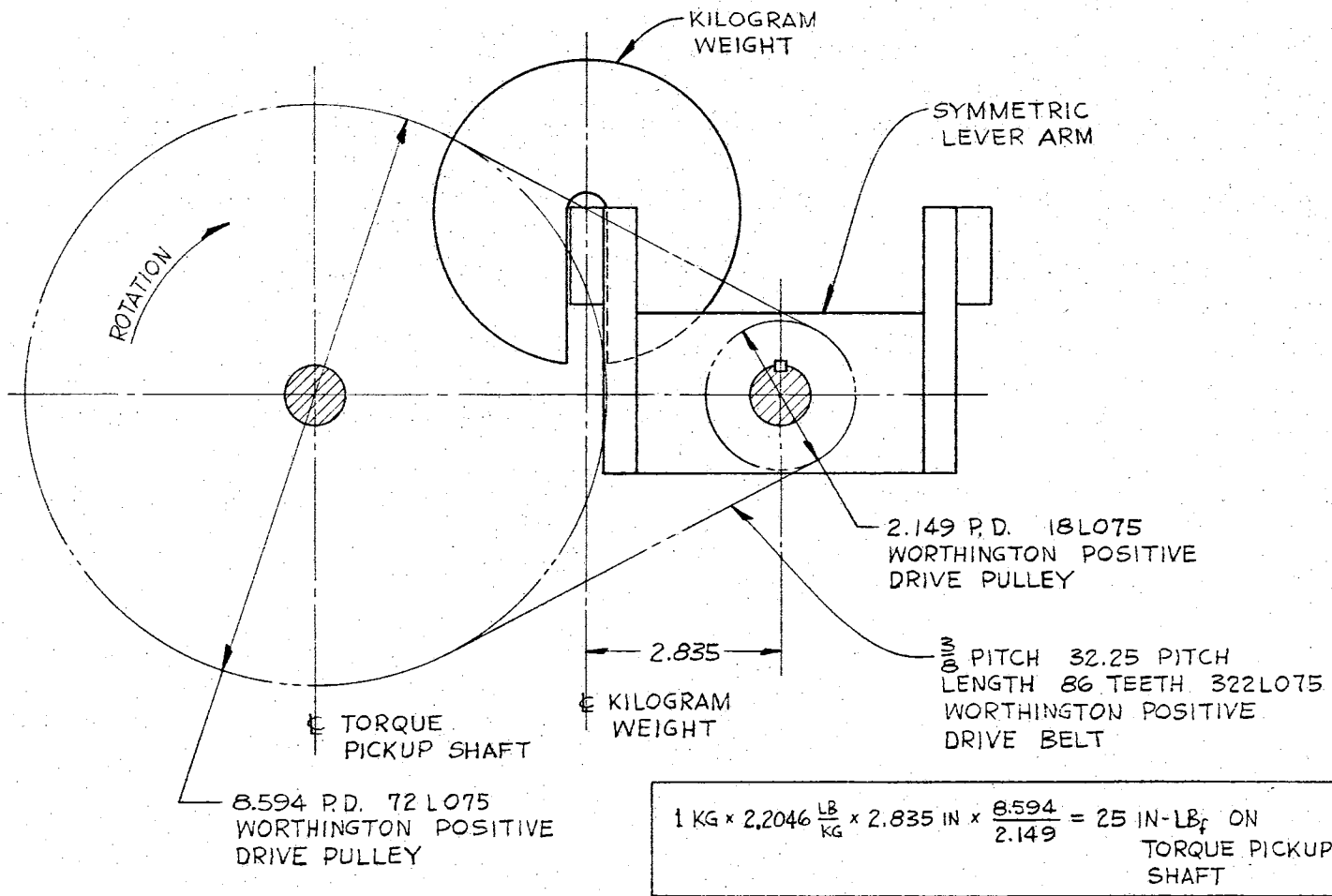


Figure 62. Dead Weight Calibration of Torque Pickup and Recorder System

on the support beam, such that its center of mass was 2.835 inches from the rotor shaft center, would apply a torque of 6.25 in-lb_f to the rotor shaft, and a torque of 25 in-lb_f to the countershaft containing the torque pickup. The mass of each kilogram calibration weight used was checked on an analytical balance. Where necessary, corrections were made by the addition of small standard metric weight clips to the symmetric lever arm when using the weight disk of incorrect mass.

Two and four kilogram weight combinations, giving torques of 50 and 100 in-lb_f on the torque pickup shaft, were used in the calibration procedure which was as follows:

1. Warm up and balance the recorder and oscilloscope.
2. Clamp the flywheel of the rotor drive system so that the symmetrical lever with the kilogram weights attached is horizontally level.
3. Set the gain on the recorder and the oscilloscope such that a torque of 50 in-lb_f (2 kilograms on lever inducing a torque of 12.5 in-lb_f on the rotor shaft) applied to the torque pickup gives full scale deflection (25mm on recorder; 50mm on oscilloscope) at the X1 position of the recorder attenuator.
4. Check the gain adjustment of step 3 by loading the torque pickup with a torque of 100 in-lb_f (4 kilograms on lever to induce a torque of 25 in-lb_f on the rotor shaft). Exactly full scale deflection.

of the recorder writing arm should result with the recorder attenuator set at the X2 position.

The plant stem physical property testing machine was calibrated in a similar way using static loads. Weights were constructed to give loads of precisely 1, 5, and 25 lb_f on the load cell of the machine. The recorder gain was set such that at the X1 attenuator position, a 1 lb_f load gave a writing arm deflection of 2 millimeters.

Figure 63 shows the equipment arrangement for calibrating the carrier-amplifier-recorder and the oscilloscope used to record the cutting torque. The flywheel stop is attached. The symmetric lever arm is attached to the rotor shaft, and one of a pair of kilogram weights to be used is mounted on the support beam of the symmetric lever. Figure 64 shows the equipment arrangement for calibrating the stem testing machine. In the photograph the force applied to the load cell by the hanging weight is one pound.

Figures 65 and 66 present typical recorder oscillograph chart calibration records. The initial calibration of the recorder and oscilloscope used for cutting torque measurements was rechecked midway through the experimental test series and after tests were completed. No change was observed. The calibration of the stem testing machine instrumentation was rechecked several times during the course of running tests and found to be accurate.

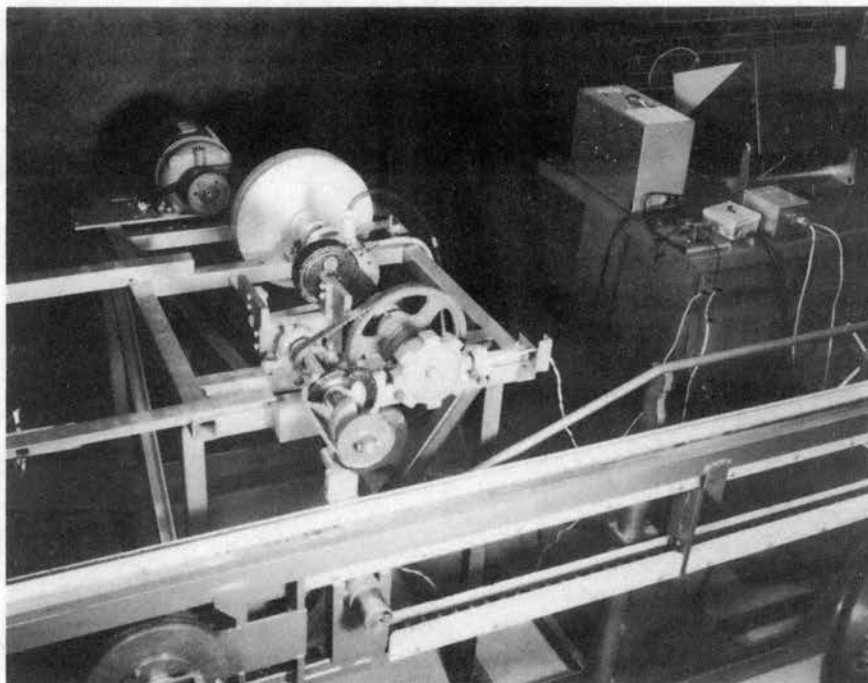


Figure 63. Torque Pickup Calibration Equipment

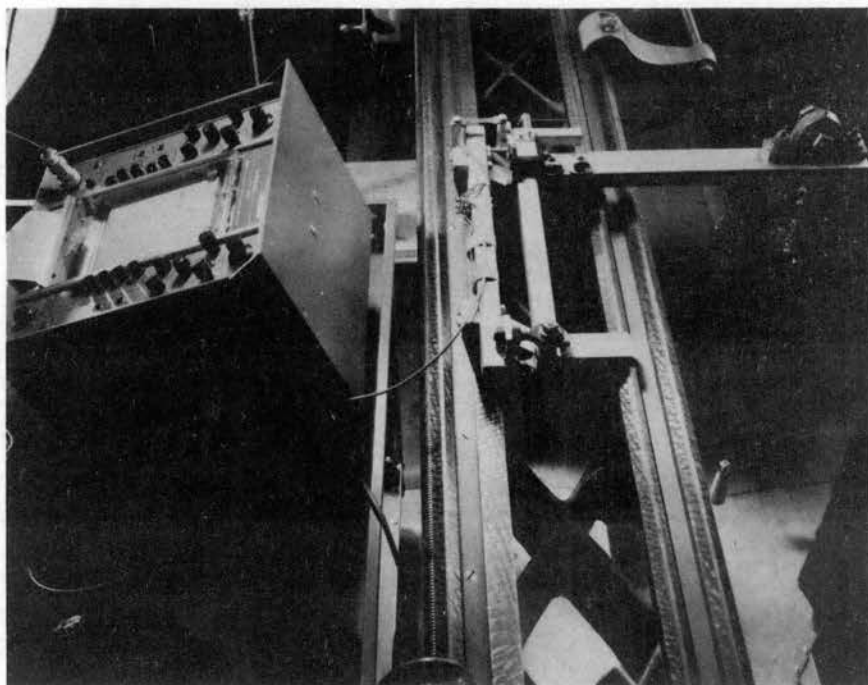


Figure 64. Stem Testing Machine Calibration Equipment

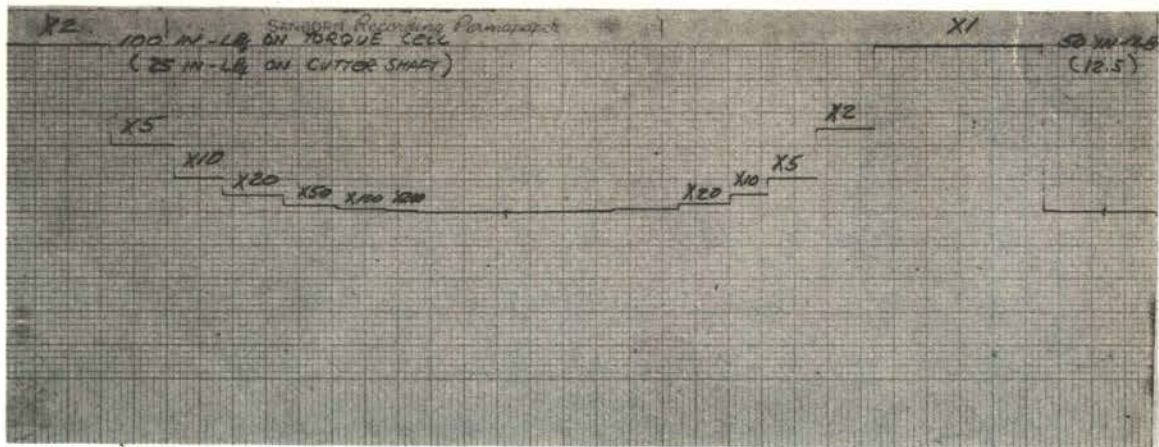


Figure 65. Oscillograph Record of Torque Pickup Calibration

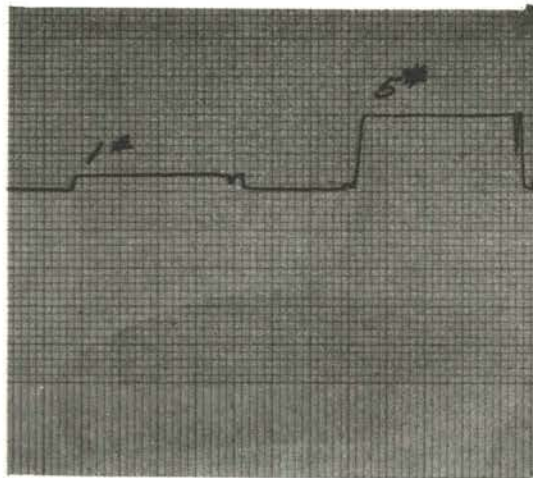


Figure 66. Oscillograph Record of Stem Testing Machine Calibration

Data Taking Procedure

The method of obtaining data for an experimental analysis of the helical cutter may be explained by considering the step by step procedure followed in conducting one trial of the main experimental plan. The plant stems were sorted according to nominal diameter and roughly according to height of the center of gravity within the diameter classifications as previously explained (Chapter VI). The stems within a classification were paired and randomly assigned to experimental trials. The trial numbers then were marked on the stems. After this preliminary assignment of experimental material, the procedure was to:

1. Check the moisture chamber nozzle to be certain a uniform mist of 180°F water was being sprayed and adjust if necessary. Place four numbered pairs of plant stems (and enough additional stems for a rerun of each size classification if required) in the holding racks under the nozzle. Leave for the time period specified by the experimental plan. (Note that enough plants for four trials were usually conditioned at the same time).
2. Install rotor assembly with the rotor angle index called for by the experimental plan. Adjust the ledger orientation to the level specified by the plan. Measure and record the clearance between the rotor and ledger blades at each end and at the center of the ledger blade. Color the edge

and top of one rotor blade with a red grease pencil; color the opposite blade with a green grease pencil such that the sector doing the cutting could be identified by the color transferred to the severed stem at the cut section.

3. Adjust the carriage track vertical height and lateral position to obtain the cutting height and lateral position indices called for by the experimental plan.
4. Adjust the friction clamp of the toothed wheel that trips the rotor shaft angular displacement monitoring proximity switch so that the switch trips just as the rotor blade leaves the ledger tube protective shroud at the lateral position where the plant stem would be engaged. This caused a blip in the shaft displacement trace on the recorder chart and oscilloscope screen at the earliest time cutting could commence.
5. Adjust the lateral position of the horizontal grid board until the base line coincided with the plant row center line.
6. Install correct stem holding blocks for the size stem to be tested on the stem physical property testing machine.
7. After the allotted time in the moisture chamber, remove the stems and let them drain thirty minutes at ambient humidity and temperature. After thirty

minutes, place all but the pair of stems to be tested in a walk-in cooler with inside temperature controlled to $40^{\circ}\text{F.} \pm 10^{\circ}\text{F.}$

8. Start the Graham variable speed drive and adjust its speed to provide the carriage propelling chain velocity called for by the experimental plan. Check the velocity by measuring the rotational speed of the chain drive sprocket with the stroboscope.
9. Start the rotor drive motor and set the speed controller dial to the predetermined value that gave the required rotor speed. Let the fluctuations due to the feedback control circuit overshooting smooth out then make final adjustment of the speed controller, checking rotor speed with the stroboscope.
10. Mark the required center of gravity height location on the stem to be cut. Check the location of the actual center of gravity on the horizontal pin fixture and adjust it to the required position by breaking off small bits of the top of the plant. Clamp the stem in the plant holding block of the carriage with its base end flush with the bottom of the lower wooden holding block. Coat stem center of gravity and about 3 to 4 inches of the lower portion of the stem with a fluorescent slurry.

- Count the number of intact seed pods on the stem and record.
11. Check operational readiness of recorder and oscilloscope. Set adjustments on oscilloscope camera. Set triggering switch on oscilloscope.
 12. Turn on ultraviolet lamp and adjust the beam to the expected position of the severed stem trajectory.
 13. Extend carriage accelerating spring assembly to the required distance by the winch and lock in place.
 14. Load polaroid film holder of graphic view camera used to record vertical displacement of the severed stem. Check camera adjustments and set shutter for operation.
 15. Have one man operate the oscilloscope camera and recorder chart drive. Have a second man operate the camera photographing the stem trajectory. Have a third man release the carriage when all is ready and the room lights are turned off by a remote switch. Run test through synchronized efforts of these men.
 16. Develop polaroid film of oscilloscope trace during cutting. Develop polaroid film of stem trajectory. Coat prints and store.
 17. Note horizontal coordinates of the severed stem center of gravity and cut end on the grid board and record.

18. Examine severed stem cut end and the cut end of the stubble for indications of the type of cut and record observations. From measurements on stubble and on the severed stem relative to the center of gravity, determine the actual height of cut above the base (base being the top of the carriage upper stem holding wooden block) and record.
19. Check severed stem on horizontal pin fixture to determine shift of center of gravity resulting from the lower end of the stem being cut off and record the shift. Note the number of seed pods intact and record.
20. Adjust the position of stem clamping block of the stem physical property testing machine to load the test stem in cantilever bending at the same height above the base as its "twin" stem was cut. Run the cantilever bending test and obtain a load-deflection curve on the recorder chart.
21. Adjust the stem testing machine for a transverse shear test at the same cross section where the cantilever bending load was applied. Run the shear failure test.
22. Cut one inch lengths from both the cut stem and the physical property test stem at a point adjacent to the cut section and shear failure section, respectively. Identify these one inch stem lengths,

weigh them on a Mettler analytic balance, and place them in an oven to dry 24 hours at 180°F.

23. At a point on the physical property test stem adjacent to the shear failure section but on the side opposite that from which the one inch length was cut, saw out a 1/8 inch thick disk, identify it, and place it in a container to later record an enlarged image of its cross section on photosensitive paper for average diameter analysis.
24. Remove one inch stem test lengths from oven after 24 hours, reweigh them and record data for moisture content and linear density determination.

For each experimental trial, the same 24 steps was repeated, except that for some of the tests, the stems had been stored in the walk-in cooler after a "batch" treatment in the moisture chamber, as noted in step 1.

Procedure for the cutting effectiveness tests with the square edge blade was basically the same as for the main experimental series. Photographs of the stem trajectory were not taken, and photographs of the torque-angular shaft displacement traces during cutting were taken for only two or three runs, randomly selected from the ten runs in each test series.

For the high speed motion picture sequences, positioning of the motion picture camera and camera operating and light adjustments, camera switching set up, film loading, etc. took the place of operating the still camera to

record stem trajectory in the main test series. Degree of illumination of the subject was measured with a Wollensak WF-327 exposure meter and camera lens diaphragm opening set to suit the light available at the operating speed desired. Also nine plants were cut in each run. These were mounted in the carriage clamping blocks and numbered with a marking pen according to order of cut. Otherwise the procedure again was basically the same as with the main experimental test series.

To record the test data in an orderly form, three data sheets were designed and used: one for the cutting effectiveness tests, one for the main test sequence, and one for the physical property tests. Typical completed data sheets are shown in Appendix B.

Data Reduction

To reduce the raw data of the main test series to a form suitable for further analysis, graphical procedures were followed. On the polaroid print of the torque-angular displacement traces, the line of no-load torque was established. The net positive area under the torque trace resulting from cutting a stem was then determined. A Kueffel and Esser Co. No. 4236 compensating polar planimeter was used to calculate the area under the curve. From five to ten determinations of the area were obtained by one operator and the results averaged for the final area figure. A second operator then made five additional determinations and

averaged them to check the results of the first operator. If a discrepancy in the results appeared, the area determination was redone. Next the vertical and horizontal scales of the photographic trace were established. The Hewlett Packard Model 197 oscilloscope camera had a specified object-to-image ratio adjustment range of 1:1 to 1:0.7. Through careful adjustment before the test sequence was commenced, it was thought that the ratio was set at 1:1. However, repeated measurements revealed that the distance between consecutive centimeters graduation lines of the photograph was actually 1.04 centimeters. Thus a correction factor was introduced to compensate for the difference. The horizontal scale on the photograph (angular displacement scale) was determined by measuring the distance between the trace blips for either four or eight complete revolutions of the rotor shaft. This amounted to either one or two complete revolutions of the toothed wheel that actuated the proximity switch to produce the trace blips. Thus the same tooth actuated both blips between which the distance measurement extended, and therefore the effect of any machining inaccuracies in the toothed wheel was eliminated. It was thought unacceptable to use the oscilloscope nominal sweep rate setting to determine the horizontal scale, for such a procedure resulted in the calculated rotor speed being higher than what actually was run. The sweep rate accuracy of the oscilloscope is specified as

+3%. This wide accuracy tolerance band could account for the discrepancy.

Once the net area under the torque curve and the horizontal and vertical scales were determined, calculation of cutting torque per stem cut was a straight forward operation. Results were recorded on the data sheets. See the sample data sheet in Appendix B. A similar procedure was followed in analyzing data from the stem physical property tests - to determine bending and shear energy input.

To ascertain the positive vertical displacement of the center of gravity and cut end of the trajected stem, measurements were made on the polaroid print of the trajectory. Since the graduation lines of the horizontal and vertical grid boards are clearly visible in the photographs, the scale of measurement was readily found. If the trajectory went outside the limits of the photograph, an estimate of the vertical displacements was made based on that portion of the trajectory shown on the photograph.

When the lower end of the plant was cut off in severing the stem from the stubble, the center of gravity of the severed stem shifted toward the top of the stem from the position previously marked. The change varied from one to four inches, averaging about $2 \frac{5}{16}$ inch. The data for center of gravity displacements refer to the marked center of gravity of the stem, determined before it was clamped in the carriage holding block.

The high speed motion picture films were analyzed according to the procedure outlined by Hyzer (44). First the films were repeatedly viewed with use of a 16mm motion picture projector. Then a frame by frame study of the films was made on a microfilm reader. Typical cutting sequences were noted, and the film strip was marked at the beginning of these. The film was stretched out on a long table top, and the distance to successive timing marks from the zero or reference frame timing mark was measured and recorded. These timing mark-distance data pairs were analyzed through use of a least squares polynomial curve fitting computer program. A second degree polynomial gave the response of elapsed time as a function of frame number with a correlation coefficient, r , of 0.99999+ for every film sequence analyzed.

A Vanguard Motion Analyzer was used to measure in successive frames the coordinates of points on a plant stem relative to a fixed reference point in the field of view recorded on the film. These measurements provided data for a plot of displacement of the point on a plant stem undergoing cutting as a function of elapsed time or film frame number. Using the elapsed time versus frame number relationship previously determined, data for plots of velocity and acceleration of the point during cutting versus elapsed time were calculated. Digital computer programs were written to carry out the calculations.

If a "micromotion" analysis like the one roughly outlined above is to provide accurate information, a point of high contrast must be selected to be followed in a frame by frame determination of displacement. Unfortunately, no such points of high contrast existed on the plant stems. As a consequence, the plots of displacement and, especially, of velocity and acceleration of a point on the stem undergoing cutting or trajectory turned out to be erratic.

CHAPTER IX

PRESENTATION AND ANALYSIS OF DATA

Cutting Effectiveness Tests

As outlined in the experimental plan (Chapter VI), the CED, PD, and PS test series were to provide data for cutting effectiveness analysis.

Classification of Severing Actions

Data collected in the three test series are tabulated in Appendix C-I. By close observation of the severed ends of the stems and of the stubble from which the stems were separated, six types of cutting action were detected. The most desirable severing action was a clean, angled cut. When the stem was completely severed but by a torn, ragged cut, the action was judged effective but less desirable. Another type of cut that effectively severed the stem at the point of blade contact produced ends that resembled those of a twig that is cut part way through with a pocket knife then broken at this weakened section by bending. This action was defined as a partial cut and break at the knife contact point. Figures 67 and 68 show typical cut ends of stems severed in the main, screening of parameter, test series. The cuts shown in Figure 67 were made with square

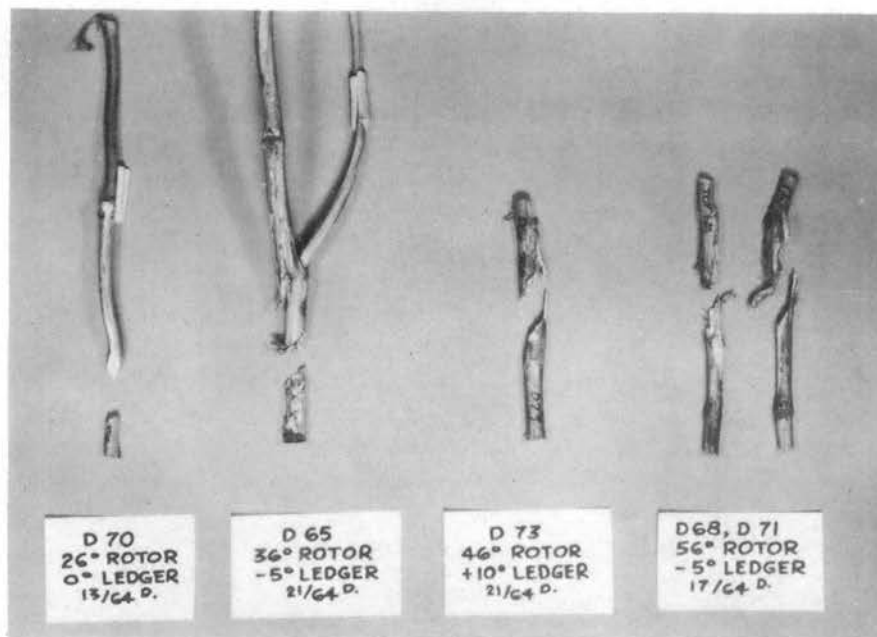


Figure 67. Typical Cut Ends of Stems Severed in the Dull Blade Test Series

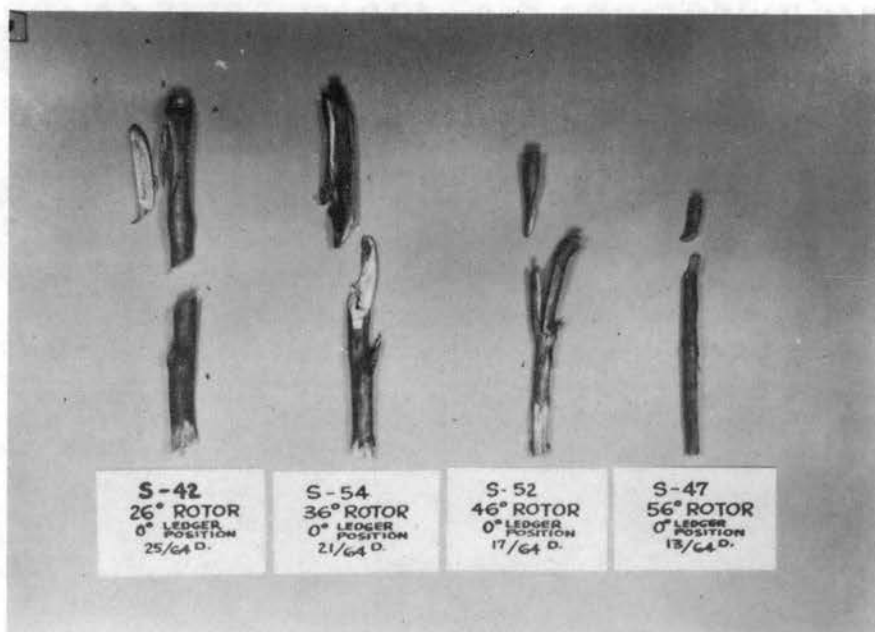


Figure 68. Typical Cut Ends of Stems Severed in the Sharp Blade Test Series

edge blades on the rotor. Note the torn, ragged cuts produced by the 56 degree rotor. Sharp blades made the cuts pictured in Figure 68.

Noneffective severing actions included those that resulted in the stem breaking at the base rather than at the blade contact point. There were a few instance in which the stem slipped under the rotor without being cut. This action resulted when the stem partially broke at the base when contacted by the rotor blade, then deflected backward and down to pass under the rotor without being severed.

Figure 69 summarizes the severing actions noted to have acted on the stems of the CED, PD, and PS test series recorded in Appendix C-I. Consideration of these results brings the following observations:

1. The 26 degree rotor was more effective than the 56 degree rotor in cutting plant stems with use of a square edge blade.
2. Moisture content of the stems had a decided effect on the type of severing action obtained when using square edge blades.
3. Rotor speed and feed rate appear to have had some effect on the cutting action of the square edge blades.
4. Overall, the sharp blade was more effective than the square edge blade in producing desirable cutting actions, and there was less difference in

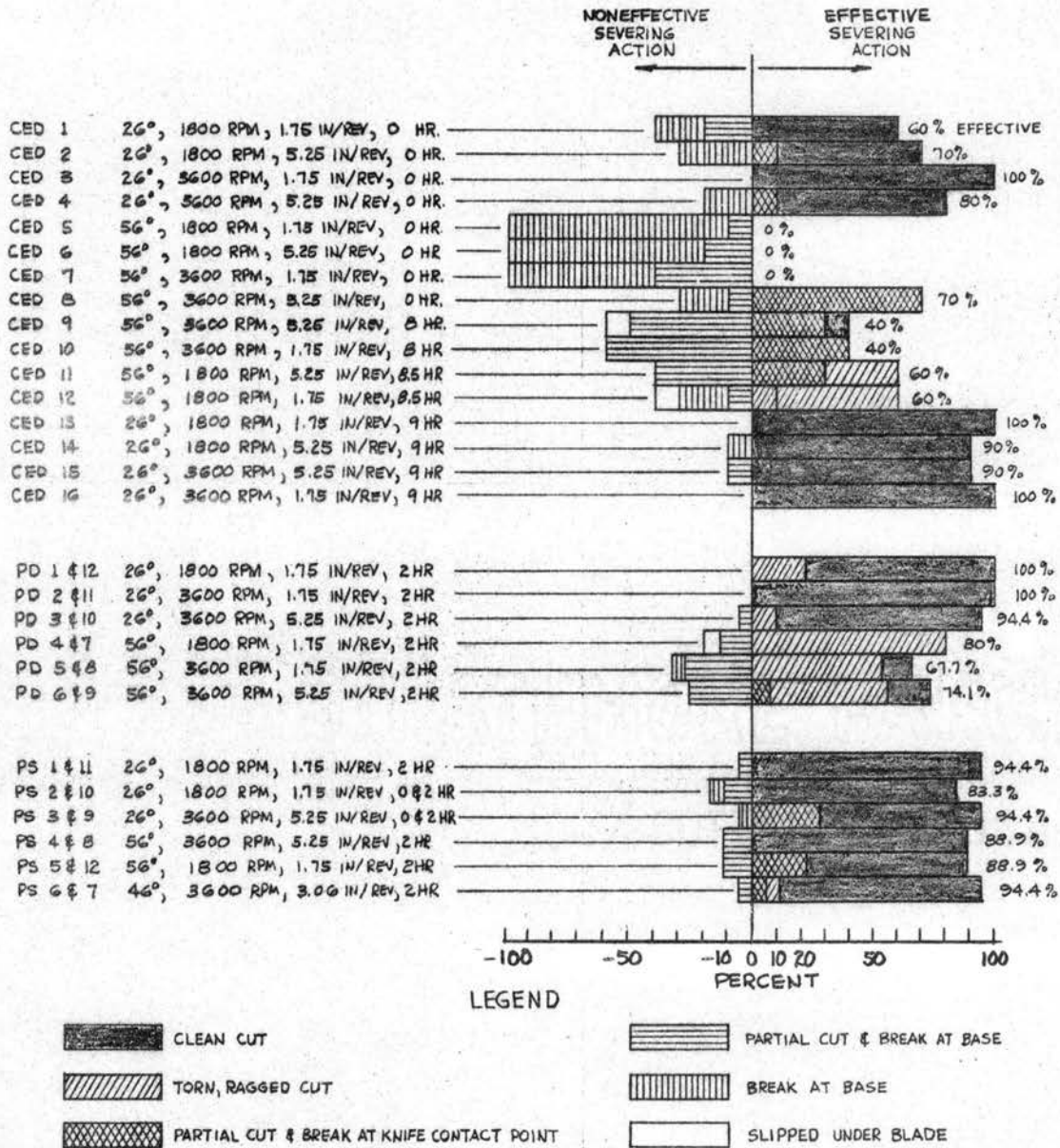


Figure 69. Summary of Cutting Effectiveness Test Results

the action of the 26 and 56 degree rotors when sharp blades were used.

Variation in Actual Cutting Height

Since stubble length is one criteria used in judging cutting devices, note the variation in actual cutting height obtained for the nominal height setting of 1 -3/4 inches used for most of the trials in the CED, PD, and PS test series. The mean cutting height, standard error of the mean, maximum and minimum values, and the range is recorded for each test series in the tables of Appendix C-I.

The cutting height data from the CED test series is biased by the large number of stems which broke at the base. When a stem broke at the base on contact with the rotor blade, the cutting height was taken as the point the blade contacted the stem. Had the stem been deflected to the fixed ledger blade and cut, however, the cutting height might well have been different from the initial point of rotor blade contact. Comparison of actual cutting height mean values therefore will be limited to results for the PD and PS test series. Figure 70 illustrates the manner in which the cutting height was defined and measured.

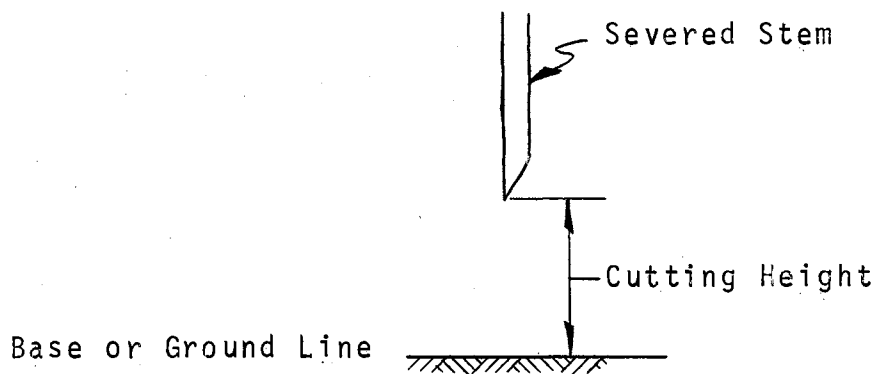


Figure 70. Cutting Height Definition

Consideration of the cutting height data for the PD and PS test series leads to these inferences:

1. With a nominal cutting height setting of 1-3/4 inches and with use of square edge blades, mean cutting height for the 26 degree rotor varied from 2.50 to 2.75 inches. Standard error of the mean varied from 0.05 to 0.11 inches. Mean cutting height for the 56 degree rotor under the same conditions varied from 2.65 to 3.00 inches with a standard error of the mean of from 0.07 to 0.21 inches. Thus the mean cutting height is significantly lower for the 26 degree rotor with the use of square edge blades.

2. When sharp blades were used with a nominal cutting height of 1-3/4 inches, mean cutting height for the 26 degree rotor varied from 2.16 to 2.40 inches. Standard error of the mean varied from 0.05 to 0.12 inches. For the 56 degree rotor, the mean cutting height varied from 2.18 to

to 2.25 inches, with a standard error of the mean of 0.07 to 0.12 inches. Thus no significant difference in mean cutting height was indicated for the two rotors when sharp blades were used.

3. For both the 26 degree and 56 degree rotors, mean cutting height was significantly lower with use of sharp blades.

Trajection of Severed Stems

Figure 71 summarizes the range of center of gravity and cut end displacements for the stems severed in the CED test series.

A desirable displacement pattern is one with positive X displacement limits, a mean c.g. X displacement of large magnitude, a mean c.g. Y displacement of low magnitude, and with an area enclosed by the range of c.g. X displacements and c.g. Y displacements of low magnitude. Positive X displacement values indicate travel of the severed stem onto the catching platform of a harvesting machine. Negative X displacement values indicate the stem being trajected in the direction of machine travel at a velocity exceeding that of the machine. Thus the stem would not fall on the catching platform. Minimum Y displacement values lessen the possibility of plants cut by adjacent sections of the cutter rotor colliding and becoming entangled while in the trajection path. A small area enclosed by the range of X and Y displacements indicates a predictable path of trajectory,

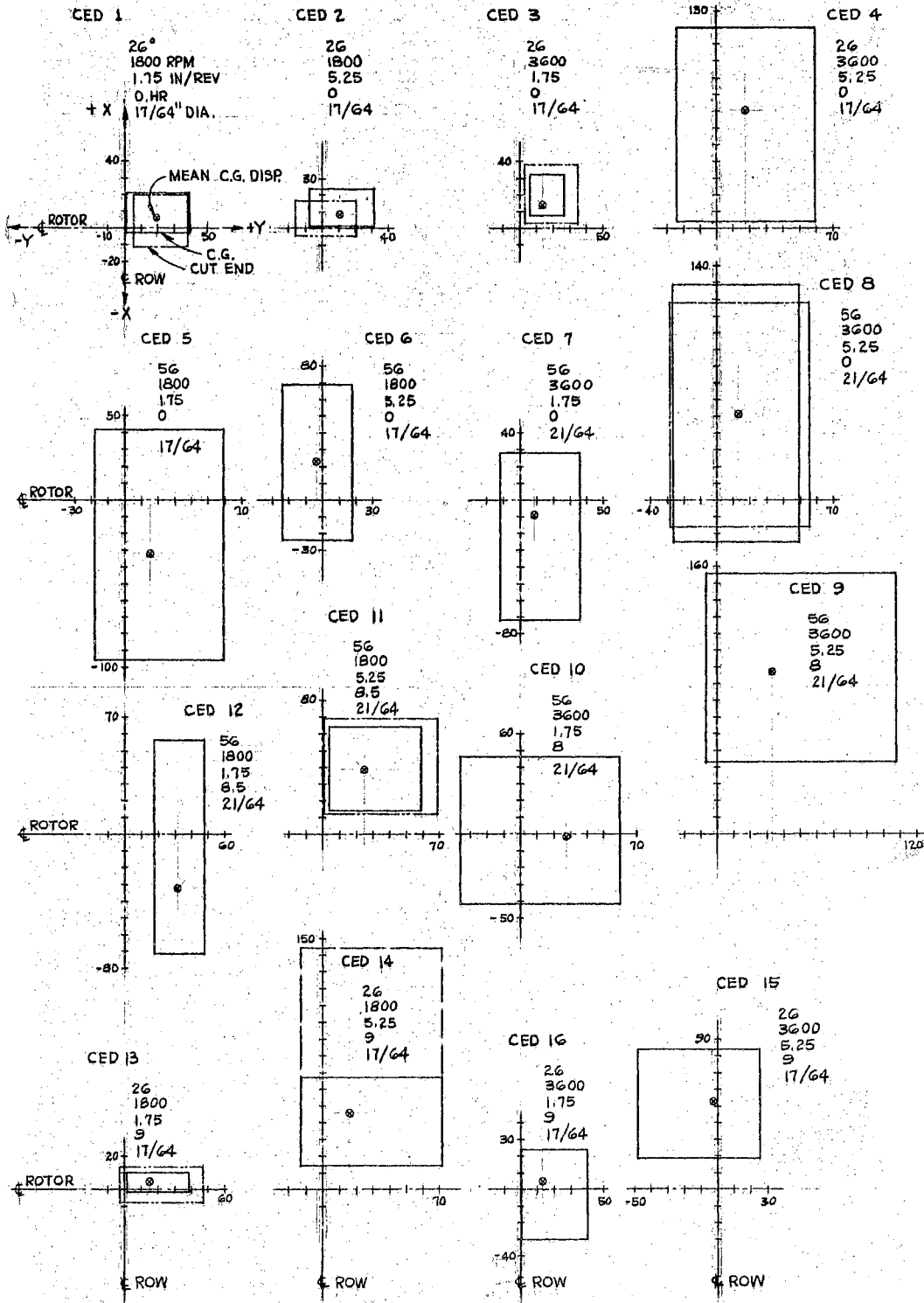


Figure 71. Severed Stem Displacement Patterns for CED Test Series

one without excessive variations.

From examination of the displacement patterns of Figure 71, in light of the above criteria, it may be concluded that:

1. In general, the 26 degree rotor trajectories the severed stems in a more desirable manner than the 56 degree rotor with the use of square edge blades - especially when stems are in the "as dried" condition.

2. Any stem that breaks at the base before being completely severed by the rotor blade plays havoc with the displacement pattern. The stem may be thrown a great distance in the positive X direction, the negative X direction, or straight up. The dashed lines for trial CED-14 represent the extension of the displacement range resulting from one stem breaking at the base.

3. High rotor speeds and feed rates insure positive X displacements of the severed stems but also increase the variability of the displacement pattern. The maximum feed rate of 5.25 inches per revolution at the 3600 rpm rotor speed resulted in displacements far exceeding the range of the grid board made to measure them.

Figure 72 shows the displacement patterns of the PD and PS test series. The superiority of the sharp blade patterns over the dull blade ones is clearly evident.

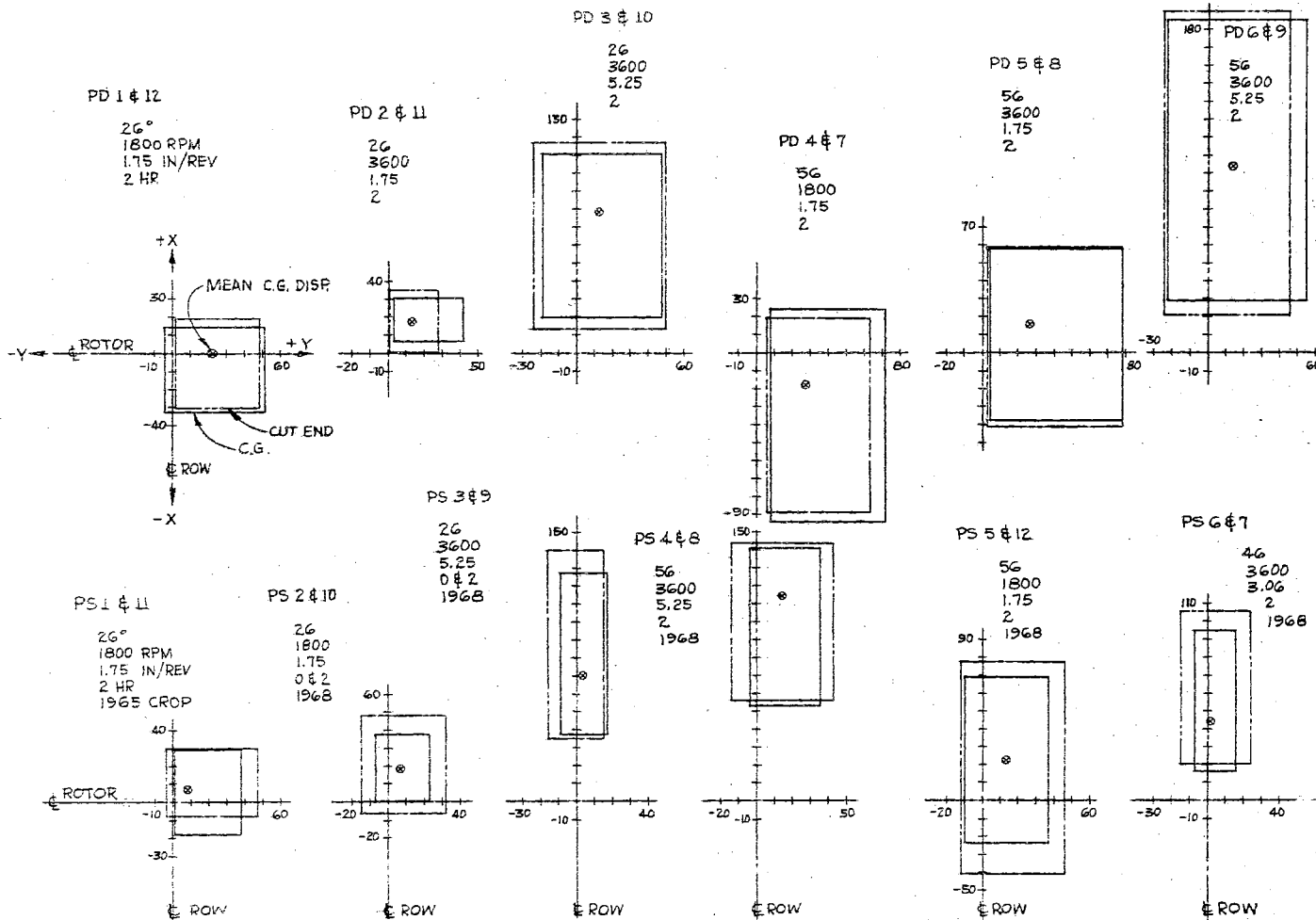


Figure 72. Severed Stem Displacement Patterns for PD and PS Test Series

Conclusions Regarding Independent Variable Ranges

The cutting effectiveness tests indicated that two changes would be necessary in the proposed limits for the levels of the independent variables considered.

Excessive breaking of stems at the base before being cut resulted when severing stems in the "as dried" condition (0 hours in the conditioning chamber) with the square edge blades. Moisture content of the as dried stems ranged from 7 to 12 percent, dry basis. This is below the range expected for stems to be harvested in the field. Accordingly, the lower limit of the "time in chamber" independent variable was increased from 0 hours to 2 hours. The 2 hour treatment provided a stem moisture content in the neighborhood of 20 to 25 percent (dry basis).

The upper limit of the feed rate index was decreased from 24×10^{-2} (5.25 inches per revolution), to 20×10^{-2} , (4.38 inches per revolution). This change was made to bring the X displacement values within convenient range of the measuring grid board.

High Speed Motion Picture Studies

The films of the cutting action and stem trajectory show clearly the cutting mechanism and motion characteristics resulting with the dull and sharp rotor blades. Examples of the detailed graphic information provided by a sequence of frames from the high speed films are shown by

Figures 73 and 74. Composite overlay drawings of such sequence of film frames provide a basis for analyzing the cutting action and resulting stem trajectory.

Cutting Mechanism - Square Edge

Blades, Low Speed Level

The films of trials PD-1 and PD-4 reveal the cutting action of square edge blades at the low level of rotor speed (1800 rpm). For these trials, nominal cutting height was 1 3/4 inches, and the lateral position of the row center line relative to the ledger blade bottom corner was 1 1/8 inches.

Figure 75 shows typical cutting actions of trial PD-1, which involved the 26 degree rotor. Five stems were cut in this trial. The oscillograph cutting torque trace for the five stems is shown at left center of the illustration. The more accurate oscilloscope trace of instantaneous cutting torque for stems 1 and 2 is at right center of the figure. The cutting action for stems 1,3, and 4 was the same. Stems 2 and 5 were cut alike but in a different manner from the others.

Part 1-A of the illustration presents a detailed analysis of the way in which stem 1 was cut. The square blade edge of one sector of the 26 degree rotor contacted the stem at frame 0. Frame 5 shows the stem position 2.79 milliseconds later. As can be seen, the stem has slid along the rotor blade edge while being deflected sharply toward the

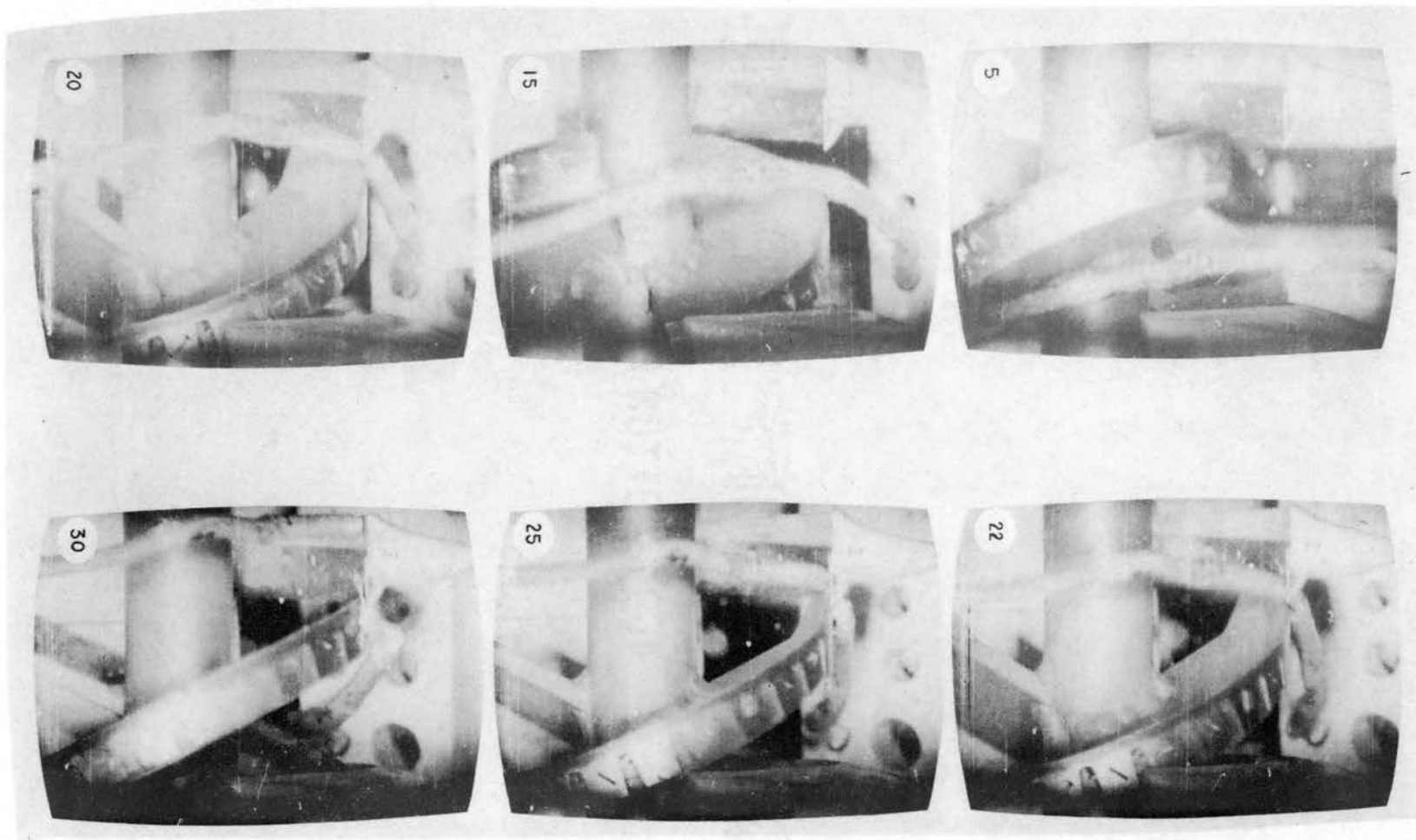


Figure 73. Cutting of Stem by 26 Degree Rotor with Square Edge Blade, 3600 RPM.
Numerals Are Frame Numbers (MPF: 4800 Frames/Sec.) Trial PD 3,
Stem No. 3

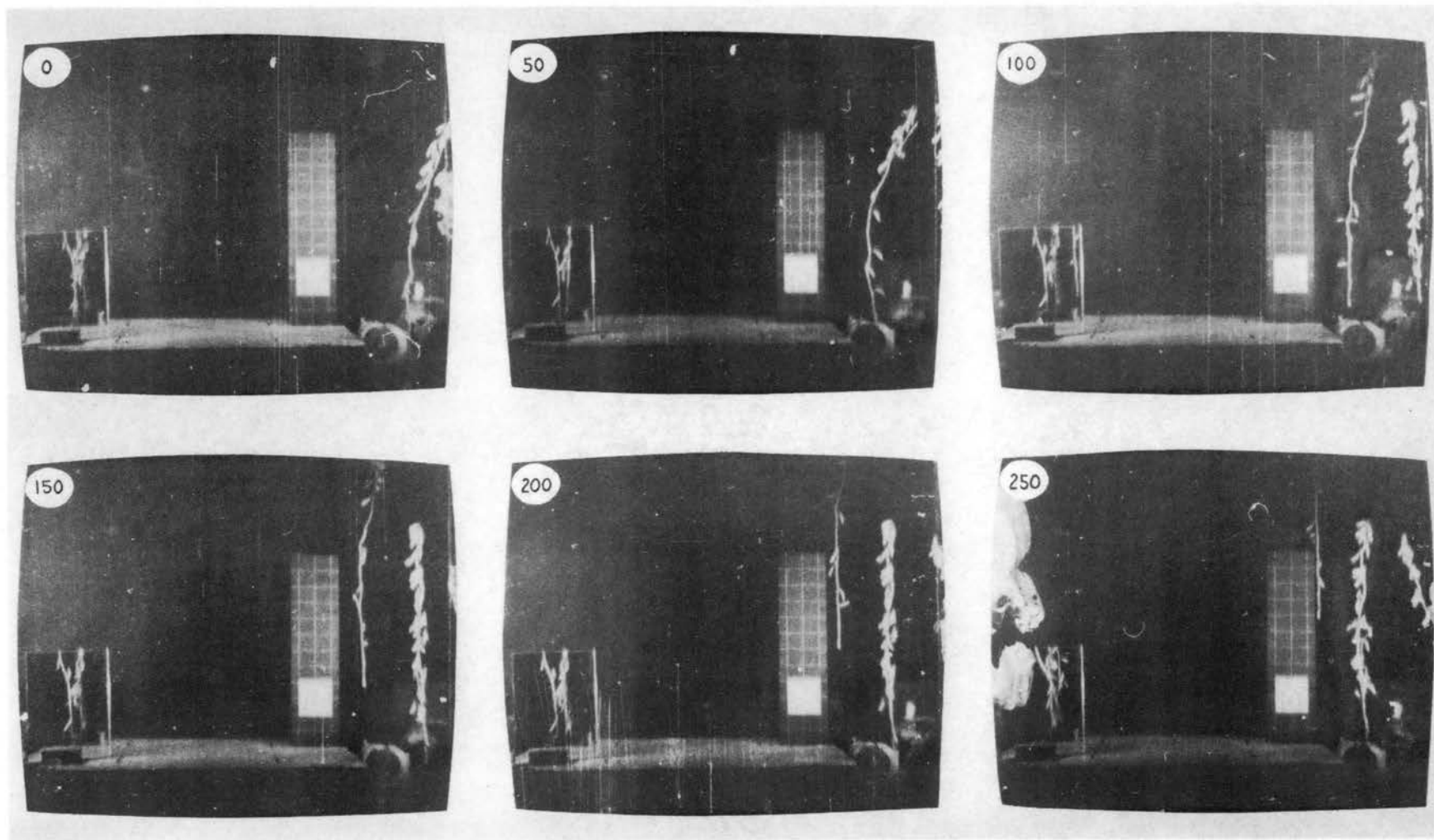


Figure 74. Trajection of Stem by 26 Degree Rotor with Sharp Blade, 1800 RPM. Numerals Are Frame Numbers (MPF: 1800 Frames/Sec.) Trial PS 10, Stem No. 1

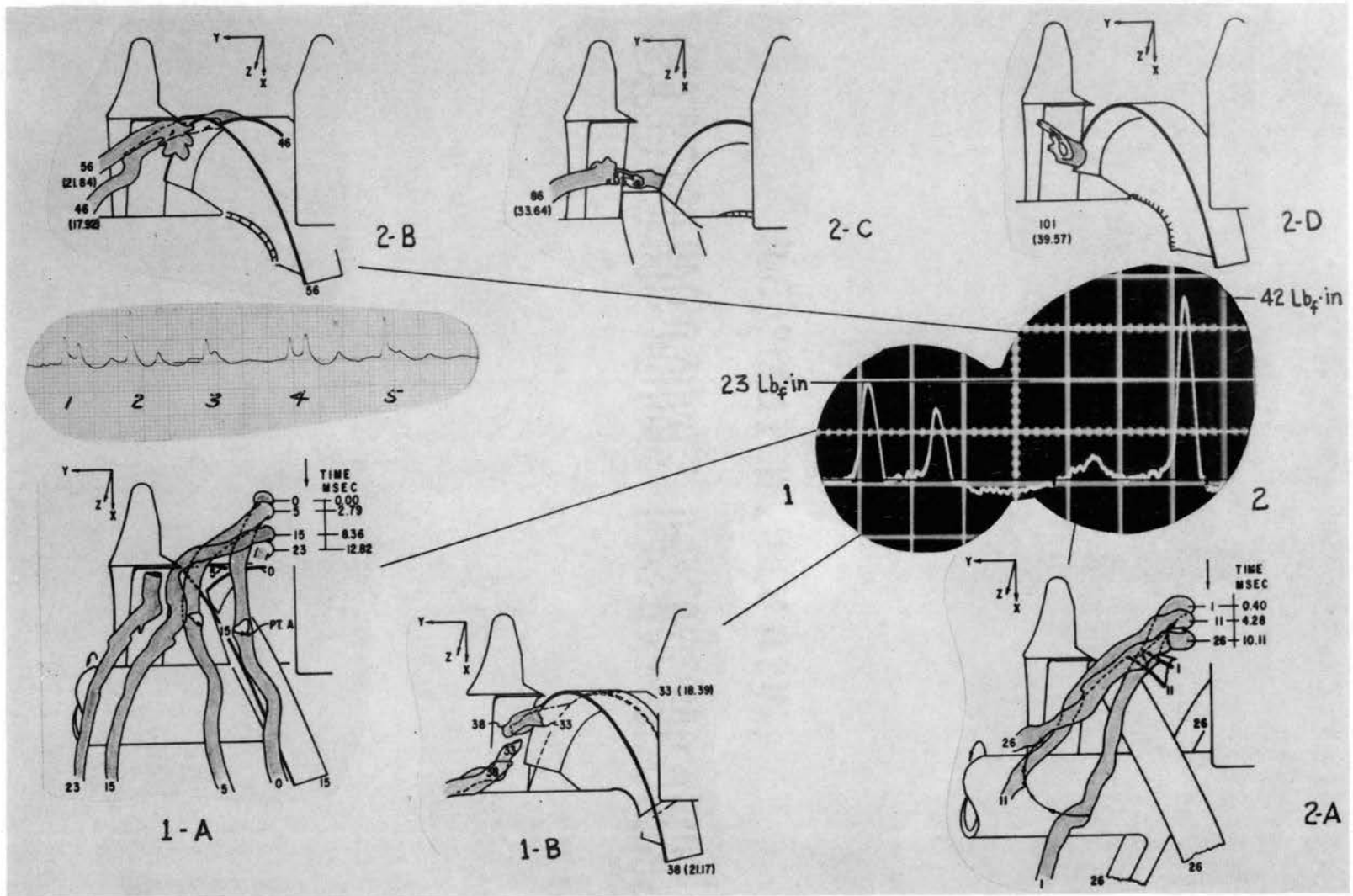


Figure 75. Cutting Mechanism With Square Edge Blades on the 26 Degree Rotor at 1800 RPM and With a Feed Rate of 1 3/4 in./rev. (Stems 1 and 2, Trial PD 1)

ledger blade. The stem is stressed in bending; the lower position of it undergoing severe deflection while the entire upper portion of it is accelerated to the left to relieve the bending load. In frame 15, 8.36 msec. after the stem was contacted by the blade, it is being severed by two element shearing between the rotor and ledger blades. The ledger blade has penetrated nearly through the stem. Frame 23, taken 12.82 msec. after the stem was contacted, shows the clean cut completed and the severed stem translating in the X and Y directions. Notice the pronounced Y component of translation. Also note that there was no contact of the severed stem with the rotor sector once the severing action was completed. Any impulse that affected the stem trajectory was imparted previous to and during the cutting.

The oscilloscope trace of instantaneous torque applied to the rotor shaft during the cutting of stem 1 indicates a peak cutting torque of 23 lb_f-in. Energy input to sever the stem was calculated to be 23.3 in-lb_f.

One of the effects of the low feed rate (1 3/4 in. per rev.) used in trial PD-1 is shown by part 1-B of Figure 75. Frame 33, taken 18.39 msec. after the stem was first contacted, shows that the rotor sector opposite to the one which cut the stem has engaged the stubble and is cutting it in two element shearing in conjunction with the ledger blade. Frame 38, exposed 21.17 msec. after frame 0, shows the completed second cut of the stubble. This action very closely resembles that predicted for low feed rates by the kinematic

analysis of Chapter IV. See Figure 26 in Chapter IV. The instantaneous torque trace reveals that a peak torque of about $18 \text{ lb}_f\text{-in.}$ was developed in second cutting of the stubble; energy input was calculated to be 14.6 in.-lb_f , more than half that required to sever the stem. Total energy expenditure for stem 1 was therefore 37.9 in.-lb_f .

Whereas stem 1 was contacted by a point on the rotor blade in the lower part of its cutting zone, stem 2 was contacted by a point about to leave its cutting zone (Refer to Figure 25, Chapter IV, for a graphic illustration of the cutting zone). The result is an impulsive deflection of the stem as shown by 2-A of Figure 75. The upper portion of the stem is moved in a clockwise direction; the lower part, in the immediate vicinity of the point of blade contact, is moved to a lesser extent in a counterclockwise direction. In 2-B of Figure 75, it is seen that stem 2 is severed by the rotor sector opposite to the one that first engaged it. Frame 46, taken 17.92 msec. after reference frame 0, shows the beginning of the cutting action. Frame 56, exposed 21.84 msec. after reference frame 0, depicts the stem about severed between the ledger and rotor blades. The cut was through a node of the stem and required a peak applied torque of $42 \text{ lb}_f\text{-in.}$, almost double that required for stem 1. The cutting action was not complete, however. A small tag of fibers still connects with the stubble in frame 86, exposed 33.64 msec. after frame 0, as shown by 2-C of Figure 75. This view emphasizes that critical clearance adjustment

must be maintained between rotor and ledger blades for clean cutting with a square edge rotor blade. As was the case with stem 1, the stubble of stem 2 is second cut, in this instance by the rotor sector that first contacted it. This action is shown in 2-D, frame 101, exposed 39.57 msec. after reference frame 0.

The initial deflection of the stem by the rotor consumed very little energy as the small instantaneous torque trace area confirms. Input energy to initially deflect, then cut the stem through a node was 57.9 in.-lb_f. This value does not include the energy expended in second cutting the stubble.

Films of trial PD-4 show the stem severing action of the 56 degree rotor fitted with square edge blades and under the same conditions defined for the 26 degree rotor shown in Figure 75. The severing action was similar to that just described for stems 1 and 2 for trial PD-1. The 56 degree rotor had a strong tendency to deflect the stems violently in the negative X direction one, two, or three times before finally bringing them against the ledger blade to be cut. The two element shearing action took place on the upper portion of the ledger blade edge; and in several instances, the rotor blade appeared to finally pull the last connecting stem fibers in two through tensile stress. The first stem of trial PD-4 partially broke at the base when contacted by the 56 degree rotor blade, then bent rearward, and passed under the rotor shaft without being cut. The remaining five

stems of the trial were completely severed, but with peak torque levels of from 35 to 65 lb_f-in. Three of the five cuts required peak torque inputs in excess of 42.5 lb_f-in. This is not surprising, since the large X and Z force components evidenced by the cutting action of the 56 degree rotor are predictable by equations (4-2) and (4-3) of Chapter IV for large values of knife angle, α .

Point A on stem 1 of trial PD 1, shown in 1-A of Figure 75, was subjected to a micromotion analysis using a Vanguard Motion Analyzer. The displacement of the point in the X and Y directions relative to its initial position in frame 0 are plotted in Figure 76. The instantaneous X and Y velocities of point A, calculated from the displacement and elapsed time-frame data for the film sequence is also plotted. Instantaneous acceleration of the point in the two orthogonal directions was calculated, in addition, but was not plotted because of the somewhat erratic nature of the data explained in Chapter VIII. The Y velocity component of point A was known to be zero before the stem was contacted by the rotor blade. Therefore the kinematic relation:

$$Y = \frac{1}{2}(A_y)_{\text{avg.}} t^2 \quad (9-1)$$

where

Y = displacement in Y direction

$(A_y)_{\text{avg.}}$ = average acceleration from rest in the Y direction

t = elapsed time for displacement from rest

can be used to calculate the average acceleration in the Y

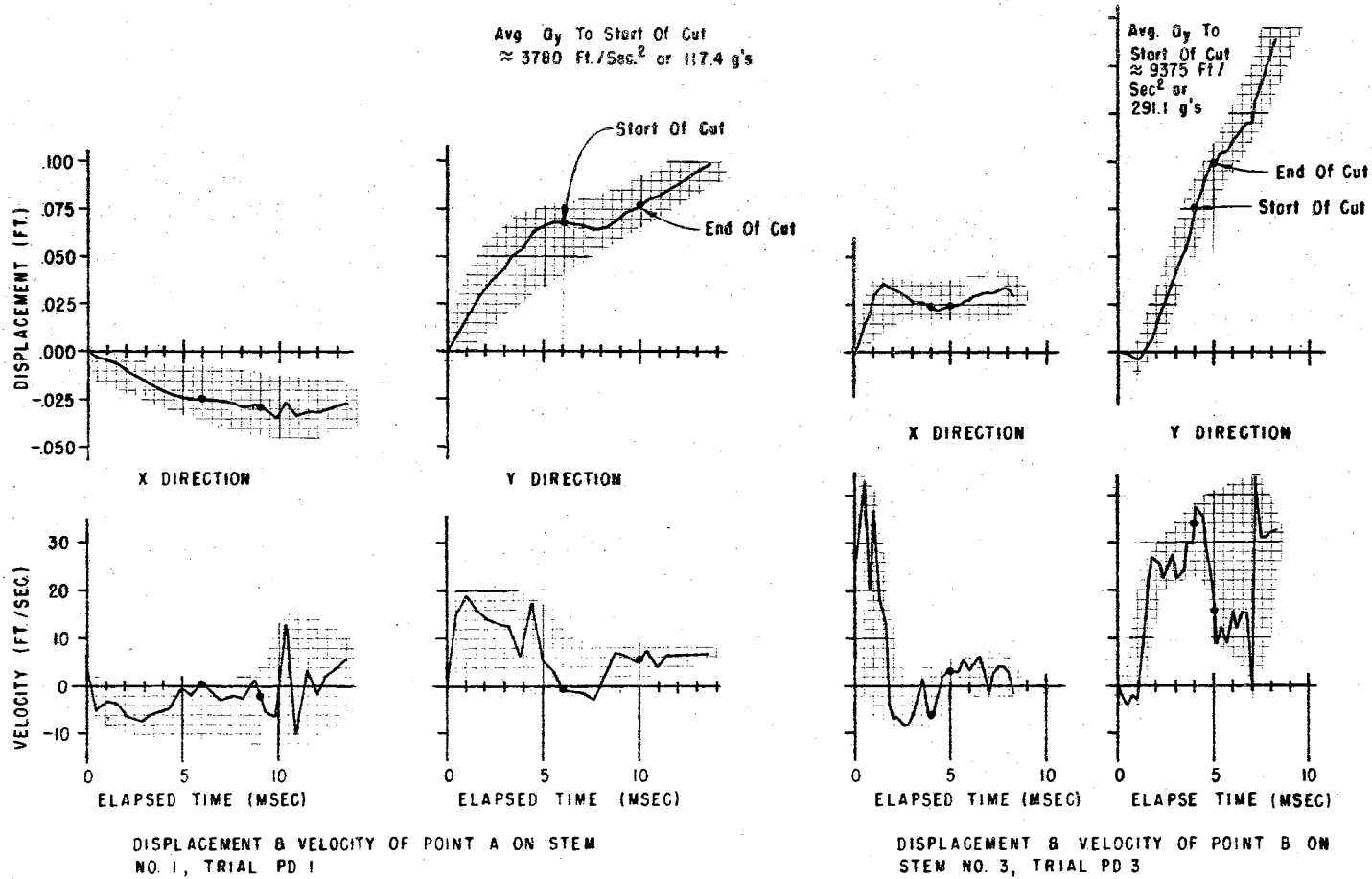


Figure 76: Displacement and Velocity of Selected Points on Stem 1, Trial PD-1 and Stem 3, Trial PD-3

direction of point A in the interval of time from when the stem was first contacted by the blade until when cutting began. This calculation is shown on Figure 76. The average Y acceleration of a point on the stem in the immediate vicinity of the blade contact gives an indication of the inertia force acting on the stem.

The typical trajectory pattern for a stem severed under the conditions defined for stem 1 of trial PD-1 is shown by Figure 77(a). The path of motion shown is that for stem 3 of trial PD-12, which was run with exactly the same specifications as trial PD-1. Observe that the stem has a pronounced Y direction displacement, and note in particular the rotation or spin about the Z axis. By following the top seed pod from frame to frame in the film sequence, it is seen that the Z rotation is approximately one revolution per 128 msec. Spinning of the severed stem about its vertical, or Z, axis indicates that it was stressed in torsion when being deflected and cut.

If point A of stem 1, shown in 1-A of Figure 75, is followed from frame to frame during the deflection and cutting sequence, it can be seen to undergo a clockwise or positive Z rotation previous to the stem being severed. Accordingly, it appears the stem is subjected to a complex stress condition at the time it is severed. Bending, transverse shear, torsion, and tensile loads all are simultaneously applied. Transverse shear is the governing load causing stem failure, however, for not until it is applied

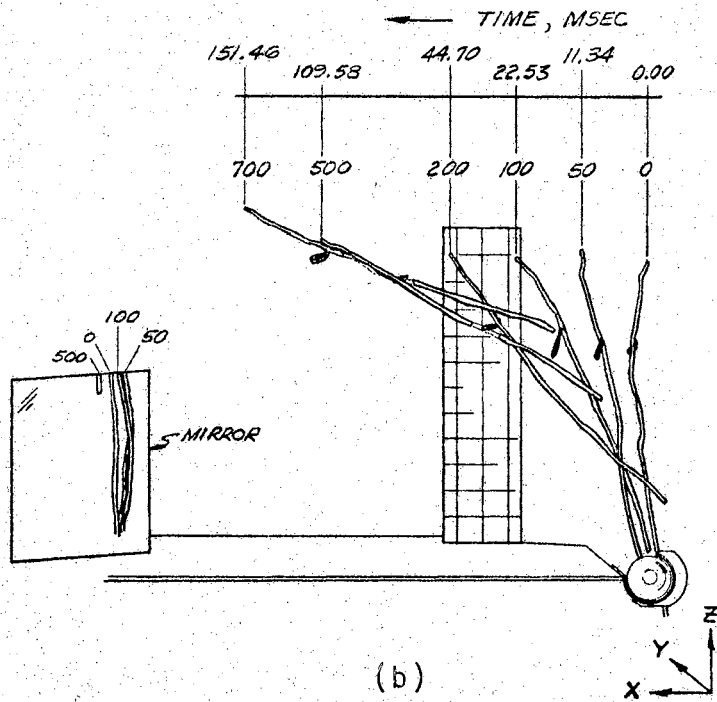
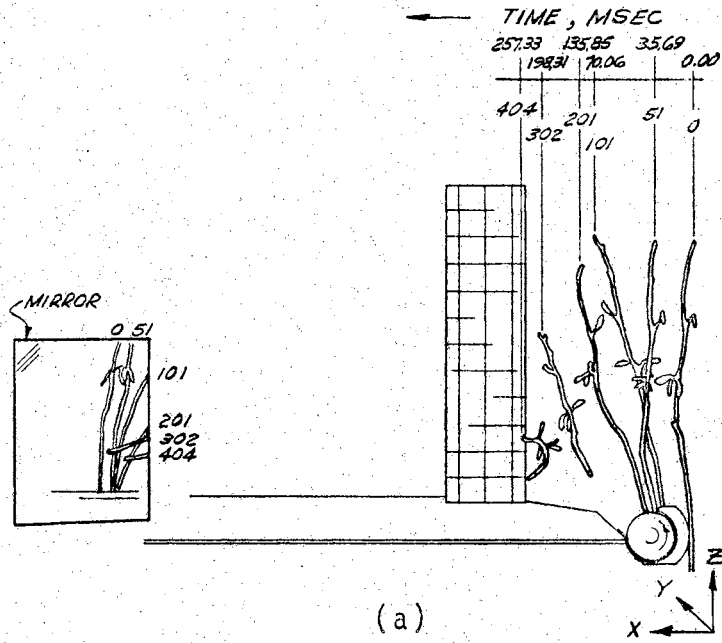


Figure 77. Trajection of Stem 3, Trial PD-12 (a); and of Stem 9, Trial PD-10 (b)

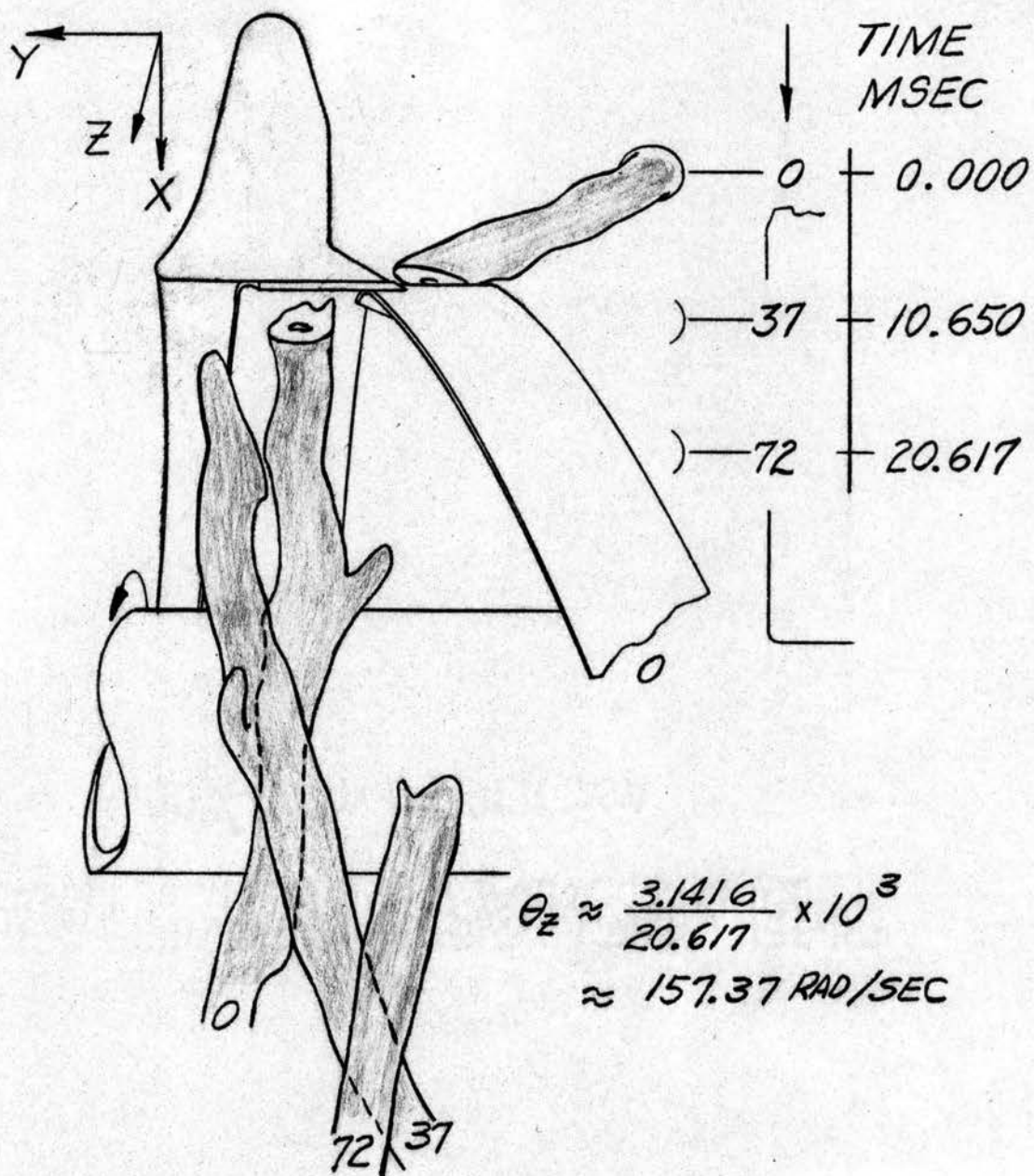


Figure 78. Rotation of Stem 3, Trial PD-1 About Its Z Axis Immediately After Being Severed

through the combined action of the rotor and ledger blades does stem failure (cutting) occur.

The inertia force due to the mass of the upper portion of the stem acts in a direction opposite to the direction of acceleration of the center of mass of this portion of the stem and thus opposite to the direction of the resultant force applied to the stem by the rotor blade edge at the point of contact (force F in Figure 28, Chapter IV). If the resultant force F and the inertial force do not lie in the same vertical plane, a couple is produced to act on the stem resulting in a torsional load about the Z axis. Rotation of the severed stem about its Z axis is thought to be a result of this applied couple.

Figure 78 shows clearly the Z rotation of stem 3, trial PD-1, immediately after it is severed.

Cutting Mechanism - Square Edge Blades, High Speed Level

The cutting action of square edge blades at the high level of rotor speed (3600 rpm) and feed rate (5 1/4 in. per rev.) is shown by the films of trials PD-3 and PD-6. Cutting height setting was 1 3/4 inches; lateral position setting was 1 1/8 inches.

Figure 79 shows the cutting action typical of trial PD-3, run with the 26 degree rotor. The composite overlay drawings comprising Figure 79 were made from some of the individual film frames shown in Figure 73. Of the nine

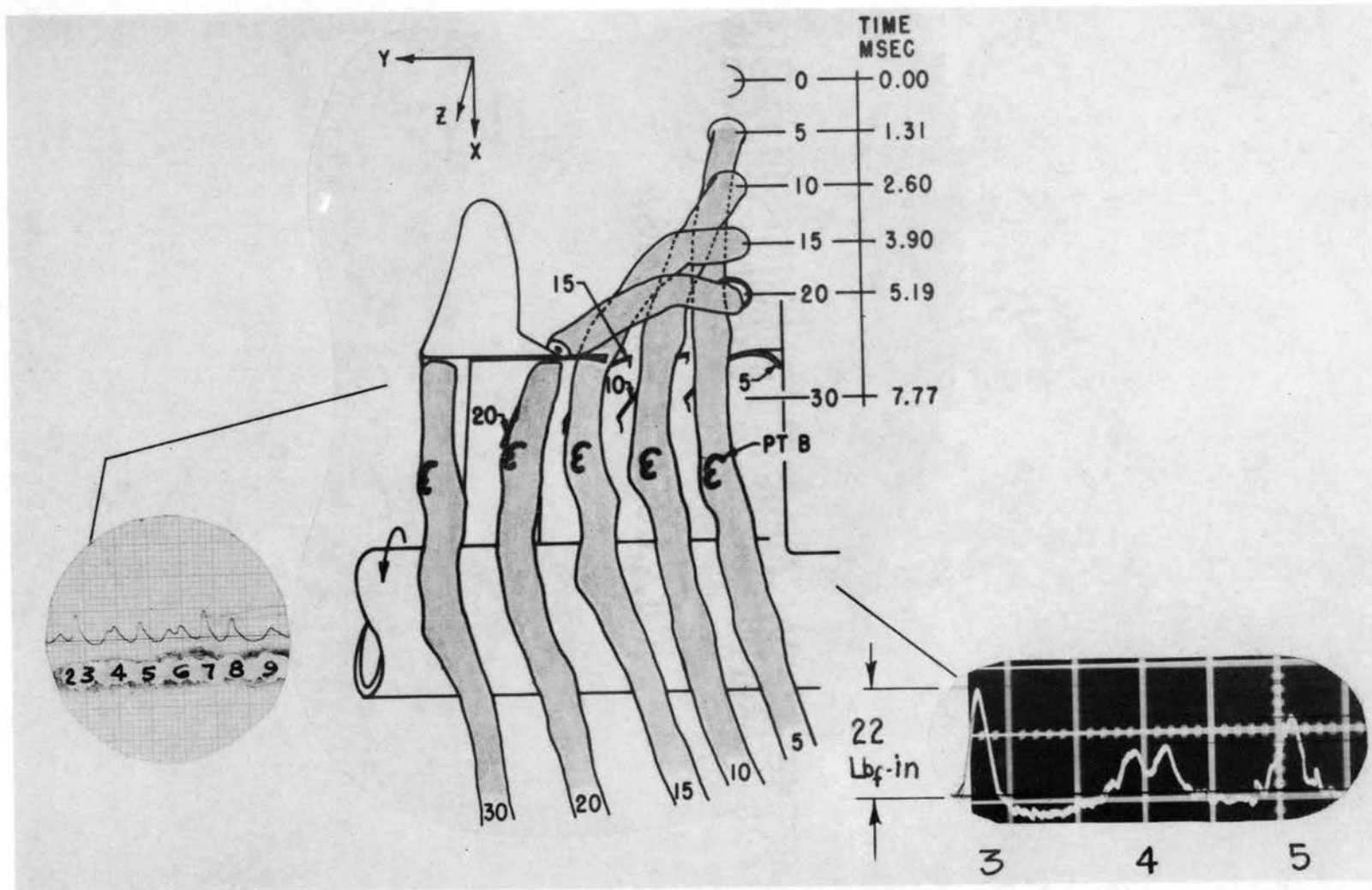


Figure 79. Mechanism of Cutting with Square Edge Blades on the 26 Degree Rotor at 3600 RPM and with a Feed Rate of 5 1/4 in/rev. (Stem 3, Trial PD-3)

stems cut in the trial, stems 1, 4, 5, 6, 7 and 9 were severed in a manner identical to that for stem 3. Stems 2 and 8 were deflected to the ledger blade first by one sector to be partially cut; the opposite sector of the rotor then completed the severing action.

The traces of instantaneous torque show that for the nine stems cut in the trial, stems 3 and 7 required the highest peak cutting torque, about 22 lb_f -in. Stems 4 and 6 required 8.5 lb_f -in; stem 5 required 13 lb_f -in. Comparing these peak torque values with those of trial PD-1 leads to the observation that lower peak torque values are required for cutting at the high level of rotor speed.

What are the reasons for this phenomena? Analysis of frames showing the progressive cutting of stem 3 reveals an action very similar to that which severed stem 1 of trial PD-1. There is one important difference, however. The top portion of the stem does not translate in the Y direction as much, so that there is greater bending of the stem about the point of blade contact. Consequently, flexural stresses in the stem must be at a much higher level than those developed in stem 1 of trial PD-1. Although two-element shearing still is the governing cause of cutting the stem, the required shear forces evidently are lower due to the increase in bending stress imposed on the stem. Possibly torsional stresses are higher also, since they too are related to the inertia force imposed by the mass of the upper portion of the stem.

The results of a micromotion analysis of point B on stem 3, trial PD-3, are plotted in Figure 76. Average acceleration of this point in the Y direction previous to cutting of the stem is calculated to be approximately 291 g's, a value more than double the 117 g average Y acceleration calculated for point A of stem 1, trial PD-1. This difference explains the increased inertia force and the resulting lower peak torque levels required to cut stems at the high level of rotor speed.

With use of the high level of feed rate, second cutting of the stubble was less frequent. Note that the stubble of stem 3, trial PD-3, broke at the base about the time the stem was cut (frame 20).

The input energy for stems of trial PD-3 is difficult to discern. Because of torsional oscillation of the rotor-counter shaft-positive drive belt system, area under the torque trace of a particular stem is confounded with the area under the torque trace of the previously cut stem. The double peaks of the cutting torque traces of stems 4 and 6 are thought to be a result of this confounding. The area under the trace for stem 5 is the "cleanest" that appears on the oscilloscope record. Input energy to cut stem 5 was calculated to be 32.7 in-lb_f.

Figure 77(b) presents the trajectory of stem 9 of trial PD-10. Conditions for this trial were the same as for trial PD-3, and the pattern of motion shown is typical. Again note the pronounced spin of the stem about its

vertical (Z) axis as it also revolves (but more slowly) about the Y axis and translates in the X, Y, and Z directions. Because of the increased inertia force involved in cutting stems of this trial, the Y translation is less than for the stems of trial PD-12.

Cutting action of the 56 degree rotor at the high level of rotor speed and feed rate and with square edge blades was nearly the same as that described for the low speed and feed rate levels. However, bending of the stem in the negative X direction on contact with the blade was much more severe due to the greater inertia forces induced by the high speed. Four of the nine stems comprising trial PD-6 were broken at the base by the impulse imparted by blade contact before cutting was completed. Three other stems had the last 1/4 of the connecting fibers to the stubble torn or pulled in two by the 56 degree blade action. Peak cutting torque ranged from 15 to 65 lb_f-in., but five of the stems were cut (or broken at the base) at peak torque levels of from 25 to 30 lb_f-in.

The high level of rotor speed was combined with the low level of feed rate in trials PD-2 and PD-5 for the 26 degree and 56 degree rotors respectively. The cutting mechanism was the same as for trials PD-3 and PD-6. Second cutting of the stubble was more common, however.

Cutting Mechanism: Sharp Blades,
Low Speed Level

Trial PS-1 for the 26 degree rotor was identical to trial PD-1 except that sharp blades were used. Figure 80 illustrates the cutting of two stems of trial PS-1. In 5-A of Figure 80, at frame 0 the rotor blade has not yet contacted stem 5. At frame 20, 4.19 msec. later, the blade has engaged the stem, deflecting it to the left, but at the same time the sharp blade edge has started to slice into the stem. Fifteen frames (3.09 msec.) later, the stem already is completely severed, through single element cutting. The cut end of the stem slides along the bevel surface of the rotor ledge until it is discharged to the left as shown by frame 65. In 5-B of Figure 80, second cutting of the stubble is illustrated. The torque trace indicates considerable torque developed and energy expended by the second cut.

Stem 6 of trial PS-1 is contacted by a rotor blade near the end of its cutting zone, as was stem 2 of trial PD-1. Instead of merely deflecting the stem as was the case in trial PD-1, however, the sharp blade slices a plug out of the stem. This action is shown by 6-A of Figure 80. The opposite sector of the rotor then completely severs the stem by single element cutting as shown in 6-B. The torque trace indicates that a higher peak torque and a greater

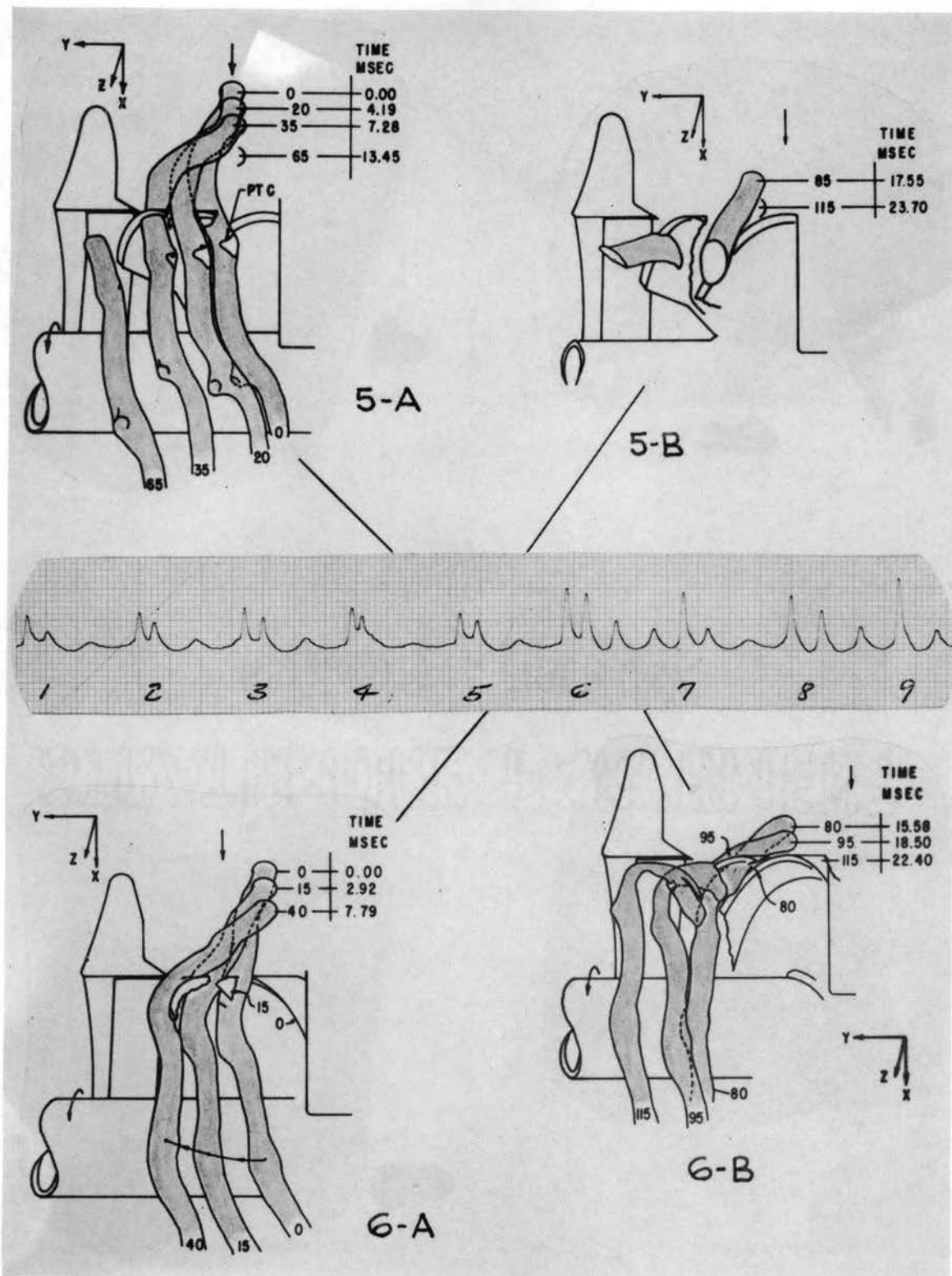


Figure 80. Mechanism of Cutting Stems with Sharp Blades on the 26 Degree Rotor at 1800 RPM and with a Feed Rate of 1 3/4 in./rev. (Stems 5 and 6, Trial PS-1)

expenditure of energy resulted from cutting the plug from the stem than from severing it at the weakened section.

Data from a micromotion analysis of point C on stem 5 of trial PS-1 is plotted in Figure 81. Average Y acceleration to the start of cut was calculated to be 552 g's. The initial translation of point A on stem 1 of trial PD-1 resulted in accelerations near this magnitude, but the resulting inertia force was not sufficient for the square edge blade to begin cutting the stem. This level of inertia force, in conjunction with the stress concentration at the edge of the sharp blade, did cause cutting of the stem.

Figure 82 illustrates the two typical stem motions resulting from cutting under the conditions of trial PS-1. Part (a) shows the trajectory of stem 1 of trial PS-11, where the stem was severed cleanly by one sector of the rotor. Part (b) shows the motion of stem 1 of trial PS-10, where one sector cut out a plug half way through the stem without severing it. The opposite sector then completed the cut. This situation was illustrated by 6-A and 6-B of Figure 80. In both cases, spin of the severed stem about its Z axis is present.

With sharp blades, the 56 degree rotor cut as cleanly as the 26 degree one. The cutting sequences filmed in trial PD-5 show that as a result of severe bending about the Y axis (stem deflected sharply in the negative X direction at the point of blade contact), the last few fibers appear to break in two ahead of the blade edge rather than being cut.

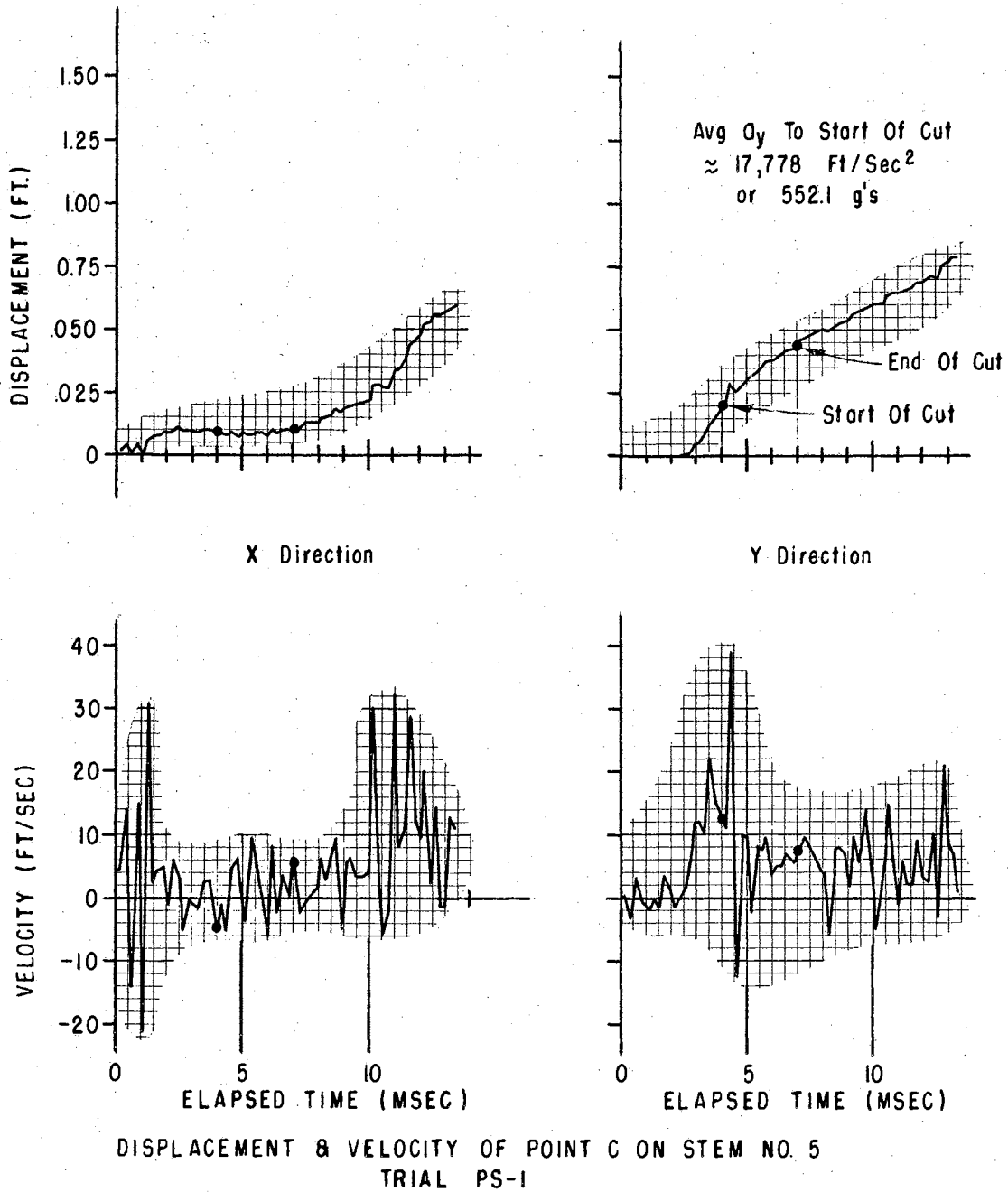


Figure 81. Displacement and Velocity Plots of Point C on Stem 5, Trial PS-1

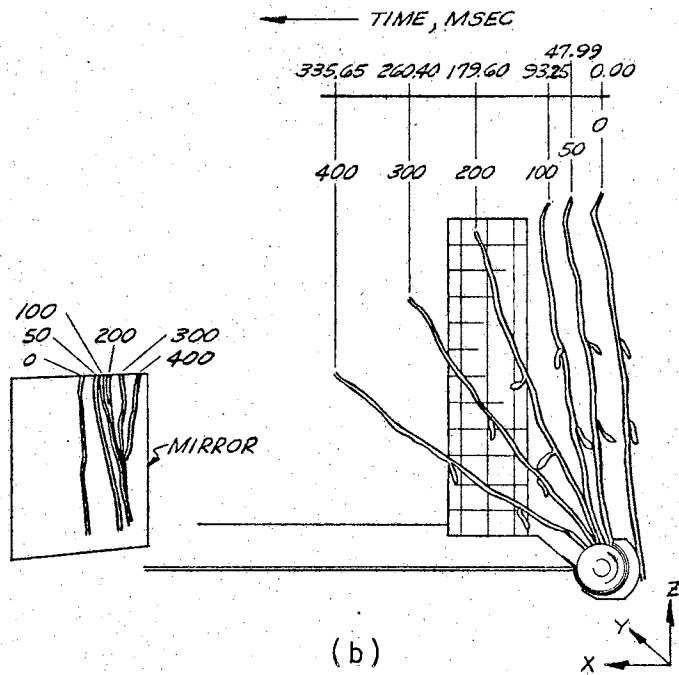
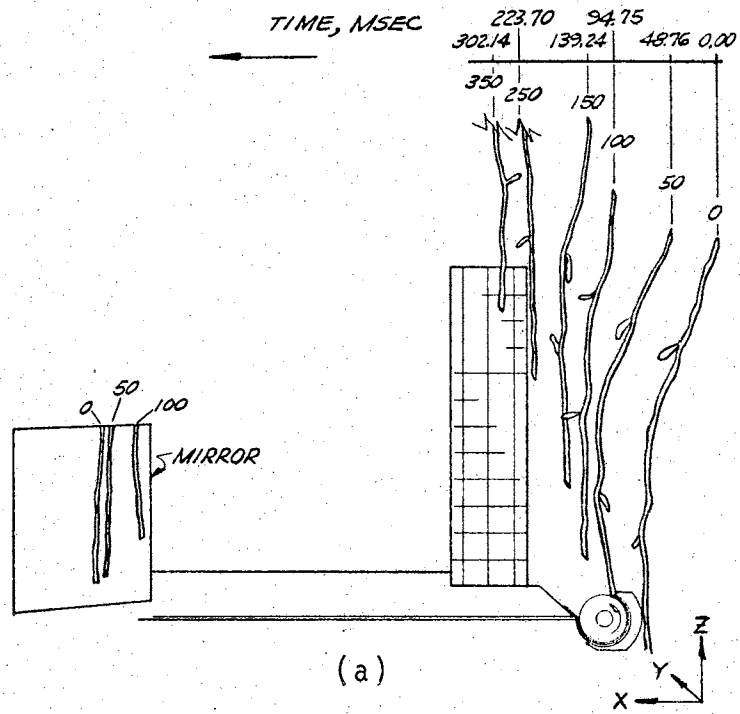


Figure 82. Trajectory of Stem 1, Trial PS-11 (a); and of Stem 1, Trial PS-10 (b)

Trajectory of the severed stems was more like that illustrated by Figure 82(a). In some instances, the cut end of the stem rotated forward to lead the stem top portion in X translation. This type of trajectory offers evidence that, in this case, the rotor sector does impart additional energy to the stem cut end after the cut is completed.

Cutting Mechanism: Sharp Blades,
High Speed Level

Figure 83 illustrates the mechanism of cutting with the 26 degree rotor fitted with sharp blades and rotating at 3600 rpm. The single element, impact type of cut shown for stem 3 in Figure 83 is typical of the manner in which the nine stems of trial PS-3 were cut. However stem 5 was deflected to the ledger blade before cutting was completed. It can be seen that the seed pod attached to stem 3, shown in the illustration, is not unduly shaken by the cutting. Point D, at the position of attachment of the seed pod, was subjected to a micromotion analysis, the results of which are shown by Figure 84. Since the X translation of point D exceeded its Y translation before cutting began, the average X acceleration was calculated to give an indication of the inertia forces involved. With the average X acceleration in excess of 1000 g's, the inertia force reached a high magnitude and provided for the almost instantaneous severing of the stem by the sharp blade, once it contacted it. As indicated by the torque traces, the peak cutting torque

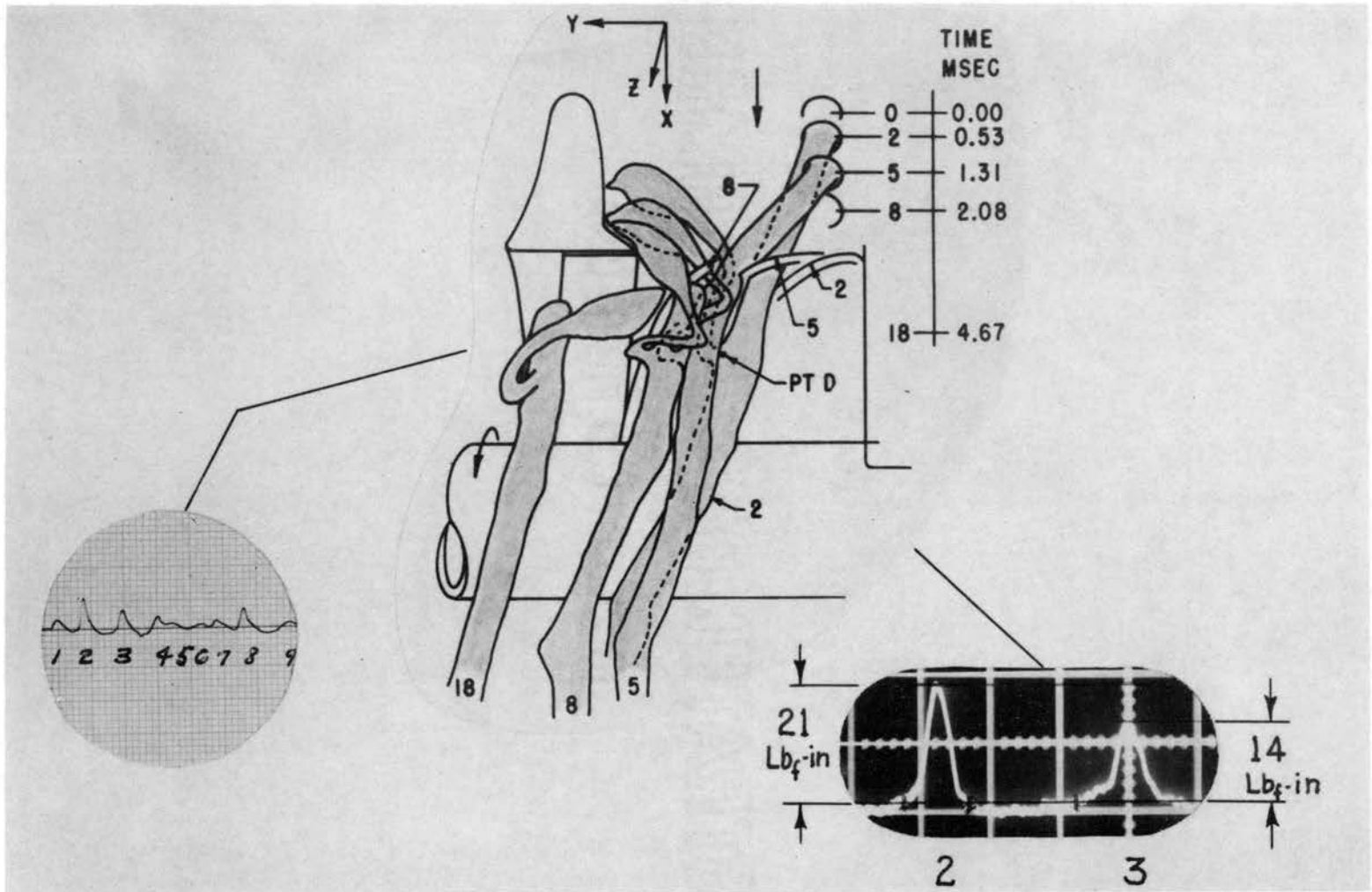


Figure 83. Mechanism of Severing Stems with Sharp Blades on the 26 Degree Rotor at 3600 RPM and with a Feed Rate of 5 1/4 in./rev. (Stem 3, Trial PS-3)

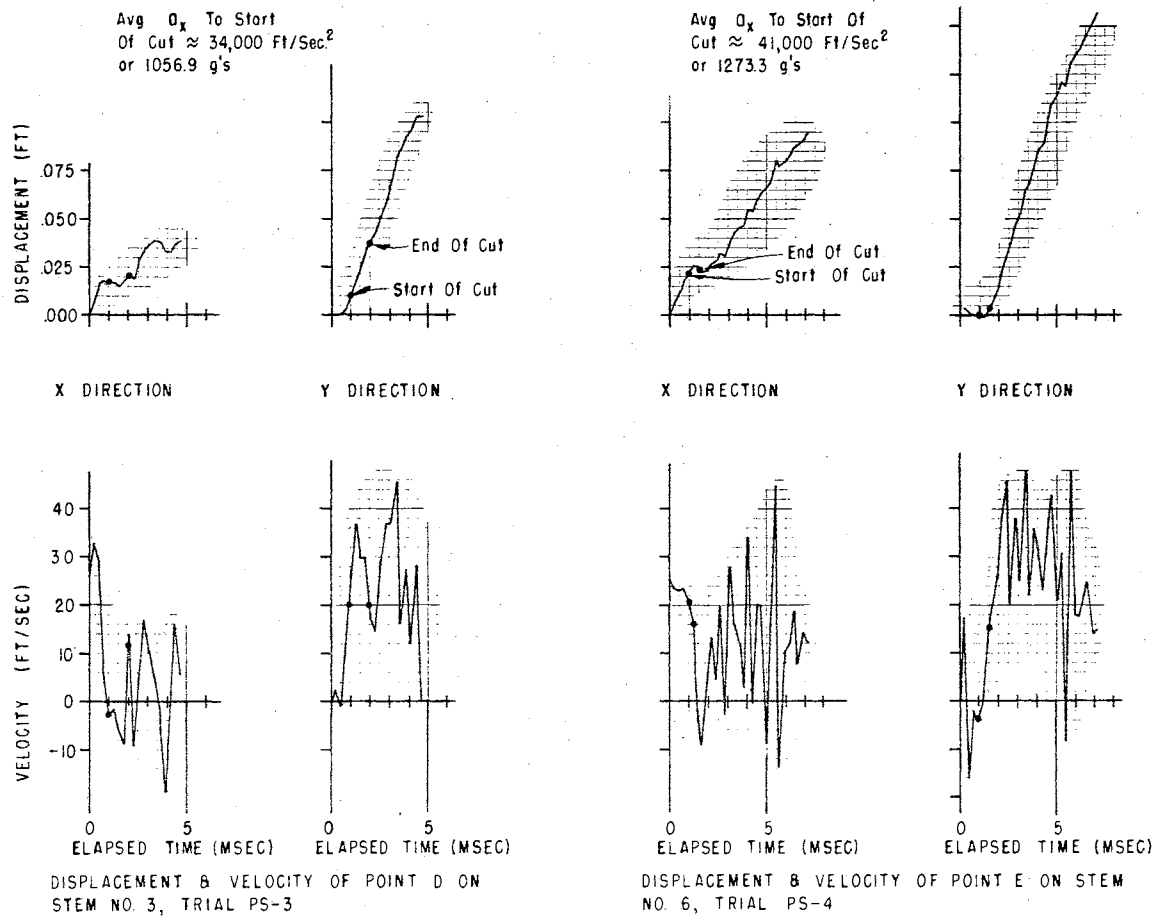


Figure 84. Displacement and Velocity of Point D on Stem 3, Trial PS-3 and of Point E on Stem 6, Trial PS-4.

required was low, just 14 lb_f -in. for stem 3. Energy input for stem 3 was calculated to be 39.9 in.- lb_f ; for stem 2 it was 51.1 in.- lb_f .

Figure 85 shows the cutting action of the 56 degree rotor fitted with sharp blades and under the same conditions as those described for trial PS-3. The film sequence is of trial PS-4, stem 6. Five of the nine stems of the trial were cut in the manner shown. The other four broke at the base before cutting was complete. The cut illustrated by Figure 85 took place in less than one millisecond, immediately after the blade contacted the stem. The cut end of the stem was then given an added impulse of energy as it slid along the rotor sector ledge to be discharged to the left. Plots of displacement and velocity of point E on stem 6 are given in Figure 84. The average X acceleration of point E before cutting began was calculated to be about 1273 g's; therefore the inertia force acting on the stem had a decisive affect on the manner of cut. The peak torque levels for those stems which did not break at the base was about 22.5 lb_f -in. consistently. The peak cutting force therefore was greater than that of the 26 degree rotor under the same conditions but less than that of the 56 degree rotor operated at 1800 rpm. Input energy varied from 48 to 59 in.- lb_f per stem cut.

The pattern of trajectory of the severed stems of trials PS-3 and PS-4 are shown in Figure 86. In (a) the motion of stem 9 of trial PS-9, run under the same

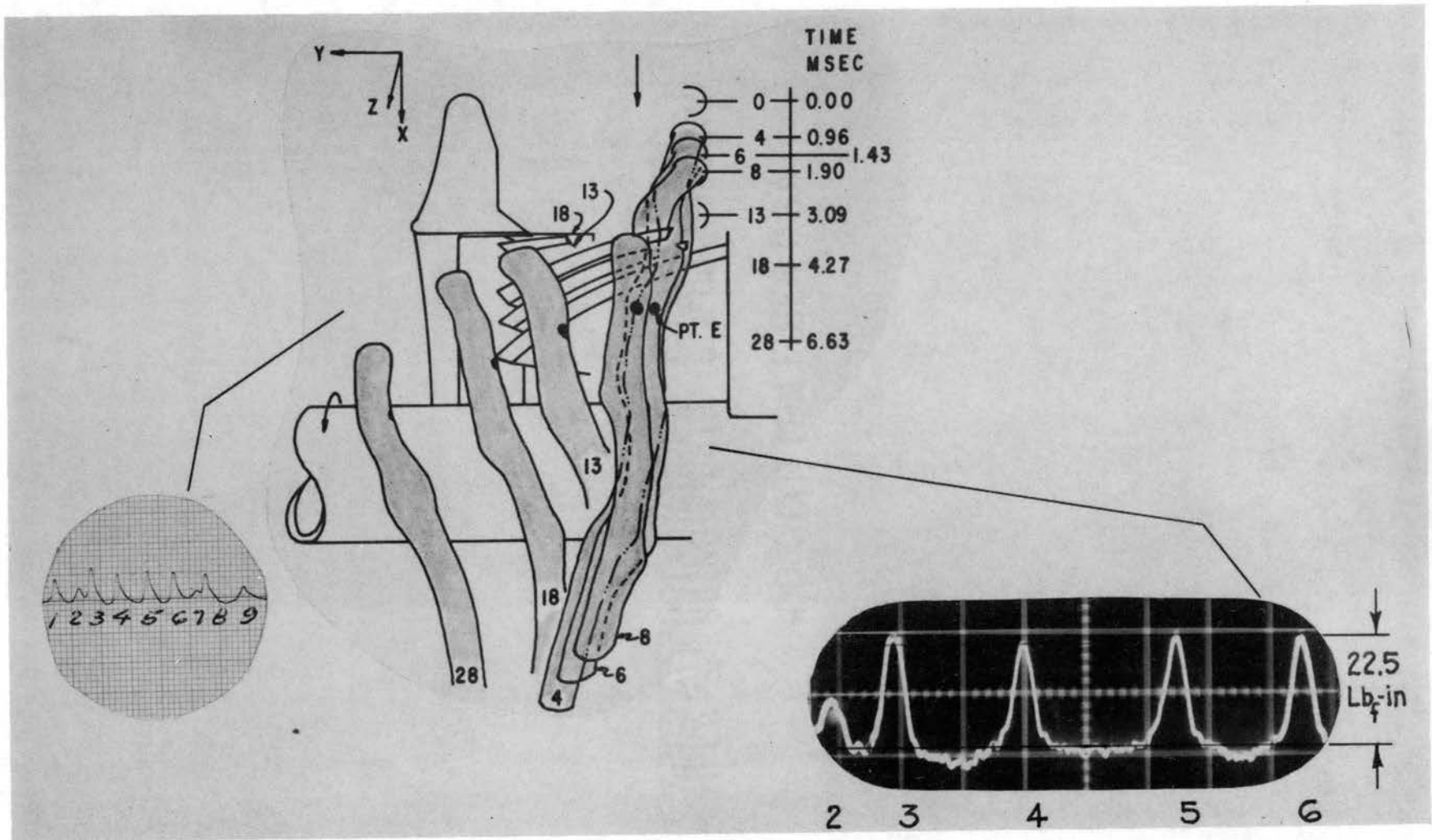


Figure 85. Cutting Mechanism of 56 Degree Rotor with Sharp Blades at 3600 RPM and with a Feed Rate of 5 1/4 in./rev. (Stem 6, Trial PS-4)

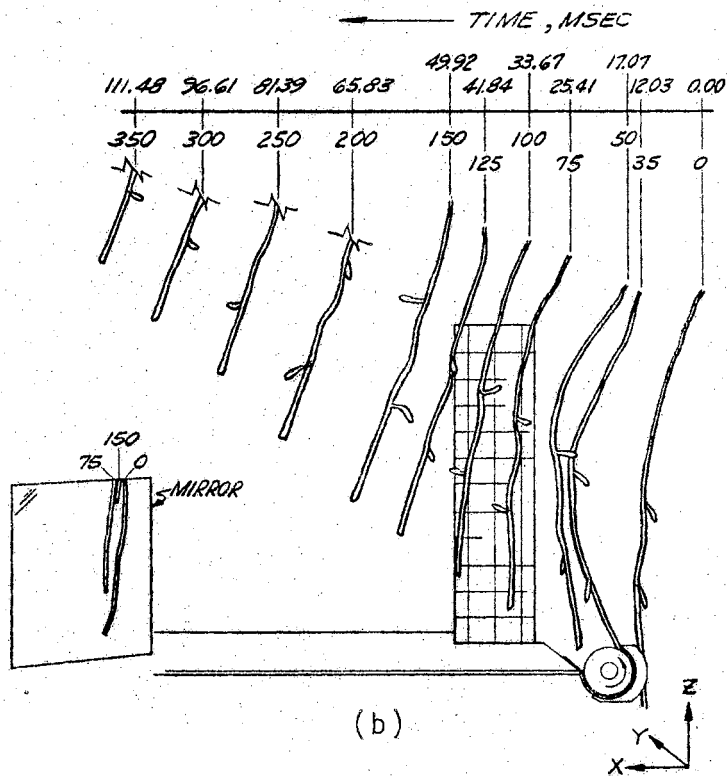
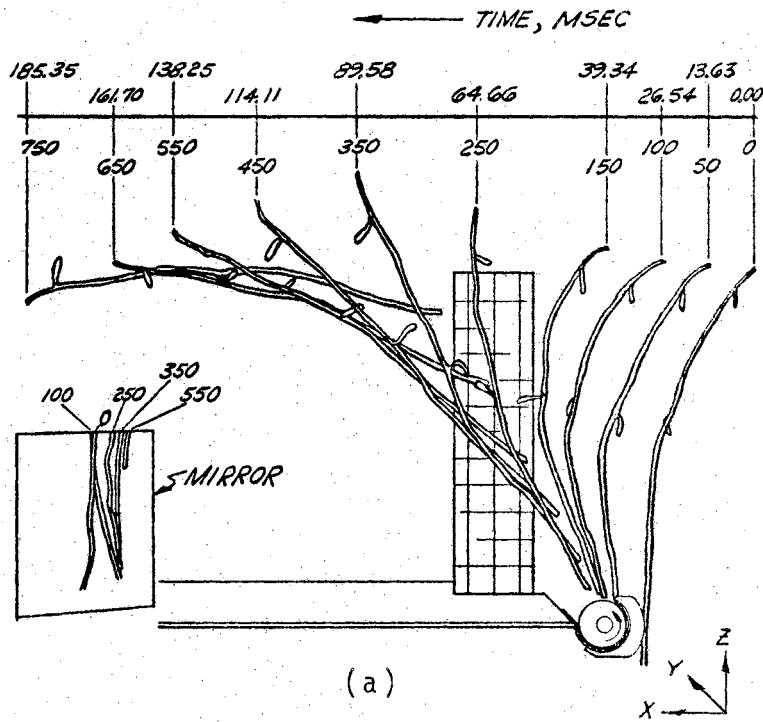


Figure 86. Trajectory of Stem 9, Trial PS-9 (a) and of Stem 1, Trial PS-8 (b)

conditions as trial PS-3, is shown. In (b) the motion of stem 1 of trial PS-8, run under the same conditions as trial PS-4, is depicted. The added energy imparted to the severed end of the stem by the 56 degree rotor is seen to "kick" the lower end ahead of the top of the plant in the XZ plane. The characteristic spin of the stem about its vertical Z axis is present in both cases.

Figure 87 illustrates the severing of stem 8 of trial PS-6. For this trial, nominal cutting height was 1 inch, lateral position was $3/8$ inch, and the stem diameter was $21/64$ inch. The 46 degree rotor fitted with sharp blades did the cutting. Feed rate was $3\ 1/16$ in./rev. With a different rotor, stem size, feed rate, lateral position, and cutting height, the cutting mechanism was still the same as for trials PS-3 and PS-4: single element impact cutting.

Further Analysis of Severed Stem Trajectory

A better understanding of the characteristic X translation of the severed stem might result from consideration of the motion of only one or two points along the stem length. The ultraviolet photographic techniques used to record the Z displacement of the cut stems in the trials of the main experiments afford a way of doing this. The trace of the center of gravity of the stem of trial 28, dull blade test series, presents a clear picture of the c.g. X displacement. This stem underwent almost pure planar motion

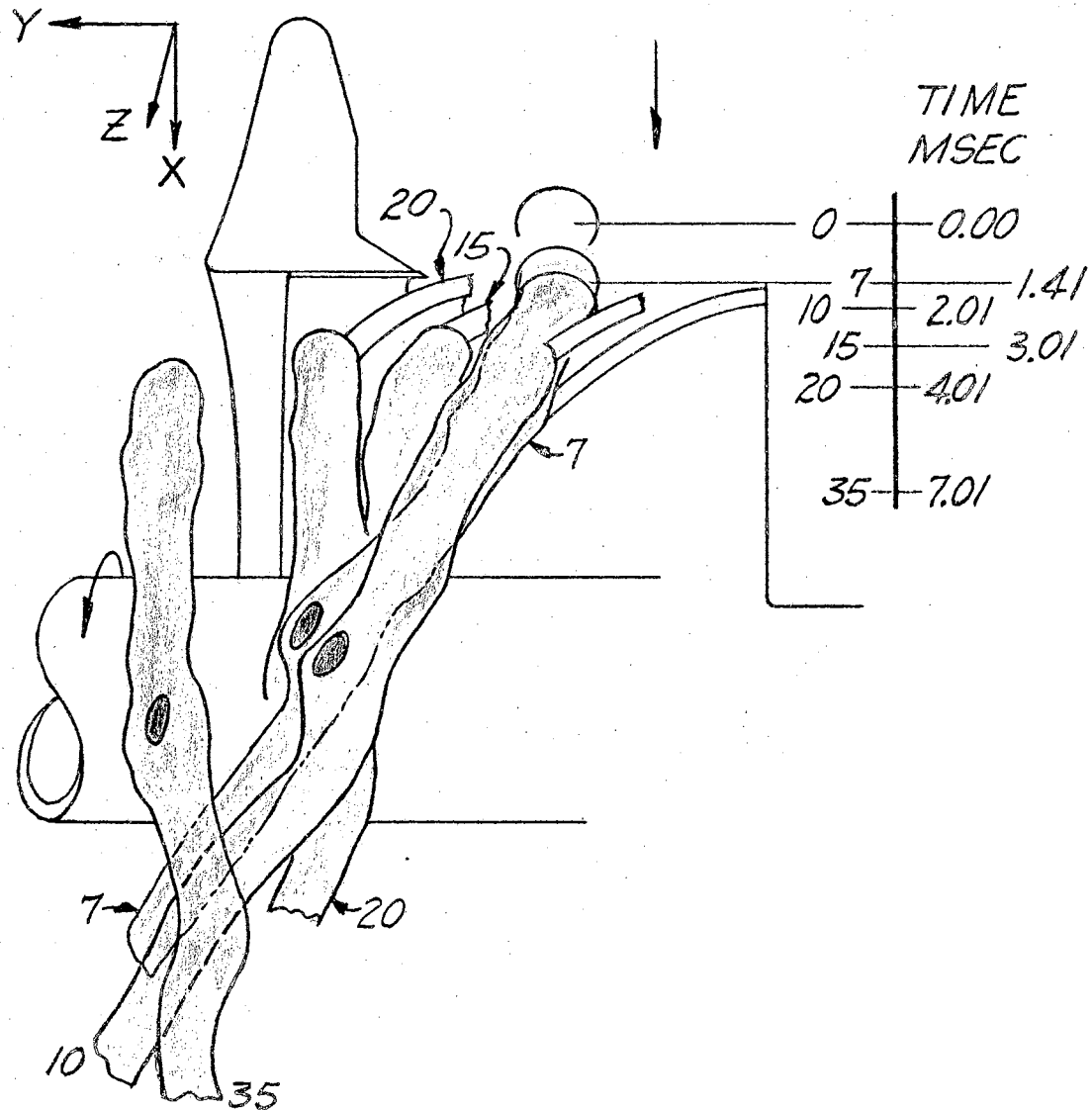


Figure 87. Cutting Mechanism for 46 Degree Rotor with Sharp Blades, Rotating at 3600 rpm with a Feed Rate of $3 \frac{1}{16}$ in./rev. (Stem 8, Trial PS-6)

after being cut. There was little or no Y translation or rotation about the X axis, as the final stem position on the horizontal grid board shows. See Figure 88. Since the ultraviolet light pulsed each 1/60 second, that is the time interval between successive trace marks in the photograph. The grid lines of the horizontal grid board are distinctively visible in the photograph and give an accurate linear scale for distance measurement. The drawing made by an overlay of the photograph is shown at the center of Figure 88. Calculated X velocity of the stem before being contacted by the rotor blade is 10.85 ft./sec.. Theoretical carriage velocity for this trial was 10.83 ft./sec.. Hence the graphic procedure gives accurate results. During cutting, the stem c.g. is decelerated to an X velocity of 6.65 ft./sec.. As it begins its descent under the influence of gravity, the stem c.g. still has an X velocity of 6.65 ft./sec.. Although this analysis is not conclusive, it does indicate that compared to gravity forces, the drag force on the severed stem has a lesser, second order effect on the motion. Therefore it appears justified not to have included drag force in the dimensional analysis of the system (Chapter V).

Check on Rotor Speed

A check on the accuracy with which rotor speed was maintained in the filming sequences was made through analysis of some of the timing and event mark data placed on the

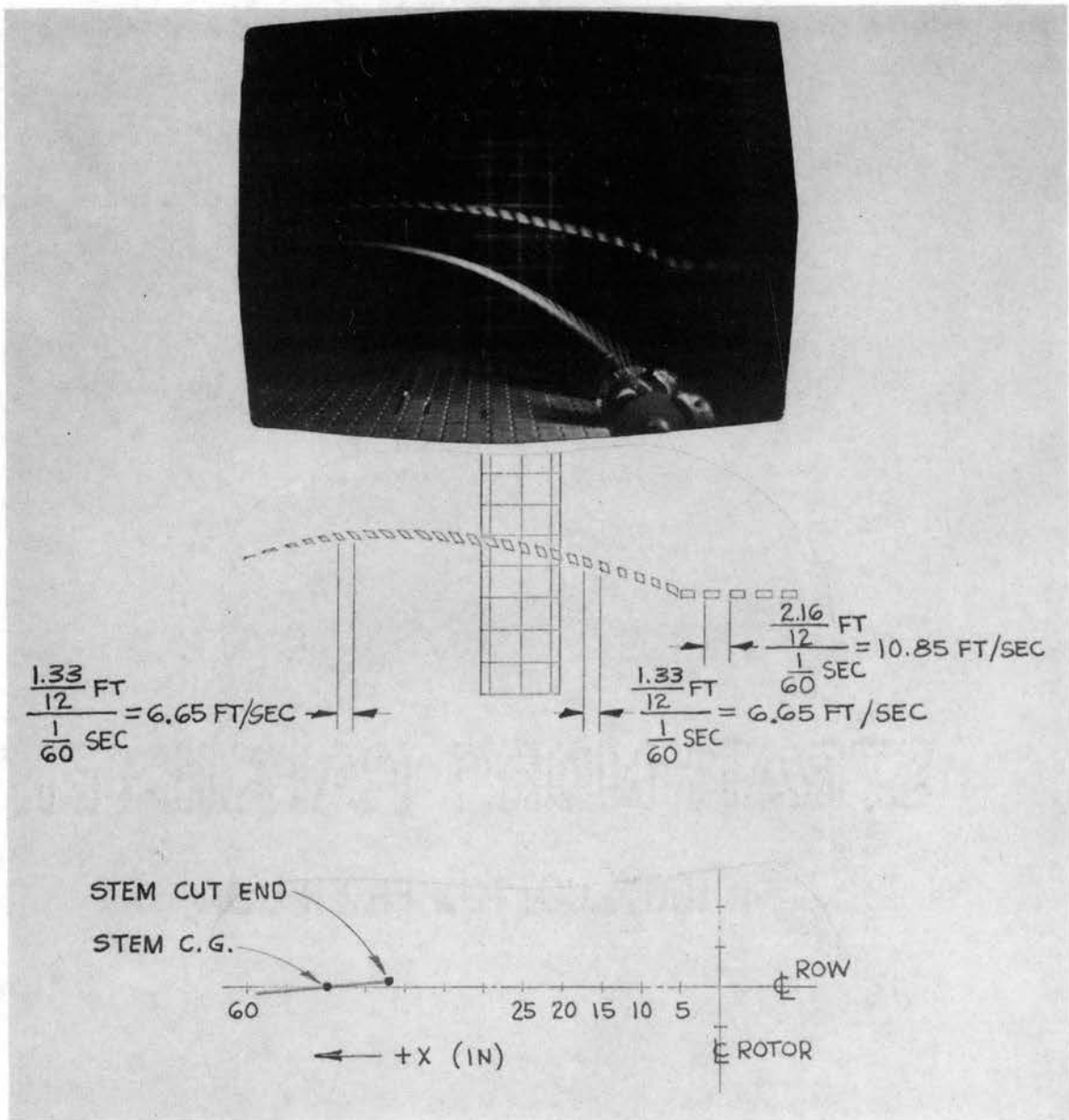


Figure 88. Analysis of Trajectory of Stem Center of Gravity

film with the equipment described in Chapter VII. Results are presented in Table XIV.

TABLE XIV
COMPARISON OF THEORETICAL AND
CALCULATED ROTOR SPEEDS

Trial No. and Stem Cutting Shown on Film Sequence	Theo. Rotor Speed		Calculated Rotor Speed From Timing Mark Data	Percent Deviation from Theo.
	1800	3600		
PS-10 #1	X		1729 Based on 8 rev.	3.9
PS-11 #1	X		1719 Based on 8 rev.	4.5
PD-12 #3	X		1702 Based on 4 rev.	5.4
PD-3 #3		X	3586 Based on 4 rev.	0.4
PS-7 #2		X	3441 Based on 4 rev.	4.4
PS-8 #1		X	3508 Based on 4 rev.	2.6
PS-9 #9		X	3481 Based on 4 rev.	3.3
PD-10 #9		X	3403 Based on 4 rev.	5.5

The variation was greater than expected, but it must be remembered that the rotor necessarily slows down momentarily when a stem is cut due to extraction of energy from the rotary system. Since the checks extended over at most eight revolutions of the rotor, the effects of the momentary speed decreases are included in the periods analyzed.

Main, Screening of Parameter, Tests

The reduced data for the main, screening of parameter experiment series are tabulated in Appendix C. The dull blade series main test data comprises Appendix C-II; the sharp blade series main test data comprises Appendix C-III. As was indicated in Chapter VI, the dull blade test series was begun with three replications of each treatment combination, but was revised to a two replication plan after 30 trials. Where three replications were run, one had to be eliminated before analysis on a two replication basis could proceed. The criteria for discarding one of the three trials was as follows:

1. If one trial involved a noneffective cutting action (breaking of the stem at the base before it was completely severed, for example) while effective cuts were made in the other two trials, the trial with the noneffective cut was discarded.

2. If all three trials resulted in effective cuts, or if there were two noneffective cuts, then the trial having the greatest deviation in moisture content or stem dry linear density was eliminated.

For statistical analysis of the data, two dimensioned response variables were added to the eight dimensionless response pi terms previously defined through dimensional analysis. The new response variables were energy input per stem cut (in.-lb_f) and maximum torque developed per stem cut (lb_f-in.).

Analysis of Variance

An analysis of variance was performed on the reduced data for each of the ten response terms in both the dull blade and the sharp blade test series. This was done on an IBM 360 digital computer. The fortran program for the computer was written to also calculate a table of treatment means for each response variable. Results of this analysis are listed in Appendix D-I for the dull blade series and in Appendix D-II for the sharp blade series.

Results of the analysis of variance are summarized in Table XV. The test of significance of an independent variable is based on the F-ratio calculated from its effect on the response term. Two confidence levels will be considered in judging the significance of independent factors. At the 85 percent confidence level, any independent factor that has the slightest non-trivial effect on a response variable will be assessed significant. At the 95 percent confidence level, there is only one chance in twenty that an independent variable will be judged significant when in fact it is not; therefore this level provides a more critical basis for judgement.

Table XVI lists the factors calculated to have a significant effect on the response terms at each of the two confidence levels. The 85 percent confidence level is the $\alpha = .15$ level; similarly, the 95 percent confidence is the $\alpha = .05$ level.

TABLE XV
SUMMARY OF RESULTS OF ANALYSIS OF VARIANCE

RESPONSE VARIABLE	BLADE	INDEPENDENT CONTROLLED VARIABLES																	
		DIA		TIME IN CHAMBER		Π_2 ROTOR SPEED INDEX		Π_3 FEED RATE INDEX		Π_4 ROTOR ANGLE INDEX		Π_5 LATERAL POSITION INDEX		Π_6 LEDGER ORIENTATION INDEX		Π_7 CUTTING HEIGHT INDEX		Π_9 PLANT C.G. HEIGHT INDEX	
		CALC F	α_L	CALC F	α_L	CALC F	α_L	CALC F	α_L	CALC F	α_L	CALC F	α_L	CALC F	α_L	CALC F	α_L	CALC F	α_L
ENERGY INPUT PER STEM CUT	D	73.311	$\leq .0005$	2.176	$\leq .15$	1.689	$\leq .25$	3.846	$\leq .05$	1.151	$\leq .35$	4.304	$\leq .05$	0.279	$\leq .85$	1.359	$\leq .30$	1.122	$\leq .35$
	S	82.550	$\leq .0005$	19.580	$\leq .0005$	1.275	$\leq .30$	0.273	$\leq .85$	11.890	$\leq .0005$	4.035	$\leq .05$	2.210	$\leq .11$	2.864	$\leq .10$	5.759	$\leq .005$
MAX. TORQUE PER STEM CUT	D	55.697	$\leq .0005$	0.389	$\leq .85$	9.142	$\leq .0005$	0.927	$\leq .40$	4.450	$\leq .05$	2.860	$\leq .10$	1.567	$\leq .25$	0.914	$\leq .40$	2.680	$\leq .10$
	S	45.344	$\leq .0005$	7.584	$\leq .005$	11.142	$\leq .0005$	0.065	$\leq .98$	9.918	$\leq .0005$	1.845	$\leq .25$	3.387	$\leq .05$	1.575	$\leq .25$	2.382	$\leq .10$
ENERGY INPUT INDEX	D	5.484	$\leq .005$	1.343	$\leq .30$	2.169	$\leq .12$	5.601	$\leq .01$	0.748	$\leq .55$	4.541	$\leq .01$	0.125	$\leq .96$	0.431	$\leq .70$	16.635	$\leq .0005$
	S	9.946	$\leq .0005$	10.576	$\leq .0005$	2.979	$\leq .05$	2.166	$\leq .15$	2.407	$\leq .10$	4.158	$\leq .02$	0.725	$\leq .55$	3.111	$\leq .07$	14.980	$\leq .0005$
MAX. TORQUE INDEX	D	2.130	$\leq .12$	2.065	$\leq .15$	3.424	$\leq .05$	1.656	$\leq .25$	1.450	$\leq .25$	1.188	$\leq .35$	0.519	$\leq .65$	0.368	$\leq .80$	9.259	$\leq .0005$
	S	5.344	$\leq .005$	3.903	$\leq .05$	8.636	$\leq .0005$	1.101	$\leq .35$	2.858	$\leq .06$	2.118	$\leq .12$	2.314	$\leq .10$	4.223	$\leq .05$	16.648	$\leq .0005$
C.G. X DISP. INDEX	D	1.227	$\leq .30$	0.448	$\leq .70$	5.620	$\leq .005$	8.454	$\leq .005$	1.404	$\leq .30$	0.911	$\leq .45$	0.525	$\leq .70$	0.575	$\leq .70$	0.739	$\leq .55$
	S	1.230	$\leq .30$	1.143	$\leq .35$	9.782	$\leq .0005$	11.599	$\leq .0005$	5.831	$\leq .005$	0.436	$\leq .75$	1.099	$\leq .35$	0.031	$\leq .99$	1.576	$\leq .25$
END X DISP. INDEX	D	1.144	$\leq .35$	0.329	$\leq .80$	4.294	$\leq .05$	8.442	$\leq .005$	1.766	$\leq .25$	0.576	$\leq .65$	0.657	$\leq .60$	0.381	$\leq .85$	0.508	$\leq .65$
	S	1.091	$\leq .35$	1.392	$\leq .30$	8.823	$\leq .0005$	7.802	$\leq .005$	5.315	$\leq .005$	0.131	$\leq .96$	1.122	$\leq .35$	0.148	$\leq .96$	0.526	$\leq .65$
C.G. Y DISP. INDEX	D	0.747	$\leq .55$	0.680	$\leq .60$	0.601	$\leq .60$	2.975	$\leq .10$	5.408	$\leq .005$	4.946	$\leq .01$	1.134	$\leq .35$	7.838	$\leq .005$	3.344	$\leq .05$
	S	0.240	$\leq .90$	1.237	$\leq .30$	4.300	$\leq .05$	0.116	$\leq .90$	1.410	$\leq .26$	2.358	$\leq .10$	0.418	$\leq .75$	0.502	$\leq .70$	0.968	$\leq .45$
END Y DISP. INDEX	D	0.774	$\leq .55$	1.032	$\leq .35$	0.679	$\leq .60$	1.513	$\leq .25$	4.285	$\leq .05$	3.581	$\leq .05$	0.816	$\leq .50$	6.486	$\leq .005$	4.569	$\leq .01$
	S	0.286	$\leq .90$	1.108	$\leq .35$	3.610	$\leq .05$	0.032	$\leq .99$	1.777	$\leq .20$	1.078	$\leq .35$	0.269	$\leq .90$	1.467	$\leq .25$	0.709	$\leq .55$
C.G. Z DISP. INDEX	D	1.994	$\leq .20$	1.589	$\leq .30$	4.857	$\leq .01$	1.239	$\leq .30$	2.228	$\leq .12$	3.046	$\leq .05$	1.480	$\leq .25$	1.950	$\leq .25$	1.322	$\leq .30$
	S	2.146	$\leq .12$	2.392	$\leq .10$	2.643	$\leq .10$	0.629	$\leq .60$	3.567	$\leq .05$	1.599	$\leq .25$	2.280	$\leq .10$	2.209	$\leq .11$	2.391	$\leq .10$
END Z DISP. INDEX	D	1.688	$\leq .25$	1.369	$\leq .30$	4.284	$\leq .05$	2.082	$\leq .15$	2.278	$\leq .10$	2.951	$\leq .05$	1.058	$\leq .30$	1.641	$\leq .25$	1.505	$\leq .25$
	S	2.348	$\leq .10$	2.678	$\leq .10$	2.713	$\leq .10$	0.969	$\leq .40$	4.229	$\leq .05$	1.559	$\leq .25$	2.821	$\leq .10$	2.751	$\leq .10$	3.547	$\leq .05$

α_L = Lowest α Level at Which H_0 : (No Diff. in Response Means for Various Levels of a Factor) can be Rejected

$F_{.50(3,32)} = .806$	$F_{.75(3,32)} = 1.44$	$F_{.90(3,32)} = 2.27$	$F_{.95(3,32)} = 2.90$	$F_{.99(3,32)} = 4.47$	$F_{.995(3,32)} = 5.09$	$F_{.9995(3,32)} = 7.79$
$F_{.50(2,32)} = .708$	$F_{.75(2,32)} = 1.45$	$F_{.90(2,32)} = 2.48$	$F_{.95(2,32)} = 3.30$	$F_{.99(2,32)} = 5.35$	$F_{.995(2,32)} = 6.29$	$F_{.9995(2,32)} = 9.77$

α is the Probability of Rejecting H_0 when it is True, of Declaring a Significant Difference in the Factor Level Response Means when in Fact no Real Difference Exists (Type I Error)

TABLE XVI

INDEPENDENT VARIABLES HAVING SIGNIFICANT EFFECT ON THE RESPONSE VARIABLES AT THE $\alpha = .15$ and $\alpha = .05$ LEVELS

RESPONSE VARIABLE	BLADE	INDEPENDENT VARIABLES HAVING SIGNIFICANT EFFECT	
		$\alpha = .15$ LEVEL	$\alpha = .05$ LEVEL
ENERGY INPUT PER STEM CUT	D	Dia., Time in Chamber, Π_3, Π_5	Dia., Π_3, Π_5
	S	Dia., Time in Chamber, $\Pi_4, \Pi_5, \Pi_6, \Pi_7, \Pi_9$	Dia., Time in Chamber, Π_4, Π_5, Π_9
MAX. TORQUE PER STEM CUT	D	Dia., $\Pi_2, \Pi_4, \Pi_5, \Pi_9$	Dia., Π_2, Π_4
	S	Dia., Time in Chamber, $\Pi_2, \Pi_4, \Pi_6, \Pi_9$	Dia., Time in Chamber, Π_2, Π_4, Π_6
ENERGY INPUT INDEX	D	Dia., $\Pi_2, \Pi_3, \Pi_5, \Pi_9$	Dia., Π_3, Π_5, Π_9
	S	Dia., Time in Chamber, $\Pi_2, \Pi_3, \Pi_4, \Pi_5, \Pi_7, \Pi_9$	Dia., Time in Chamber, Π_2, Π_5, Π_9
MAX. TORQUE INDEX	D	Dia., Time in Chamber, Π_2, Π_9	Π_2, Π_9
	S	Dia., Time in Chamber, $\Pi_2, \Pi_4, \Pi_5, \Pi_6, \Pi_7, \Pi_9$	Dia., Time in Chamber, Π_2, Π_7, Π_9
C.G. X DISP. INDEX	D	Π_2, Π_3	Π_2, Π_3
	S	Π_2, Π_3, Π_4	Π_2, Π_3, Π_4
END X DISP. INDEX	D	Π_2, Π_3	Π_2, Π_3
	S	Π_2, Π_3, Π_4	Π_2, Π_3, Π_4
C.G. Y DISP. INDEX	D	$\Pi_3, \Pi_4, \Pi_5, \Pi_7, \Pi_9$	$\Pi_4, \Pi_5, \Pi_7, \Pi_9$
	S	Π_2, Π_5	Π_2
END Y DISP. INDEX	D	$\Pi_4, \Pi_5, \Pi_7, \Pi_9$	$\Pi_4, \Pi_5, \Pi_7, \Pi_9$
	S	Π_2	Π_2
C.G. Z DISP. INDEX	D	Π_2, Π_4, Π_5	Π_2, Π_5
	S	Dia., Time in Chamber, $\Pi_2, \Pi_4, \Pi_6, \Pi_7, \Pi_9$	Π_4
END Z DISP. INDEX	D	$\Pi_2, \Pi_3, \Pi_4, \Pi_5$	Π_2, Π_5
	S	Dia., Time in Chamber, $\Pi_2, \Pi_4, \Pi_6, \Pi_7, \Pi_9$	Π_4, Π_9

Graphs of Treatment Means and Discussion of Results

To answer the question of what type of effect - linear, quadratic, cubic - that each significant factor (at the 85 percent confidence level) has on the response variables, the treatment means are graphed in Figures 89 through 96. Analysis of variance data were utilized to draw the correct type of curve representing the response. With reference to Figures 89 through 96, and to Tables XV and XVI, consider now each response variable in turn.

Energy input per stem cut depended primarily on the plant stem nominal diameter, or on those stem physical properties having a one to one correspondence with the nominal diameter, for both the dull and sharp blades. The relationship was linear for the sharp blades and linear tending toward quadratic at the larger diameters for the dull blade, as Figure 89 shows.

For the sharp blade, the next most significant factor affecting energy input was time in the conditioning chamber, which is a measure of moisture content of the stem. For the dull blade, time in chamber was barely significant at the 85 percent confidence level. The effect was cubic for both the sharp and dull blades. Mean input energy for cutting was greatest for stems treated six hours in the chamber. This treatment time corresponds to mean moisture

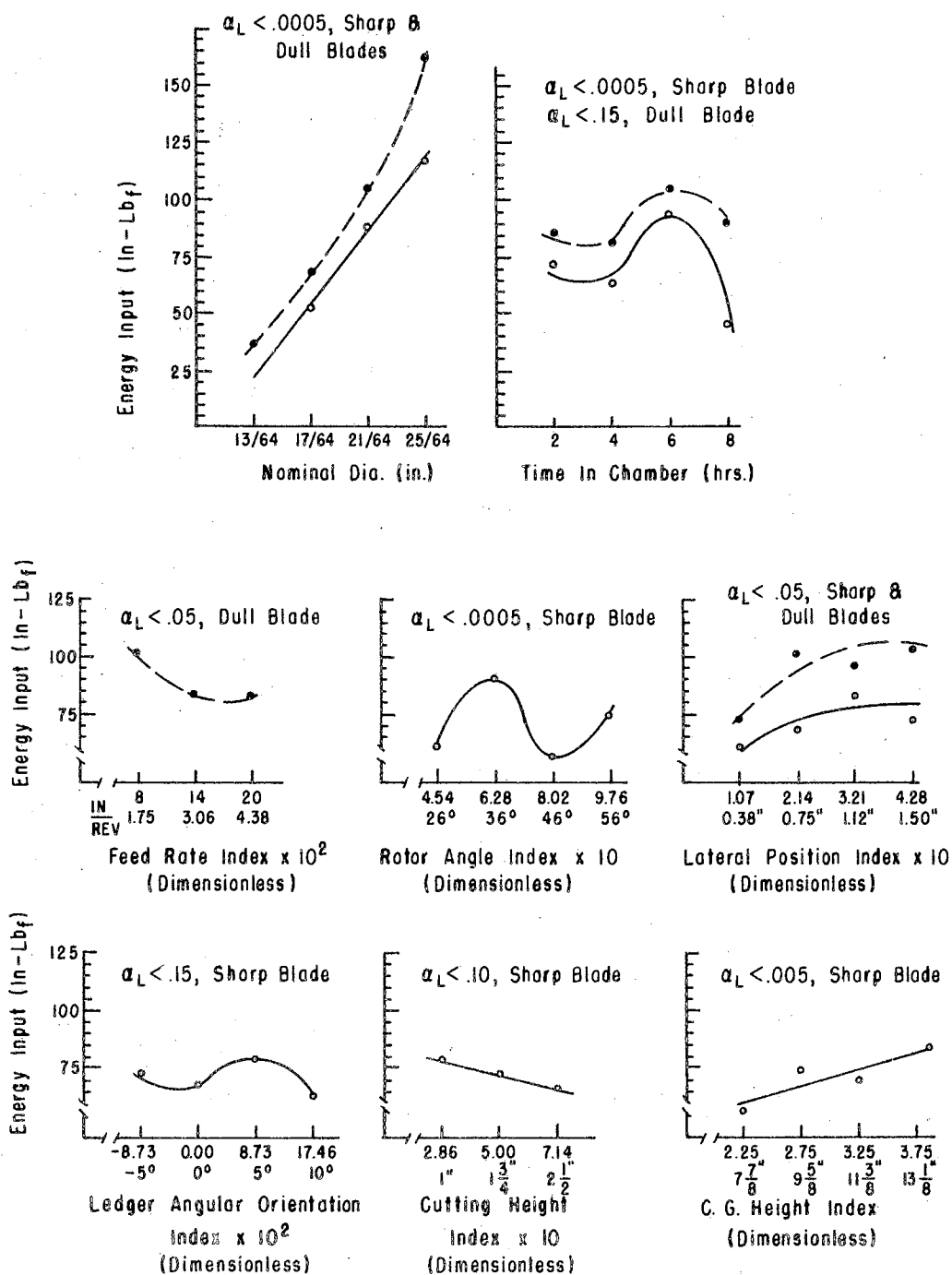


Figure 89. Energy Input Per Stem Cut Versus Independent Variable Parameters (Solid Line = Sharp Blade; Dashed Line = Dull Blade)

contents of 35 percent (D.B.) for the dull blade series of tests and 43 percent (D.B.) for the sharp blade series of tests.

After diameter, the lateral position index had the greatest effect on energy input for the dull blade test series, and had a significant effect for the sharp blade series, too, but not so much as the rotor angle index. The rotor angle index did not have appreciable effect with use of the dull blade. With both the dull and sharp blades, the effect of lateral position was quadratic. There was a noticeable increase in energy input between the first and second levels of lateral position index, but the increase "tapered off" among the second, third and fourth levels. This effect may be attributed to the added energy required to bend the stem to the ledger blade with increasing distance for the dull blade. For the sharp blade, it may be attributed to increased energy imparted to the severed end of the stem while it is in contact with the rotor sector after cutting. This added energy affects the stem trajectory.

The rotor angle index had a cubic effect with use of sharp blades. The 46 degree rotor required the least mean energy input per stem cut; the 36 degree rotor required the most. On examining the trials involving the 36 degree rotor, it was noted that there were many instances where one sector sliced a plug from the stem without severing it completely; the opposite sector then completed the cut. This "double

contact" type of cutting expends considerable amounts of energy, as was shown in the previous section describing the cutting mechanism involved. Although rotor angle index did not have a significant effect with use of the dull blade, examination of the table of mean values reveals that the 26 degree rotor required the least mean energy input, followed in order by the 36, 46, and 56 degree rotors. This was the expected result since two element cutting was involved.

The feed rate index is the final independent variable considered which had a significant effect on energy input per stem cut for the dull blade series. Surprisingly, the feed rate index did not have a significant effect in the sharp blade tests. For the dull blade, the effect was quadratic; the energy input dropped rapidly between the first and second levels; it was about the same for the second and third levels.

The plant stem center of gravity height index was highly significant for the sharp blade test series. It had primarily a linear effect but tended toward a cubic effect, with energy input per stem cut increasing with increasing height of center of gravity of the plant.

The ledger orientation index and the cutting height index were of about the same order of importance in affecting the input energy. The ledger orientation had a cubic effect, with the +10 degree setting giving best mean results,

followed by the 0 degree setting. Effect of the cutting height was linear, energy input decreasing with increasing cutting height.

The rotor speed index did not have a significant effect on energy input per stem cut for either the dull or sharp blade test series.

Figure 90 illustrates the influence on maximum torque developed per stem cut for each of the independent variables which affected it at the 85 percent confidence level. As was the case with the response of energy input, nominal diameter of the stems had the greatest effect on maximum torque developed for both the dull and sharp blade test series. Again the effect was linear for the sharp blade and linear tending toward quadratic for the dull blade.

Following nominal diameter, the rotor speed index was the next most important independent variable affecting cutting torque. Its effect was quadratic for both the dull and sharp blades. With increasing rotor speed, the maximum cutting torque dropped rapidly at the low level of the speed range. Then it leveled off and began to increase slightly at the upper end of the range. Minimum values of peak cutting torque occurred for rotor speeds between 3100 and 3600 rpm for both the dull and sharp blade rotors.

Next to rotor speed index in importance was the rotor angle index - for both dull and sharp blades. For dull blades the effect was linear, peak torque levels increasing with increase of the rotor angle. With sharp blades, the

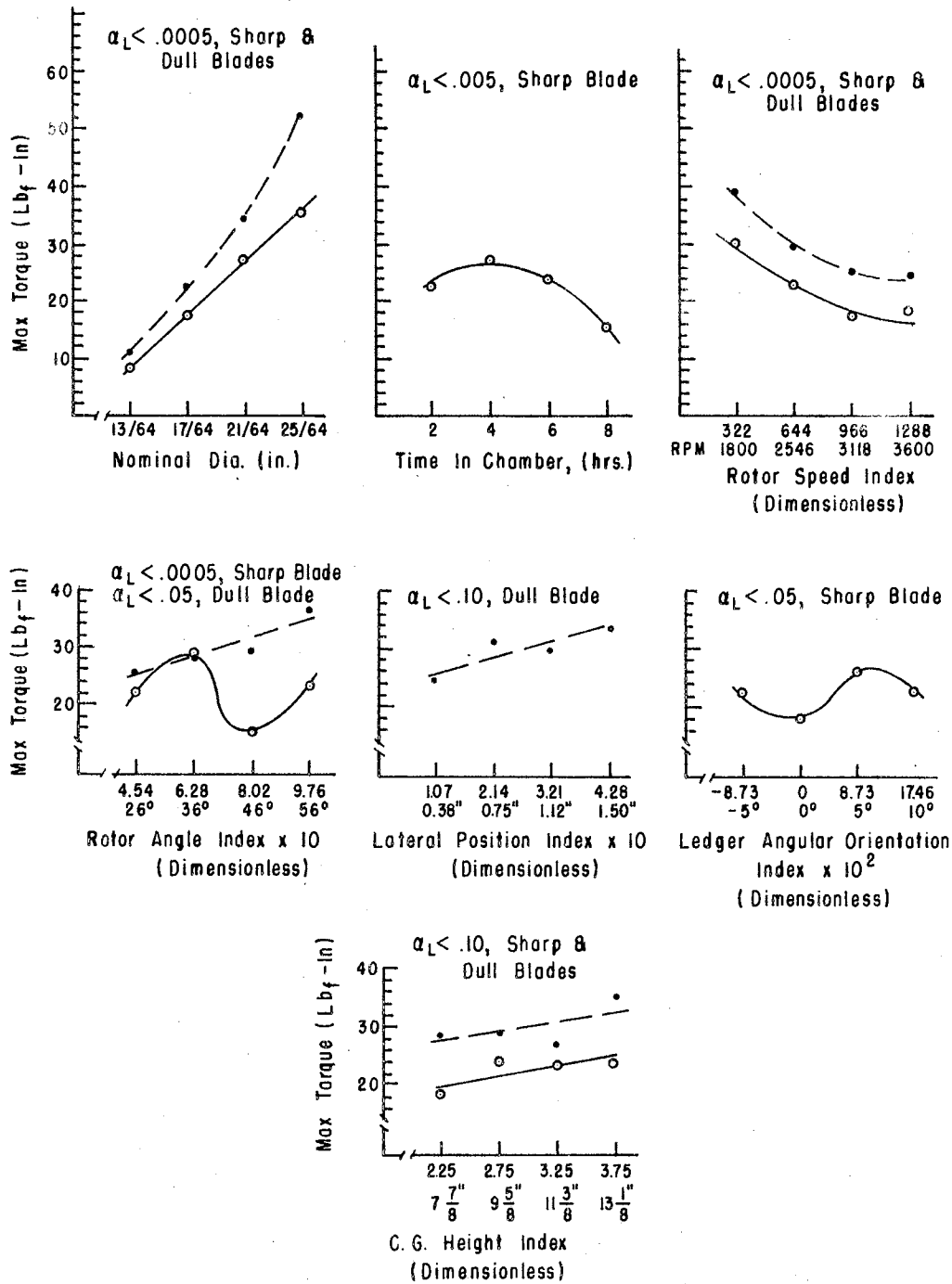


Figure 90. Maximum Torque Per Stem Cut Versus Independent Variable Parameters (Solid Line = Sharp Blade; Dashed Line = Dull Blade)

effect was cubic. The 46 degree rotor developed the least mean peak torque, followed by the 26 degree rotor. The 36 degree rotor produced the maximum mean peak torque value.

Time in chamber had a highly significant effect for the sharp blade series and no effect (at the 85 percent confidence level) for the dull blade series. The effect was quadratic for the sharp blade series. Stems treated four hours required slightly greater torque levels for cutting than those treated two hours. The required cutting torque level decreased with increasing time in chamber for the six and eight hour treatment times.

Ledger orientation significantly affected peak torques developed in the sharp blade test series only. The effect was cubic with the 0 degree setting developing the least mean peak torque.

The lateral position index had a significant effect on peak torque for the dull blade test series only. The effect was linear (with a slight cubic tendency). Peak torque per stem cut became greater with increase in lateral position.

In both the dull and sharp blade series, maximum torque developed was dependent on the plant center of gravity index. The effect was linear with quadratic tendencies for both series. With increasing values of the C.G. height index, the maximum torque per stem cut mean values increased.

The feed rate index had no effect on the maximum torque per stem cut at the 85 percent confidence level for either the dull or sharp blade series.

As stated in Chapter V, it was hoped that the dimensionless response variables, energy input index and maximum torque index, would be related to the independent variables in nearly the same manner as the dimensioned response variables, energy input per stem cut and maximum torque per stem cut. The principal exception desired was that the effects of diameter and moisture content would be removed by the denominator terms of the dimensionless variables. Examination of Figures 91 and 92, which show how the energy input index and maximum torque index relate to the independent variables, will confirm that the goals sought were only partly realized. The effects of diameter and time in chamber are still present - although less significant. The other relationships are fairly parallel for the dimensioned and dimensionless response variables in most but not all cases. For instance, in the case of energy input per stem cut, the effects of the plant C.G. height index are magnified and give a curve of reverse slope for the dimensionless response term. And rotor speed index comes into significance whereas it was not for the dimensioned response term. In the case of maximum torque per stem cut, the C.G. height index again gives a magnified curve of reverse slope, and cutting height index becomes a significant variable for the sharp blade series.

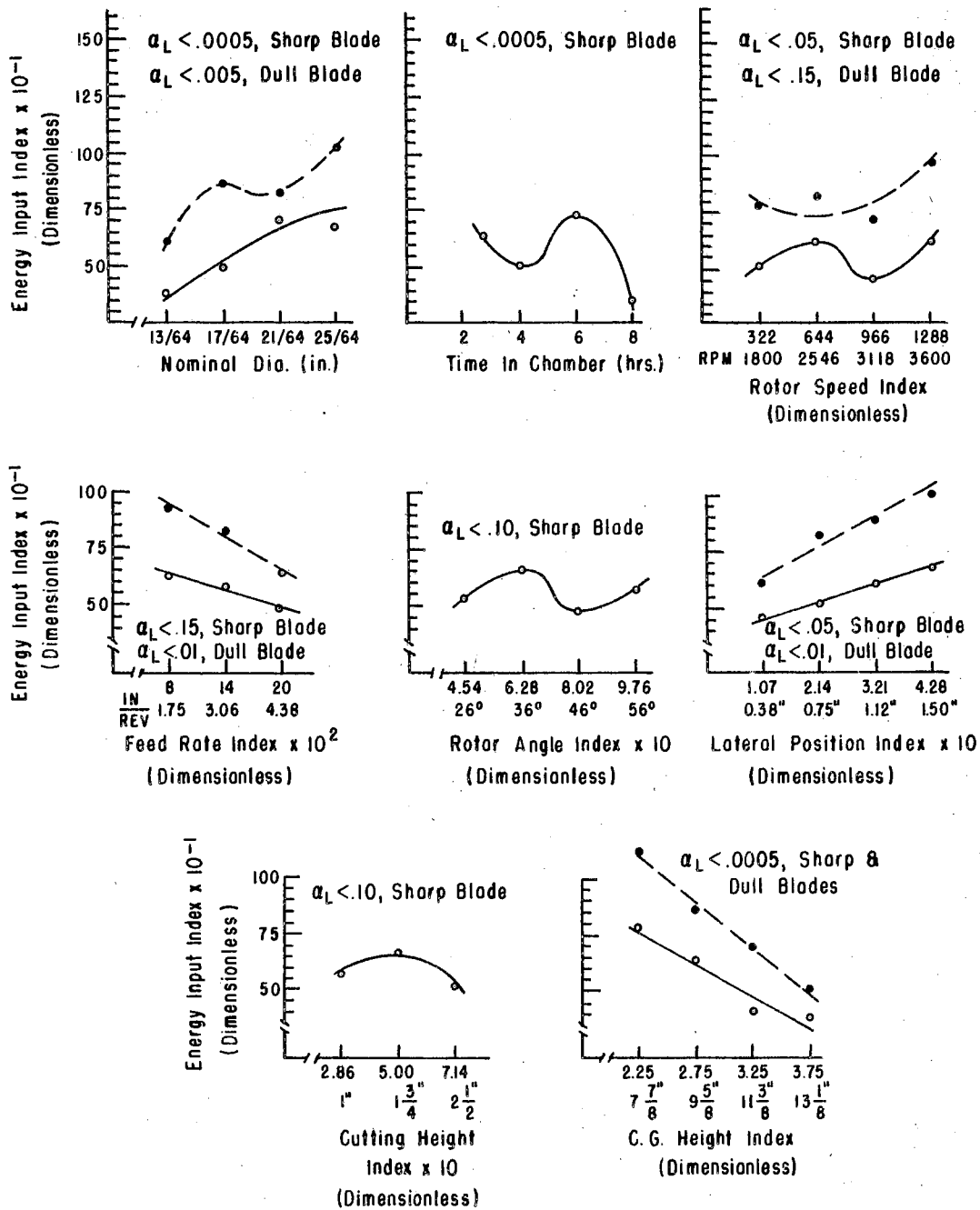


Figure 91. Energy Input Index Versus Independent Variable Parameters (Solid Line = Sharp Blade; Dashed Line = Dull Blade)

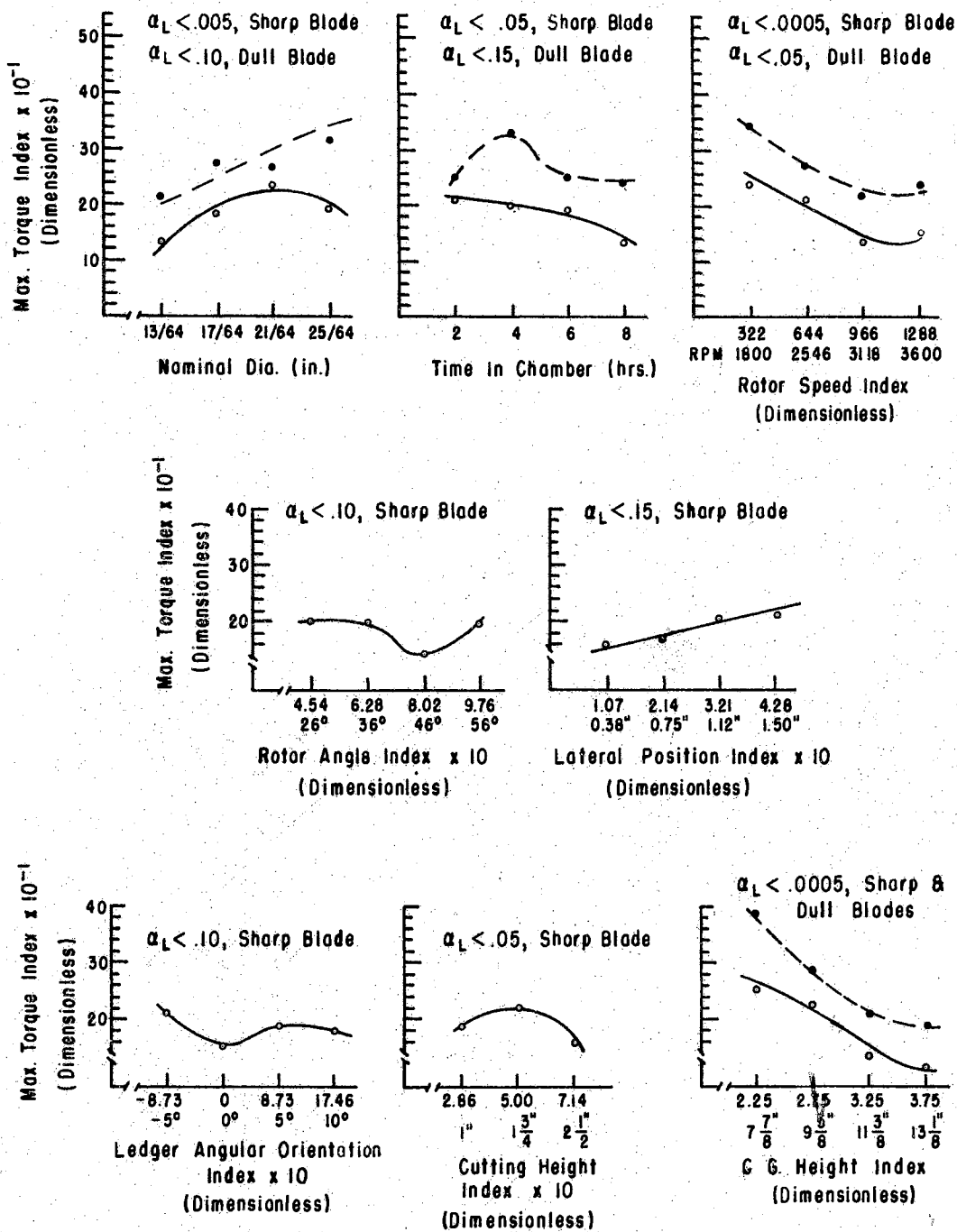


Figure 92. Maximum Torque Index Versus Independent Variable Parameters (Solid Line = Sharp Blade; Dashed Line = Dull Blade)

Relationships of the severed stem displacement indices to the significant independent variables are shown by Figures 93, 94, and 95. Rotor speed index and feed rate index affect the X displacement both for the dull and sharp blade test series. Increasing values of these indices give increasing X displacement - in an almost linear manner. The rotor angle index affects X displacement for the sharp blade series only. The effect is cubic, and it is the 46 degree rotor that gives the best response.

The Y displacement indices are affected by a number of independent variables with use of dull blades. Only the rotor speed and lateral position indices are significant with use of sharp blades. The rotor speed index invokes a cubic response, with minimum Y displacements at a rotor speed of 3118 rpm. The Y displacement of the stem cut end increases linearly with increase of the lateral position index.

The Z displacement indices are affected by a number of independent variables with use of sharp blades. With dull blades, the rotor speed, feed rate, rotor angle, and lateral position indices are significant.

In Chapter IV, from consideration of the kinematic and force analysis, a prediction of maximum X displacement for the stem C.G. and maximum Z displacement for the severed end of the stem was made for the 26 degree rotor with a +10 degree ledger orientation. This prediction is partly verified and partly revoked by test results. With dull blades, the 26 degree rotor did give the greatest mean X displacement

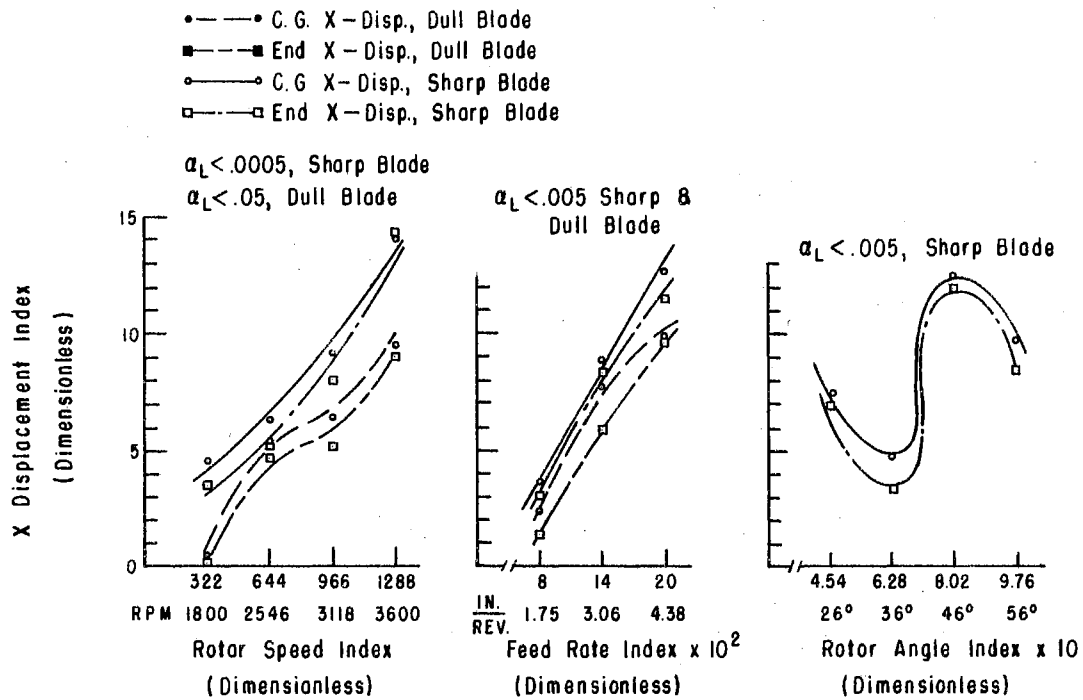


Figure 93. X Displacement Index Versus Independent Variable Parameters

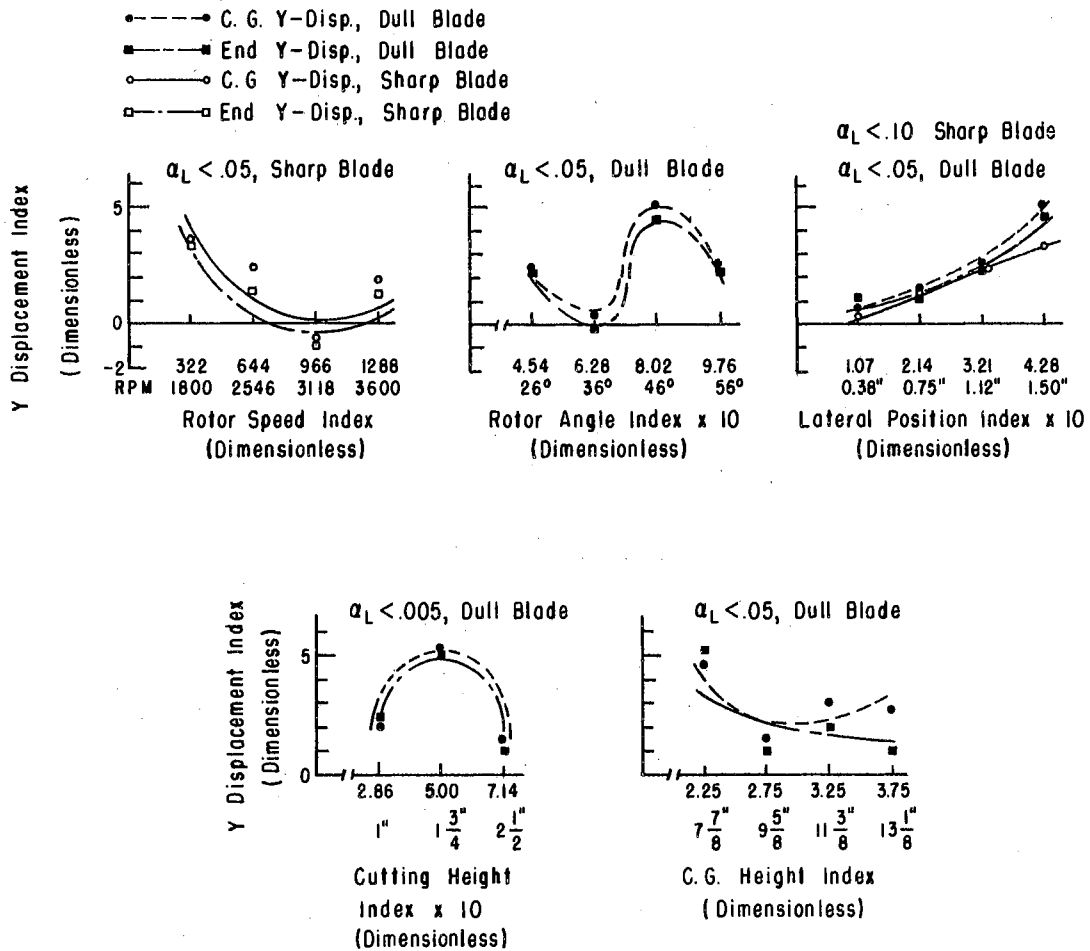


Figure 94. Y Displacement Index Versus Independent Variable Parameters

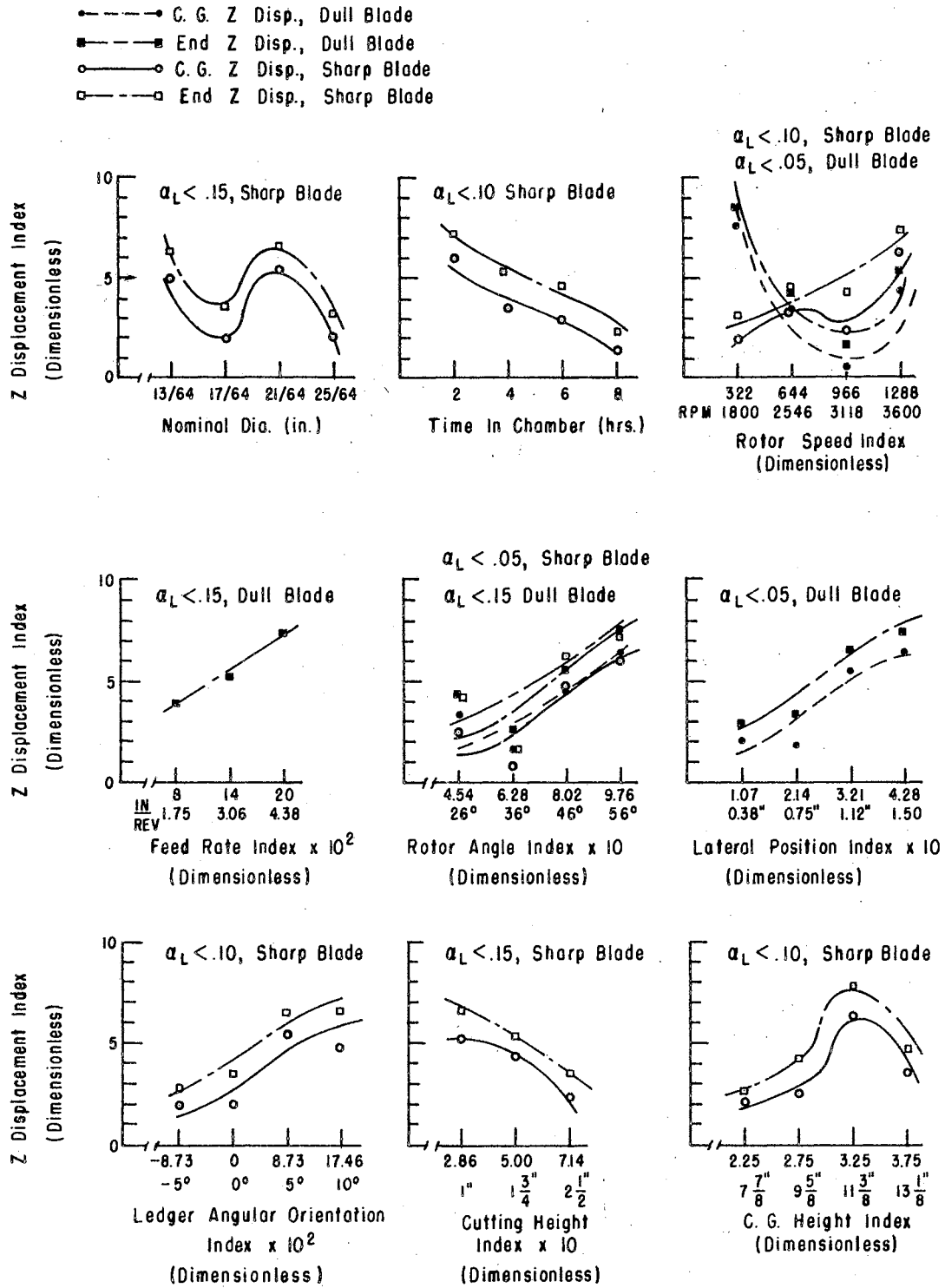


Figure 95. Z Displacement Index Versus Independent Variable Parameters

of the stem C.G., but the 56 degree rotor produced a mean displacement almost as great, the response over the rotor angle index range being quadratic. This result indicates that even with two element cutting, the 56 degree rotor imparts energy to the stem after it is severed. The ledger orientation index did not significantly affect the end Z displacement index for the dull blade tests. With sharp blades, the ledger orientation index did significantly affect the end X displacement, and the +10 degree level did produce the greatest response.

Comparison of Responses for Dull and Sharp Blades

A review of the response curves shows a consistent difference in the curves representing the dull and sharp blade test data. A comparison in the overall means for the two blade types, for each response variable considered in the tests, is presented in Table XVII.

A listing of criteria for evaluating parameter combinations for a rotary sickle type of helical cutter considered in this investigation was begun in the first section of the chapter. With inclusion of input energy and maximum torque, the criteria can be extended such that evaluation of the parameter combinations is based on the determination of mean:

1. Energy input per stem cut; minimum value best.
2. Peak torque per stem cut; minimum value best.
3. Stem C.G. X displacement; maximum value best.

TABLE XVII
 99 PER CENT CONFIDENCE LIMITS FOR DIFFERENCE
 IN OVERALL RESPONSE MEANS BETWEEN
 DULL AND SHARP BLADE TEST SERIES

RESPONSE VARIABLE	BLADE	OVERALL MEAN	STD ERROR OF MEAN	99 PER CENT CONFIDENCE LIMITS FOR DIFFERENCE IN MEANS		COMMENT
				Lower	Upper	
ENERGY INPUT PER STEM CUT	D	92.5147	3.2543	11.63	32.14	
	S	70.6307	2.2797			
MAX. TORQUE PER STEM CUT	D	29.6547	1.1159	3.67	10.99	
	S	22.3266	0.8749			
ENERGY INPUT INDEX $\times 10^{-1}$	D	82.7694	3.6831	15.32	38.07	
	S	56.0741	2.4235			
MAX. TORQUE INDEX $\times 10^{-1}$	D	26.7171	1.4613	4.17	12.85	
	S	18.2055	0.8297			
C.G. X DISP. INDEX	D	5.5452	0.8269	0.27	5.73	
	S	8.5482	0.6605			
END X DISP. INDEX	D	4.8606	0.8820	-0.06	5.98	Since interval contains zero, no significant difference in means at 99% confidence level
	S	7.8196	0.7704			
C.G. Y DISP. INDEX	D	2.5858	0.4133	-0.73	2.31	Same as for End X Disp. Index
	S	1.7946	0.4072			
END Y DISP. INDEX	D	2.3379	0.4663	-0.80	2.66	Same as for End X Disp. Index
	S	1.4054	0.4665			
C.G. Z DISP. INDEX	D	3.9741	0.6667	-1.90	2.74	Same as for End X Disp. Index
	S	3.5571	0.6040			
END Z DISP. INDEX	D	5.1259	0.6638	-2.03	2.58	Same as for End X Disp. Index
	S	4.8545	0.5960			

4. Stem C.G. Y displacement; minimum value best.
5. Stem cut end Z displacement; maximum value best.
6. Actual cutting height; minimum value best.

The cutting effectiveness tests showed the sharp blade superior on the basis of mean actual cutting height. The data in Table XVII show the sharp blade superior on the basis of energy input, peak torque, and X displacement of the stem C.G. - at the 99 percent confidence level. For the other displacements there was no difference in results with the two blade types.

For the range of values of the independent variables comprising the main experiment test series, optimum values can be defined for those parameters which allow selective control. These values, presented in Table XVIII, are based on the response data previously analyzed in this chapter. Parameters like stem diameter, moisture content, stem C.G. height index, and lateral position index, which would be random variables in relation to a field going cutting device, are not considered in the list.

TABLE XVIII
OPTIMUM VALUES OF SELECTED INDEPENDENT
PARAMETERS BASED ON MAIN
EXPERIMENT DATA

Parameter	Value	
	Dull Blade	Sharp Blade
Rotor Speed	3118 or 3600 rpm	3118 rpm
Feed Rate	4.38 in./rev.	not critical but 4.38 in./rev. best
Rotor Angle	26°	46°
Ledger Orientation	-5° or 0°	0°
Cutting Height	not critical but 2 1/2" best	not critical but 2 1/2" best

Stem Physical Property Tests

The reduced data from the stem physical property tests are tabulated in Appendix E. In the tables, the data are classified first into four levels of nominal diameter. Within each nominal diameter section, the listings are further classified according to cutting height and are ranked in order of moisture content within each cutting height group. Since 30 trials of the dull blade test series were run on a three replication plan, there are nine more test results in this group of data than in the sharp blade results. Overall, 137 trials are included in the tabulated data.

It was anticipated that Π_g , Se/Be, could be related to stem moisture content by a polynomial prediction equation for each cutting height range within each diameter classification. A family of curves would result such that by knowing stem nominal diameter, the height of cut, and the stem moisture content, a fairly exact value of Π_g could be determined. An attempt was made to analyze the data in such a manner. Trials with wide variation in stem average diameter, dry linear density, or actual cutting height were treated as outliers, as stated in the footnote to Appendix E, and were not included in the curve fitting analyses. Still the results were disappointing. Figures 96 and 97 show that the curves obtained could not be classified as a family. The summary of results of the regression analyses, listed in Table XIX, shows that correlation coefficients for most of the curves were low. Thus the equations would give imprecise

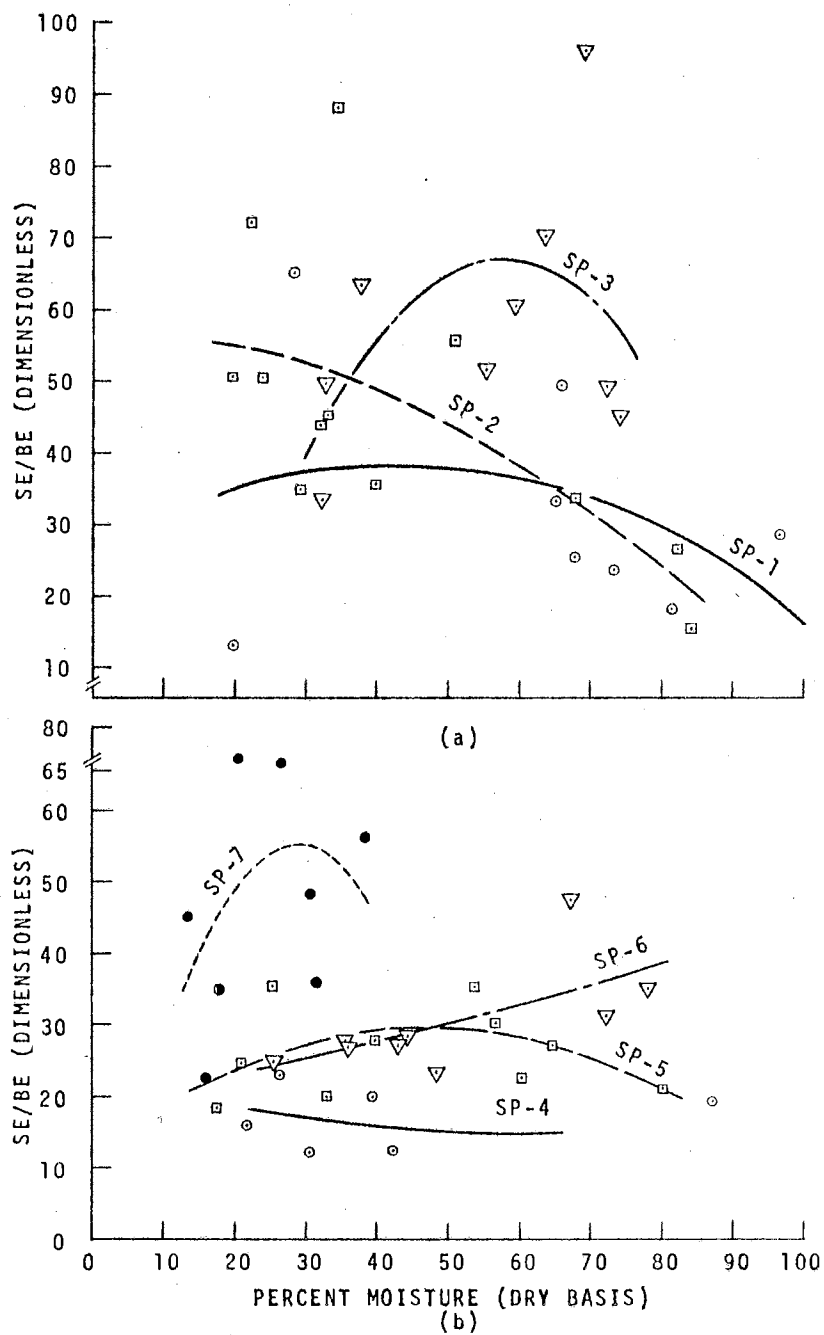


Figure 96. $\Pi_8 = Se/Be$ Versus Percent Moisture:
 (a) 13/64 Diameter Stems;
 (b) 17/64 Diameter Stems

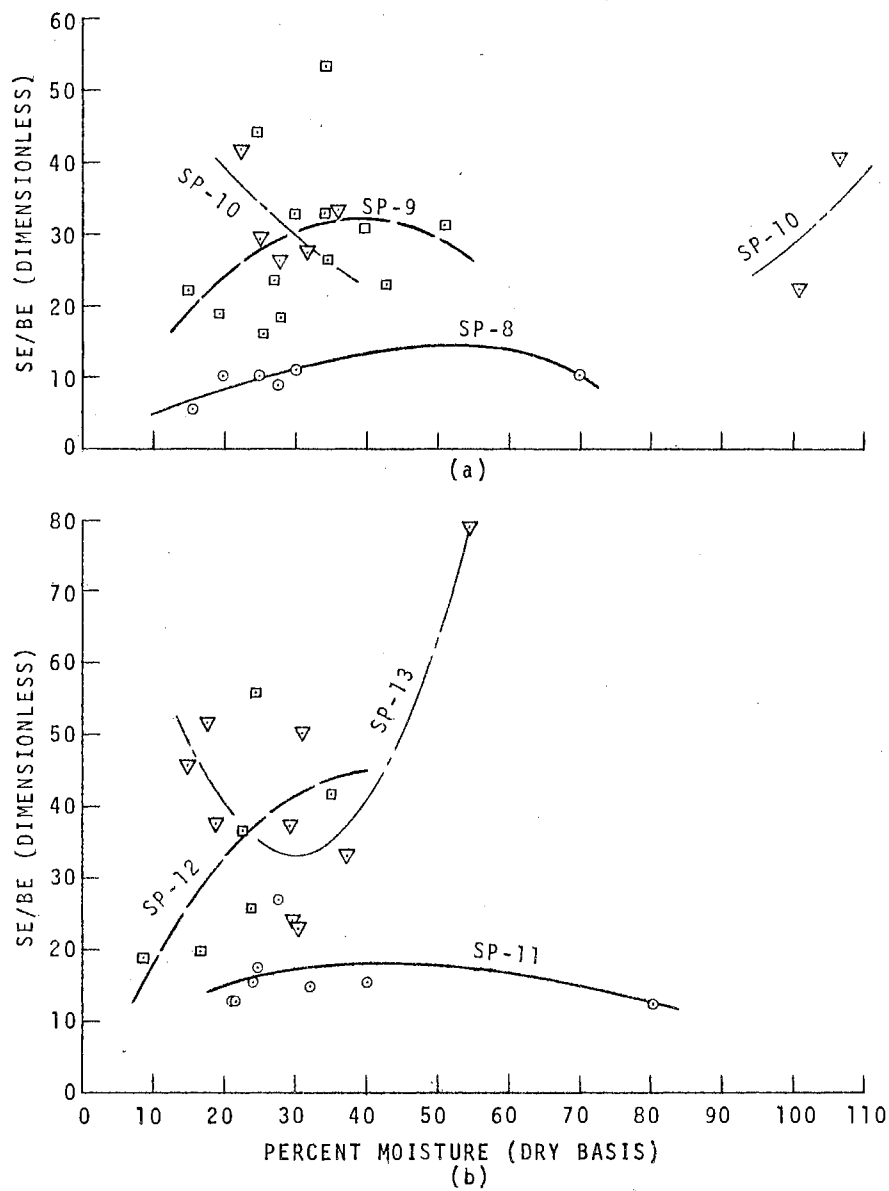


Figure 97. $\Pi_8 = Se/Be$ Versus Percent Moisture:
 (a) 21/64 Diameter Stems;
 (b) 25/64 Diameter Stems

TABLE XIX
SUMMARY OF REGRESSION ANALYSIS FOR $\Pi_8 = Se/Be$
VERSUS STEM MOISTURE CONTENT

Nominal Stem Dia (In)	Cutting Height (In)	No Data Pairs Included in Analysis	Quadratic Functional Relationship Coefficients $Y=A+Bx+Cx^2$ ($Y=Se/Be$; $X=\%Moist., D.B.$)	Curve No.	Corr. Coeff.	Deviations About Regression Mean Square	Range of Moisture Content (Dry Basis)
13/64	1 1/4 - 1 3/4	8	A = 25.11512 B = 0.61934 C = -0.00708	SP-1	.344	17.44	20 - 81%
13/64	2 - 2 7/8	14	A = 56.89900 B = -0.00681 C = -0.00503	SP-2	.627	14.88	19 - 84%
13/64	3 - 3 5/8	9	A = -51.27068 B = 4.08417 C = -0.03530	SP-3	.502	16.67	32 - 90%
17/64	1 1/8 - 1 7/8	6	A = 23.73134 B = -0.32285 C = 0.00311	SP-4	.319	4.55	22 - 86%
17/64	2 - 2 1/4	10	A = 11.63094 B = 0.74928 C = -0.00788	SP-5	.488	5.54	18 - 80%
17/64	2 1/2 - 2 7/8	9	A = 18.93596 B = 0.18616 C = 0.00071	SP-6	.660	5.81	26 - 78%
17/64	3 3/8 - 3 5/8	8	A = -10.32384 B = 4.51838 C = -0.07794	SP-7	.392	17.32	14 - 38%
21/64	1 1/8 - 1 3/8	6	A = -0.40295 B = 0.54314 C = -0.00558	SP-8	.791	1.38	15 - 70%
21/64	2 - 2 7/8	13	A = -2.12216 B = 1.74140 C = -0.02216	SP-9	.353	10.42	15 - 51%
21/64	3 - 3 1/4	7	A = 66.60173 B = -1.59809 C = 0.01216	SP-10	.563	6.64	22 - 106%
25/64	1 - 1 7/8	8	A = 8.35174 B = 0.44017 C = -0.00493	SP-11	.383	4.80	21 - 80%
25/64	2 1/2 - 2 7/8	6	A = -2.43609 B = 2.35906 C = -0.02959	SP-12	.685	11.68	8 - 35%
25/64	3 1/8 - 4	9	A = 96.97622 B = -4.33682 C = 0.07347	SP-13	.855	9.48	14 - 54%

results if used for prediction. In some instances, polynomials of higher degree than the second degree ones listed gave better correlation; but the improvement was considered artificial, since no dramatic differences pointing to a true relationship were obtained.

The poor results experienced with the stem physical property analyses may be attributed to several causes:

1. Inability to accurately control moisture content of the stems.
2. High inherent variability of physical properties of seemingly identical stems.
3. Strong influence of cutting height differences on physical property variation.
4. Strong influence of stem average diameter differences on physical property variation.

More precise results might have resulted if a realistic average cutting height had been used for all the physical property tests, and a greater number of replications of each treatment had been run. Better control over the moisture content and the general similarities of stems used as the experimental units for the replications of a given trial are additional prerequisite conditions for more precise test results.

Prediction Equations

Attempts to precisely determine the stem physical property π terms were not successful; and since analysis of

variance results indicate these terms are highly significant in determining energy input and maximum torque index responses, accurate prediction equations for these responses cannot be determined from the data of this experiment. However, an attempt was made to determine the general form of the prediction equation for the energy input index, using average values of π_8 and π_{10} .

With the highly variable stem test material, and the random position of a given stem in the cutting zone when first contacted by a rotor blade, it was doubted that displacement indices could be accurately related to independent π terms either. Average values calculated from more than just two replications of each treatment combination would be needed for precise results. But in this case also, the general form of the equation relating the stem C.G. X displacement index to the significant variables affecting it was sought through multivariable regression techniques.

Since the sharp blades gave results superior to dull blades, the analysis was restricted to the sharp blade test data. Table XX lists the variation of stem mean moisture content with the levels of time in conditioning chamber for different parts of the experiment. The information in this table is plotted in Figure 98. It is seen that roughly linear relationships existed between mean moisture content and time in chamber for the stems cut in the main test series, but that the group of stems subjected to physical property tests in the sharp blade series gave a roughly

TABLE XX
 MEAN VALUES OF MOISTURE CONTENT VERSUS TIME IN CHAMBER
 FOR VARIOUS PARTS OF THE EXPERIMENT

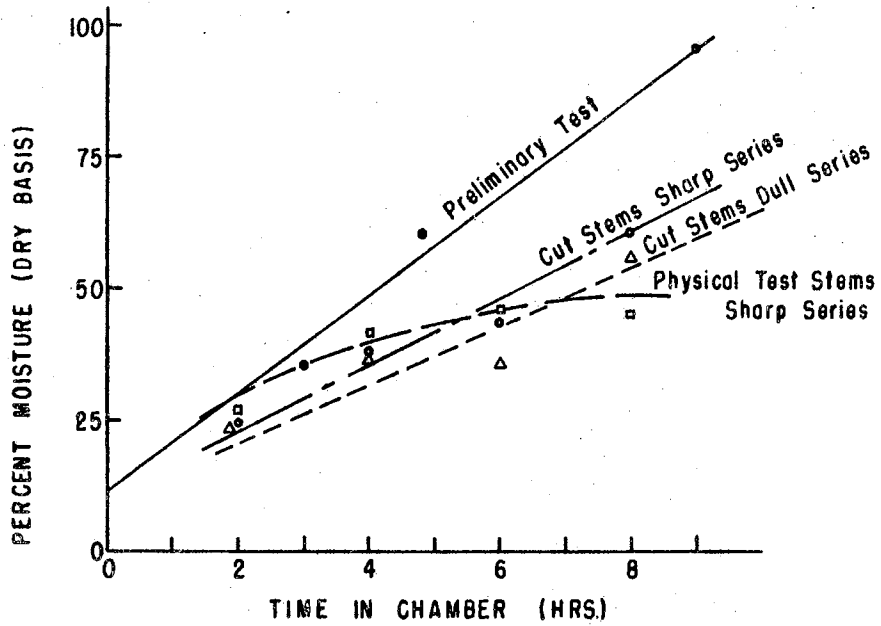
TIME IN CHAMBER (HRS)	PER CENT MOISTURE (DRY BASIS) MEAN VALUES			
	DULL BLADE SERIES CUT STEMS	DULL BLADE SERIES PHYSICAL PROPERTY TEST STEMS	SHARP BLADE SERIES CUT STEMS	SHARP BLADE SERIES PHYSICAL PROPERTY TEST STEMS
2	23.6	27.9	24.4	26.1
4	36.8	35.9	37.9	39.6
6	35.2	38.9	43.4	46.3
8	55.9	52.0	61.2	46.2

TABLE XXI
 MEAN VALUES OF π_8 AND π_{10} FOR
 LEVELS OF NOMINAL DIAMETER
 SHARP BLADE SERIES

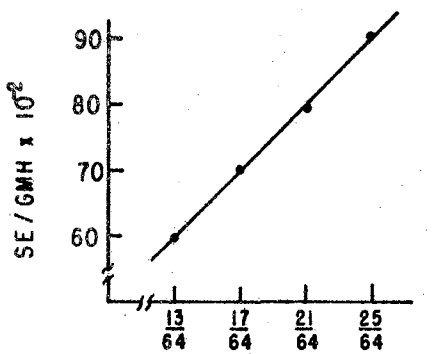
NOMINAL DIAMETER	$\pi_8 = \frac{Se}{Be}$	$\pi_{10} = \frac{Se}{Gmh}$
13/64	38.7	5790
17/64	25.9	7006
21/64	21.8	7932
25/64	19.9	9064

TABLE XXII
 MEAN VALUES OF MOISTURE CONTENT
 π_8 , $1/\pi_8$, AND π_{10} FOR LEVELS
 OF TIME IN CHAMBER
 SHARP BLADE SERIES

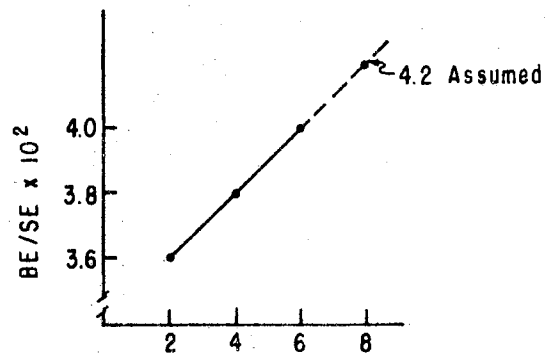
TIME IN CHAMBER (HRS)	PERCENT MOISTURE (DRY BASIS)	$\pi_8 = \frac{Se}{Be}$	$1/\pi_8 = \frac{Be}{Se}$	$\pi_{10} = \frac{Se}{Gmh}$
2	26.1	27.7	3.6×10^{-2}	8174
4	39.6	26.0	3.8×10^{-2}	7932
6	46.3	25.1	4.0×10^{-2}	6788
8	46.2	27.2	3.7×10^{-2}	7097



MOISTURE CONTENT VERSUS TIME IN CHAMBER FOR DIFFERENT PHASES OF THE EXPERIMENT



SE/GMH VS NOM. DIA.



BE/SE VS TIME IN CHAMBER

Figure 98. Graphs of Percent Moisture Content Versus Time in Chamber, Π_{10} Versus Nominal Diameter, and $1/\Pi_8$ Versus Time in Chamber

linear response only over the first three levels. Moisture content values for six and eight hour treatment times were the same. Tables XXI and XXII list the mean values of Π_8 and Π_{10} , the physical property pi terms, for the different levels of nominal diameter and time in chamber. If the mean values of either Π_8 or Π_{10} are to be substituted for the levels of nominal diameter and time in chamber in a regression analysis, then a linear relationship existing between the pi terms and the diameter and time in chamber must be found. From the information in Tables XXI and XXII, it was judged that nominal diameter varied approximately linearly with the mean values of Π_{10} . For the first three levels of time in chamber, mean values of the reciprocal of Π_8 varied approximately linearly with time in chamber. Figure 98 shows graphs of these relationships, and also shows the assumed value of $1/\Pi_8$ for the eight hour time in chamber level.

For the multivariate regression analysis, all factors having a significant effect at the 90 percent confidence level were included. Thus from Table XV, for the energy input index, factors to be included are nominal diameter (substitute Π_{10}), time in chamber (substitute $1/\Pi_8$) Π_2 , Π_4 , Π_7 , and Π_9 . For the stem C.G. X displacement index, factors to be included are Π_2 , Π_3 , and Π_4 .

Using the additive model defined by the AOV data for Π_1 , energy input index, resulted in a multiple correlation coefficient, r , of only 0.439. Thirty-two input data points

were used - after averaging the two replications of each treatment combination to eliminate variation between replications. A multiplicative model for Π_1 resulted in a value for r of 0.798, a significant improvement over the additive model. The resulting prediction equation is:

$$\begin{aligned} \Pi_1 \times 10^{-1} = & (4.6 \times 10^{-9}) (\Pi_{10})^{1.86} (1/\Pi_8)^{-2.46} \\ & (\Pi_2)^{.076} (\Pi_4)^{.24} (\Pi_7)^{-.105} (\Pi_9)^{-1.56} \quad (9-2) \end{aligned}$$

The additive model for the stem C.G. X displacement index, $\Pi_1''(1)$, resulted in a prediction equation with a value for r of 0.774. The equation is:

$$\begin{aligned} \Pi_1''(1) = & -16.56 + 64\Pi_3 + 0.01\Pi_2 + 14.8\Pi_4 \\ & -4.97\Pi_4^3 \quad (9-3) \end{aligned}$$

CHAPTER X

SUMMARY AND CONCLUSIONS

Summary

The objectives of this study were to: (1) design a balanced, rotary sickle with detachable blades approximately helical in configuration; (2) test the device to determine if it could effectively cut and traject stems of a typical seed-bearing crop in one operation; (3) determine the mechanism of cutting involved with such a device when equipped with square edge (dull) and sharp blades through high speed motion picture photography; (4) identify and screen the pertinent design, operating, and plant physical property parameters that might affect the responses of energy input per stem cut, peak torque developed per stem cut, and resulting displacement of the trajected stem to determine which parameters do have a non-trivial effect; (5) determine the form of dimensionally correct prediction equations relating the response terms with significant independent parameters.

A careful review of the literature was made to learn the nature and significance of design, operating, and plant physical property parameters affecting conventional cutting devices. The results are summarized in Tables I through IV.

The rotor segment bevel angle specification and the range of knife angles to include in this investigation were determined from these data.

To develop design ideas, a model auger knife was constructed. Through qualitative cutting effectiveness tests with two rotor and ledger tube designs for the model, it was decided the prototype cutter should have a ledge on the leading surface of the rotor disk to provide the effective acute bevel angle of sharp blades.

The rotary sickle was designed utilizing a rotor and concentric ledger tube with the blades of each approximately helical in configuration. Rotor diameter was 3 1/2 inches. Details of the design are described and illustrated in Chapter III. Previous helical cutters are described in Chapter II.

Through kinematic, force, and dimensional analysis, ten parameters that might have an effect on energy input, peak torque, or stem displacement responses for the rotary sickle were identified. These are listed in Chapter V.

An experimental plan to test the significance of the independent parameters on the response terms was adopted, and a special test stand and instrumentation were designed and built or procured to run the experiment.

Initial cutting tests identified effective and non effective types of severing actions. A clean, angled cut typifies effective severing; the stem breaking at the base before being completely severed typifies non effective

severing. It was determined that stubble length was significantly lower with use of sharp blades.

High speed motion picture films were taken which give a clear description of the cutting mechanism involved with square edge (dull) and sharp blades on the rotor.

With square edge blades, the stem slides along the rotor blade edge without damage as it is deflected toward the ledger to be severed in two element shear between the rotor and ledger blades. Once severed the stem loses contact with the rotor sector. The stem trajectory is characterized by a noticeable spin of the stem about its vertical axis.

With sharp blades, when the stem is contacted by the blade edge and deflection toward the ledger is started, the sharp edge immediately slices into the stem cross section and single element, impact cutting results. The severed end of the stem then slides along the beveled rotor sector ledge until discharged to the side. Additional energy to affect the stem trajectory is imparted during this phase. The stem trajectory is characterized by the same spin about the vertical axis as when cut by the square edge blade. Through micromotion analysis, points on the stem near the point of blade contact were determined to be subjected to accelerations in excess of 1000 g's at the 3600 rpm rotor speed.

For both blade types, deformations of the stem during cutting indicate that bending, torsional, and tensile

stresses, as well as transverse shear, act on the stem to cause failure.

The main, screening of parameter, test series proves statistically that the sharp blade is superior to the dull with respect to minimum input energy, minimum peak torque developed, and maximum stem C.G. X displacement responses. The most significant parameters affecting energy input were stem physical properties relating to nominal diameter and moisture content for both the dull and sharp blades. Rotor angle was highly significant with use of sharp blades. In addition to the stem physical properties, rotor speed had a highly significant effect on peak torque developed. Rotor speed, feed rate, and rotor angle had significant effect on severed stem displacements. Table XV summarizes the factor effects.

Attempts to characterize significant stem physical properties by one dimensionless term were not successful. Lack of control over moisture content, failure to consider just one mean cutting height, and insufficient replication of tests were contributing causes. The special testing machine built to determine the stem physical properties gave accurate results.

Prediction equations relating the energy input index and stem C.G. X displacement index to significant independent pi terms had low correlation coefficients (.798 and .774 respectively). A multiplicative model gave best results for

the energy input index; an additive, polynomial type model was used for the displacement index.

Conclusions

1. The rotary, helical sickle designed in this study can effectively cut and traject plant stems in one operation. The limiting factor in trajecting severed stems onto the catching platform of a field going machine using the rotary sickle might be insufficient forward velocity, since the lowest level of forward velocity considered in this study was 2.98 mph (with 1800 rpm rotor speed).

2. The governing mechanism of cutting for the rotary sickle fitted with square edge blades is two element shearing between the rotor and ledger blades.

3. The governing mechanism of cutting for the rotary sickle fitted with sharp blades is single element impact cutting. The stem rarely is deflected to the ledger blade before it is severed.

4. A suitable structural model for a stem undergoing cutting by the rotary sickle, with either dull or sharp blades, is that of a propped cantilever beam with an eccentric, inclined, concentrated load applied at the point of blade contact. The inertia of the top portion of the stem acts as the prop. The characteristic spin about its vertical axis of a stem trajected by action of the rotary sickle results from the load being eccentrically applied.

5. The important design parameters considered in this study were knife sharpness index (sharp blade is superior) and rotor angle index (26 degree angle best for dull blades; 46 degree angle best for sharp blades). Ledger orientation index was not significant at a confidence level greater than 90 percent, except for the response of maximum torque per stem cut for the sharp blade where the confidence level was 95 percent. Lateral position index might be considered a design parameter in that a wider feed opening than the one used in this study (1.5 inches) would increase energy input requirements.

6. The important operating parameters considered were rotor speed index (highly significant on peak torque and stem displacement responses), feed rate index (highly significant on energy input for dull blade rotor and on stem displacements), and cutting height index (highly significant on peak torque and energy input indices for sharp blade rotors).

7. All three stem physical property parameters, nominal diameter, time in chamber, and C.G. height index had highly significant effects on one or more response variables.

8. For design of a field-going rotary sickle, sharp blades, a 46 degree knife angle, zero degree ledger tube orientation, 3118 rpm rotor speed, and a feed rate of 4.38 in./rev. should be specified, in accordance with the best results obtained in this experiment. Judging from the response curves, however, probably a range of values,

extending +5 percent of the nominal values cited, would be entirely satisfactory.

Suggestions for Further Study

1. Evaluate a prototype rotary sickle in field conditions with special consideration to effect of the interaction of masses of plants on trajectory pattern and to seed shattering effects.

2. Initiate a study of ledger tube design features to determine optimum values of ledger blade knife angle and extent of arc length.

3. Adopt principles used in low acceleration cam development to perfecting a guard design for the ledger tube. Plants impacting against the guard surface before being guided into the cutting zone suffered seed shattering effects (the cutting of stem 1 of trial PS-4 exhibited this action very clearly on the high speed films).

4. Plan and execute controlled experiments to accurately determine Π_8 as a function of moisture content for soybean stems. If a dimensionless term such as Π_8 can adequately characterize stem physical properties for cutting energy, torque, and displacement relationships, it should prove useful in comparing cutting energy required for different crops.

BIBLIOGRAPHY

- (1) Bainer, Roy, R. A. Kepner, and E. L. Barger. Principles of Farm Machinery. New York: John Wiley and Sons, 1955, pp 388-389.
- (2) Kepner, Robert A. "Analysis of the Cutting Action of a Mower." Agricultural Engineering, 33:11 (November, 1952), pp. 693-697, 704.
- (3) Lamp, B. J., W. H. Johnson, and K. A. Harkness. "Soybean Harvesting Losses - Approaches to Reduction." Transactions of the ASAE, 4:2 (April, 1961), pp. 203-205, 207.
- (4) Arms, Milo F. "A Harvester for Castor Seed." (unpub. M. S. thesis, University of Nebraska, July, 1951) pp. 5-6.
- (5) Elfes, L. E. "Design and Development of a High-Speed Mower." Agricultural Engineering, 35:3 (March, 1954), pp. 147-153.
- (6) Domingo, W. E. "Circular Saw Cutter Tests." (unpub. Non-Technical Report, The Baker Castor Oil Company, April 24, 1952).
- (7) Chancellor, W. J. "Energy Requirements for Cutting Forage." Agricultural Engineering, 39:10 (October, 1958), pp. 633-636.
- (8) Prince, R. P., W. C. Wheeler, and D. A. Fisher. "Discussion on Energy Requirements for Cutting Forage." Agricultural Engineering, 39:10 (October, 1958) pp. 638-639, 652.
- (9) Harbage, R. P. and R. V. Morr. "Development and Design of a Ten Foot Mower." Agricultural Engineering, 43:4 (April, 1962), pp. 208-211, 219.
- (10) * Richey, C. B. "Discussion on Energy Requirements For Cutting Forage." Agricultural Engineering, 39:10 (October, 1958), pp. 636-637.

- (11) Stroppe, Th. Zur Systematik der Technologie des Schneidens (On the Systematics of the Technology of Cutting). Grundl. Landtech. 5 (1953), pp. 120-134.
- (12) Feller, R. "Effects of Knife Angles and Velocities on Cutting of Stalks without a Counter-Edge." Journal of Agricultural Engineering Research, 4:4 (1959), pp. 277-293.
- (13) Koniger, R. Versuch einer Theorie des Scherenschnittes von Halmen (Attempt at a Theory on the Shearing of Grass Blades). Grundl. Landtech., 5 (1953), pp. 96-97.
- (14) Svahn, Olov and Kjell Lundstrom. "An Investigation into Shearing by the Short-Stroke Method." Sheet Metal Industries, 40:434 (June, 1963), pp. 409-417, 422.
- (15) Fisher, David A., J. J. Kolega, and W. C. Wheeler. "An Evaluation of the Energy Required to Cut Forage Grasses and Legumes." Storrs (Connecticut) Agricultural Experiment Station, Progress Report 17 (January, 1957).
- (16) Chancellor, W. J. "Basic Concepts of Cutting Hay." (unpub. Ph.D. Thesis, Cornell University, 1957).
- (17) McClelland, J. H. and R. E. Spielrein. "An Investigation of the Ultimate Bending Strength of Some Common Pasture Plants." Journal of Agricultural Engineering Research, 2:4 (1954), pp. 288-292.
- (18) Prince, Ralph P. "Measurement of Ultimate Strength of Forage Stalks.: Transactions of the ASAE, 4:2 (1961), pp. 208-209.
- (19) Johnston, R. C. R. "Crop Behavior During Mowing." Journal of Agricultural Engineering Research, 4:3 (1959), pp. 193-203.
- (20) Bosoi, E. S. The Angle of Slope of the Blade of the Cutting Apparatus of Harvesting Machines (in Russian) SetKhoz Mashina, No. 5 (1949), pp. 7-9.
- (21) Harris, P. "Cutting Action of Tools." Research, 9:3 (March, 1956), pp. 109-113.
- (22) "After Decades A Revolution in Saws." Fortune, 47 (January, 1953), p. 49.

- (23) McClelland, J. H. and R. E. Spielrein. "A Study of Some Design Factors Affecting the Performance of Mower Knives." Journal of Agricultural Engineering Research, 3:2 (1958), pp. 137-145.
- (24) Liljedahl, J. B., G. L. Jackson, R. P. Degraff, and M. E. Schroeder. "Measurement of Shearing Energy." Agricultural Engineering, 42:6 (June, 1961), pp. 298-301.
- (25) Prine, R. P. and W. C. Wheeler. "Some Factors Affecting the Cutting Process of Forage Crops." Storrs (Connecticut) Agricultural Experiment Station, Progress Report 37 (1960).
- (26) Beekman, Gerard. "Reaping or Mowing Machine." U.S. Patent No. 490,781 (January 31, 1893).
- (27) Beekman, Gerard. "Reaping or Mowing Machine." U.S. Patent No. 490,782 (January 31, 1893).
- (28) Newton, Richard T. "Lawn Mower For Grass, Grains, and the Like." U.S. Patent No. 2,282,238 (May 5, 1942).
- (29) Brauer, Walter, "Lawn Mower." U.S. Patent No. 2,484,071 (October 11, 1949).
- (30) Chambliss, John A. "Multiple Blade Oblique Vegetation Cutter." U.S. Patent No. 2,860,477 (November 18, 1958).
- (31) Miller, Martin R. "Developing a High-Capacity Stalk Cutter." Report No 1-001, ASAE, St. Joseph, Michigan (1968).
- (32) "The Spinslicer Mower." Sales Brochure, Spinslicer Company, P. O. Box 9175, South Charleston, W. Va. (1968).
- (33) Murphy, Glenn. Similitude in Engineering. New York: The Ronald Press Company, 1950.
- (34) Kline, Stephen J. Similitude and Approximation Theory. New York: McGraw Hill Book Company Inc., 1965.
- (35) Schenck, Hilbert Jr. Theories of Engineering Experimentation. New York: McGraw Hill Book Company Inc., 1961.

- (36) Addelman, Sidney and Oscar Kempthorne. Orthogonal Main-Effect Plans. Aeronautical Research Laboratory Technical Report-ARL 79 (November 1961). Available from Clearinghouse for Federal Scientific and Technical Information, Springfield, Va. 22151.
- (37) Ostle, Bernard. Statistics in Research. Ames, Iowa: The Iowa State University Press, 1963.
- (38) Phillips, Richard C., (Sales Engineer, Lebow Associates, Inc., Oak Park Michigan). Private Communication (July 7, 1966).
- (39) Suggs, C. W. and W. E. Splinter. "Mechanical Properties of Tobacco Stalks." Transactions of the ASAE, 8:3 (1965), pp. 361-364.
- (40) Halyk, R. M. and L. W. Hurlbut. "Tensile and Shear Strength Characteristics of Alfalfa Stems." ASAE Paper No. 64-816, New Orleans, Louisiana (1964).
- (41) Bartok, J. W. Jr. and R. P. Prince. "Cutoff Saw Sizes Forage Stalk Specimens." Agricultural Engineering, 45:10 (October, 1964), p. 559.
- (42) Hyzer, William G. "High Speed Photography in Product Development." Machine Design, 27:2 (February, 1955), pp. 150-158.
- (43) Hyzer, William G. Engineering and Scientific High Speed Photography. New York: The Macmillan Co., 1962.
- (44) Hyzer, William G. "Measuring Motion with High-Speed Movies." Machine Design, 31:7 (April 2, 1959), pp. 102-108.

APPENDIX A

CALCULATIONS FOR FLYWHEEL AND
SHEAR BOLT DESIGN

APPENDIX A
 CALCULATIONS FOR FLYWHEEL AND
 SHEAR BOLT DESIGN

1/2	9.20-20	9.20-20	9.20-20	9.20-20	9.20-20	9.20-20
<p>DRIVE DRIVE</p> <p>ACTIVE DRIVE WITH ALLY'S DESIGN</p> <p>$\frac{1}{2} = 1.0$ $\frac{1}{2} = 1.0$ $\frac{1}{2} = 1.0$ $\frac{1}{2} = 1.0$</p>	<p>FLYWHEEL</p> <p>ACTIVE DRIVE WITH ALLY'S DESIGN</p> <p>$\frac{1}{2} = 1.0$ $\frac{1}{2} = 1.0$ $\frac{1}{2} = 1.0$ $\frac{1}{2} = 1.0$</p>	<p>DRIVE DRIVE</p> <p>ACTIVE DRIVE WITH ALLY'S DESIGN</p> <p>$\frac{1}{2} = 1.0$ $\frac{1}{2} = 1.0$ $\frac{1}{2} = 1.0$ $\frac{1}{2} = 1.0$</p>	<p>FLYWHEEL</p> <p>ACTIVE DRIVE WITH ALLY'S DESIGN</p> <p>$\frac{1}{2} = 1.0$ $\frac{1}{2} = 1.0$ $\frac{1}{2} = 1.0$ $\frac{1}{2} = 1.0$</p>	<p>DRIVE DRIVE</p> <p>ACTIVE DRIVE WITH ALLY'S DESIGN</p> <p>$\frac{1}{2} = 1.0$ $\frac{1}{2} = 1.0$ $\frac{1}{2} = 1.0$ $\frac{1}{2} = 1.0$</p>	<p>FLYWHEEL</p> <p>ACTIVE DRIVE WITH ALLY'S DESIGN</p> <p>$\frac{1}{2} = 1.0$ $\frac{1}{2} = 1.0$ $\frac{1}{2} = 1.0$ $\frac{1}{2} = 1.0$</p>	<p>DRIVE DRIVE</p> <p>ACTIVE DRIVE WITH ALLY'S DESIGN</p> <p>$\frac{1}{2} = 1.0$ $\frac{1}{2} = 1.0$ $\frac{1}{2} = 1.0$ $\frac{1}{2} = 1.0$</p>

APPENDIX B

- B-I SUMMARY OF ROTOR AND CARRIAGE VELOCITIES USED IN THE EXPERIMENT
- B-II SAMPLE DATA SHEET FOR CUTTING EFFECTIVENESS TESTS
- B-III SAMPLE DATA SHEET FOR SCREENING OF PARAMETER (MAIN EXPERIMENT) TEST SERIES
- B-IV SAMPLE DATA SHEET FOR STEM PHYSICAL PROPERTY TESTS
- B-V SAMPLE DATA SHEET FOR DETERMINING AVERAGE DIAMETER OF STEM CROSS SECTION

Explanation of Table in Appendix B-I

In the column headed "Corresponding Blade Edge Velocity (.01528 N Ft/Sec)," N represents the rotor speed in rpm.

Information in the upper left hand cell of the "Required Carriage Velocity for Specified Feed Rates" table is typical and will be explained in detail. The first line is the required carriage velocity in ft/sec. The second line lists this same velocity in mph. The third line gives the theoretical distance on the recorder chart (100 mm/sec chart speed) between blips representing a 3 ft. travel of the carriage. The fourth line lists the theoretical rotational speed of the carriage drive chain sprocket (7.991 P.D.) to provide the correct carriage velocity. In the divided sub-cell, the number combination on the left indicates the spring set (48 lb) and its deflection (12 inches) to accelerate the carriage to the required velocity. The number on the right (3.7) is the approximate dial setting for the Graham variable speed drive to give the correct chain velocity.

APPENDIX B-I

SUMMARY OF ROTOR AND CARRIAGE VELOCITIES
USED IN THE EXPERIMENT

Rotor Speed (RPM)	Corresponding Blade Edge Velocity (.01528 N Ft/Sec)	Π_2 $\frac{\omega^2 NeG}{D}$	Required Carriage Velocity For Specified Feed Rates											
			$\Pi_3 = \frac{V}{\omega D} = 8 \times 10^{-2}$ $L = \frac{D}{2} \frac{IN}{REV} =$ 1.75 IN/REV	$\Pi_3 = \frac{V}{\omega D} = 14 \times 10^{-2}$ $L = \frac{7}{8} D =$ 3.0625 IN/REV	$\Pi_3 = \frac{V}{\omega D} = 20 \times 10^{-2}$ $L = \frac{5}{4} D =$ 4.375 IN/REV	$\Pi_3 = \frac{V}{\omega D} = 24 \times 10^{-2}$ $L = \frac{3}{2} D =$ 5.25 IN/REV								
1800 60 Cutting Cycles/Sec 8 Lobe Cam 1.67 mm/Cutting Cy. 16.7 Milliseconds/Cut	27.504 Ft/Sec 306.048 In/Sec	4.805 x 10 ⁷	4.38 Ft/Sec 2.98 MPH 68.6 mm/3Ft 125.48 RPM (7.991 P.D. Sprocket)	8.26 Ft/Sec 5.22 MPH 39.18 mm 219.58 RPM	10.94 Ft/Sec 7.46 MPH 27.43 mm 313.69 RPM	13.12 Ft/Sec 8.95 MPH 22.9 mm 376.43 RPM	48-12	3.7	48-20	6.7	48-30	10	80-22	12.6
			6.19 Ft/Sec 4.22 MPH 48.5 mm 177.48 RPM	10.83 Ft/Sec 7.38 MPH 27.70 mm 310.59 RPM	15.47 Ft/Sec 10.55 MPH 19.39 mm 443.70 RPM	18.52 Ft/Sec 12.63 MPH 16.2 mm 531.24 RPM	48-16	5.4	48-30	9.9	80-29	14.5	128-28	18.10
2546 84.87 Cutting Cy/Sec 8 Lobe Cam 1.18 mm/Cutting Cy. 11.8 Milliseconds/Cut	38.903 Ft/Sec 466.836 In/Sec	9.610 x 10 ⁷	7.58 Ft/Sec 5.17 MPH 39.6 mm 217.35 RPM	13.26 Ft/Sec 9.04 MPH 22.62 mm 380.36 RPM	18.95 Ft/Sec 12.92 MPH 15.83 mm 543.38 RPM	22.73 Ft/Sec 15.61 MPH 13.2 mm 652.06 RPM	48-20	6.7	80-24	12	128-32	18.5	128-36	22
			8.75 Ft/Sec 5.97 MPH 34.3 mm 250.95 RPM	15.31 Ft/Sec 10.44 MPH 19.59 mm 439.16 RPM	21.88 Ft/Sec 14.91 MPH 13.71 mm 627.38 RPM	26.25 Ft/Sec 17.90 MPH 11.43 mm 752.85 RPM	48-24	8.0	80-28	14.5	128-36	21.5	128-41	26.1
3118 103.93 Cutting Cy/Sec 8 Lobe Cam 0.964 mm/Cutting Cy. 9.64 Milliseconds/Cut	47.643 Ft/Sec 571.716 In/Sec	14.415 x 10 ⁷	8.75 Ft/Sec 5.97 MPH 34.3 mm 250.95 RPM	15.31 Ft/Sec 10.44 MPH 19.59 mm 439.16 RPM	21.88 Ft/Sec 14.91 MPH 13.71 mm 627.38 RPM	26.25 Ft/Sec 17.90 MPH 11.43 mm 752.85 RPM	48-24	8.0	80-28	14.5	128-36	21.5	128-41	26.1
			8.75 Ft/Sec 5.97 MPH 34.3 mm 250.95 RPM	15.31 Ft/Sec 10.44 MPH 19.59 mm 439.16 RPM	21.88 Ft/Sec 14.91 MPH 13.71 mm 627.38 RPM	26.25 Ft/Sec 17.90 MPH 11.43 mm 752.85 RPM	48-24	8.0	80-28	14.5	128-36	21.5	128-41	26.1
3600 120 Cutting Cy/Sec 8 Lobe Cam 0.833 mm/Cutting Cy. 8.33 Milliseconds/Cut	55.008 Ft/Sec 660.096 In/Sec	19.220 x 10 ⁷	8.75 Ft/Sec 5.97 MPH 34.3 mm 250.95 RPM	15.31 Ft/Sec 10.44 MPH 19.59 mm 439.16 RPM	21.88 Ft/Sec 14.91 MPH 13.71 mm 627.38 RPM	26.25 Ft/Sec 17.90 MPH 11.43 mm 752.85 RPM	48-24	8.0	80-28	14.5	128-36	21.5	128-41	26.1
			8.75 Ft/Sec 5.97 MPH 34.3 mm 250.95 RPM	15.31 Ft/Sec 10.44 MPH 19.59 mm 439.16 RPM	21.88 Ft/Sec 14.91 MPH 13.71 mm 627.38 RPM	26.25 Ft/Sec 17.90 MPH 11.43 mm 752.85 RPM	48-24	8.0	80-28	14.5	128-36	21.5	128-41	26.1

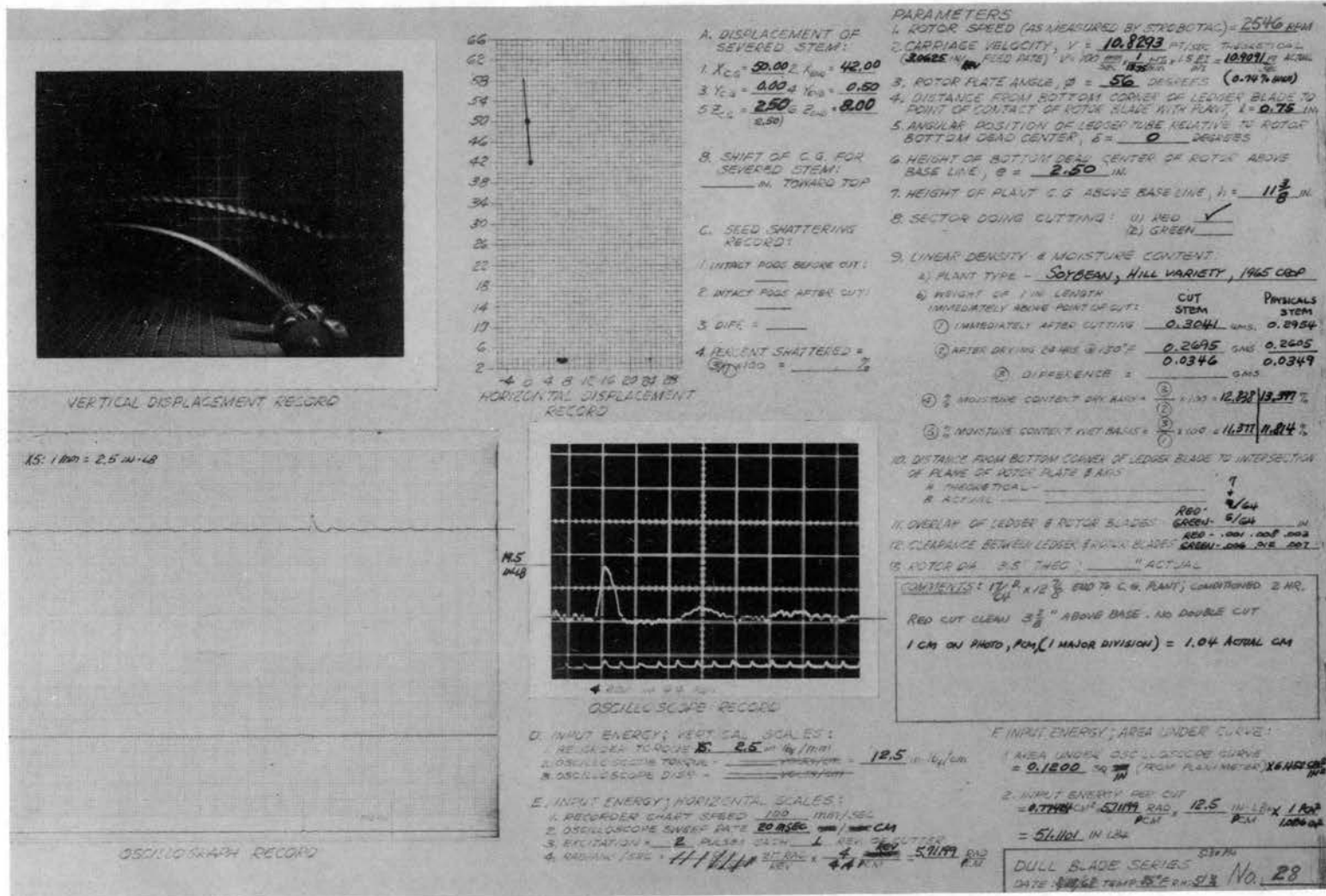
APPENDIX B-II

SAMPLE DATA SHEET FOR CUTTING EFFECTIVENESS TESTS

CUTTING EFFECTIVENESS TEST											
TEST No. <u>CED-3</u>		CONDITION <u>AS DRIED</u>			DATE <u>7/25/68</u>						
STEM NOM. DIA. <u>17/64</u> IN.		ROTOR <u>26°</u>			C. G. LOCATION <u>≈ 12 7/8</u> FROM END						
CUTTING HEIGHT <u>1.75</u> IN.		LEDGER TUBE ANGLE <u>0°</u>			ROTOR SPEED <u>3600</u>						
STEM LATERAL POSITION <u>1.125</u> IN.		BLADE <u>DULL</u>			FEED RATE <u>1.75 IN/REV</u>						
STEM AVG DIA. AT CUT _____		STEM AVG SHEAR STRENGTH _____			STEM STIFFNESS (AVG) _____						
SECTOR DOING CUTTING _____		<input type="checkbox"/> RED <input type="checkbox"/> GREEN									
DIST FROM END TO C.G. BEFORE CUT	SAMPLE NO.	DISTANCE OF CUT ABOVE BASE	DESC OF KNIFE ACTION				PLANT DISPLACEMENT AFTER CUT (REF. & CUTTER & PLANT ROW)				COMMENTS
			CLEAN CUT	PARTIAL CUT	STEMS BENT	SLIPPERY PLANT	C.G.		END		
							X+	Y+	X+	Y+	
12.750	8	2.375	✓				11.250	7.000	3.000	3.750	
12.625	11	1.875	✓				18.000	6.500	11.500	8.500	END OF PLANT PARTIALLY CUT A SECOND TIME
13.000	⑦	2.750	✓				7.875	13.500	10.250	5.250	TORQUE RECORDED @ X1
2.500	4	2.250	✓				8.375	10.875	9.625	3.000	TORQUE RECORDED @ X2
12.875	⑩	3.000	✓				9.750	20.250	14.500	27.500	TORQUE RECORDED @ X2 PLANT # 6
13.125	⑤	2.750	✓				17.500	7.250	9.000	9.000	TORQUE RECORDED @ X2
13.062	⑨	2.375	✓				32.000	27.000	29.000	35.000	T&P FELL IN KNIFE & WAS CUT ABOUT 1 FT. TO FRONT & 2 FT TO R. SIDE
12.000	13	2.750	✓				—	—	—	—	
12.375	②	2.500	✓				20.000	21.000	38.000	18.000	TORQUE RECORDED @ X1 PLANT # 1
12.875	3	2.375	✓				17.000	17.000	20.000	8.000	

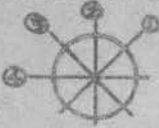
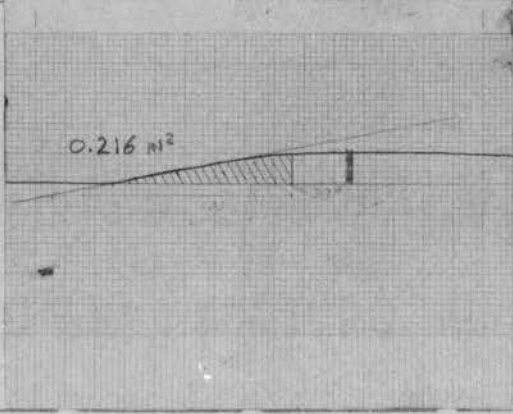
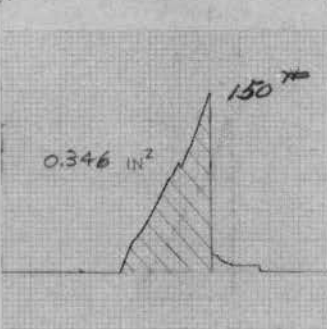
APPENDIX B-III

SAMPLE DATA SHEET FOR SCREENING OF PARAMETER (MAIN EXPERIMENT) TEST SERIES



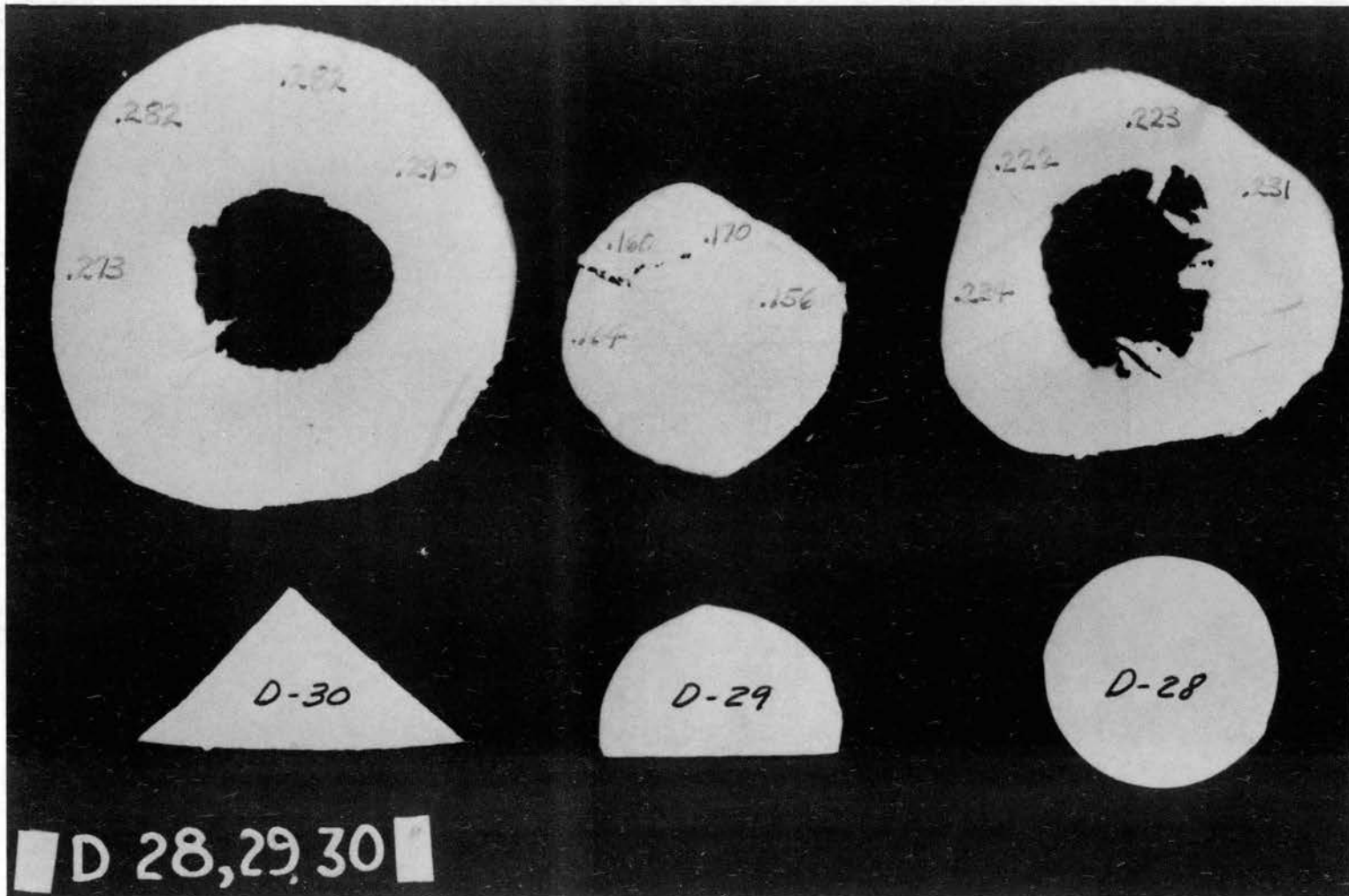
APPENDIX B-IV

SAMPLE DATA SHEET FOR STEM PHYSICAL PROPERTY TESTS

STEM PHYSICAL PROPERTIES		CONDITIONED 2HR
SAMPLE IDENTIFICATION		
TEST NO. [REDACTED]	DATE 8/28/68	NOM. SIZE OF STEM $1\frac{7}{64} \times 12\frac{7}{8}$ END TO C.G.
TEST LENGTH (FROM BASE OF STEM TO APPLIED LOAD) 3.375		IN.
MOISTURE CONTENT: (DRY BASIS) 13.397%		(WET BASIS) 11.814%
STEM LINEAR DENSITY AT TEST SECTION 0.2605 GMS/IN (DRY)		0.2954 GMS/IN (WET)
STEM CROSS SECTION DATA		
SHADOWGRAPH IDENTIFICATION SYMBOL 		
DIAMETER AT SHEAR SECTION (FROM MEASUREMENTS OF SHADOWGRAPH)		
LOCATION ①	.231	IN.
LOCATION ②	.223	IN.
LOCATION ③	.222	IN.
LOCATION ④	.234	IN.
AVG		0.2275 IN.
AREA		_____ SQ. IN.
LOAD-DEFLECTION DATA		
		
RAM SPEED 7.44187	IN/MIN	PHOTO VERT. SCALE _____ LB/CM
CHART SPEED 5	MM/SEC	PHOTO HORI. SCALE _____ IN/CM
SCOPE SWEEP RATE _____	CM/SEC	CHART VERT. SCALE 0.5 LB/MM
		CHART HORI. SCALE 0.25 IN/CM
STIFFNESS (LINEAR PORTION OF CURVE) = 3.9 LB / 1.0 IN = 3.9 LB/IN		
SHEAR TEST DATA		
		
RAM SPEED 0.96937	IN/MIN	CHART VERT. SCALE X10: 5.0 LB/MM
CHART SPEED 1	MM/SEC	CHART HORI. SCALE 0.016 IN/MM
SHEAR STRENGTH PER UNIT AVG DIA = 150 LB / 0.2275 IN. = 659.341 LB/IN		
SHEAR STRENGTH PER UNIT AREA = _____ LB/IN ²		

APPENDIX B-V

SAMPLE DATA SHEET FOR DETERMINING AVERAGE DIAMETER
OF STEM CROSS SECTION



APPENDIX C

- C-I CUTTING EFFECTIVENESS TEST DATA
- C-II DULL BLADE SERIES MAIN TEST DATA
- C-III SHARP BLADE SERIES MAIN TEST DATA

Explanation of Tables

C-I

The column headings under the description of cutting action section of the tables are to interpreted as follows:

Effective

CC - clean cut
 TRC - torn, ragged cut
 PCBKC - partial cut and break at knife contact point

Noneffective

PCBB - partial cut and break at base
 BB - break at base
 SUB - slipped under blade without being cut

C-II and C-III

The comment code letters have the following meaning:

- A - One sector hit and deflected stem without completely cutting it; opposite sector then severed stem.
- B - Torn, ragged cut.
- C - Stem was cut 1/2 to 7/8 through then broke at base.
- D - One sector cut 1/2 to 7/8 through stem then opposite sector completed cut.
- E - Second cut of stubble.
- F - Clean cut.
- G - Cut through node of stem.

H - Stem partially cut, then partially broke at base and was deflected under rotor without being cut.

I - One sector cut stem 1/2 to 7/8 through then opposite sector hit and broke stem at base.

Coded values of independent variable pi terms are explained as follows. It should be noted that these coded numbers are not the same as those listed in the experimental plan.

$$\begin{aligned} \Pi_2 : \quad 0 &= 322 \quad (1800 \text{ rpm}) \\ 1 &= 644 \quad (2546 \text{ rpm}) \\ 2 &= 966 \quad (3118 \text{ rpm}) \\ 3 &= 1288 \quad (3600 \text{ rpm}) \end{aligned}$$

$$\begin{aligned} \Pi_3 : \quad 0 &= 8 \times 10^{-2} \quad (1.75 \text{ in/rev.}) \\ 1 &= 14 \times 10^{-2} \quad (3.06 \text{ in/rev.}) \\ 2 &= 20 \times 10^{-2} \quad (4.38 \text{ in/rev.}) \end{aligned}$$

$$\begin{aligned} \Pi_4 : \quad 0 &= 4.54 \times 10^{-1} \quad (26^\circ) \\ 1 &= 6.28 \times 10^{-1} \quad (36^\circ) \\ 2 &= 8.02 \times 10^{-1} \quad (46^\circ) \\ 3 &= 9.76 \times 10^{-1} \quad (56^\circ) \end{aligned}$$

$$\begin{aligned} \Pi_5 : \quad 0 &= 1.07 \times 10^{-1} \quad (0.38 \text{ in.}) \\ 1 &= 2.14 \times 10^{-1} \quad (0.75 \text{ in.}) \\ 2 &= 3.21 \times 10^{-1} \quad (1.12 \text{ in.}) \\ 3 &= 4.28 \times 10^{-1} \quad (1.50 \text{ in.}) \end{aligned}$$

$$\begin{aligned} \Pi_6 : \quad 0 &= -8.73 \times 10^{-2} \quad (-5^\circ) \\ 1 &= 0.00 \times 10^{-2} \quad (0^\circ) \\ 2 &= 8.73 \times 10^{-2} \quad (5^\circ) \\ 3 &= 17.46 \times 10^{-2} \quad (10^\circ) \end{aligned}$$

$$\begin{aligned} \Pi_7 : \quad 0 &= 2.86 \times 10^{-1} \quad (1.00 \text{ in.}) \\ 1 &= 5.00 \times 10^{-1} \quad (1.75 \text{ in.}) \\ 2 &= 7.14 \times 10^{-1} \quad (2.50 \text{ in.}) \end{aligned}$$

$$\begin{aligned} \Pi_9 : \quad 0 &= 2.25 \quad (7.88 \text{ in.}) \\ 1 &= 2.75 \quad (9.62 \text{ in.}) \\ 2 &= 3.25 \quad (11.38 \text{ in.}) \\ 3 &= 3.75 \quad (13.12 \text{ in.}) \end{aligned}$$

APPENDIX C-I
CUTTING EFFECTIVENESS TEST DATA

Test No	No. Stems in Test	Conditions Rotor Angle, Rotor Speed, Feed Rate, Nom. Dia., Time in Chamber, C.G. Height, Crop Year	Description of Severing Action						Response Variable	No. Items Analyzed	Mean (In)	Std Error of Mean (In)	Max Value (In)	Min Value (In)	Range (In)
			Effective			Noneffective									
			CC	TRC	PCBKC	PCBB	BB	SUB							
CED 1	10	26°, 1800 RPM, 1.75 In/Rev, 17/64 In., 0 Hrs., 12 1/4 to 13 1/8 In., 1965	6				2	2	Cutting Height	9	2.75	0.07	3.12	2.38	0.74
									C. G. X-Disp	6	6.0	3.8	21.0	-3.0	24.0
									C. G. Y-Disp	6	19.2	5.7	39.0	0.5	38.5
									Cut End X-Disp	6	2.6	4.8	20.0	-11.0	31.0
									Cut End Y-Disp	6	17.9	5.0	38.5	5.0	33.0
CED 2	10	26°, 1800 RPM, 5.25 In/Rev, 17/64 In., 0 Hrs., 12 3/8 to 13 1/8 In., 1965	6		1			3	Cutting Height	10	2.52	0.12	3.25	2.00	1.25
									C. G. X-Disp	5	8.6	4.0	23.2	1.0	22.2
									C. G. Y-Disp	5	10.9	6.2	25.0	-8.0	33.0
									Cut End X-Disp	4	3.5	4.8	16.5	-5.0	21.5
									Cut End Y-Disp	4	0.2	7.7	20.5	-16.0	36.5
CED 3	10	26°, 3600 RPM, 1.75 In/Rev, 17/64 In., 0 Hrs., 12 to 13 1/8 In., 1965	10						Cutting Height	10	2.50	0.10	3.00	1.88	1.12
									C. G. X-Disp	9	16.9	3.0	32.0	7.9	24.1
									C. G. Y-Disp	9	14.5	2.4	27.0	6.5	20.5
									Cut End X-Disp	9	16.1	3.7	38.0	3.0	35.0
									Cut End Y-Disp	9	13.1	3.8	35.0	3.0	32.0
CED 4	10	26°, 3600 RPM, 5.25 In/Rev, 17/64 In., 0 Hrs., 10 1/8 to 11 1/2 In., 1965	7		1			2	Cutting Height	7	2.54	0.14	3.00	2.00	1.00
									C. G. X-Disp	7	70.9	15.2	120.0	4.0	116.0
									C. G. Y-Disp	7	17.4	10.7	60.0	-24.0	84.0
									Cut End X-Disp	1	-4.0				
									Cut End Y-Disp	1	14.0				
CED 5	10	56°, 1800 RPM, 1.75 In/Rev, 17/64 In., 0 Hrs., 14 1/2 to 15 In., 1965					1	9	Cutting Height	10	2.69	0.07	3.00	2.50	0.50
									C. G. X-Disp	10	-31.8	12.3	42.0	-96.0	138.0
									C. G. Y-Disp	10	15.6	7.2	60.0	-18.0	78.0
									Cut End X-Disp	0					
									Cut End Y-Disp	0					

APPENDIX C-I (Continued)

Test No	No. Stems in Test	Conditions Rotor Angle, Rotor Speed, Feed Rate, Nom. Dia., Time in Chamber, C.G. Height, Crop Year	Description of Severing Action						Response Variable	No. Items Analyzed	Mean (In)	Std Error of Mean (In)	Max Value (In)	Min Value (In)	Range (In)	
			Effective			Noneffective										
			CC	TRC	PCBKC	PCBB	BB	SUB								
CED 6	10	56°, 1800 RPM, 5.25 In/Rev, 17/64 In., 0 Hrs., 12 7/8 to 16 3/8 In., 1965				2	8		Cutting Height	10	2.96	0.11	3.50	2.50	1.00	
									C. G. X-Disp	10	23.2	10.3	69.0	-24.0	93.0	
										C. G. Y-Disp	10	-3.6	4.8	18.0	-24.0	42.0
										Cut End X-Disp	2	58.2	19.8	78.0	38.5	39.5
										Cut End Y-Disp	2	4.8	8.2	13.0	-3.5	16.5
CED 7	10	56°, 3600 RPM, 1.75 In/Rev, 21/64 In., 0 Hrs., 12 3/4 to 13 1/8 In., 1965				4	6		Cutting Height	9	2.65	0.11	3.25	2.00	1.25	
									C. G. X-Disp	6	-8.6	15.7	28.2	-72.0	100.2	
										C. G. Y-Disp	6	8.7	8.0	36.0	-12.0	48.0
										Cut End X-Disp	2	15.0	6.0	21.0	9.0	12.0
										Cut End Y-Disp	2	25.5	3.5	29.0	22.0	7.0
CED 8	10	56°, 3600 RPM, 5.25 In/Rev, 21/64 In., 0 Hrs., 12 5/8 to 13 In., 1965			7	1	2		Cutting Height	9	2.58	0.06	2.88	2.38	0.50	
									C. G. X-Disp	8	51.8	16.6	129.0	-25.0	154.0	
										C. G. Y-Disp	8	13.4	9.6	50.0	-26.5	76.5
										Cut End X-Disp	8	53.5	15.4	118.0	-16.5	134.5
										Cut End Y-Disp	8	15.0	9.9	56.0	-28.0	84.0
CED 9	10	56°, 3600 RPM, 5.25 In/Rev, 21/64 In., 8 Hr., 10 1/8 to 10 3/8 In., 1965	1		3	5	1		Cutting Height	8	2.27	0.16	3.25	1.88	1.37	
									C. G. X-Disp	6	97.0	19.0	156.0	43.0	113.0	
										C. G. Y-Disp	6	33.5	18.6	108.0	-6.5	114.5
										Cut End X-Disp	4	87.5	26.4	150.0	37.0	113.0
										Cut End Y-Disp	4	4.5	3.0	10.0	-4.0	14.0
CED 10	10	56°, 3600 RPM, 1.75 In/Rev, 21/64 In., 8 Hr., 10 1/8 to 10 3/8 In., 1965			4	6			Cutting Height	10	2.78	0.08	3.25	2.50	0.75	
									C. G. X-Disp	10	-1.8	10.0	46.0	-42.0	88.0	
										C. G. Y-Disp	10	28.0	8.9	60.0	-36.0	96.0
										Cut End X-Disp	6	17.3	7.9	50.0	-2.5	52.5
										Cut End Y-Disp	6	26.5	7.2	55.0	5.5	49.5

APPENDIX C-I (Continued)

Test No	No. Stems in Test	Conditions Rotor Angle, Rotor Speed, Feed Rate, Nom. Dia., Time in Chamber, C.G. Height, Crop Year	Description of Severing Action						Response Variable	No. Items Analyzed	Mean (In)	Std Error of Mean (In)	Max Value (In)	Min Value (In)	Range (In)
			Effective			Noneffective									
			CC	TRC	PCBKC	PCBB	BB	SUB							
CED 11	10	56°, 1800 RPM, 5.25 In/Rev, 21/64 In., 8.5 Hr., 12 7/8 to 13 1/8 In., 1965		3	3	4			Cutting Height	10	2.78	0.05	3.00	2.50	0.50
									C. G. X-Disp	10	38.7	6.0	64.0	14.0	50.0
									C. G. Y-Disp	10	25.0	5.1	59.0	4.0	55.0
									Cut End X-Disp	10	41.2	6.0	69.0	12.0	57.0
									Cut End Y-Disp	10	28.2	6.6	69.5	0.2	69.3
CED 12	10	56°, 1800 RPM, 1.75 In/Rev, 21/64 In., 8.5 Hr., 12 7/8 to 14 5/8 In., 1965		5	1	1	2	1	Cutting Height	10	2.68	0.11	3.00	2.00	1.00
									C. G. X-Disp	9	-12.4	13.3	56.0	-72.0	128.0
									C. G. Y-Disp	9	32.2	3.3	48.0	18.0	30.0
									Cut End X-Disp	0					
									Cut End Y-Disp	0					
CED 13	10	26°, 1800 RPM, 1.75 In/Rev, 17/64 In., 9 Hr., 12 7/8 to 14 3/4 In., 1965	10						Cutting Height	10	2.52	0.06	2.88	2.25	0.63
									C. G. X-Disp	10	5.0	1.1	10.0	-1.5	11.5
									C. G. Y-Disp	10	15.4	3.6	39.0	2.0	37.0
									Cut End X-Disp	10	5.5	2.0	13.5	-8.0	21.5
									Cut End Y-Disp	10	11.4	5.4	47.5	-2.5	50.0
CED 14	10	26°, 1800 RPM, 5.25 In/Rev, 17/64 In., 9 Hr., 12 to 17 In., 1965	9					1	Cutting Height	10	2.41	0.06	2.75	2.12	0.63
									C. G. X-Disp	10	45.6	12.2	144.0	14.0	130.0
									C. G. Y-Disp	10	16.0	7.3	72.0	-13.0	85.0
									Cut End X-Disp	9	31.6	8.0	69.0	2.0	67.0
									Cut End Y-Disp	9	10.0	3.6	22.0	-4.5	26.5
CED 15	10	26°, 3600 RPM, 5.25 In/Rev, 17/64 In., 9 Hr., 10 1/8 to 12 7/8 In., 1965	9			1			Cutting Height	10	2.59	0.08	3.00	2.25	0.75
									C. G. X-Disp	10	52.3	7.7	84.0	18.2	65.8
									C. G. Y-Disp	10	-2.3	6.6	25.5	-48.0	73.5
									Cut End X-Disp	4	51.2	16.2	81.0	12.5	68.5
									Cut End Y-Disp	4	11.1	9.5	30.5	-9.0	39.5

APPENDIX C-I (Continued)

Test No	No. Stems in Test	Conditions Rotor Angle, Rotor Speed, Feed Rate, Nom. Dia., Time in Chamber, C.G. Height, Crop Year	Description of Severing Action						Response Variable	No. Items Analyzed	Mean (In)	Std Error of Mean (In)	Max Value (In)	Min Value (In)	Range (In)
			Effective			Noneffective									
			CC	TRC	PCBKC	PCBB	BB	SUB							
CED 16	10	26°, 3600 RPM, 1.75 In/Rev, 17/64 In., 9 Hr., 9 7/8 to 13 1/4 In., 1965	10						Cutting Height	10	2.42	0.08	2.88	2.19	0.69
									C. G. X-Disp	10	4.7	4.5	23.6	-30.0	53.6
									C. G. Y-Disp	10	13.0	3.9	40.0	0.0	40.0
									Cut End X-Disp	7	9.4	3.5	29.1	2.0	27.1
									Cut End Y-Disp	7	5.9	2.4	19.0	-0.5	19.5
PD 1	5	26°, 1800 RPM, 1.75 In/Rev, 17/64 In., 2 Hr., 13 1/2 to 15 1/4 In., 1965	4	1					Cutting Height	5	2.81	0.08	3.12	2.69	0.43
									C. G. X-Disp	5	6.0	2.4	14.5	0.5	14.0
									C. G. Y-Disp	5	16.0	8.9	49.5	-4.0	53.5
									Cut End X-Disp	5	4.2	5.5	19.0	-9.5	28.5
									Cut End Y-Disp	5	12.5	7.2	39.0	1.5	37.5
PD 2	9	26°, 3600 RPM, 1.75 In/Rev, 17/64 In., 2 Hr., 12 1/4 to 16 In., 1965	9						Cutting Height	9	2.65	0.08	3.12	2.38	0.74
									C. G. X-Disp	9	19.1	1.9	27.5	12.8	14.7
									C. G. Y-Disp	9	12.7	2.7	28.2	3.2	25.0
									Cut End X-Disp	9	11.9	3.6	35.0	2.5	32.5
									Cut End Y-Disp	9	10.3	2.5	27.8	2.0	25.8
PD 3	9	26°, 3600 RPM, 5.25 In/Rev, 17/64 In., 2 Hr., 13 1/2 to 14 7/8 In., 1965	8	1					Cutting Height	9	2.45	0.08	2.88	2.12	0.76
									C. G. X-Disp	9	87.4	6.4	107.0	46.0	61.0
									C. G. Y-Disp	9	13.3	2.9	29.0	-2.5	31.5
									Cut End X-Disp	9	84.1	7.7	110.0	33.0	77.0
									Cut End Y-Disp	9	11.6	3.3	30.0	-3.0	33.0
PD 4	6	56°, 1800 RPM, 1.75 In/Rev, 17/64 In., 2 Hr., 13 1/2 to 14 1/2 In., 1965	5					1	Cutting Height	6	2.62	0.21	3.12	1.62	1.50
									C. G. X-Disp	5	6.2	7.8	24.5	-22.0	46.5
									C. G. Y-Disp	5	15.0	2.5	25.0	11.0	14.0
									Cut End X-Disp	5	7.2	5.1	19.0	-12.0	31.0
									Cut End Y-Disp	5	17.0	3.1	22.2	6.0	16.2

APPENDIX C-I (Continued)

Test No	No Stems in Test	Conditions Rotor Angle, Rotor Speed, Feed Rate, Nom. Dia., Time in Chamber, C. G. Height, Crop Year	Description of Severing Action						Response Variable	No. Items Analyzed	Mean (In)	Std Error of Mean (In)	Max Value (In)	Min Value (In)	Range (In)
			Effective			Noneffective									
			CC	TRC	PCBKC	PCBB	BB	SUB							
PD 5	9	56°, 3600 RPM, 1.75 In/Rev, 17/64 In., 2 Hrs., 12 1/4 to 13 1/4 In., 1965		7		1	1		Cutting Height	9	3.01	0.14	3.50	2.12	1.38
									C. G. X-Disp	9	24.5	6.6	56.0	2.0	54.0
									C. G. Y-Disp	9	25.6	5.3	55.0	3.8	51.2
									Cut End X-Disp	9	23.2	7.4	59.0	2.0	57.0
									Cut End Y-Disp	9	22.9	5.1	46.5	2.5	44.0
PD 6	18	56°, 3600 RPM, 5.25 In/Rev, 17/64 In., 2 Hr., 11 1/2 to 13 In., 1965	2	9	1	6			Cutting Height	14	2.82	0.11	3.38	2.12	1.26
									C. G. X-Disp	18	117.0	11.7	185.5	34.5	151.0
									C. G. Y-Disp	18	11.1	4.7	55.0	-22.5	77.5
									Cut End X-Disp	18	116.6	12.3	190.5	22.0	168.5
									Cut End Y-Disp	18	11.2	4.3	46.0	-24.0	70.0
PD 7	9	56°, 1800 RPM, 1.75 In/Rev, 17/64 In., 2 Hr., 10 1/2 to 13 5/8 In., 1965	1	6		1	1		Cutting Height	9	2.71	0.07	3.00	2.50	0.50
									C. G. X-Disp	9	-31.2	14.4	8.2	-94.0	102.2
									C. G. Y-Disp	9	34.8	8.3	71.8	7.8	64.0
									Cut End X-Disp	9	-25.4	14.5	19.5	-88.0	107.5
									Cut End Y-Disp	9	33.4	7.4	63.0	5.5	57.5
PD-8	9	56°, 3600 RPM, 1.75 In/Rev, 17/64 In., 2 Hr., 11 1/2 to 13 5/8 In., 1965	2	3		4			Cutting Height	9	2.94	0.11	3.25	2.19	1.06
									C. G. X-Disp	9	8.0	9.9	58.0	-37.5	95.5
									C. G. Y-Disp	9	26.8	6.9	77.5	9.0	68.5
									Cut End X-Disp	9	6.1	10.9	59.0	-41.2	100.2
									Cut End Y-Disp	9	26.1	7.0	77.5	5.5	72.0
PD 9	9	56°, 3600 RPM, 5.25 In/Rev, 17/64 In., 2 Hr., 12 1/4 to 13 1/2 In., 1965	3	4	1	1			Cutting Height	9	2.92	0.13	3.25	2.12	1.13
			3	4	1	1			C. G. X-Disp	9	77.9	13.0	135.8	29.0	106.8
			3	4	1	1			C. G. Y-Disp	9	19.1	4.3	38.0	-5.2	43.2
									Cut End X-Disp	9	79.4	12.7	135.9	21.0	114.9
									Cut End Y-Disp	9	21.0	5.0	41.5	-7.5	49.0

APPENDIX C-1 (Continued)

Test No	No Stems in Test	Conditions Rotor Angle, Rotor Speed, Feed Rate, Nom. Dia., Time in Chamber, C. G. Height, Crop Year	Description of Severing Action						Response Variable	No. Items Analyzed	Mean (In)	Std Error of Mean (In)	Max Value (In)	Min Value (In)	Range (In)
			Effective			Noneffective									
			CC	TRC	PCBKC	PCBB	BB	SUB							
PD 10	9	26°, 3600 RPM, 5.25 In/Rev, 17/64 In., 2 Hr., 10 3/8 to 11 3/8 In., 1965	7	1		1			Cutting Height	9	2.62	0.11	3.12	2.12	1.00
									C. G. X-Disp	9	69.8	10.9	111.0	19.8	91.2
									C. G. Y-Disp	9	11.3	7.7	47.5	-19.0	66.5
									Cut End X-Disp	9	69.5	12.7	117.0	13.2	103.8
									Cut End Y-Disp	9	10.8	8.7	49.0	-24.0	73.0
PD 11	9	26°, 3600 RPM, 1.75 In/Rev, 17/64 In., 2 Hr., 9 5/8 to 12 5/8 In., 1965	9						Cutting Height	9	2.74	0.10	3.38	2.38	1.00
									C. G. X-Disp	9	16.3	2.7	31.0	6.8	24.2
									C. G. Y-Disp	9	14.1	3.9	42.0	3.5	38.5
									Cut End X-Disp	8	12.3	3.4	25.2	0.2	25.0
									Cut End Y-Disp	8	6.9	1.6	13.5	0.2	13.3
PD 12	18	26°, 1800 RPM, 1.75 In/Rev, 17/64 In., 2 Hr., 9 5/8 to 13 7/8 In., 1965	14	4					Cutting Height	18	2.63	0.05	2.88	2.25	0.63
									C. G. X-Disp	18	-1.4	3.5	14.0	-32.5	46.5
									C. G. Y-Disp	18	23.2	2.7	51.2	5.5	45.7
									Cut End X-Disp	18	2.0	3.9	19.1	-31.0	50.1
									Cut End Y-Disp	18	22.4	3.3	48.5	2.0	46.5
PS 1	9	26°, 1800 RPM, 1.75 In/Rev, 17/64 In., 2 Hr., 14 1/2 to 17 5/8 In., 1965	9						Cutting Height	9	2.40	0.12	2.88	1.88	1.00
									C. G. X-Disp	9	10.3	2.5	29.0	3.2	25.8
									C. G. Y-Disp	9	6.1	1.5	15.5	0.2	15.3
									Cut End X-Disp	9	2.4	3.8	29.5	-6.5	36.0
									Cut End Y-Disp	9	2.9	0.6	6.8	1.5	5.3
PS 2	9	26°, 1800 RPM, 1.75 In/Rev, 17/64 In., 0 Hr., 14 1/8 to 17 1/4 In., 1968	7			1	1		Cutting Height	9	2.44	0.08	3.00	2.25	0.75
									C. G. X-Disp	8	13.8	3.1	29.1	6.0	23.1
									C. G. Y-Disp	8	7.4	1.8	16.2	0.0	16.2
									Cut End X-Disp	8	2.6	3.2	17.8	-6.5	24.3
									Cut End Y-Disp	8	5.2	3.2	20.0	-9.1	29.1

APPENDIX C-I (Continued)

Test No	No Stems in Test	Conditions Rotor Angle, Rotor Speed, Feed Rate, Nom. Dia., Time in Chamber, C. G. Height, Crop Year	Description of Severing Action						Response Variable	No. Items Analyzed	Mean (in)	Std Error of Mean (in)	Max Value (in)	Min Value (in)	Range (in)
			Effective			Noneffective									
			CC	TRC	PCBKC	PCBB	BB	SUB							
PS 3	9	26°, 3600 RPM, 5.25 In/Rev, 17/64 In., 0 Hr., 15 3/4 to 18 3/4 In., 1968	5		3		1	Cutting Height	9	2.28	0.07	2.62	2.00	0.62	
								C. G. X-Disp	9	61.9	6.8	105.0	37.0	68.0	
								C. G. Y-Disp	9	5.8	2.9	17.0	-5.5	22.5	
								Cut End X-Disp	9	66.5	8.3	117.0	35.0	82.0	
								Cut End Y-Disp	9	6.4	2.8	15.0	-12.0	27.0	
PS 4	9	56°, 3600 RPM, 5.25 In/Rev, 17/64 In., 2 Hr., 14 5/8 to 19 3/4 In., 1968	1	3	4		1	Cutting Height	9	2.17	0.12	2.88	1.75	1.13	
								C. G. X-Disp	8	110.6	9.8	141.0	53.0	88.0	
								C. G. Y-Disp	8	19.9	4.2	35.5	4.0	31.5	
								Cut End X-Disp	8	113.3	10.5	144.0	56.0	88.0	
								Cut End Y-Disp	8	18.9	6.9	42.5	-5.5	48.0	
PS 5	9	56°, 1800 RPM, 1.75 In/Rev, 17/64 In., 2 Hr., 15 3/8 to 20 In., 1968	8		1			Cutting Height	9	2.39	0.07	2.50	1.88	0.62	
								C. G. X-Disp	9	21.6	5.7	65.8	11.2	54.6	
								C. G. Y-Disp	9	11.2	4.6	34.5	-1.8	36.3	
								Cut End X-Disp	9	12.9	8.4	77.8	-2.2	80.0	
								Cut End Y-Disp	9	16.2	5.2	46.0	3.5	42.5	
PS 6	9	46°, 3600 RPM, 3.06 In/Rev, 21/64 In., 2 Hr., 15 1/4 to 17 7/8 In., 1968	9					Cutting Height	9	1.38	0.08	1.75	1.00	0.75	
								C. G. X-Disp	9	50.2	5.7	95.0	39.0	56.0	
								C. G. Y-Disp	9	1.6	1.8	9.0	-6.0	15.0	
								Cut End X-Disp	9	48.7	8.1	106.0	28.8	77.2	
								Cut End Y-Disp	9	0.6	2.5	9.5	-14.5	24.0	
PS 7	9	46°, 3600 RPM, 3.06 In/Rev, 21/64 In., 2 Hr., 13 3/4 to 21 1/2 In., 1968	6	1	1	1		Cutting Height	9	1.53	0.10	2.00	1.25	0.75	
								C. G. X-Disp	9	37.9	4.1	58.0	16.2	41.8	
								C. G. Y-Disp	9	1.8	2.0	16.0	-4.0	20.0	
								Cut End X-Disp	9	36.8	5.6	69.5	20.5	49.0	
								Cut End Y-Disp	9	4.5	3.9	24.0	-15.0	39.0	

APPENDIX C-I (Continued)

Test No	No Stems in Test	Conditions Rotor Angle, Rotor Speed, Feed Rate, Nom. Dia., Time in Chamber, C. G. Height, Crop Year	Description of Severing Action						Response Variable	No. Items Analyzed	Mean (In)	Std Error of Mean (In)	Max Value (In)	Min Value (In)	Range (In)
			Effective			Noneffective									
			CC	TRC	PCBKC	PCBB	BB	SUB							
PS 8	9	56°, 3600 RPM, 5.25 In/Rev, 17/64 In., 2 Hr., 18 3/4 to 22 5/8 In., 1968	5		3	1			Cutting Height	9	2.22	0.11	2.62	1.75	0.87
									C. G. X-Disp	9	117.7	4.3	127.5	90.0	37.5
									C. G. Y-Disp	9	9.9	2.9	23.0	-3.5	26.5
									Cut End X-Disp	9	127.3	6.7	142.5	80.5	62.0
									Cut End Y-Disp	9	7.9	5.9	32.0	-14.0	46.0
PS 9	9	26°, 3600 RPM, 5.25 In/Rev, 17/64 In., 2 Hr., 15 5/8 to 22 3/8 In., 1968	7		2				Cutting Height	9	2.04	0.05	2.25	1.75	0.50
									C. G. X-Disp	9	79.6	7.6	127.5	47.0	80.5
									C. G. Y-Disp	9	1.0	2.5	14.0	-9.0	23.0
									Cut End X-Disp	9	85.1	9.2	140.0	39.0	101.0
									Cut End Y-Disp	9	0.4	3.0	13.2	-16.0	29.2
PS 10	9	26°, 1800 RPM, 1.75 In/Rev, 17/64 In., 2 Hr., 18 1/4 to 21 1/2 In., 1968	8			1			Cutting Height	9	2.35	0.11	2.75	1.88	0.87
									C. G. X-Disp	9	22.6	3.9	37.5	0.0	37.5
									C. G. Y-Disp	9	6.6	3.5	23.0	-7.0	30.0
									Cut End X-Disp	9	17.1	5.5	48.0	-5.0	53.0
									Cut End Y-Disp	9	9.2	4.7	32.8	-15.0	47.8
PS 11	9	26°, 1800 RPM, 1.75 In/Rev, 17/64 In., 2 Hr., 15 1/4 to 17 3/8 In., 1965	8			1			Cutting Height	9	2.22	0.10	2.88	1.88	1.00
									C. G. X-Disp	9	3.9	3.0	9.8	-18.0	27.8
									C. G. Y-Disp	9	10.6	3.7	38.0	2.0	36.0
									Cut End X-Disp	9	-1.4	2.4	16.8	-8.0	24.8
									Cut End Y-Disp	9	9.5	5.5	47.0	-3.2	50.2
PS-12	9	56°, 1800 RPM, 1.75 In/Rev, 17/64 In., 2 Hr., 15 3/8 to 20 1/8 In., 1968	4		3	2			Cutting Height	9	2.11	0.07	2.50	1.75	0.75
									C. G. X-Disp	9	23.5	9.6	69.2	-24.0	93.2
									C. G. Y-Disp	9	15.2	4.1	37.0	-10.0	47.0
									Cut End X-Disp	9	11.8	10.0	57.0	-41.0	98.0
									Cut End Y-Disp	9	17.0	4.4	31.2	-12.0	43.2

APPENDIX C-II
DULL BLADE SERIES MAIN TEST DATA

Run No.	Comment Code	Energy Input In-Lb _f	Max Torque Lb _f -In	Theo Relative Contact Velocity Ft/Sec	X Disp				Y Disp				Positive Z Disp		Actual Ht. of Cut Above Base In	Per Cent Moisture Dry Basis %	Wet Linear Density Gm/In	Dry Linear Density Gm/In	Plant Size Dia X Ht. from End to C.G. In	Time in Chamber Hrs.	Coded Values of Independent Variable Pi Terms								
					C.G.		End		C.G.		End		C.G.	End							C.G.	End	π ₂	π ₃	π ₄	π ₅	π ₆	π ₇	π ₉
D1	A,B	114.1265	20.0	45.09	7.4	1.2	10.0	3.2	1.5	2.0	2.38	35.286	0.3025	0.2236	17/64 x 12 7/8	6	1	0	1	3	3	0	2						
D11 ^a	C	84.2263	36.0	45.09	0.0	6.0	40.0	48.0	85.0 ^b	85.0 ^b	2.00	46.814	0.4356	0.2967	17/64 x 12 7/8	6	1	0	1	3	3	0	2						
D16	D	132.8119	37.5	45.09	22.5	21.2	17.9	27.2	3.0	3.0	2.00	36.800	0.3472	0.2500	17/64 x 12 7/8	6	1	0	1	3	3	0	2						
D2 ^a	C,E	136.6230	33.8	70.32	0.0	7.0	21.0	15.0	36.0 ^b	40.0 ^b	3.38	35.106	0.5248	0.3911	21/64 x 11 1/8	6	3	1	3	2	3	2	1						
D6	B	130.5778	33.0	70.32	58.0	57.0	30.5	24.2	14.6	25.0	3.25	26.580	0.4271	0.3374	21/64 x 11 1/8	6	3	1	3	2	3	2	1						
D17	C	143.9259	33.0	70.32	38.5	31.0	-5.0	-14.0	60.0 ^b	64.0 ^b	3.75	23.857	0.5202	0.4200	21/64 x 11 1/8	6	3	1	3	2	3	2	1						
D3	C,E	148.7039	56.0	38.44	4.0	6.0	24.0	15.0	84.0 ^b	84.0 ^b	4.00	30.769	0.6392	0.4888	25/64 x 14 5/8	6	0	2	3	3	1	1	3						
D10	D,E	251.0605	95.0	38.44	0.0	6.0	16.0	20.0	84.0 ^b	84.0 ^b	2.88	19.496	0.5694	0.4765	25/64 x 14 5/8	6	0	2	3	3	1	1	3						
D22 ^a	C,E	112.0864	42.0	38.44	-22.0	-24.0	32.0	36.0	0.0	4.0	2.75	35.741	0.5655	0.4166	25/64 x 14 5/8	6	0	2	3	3	1	1	3						
D4	F,E	197.5170	37.0	63.76	13.8	4.5	2.4	4.5	6.0	8.0	1.88	40.432	0.5644	0.4019	25/64 x 12 7/8	6	3	0	0	0	2	0	2						
D9	B,E	136.8343	28.0	63.76	37.2	44.2	7.8	14.2	22.0	26.0	1.88	35.193	0.5305	0.3924	25/64 x 12 7/8	6	3	0	0	0	2	0	2						
D20 ^a	G,F,E	193.9485	40.0	63.76	-18.0	-9.2	-3.5	-2.0	3.0	3.0	1.38	21.895	0.6920	0.5677	25/64 x 12 7/8	6	3	0	0	0	2	0	2						
D5 ^a	A	45.9439	23.0	31.88	-14.2	-9.0	0.0	0.0	0.0	3.0	2.75	34.255	0.3884	0.2893	21/64 x 9 3/8	6	0	0	0	1	0	2	0						
D19	F,E	112.7423	30.0	31.88	-4.0	0.0	8.0	7.0	3.0	8.0	3.38	21.658	0.4005	0.3292	21/64 x 9 3/8	6	0	0	0	1	0	2	0						
D21	F,E	147.5617	40.0	31.88	-4.0	-2.0	2.0	4.0	0.8	2.0	2.88	42.483	0.5668	0.3978	21/64 x 9 3/8	6	0	0	0	1	0	2	0						
D7	F,E	27.4857	13.8	60.90	60.0	53.0	50.0	42.0	6.0	19.0	2.25	37.145	0.2854	0.2081	17/64 x 14 5/8	6	2	1	2	0	0	1	3						
D12	F	40.0832	15.0	60.90	29.5	18.5	7.2	8.5	0.8	2.5	1.88	33.102	0.3320	0.2496	17/64 x 14 5/8	6	2	1	2	0	0	1	3						
D15 ^a	D,B	56.8672	16.8	60.90	40.5	30.0	4.0	4.5	0.8	12.0	2.12	79.230	0.2891	0.1613	17/64 x 14 5/8	6	2	1	2	0	0	1	3						
D8 ^a	B	30.2430	15.3	54.37	27.8	25.8	5.5	11.2	1.0	7.0	3.38	73.182	0.1905	0.1100	13/64 x 11 1/8	6	1	2	2	1	2	2	1						
D14	B	38.8437	15.0	54.37	55.0	49.2	7.0	3.8	12.0	19.0	3.12	35.836	0.1827	0.1345	13/64 x 11 1/8	6	1	2	2	1	2	2	1						
D24	F	25.9189	6.5	54.37	31.0	30.2	1.5	-5.5	3.0	8.5	2.88	36.654	0.1454	0.1064	13/64 x 11 1/8	6	1	2	2	1	2	2	1						

APPENDIX C-II (Continued)

Run No.	Comment Code	Energy Input In-Lb _f	Max Torque Lb _f -In	Theo Relative Contact Velocity Ft/Sec	X Disp						Y Disp						Positive Z Disp						Actual Ht. of Cut Above Base In	Per Cent Moisture Dry Basis %	Wet Linear Density Gm/In	Dry Linear Density Gm/In	Plant Size Dia X Ht. from End to C.G. In	Time in Chamber Hrs.	Coded Values of Independent Variable Pi Terms								
					C.G.		In		End		C.G.		In		End		C.G.		In		End								π ₂	π ₃	π ₄	π ₅	π ₆	π ₇	π ₉		
D13	F	23.6612	6.5	55.22	7.2	1.0	4.2	4.0	0.0	1.0	3.00	53.353	0.1509	0.0984	13/64 x 9 3/8	6	2	0	1	2	1	2	0														
018	F,E	25.6417	10.0	55.22	-2.0	2.0	4.0	5.2	0.0	3.0 ^b	3.12	54.376	0.1164	0.0754	13/64 x 9 3/8	6	2	0	1	2	1	2	0														
D23 ^a	B	33.0864	13.5	55.22	33.2	29.1	15.4	16.5	11.5	11.5	3.62	68.054	0.1978	0.1177	13/64 x 9 3/8	6	2	0	1	2	1	2	0														
025	F,E	103.2932	23.0	63.76	43.0	39.0	0.0	-6.0	7.2	7.8	2.38	14.001	0.4128	0.3621	21/64 x 11 1/8	2	3	0	1	0	1	1	1														
041	A,B,E	101.0221	32.0	63.76	-26.0	-24.0	-7.0	-3.0	12.5	13.0	2.38	36.396	0.4467	0.3275	21/64 x 11 1/8	2	3	0	1	0	1	1	1														
D26	H	74.8408 ^b	40.0 ^b	35.76	-6.0 ^b	-10.0 ^b	30.0 ^b	25.0 ^b	20.0 ^b	24.0 ^b	2.00	36.953	0.6356	0.4641	21/64 x 9 3/8	2	0	1	2	3	2	0	0														
D35	A,B	116.1902	52.0	35.76	-12.0	-12.0	51.0	56.0	72.0 ^b	72.0 ^b	2.50	24.867	0.3756	0.3008	21/64 x 9 3/8	2	0	1	2	3	2	0	0														
027	D	71.3918	24.0	55.22	5.0	-3.4	11.0	5.2	0.5	3.8	3.38	17.032	0.2824	0.2413	17/64 x 14 5/8	2	2	0	0	2	2	2	3														
D33	F,E	80.5710	16.0	55.22	13.4	9.5	3.5	-5.6	3.8	6.2	3.38	13.804	0.2333	0.2050	17/64 x 14 5/8	2	2	0	0	2	2	2	3														
028	F	51.1101	19.5	49.73	50.0	42.0	0.0	0.5	2.5	8.0	3.38	12.838	0.3041	0.2695	17/64 x 12 7/8	2	1	1	3	1	1	2	2														
D39	B	56.6373	26.5	49.73	28.5	22.0	-6.5	-10.2	5.2	11.8	3.38	23.558	0.3000	0.2428	17/64 x 12 7/8	2	1	1	3	1	1	2	2														
D29 ^a	F,E	32.1744	10.0	45.09	4.0	-2.5	8.2	8.5	0.0	2.0	2.88	35.211	0.1344	0.0994	13/64 x 11 1/8	2	1	0	0	3	0	1	1														
D31	F	28.3187	8.5	45.09	1.0	-5.0	7.5	4.2	3.2	11.8	2.62	31.260	0.1625	0.1238	13/64 x 11 1/8	2	1	0	0	3	0	1	1														
D34	F,E	32.4832	7.5	45.09	4.0	10.0	33.0	38.0	10.0	10.5	2.75	22.248	0.1577	0.1290	13/64 x 11 1/8	2	1	0	0	3	0	1	1														
D30	I	172.3517	25.0	76.88	12.2	2.5	8.5	15.0	14.0	24.0	4.00	24.231	0.5091	0.4098	25/64 x 12 7/8	2	3	2	2	2	0	2	2														
D37	F	185.5896	50.0	76.88	44.0	35.0	-8.0	-8.0	0.5	6.5	2.50	23.265	0.4726	0.3834	25/64 x 12 7/8	2	3	2	2	2	0	2	2														
D32	F	10.4027	5.5	66.59	70.0	63.0	-5.0	-7.0	3.6	9.5	1.75	30.346	0.1353	0.1036	13/64 x 9 3/8	2	2	2	3	0	3	0	0														
D40	B	20.2652	5.0	66.59	35.0	33.0	-3.5	4.0	0.0	6.3	1.50	31.521	0.1815	0.1380	13/64 x 9 3/8	2	2	2	3	0	3	0	0														
D36	F,E	137.9290	63.0	31.88	4.9	0.0	8.8	0.0	1.8	-2.0	3.25	16.725	0.3657	0.3133	25/64 x 14 5/8	2	0	0	1	1	3	2	3														
D38	F,E	153.4641	65.0	31.88	1.5	-2.0	-2.5	-10.0	48.0 ^b	60.0 ^b	3.12	18.472	0.5195	0.4385	25/64 x 14 5/8	2	0	0	1	1	3	2	3														

APPENDIX C-II (Continued)

Run No.	Comment Code	Energy Input In-Lb _f	Max Torque Lb _f -In	Theo Relative Contact Velocity Ft/Sec	X Disp		Y Disp		Positive Z Disp		Actual Ht. of Cut Above Base In	Per Cent Moisture Dry Basis %	Wet Linear Density Gm/In	Dry Linear Density Gm/In	Plant Size Dia X Ht. from End to C.G. In	Time in Chamber Hrs.	Coded Values of Independent Variable Pi Terms							
					C.G.		C.G.		C.G.								π ₂	π ₃	π ₄	π ₅	π ₆	π ₇	π ₉	
					In	End	In	End	In	End														
D42	A,B,E	136.5732	40.0	55.22	12.0	3.8	6.0	6.2	1.3	3.1	2.88	51.369	0.3925	0.2593	21/64 x 12 3/8	4	2	0	3	1	2	1	2	
D54	A,F	143.2482	42.5	55.22	4.0	-3.8	7.5	3.0	3.0	4.8	2.12	38.017	0.4763	0.3451	21/64 x 12 3/8	4	2	0	3	1	2	1	2	
D43	F	44.7390	10.0	70.32	64.0	77.0	-15.0	-20.0	2.0	15.0	1.50	45.822	0.1623	0.1113	13/64 x 14 5/8	4	3	1	1	1	0	0	3	
D47	D,F	40.9945	9.0	70.32	25.6	14.0	0.5	1.0	0.0	5.3	1.38	59.263	0.1470	0.0923	13/64 x 14 5/8	4	3	1	1	1	0	0	3	
D44	B,E	36.5810	27.5	38.44	12.0	6.0	-15.0	-15.5	0.8	2.0 ^b	3.62	16.316	0.2103	0.1808	17/64 x 11 1/8	4	0	2	1	0	2	2	1	
D49	B,E	22.9047	16.0	38.44	-5.0	-11.0	-24.0	-25.0	4.0	6.0 ^b	3.50	29.077	0.2042	0.1582	17/64 x 11 1/8	4	0	2	1	0	2	2	1	
D45	A,F	128.2234	34.0	60.90	5.0	0.0	6.0	2.0	0.5	1.5 ^b	3.25	22.416	0.4407	0.3600	25/64 x 11 1/8	4	2	1	0	3	3	2	1	
D52	F	144.8227	46.0	60.90	46.0	49.0	9.0	3.0	15.0	20.0	3.25	29.002	0.4359	0.3379	25/64 x 11 1/8	4	2	1	0	3	3	2	1	
D46	A,F	123.5707	36.0	63.76	5.0	0.5	13.0	12.0	6.0	8.0	3.38	30.913	0.2507	0.1915	17/64 x 9 3/8	4	3	0	2	3	1	2	0	
D50	A,F,E	66.0371	10.0	63.76	2.0	7.0	41.0	41.5	36.0 ^b	44.0 ^b	3.50	22.080	0.1913	0.1567	17/64 x 9 3/8	4	3	0	2	3	1	2	0	
D48	F	53.0624	39.0	54.37	53.5	65.0	-11.0	-11.2	5.5	14.4	1.38	24.658	0.4565	0.3662	21/64 x 14 5/8	4	1	2	0	2	1	0	3	
D53	C	89.5371	45.0	54.37	44.0	55.0 ^b	-10.0	-14.0 ^b	84.0 ^b	84.0 ^b	1.25	57.220	0.5770	0.3670	21/64 x 14 5/8	4	1	2	0	2	1	0	3	
D51	B,E	23.7852	15.3	31.88	28.0	35.0	40.5	35.0	10.0	14.0 ^b	2.88	29.181	0.1421	0.1100	13/64 x 12 7/8	4	0	0	2	2	3	1	2	
D56	B,E	51.3270	23.8	31.88	-56.0	-49.0	24.0	19.0	72.0 ^b	72.0 ^b	2.88	30.229	0.1874	0.1439	13/64 x 12 7/8	4	0	0	2	2	3	1	2	
D55	D,B	161.4170	65.0	45.09	-13.0	-9.2	1.0	2.0	0.0	2.0 ^b	3.75	87.735	0.6567	0.3498	25/64 x 9 3/8	4	1	0	3	0	0	2	0	
D57	B,E	85.1834	40.0	45.09	20.0	16.0	32.0	35.0	48.0 ^b	48.0 ^b	3.12	14.746	0.3774	0.3289	25/64 x 9 3/8	4	1	0	3	0	0	2	0	
D58	B,E	166.6724	46.0	55.22	8.5	0.5	4.2	1.8	0.0	4.9	1.38	95.503	0.6782	0.3469	25/64 x 11 1/8	8	2	0	2	1	1	0	1	
D61	D,B	243.7522	58.0	55.22	7.5	0.5	7.5	2.2	0.7	1.4 ^b	1.00	61.432	0.8945	0.5541	25/64 x 11 1/8	8	2	0	2	1	1	0	1	

APPENDIX C-II (Continued)

Run No.	Comment Code	Energy Input In-Lb _F	Max Torque Lb _F -In	Theo Relative Contact Velocity Ft/Sec	X Disp		Y Disp		Positive Z Disp		Actual Ht. of Cut Above Base In	Per Cent Moisture Dry Basis %	Net Linear Density Gm/In	Dry Linear Density Gm/In	Plant Size Dia X Ht. from End to C.G. In	Time in Chamber Hrs.	Coded Values of Independent Variable Pi Terms								
					C.G.	End	C.G.	End	C.G.	End							π ₂	π ₃	π ₄	π ₅	π ₆	π ₇	π ₉		
D59	D	144.8118	47.0	49.73	-9.0	-5.5	28.0	31.5	13.0	15.0 ^b	2.25	23.464	0.6935	0.5617	25/64 x 9 3/8	8	1	1	1	2	2	1	0		
D63	F,E	149.9224	39.0	49.73	2.2	-3.2	3.1	3.5	0.0	3.1	2.38	34.800	0.3552	0.2635	25/64 x 9 3/8	8	1	1	1	2	2	1	0		
D60	F	71.3675	20.0	66.59	23.2	15.0	4.0	4.2	1.0	12.8	2.88	36.991	0.3570	0.2606	21/64 x 12 7/8	8	2	2	1	3	0	2	2		
D65	D,F	93.4446	22.0	66.59	40.4	46.2	1.8	-3.5	1.0	8.0	3.12	51.550	0.5765	0.3804	21/64 x 12 7/8	8	2	2	1	3	0	2	2		
D62	F,E	77.8762	29.0	45.09	6.0	-4.0	1.0	2.0	0.0	1.8 ^b	3.25	35.325	0.4076	0.3012	21/64 x 14 5/8	8	1	0	2	0	3	2	3		
D73	D	94.3336	32.0	45.09	4.5	-5.5	3.0	-0.5	0.2	3.1	2.75	33.521	0.3792	0.2840	21/64 x 14 5/8	8	1	0	2	0	3	2	3		
D64	F,E	21.5889	11.0	35.76	15.4	14.8	10.8	17.2	4.8	5.6	3.25	32.841	0.1889	0.1422	13/64 x 12 7/8	8	0	1	0	0	1	2	2		
D70	F,E	26.9742	11.0	35.76	39.0	44.0	-11.0	-12.0	0.0	2.0	3.25	87.782	0.2930	0.1603	13/64 x 12 7/8	8	0	1	0	0	1	2	2		
D66	D,B	53.2524	11.5	63.76	24.5	16.2	5.0	8.8	2.8	4.0 ^b	4.12	121.416	0.2564	0.1158	13/64 x 14 5/8	8	3	0	3	3	2	2	3		
D72	G,B	47.9752	27.0	63.76	73.0	64.0	16.0	15.0	18.6 ^b	26.8 ^b	3.62	37.305	0.1855	0.1351	13/64 x 14 5/8	8	3	0	3	3	2	2	3		
D67	F	20.8225	4.0	76.88	20.0 ^b	23.0 ^b	28.0 ^b	33.0 ^b	1.0	10.5	2.00	73.460	0.4085	0.2355	17/64 x 9 3/8	8	3	2	0	1	3	1	0		
D69	F	88.0503	22.0	76.88	115.0	120.0	33.5	36.5	22.0 ^b	29.0 ^b	2.12	25.199	0.3294	0.2631	17/64 x 9 3/8	8	3	2	0	1	3	1	0		
D68	D,B	108.3101	43.0	31.88	1.2	-5.2	14.5	19.0	5.5	7.0 ^b	2.00	23.826	0.2822	0.2279	17/64 x 11 1/8	8	0	0	3	2	0	0	1		
D71	D,B	66.4240	27.5	31.88	-3.0	-10.0	16.0	19.0	26.0 ^b	33.0 ^b	1.88	125.669	0.4466	0.1979	17/64 x 11 1/8	8	0	0	3	2	0	0	1		

^aNot Used in Analysis of Results
^bEstimated Value; Exact Value Unobtainable Because the Vertical Trace Extended Out of the Camera Field or Stem Fell Outside Limits of Horizontal Grid Board

APPENDIX C-III
SHARP BLADE SERIES MAIN TEST DATA

Run No.	Comment Code	Energy Input In-Lb _f	Max Torque Lb _f -In	Theo Relative Contact Velocity Ft/Sec	X Disp		Y Disp		Positive Z Disp		Actual Ht. of Cut Above Base In	Per Cent Moisture Dry Basis %	Wet Linear Density Gm/In	Dry Linear Density Gm/In	Plant Size Dia X Ht. from End to C.G. In	Time in Chamber Hrs.	Coded Values of Independent Variable Pi Terms								
					C.G.	End	C.G.	End	C.G.	End							π ₂	π ₃	π ₄	π ₅	π ₆	π ₇	π ₉		
S1	F,E	39.2512	8.2	63.76	42.0	36.0	-6.0	-5.0	60.0 ^a	60.0 ^a	2.00	23.149	0.2080	0.1689	13/64 x 9 3/8	6	3	0	0	3	2	1	0		
S16	F,E	36.7778	10.0	63.76	22.6	26.5	18.5	14.2	1.5	4.0 ^a	2.12	45.884	0.1790	0.1227	13/64 x 9 3/8	6	3	0	0	3	2	1	0		
S2	F,E	29.3736	9.6	38.44	80.5 ^a	71.5 ^a	42.0 ^a	45.0 ^a	28.5 ^a	33.0 ^a	2.38	41.529	0.2757	0.1948	13/64 x 12 7/8	6	0	2	2	1	0	1	2		
S13	D,F,E	36.3593	18.5	38.44	10.0	2.0	6.0	10.0	2.5	14.0	2.62	42.747	0.2234	0.1565	13/64 x 12 7/8	6	0	2	2	1	0	1	2		
S3	D,F	181.5397	40.0	55.22	9.0	14.0	-17.0	-11.0	30.0 ^a	35.0 ^a	1.38	21.950	0.6978	0.5722	25/64 x 11 1/8	6	2	0	3	0	2	0	1		
S10	D,F	132.3438	32.0	55.22	6.5	12.5	-9.0	-15.0	20.0 ^a	26.0 ^a	1.25	28.526	0.5276	0.4105	25/64 x 11 1/8	6	2	0	3	0	2	0	1		
S4	D,F,E	171.3408	40.0	49.73	-2.0	-6.2	5.8	2.5	3.0 ^a	4.0 ^a	2.50	42.896	0.4144	0.2900	21/64 x 9 3/8	6	1	1	1	3	3	2	0		
S9	D,F	73.3141	17.5	49.73	10.8	6.2	5.2	3.2	0.8	2.0	3.00	62.626	0.4186	0.2574	21/64 x 9 3/8	6	1	1	1	3	3	2	0		
S5	D,F,E	208.4096	41.0	54.37	23.6	15.0	0.0	-7.8	0.8	5.0	1.75	24.179	0.6132	0.4938	25/64 x 14 5/8	6	1	2	1	2	0	0	3		
S12	O,F	191.1932	52.0	54.37	27.5	22.8	13.2	2.2	0.5	5.5	1.00	27.671	0.5449	0.4268	25/64 x 14 5/8	6	1	2	1	2	0	0	3		
S6	F,E	84.2589	18.0	70.32	41.0	45.5	-20.0	-29.0	8.0	16.0	3.12	43.973	0.3500	0.2431	17/64 x 14 5/8	6	3	1	0	2	1	2	3		
S15	F,E	84.3317	22.0	70.32	44.5	42.0	20.0	30.0	1.5	7.0	2.88	38.774	0.3783	0.2726	17/64 x 14 5/8	6	3	1	0	2	1	2	3		
S7	F,E	98.5266	18.5	60.90	65.0	68.0	-11.5	-3.5	7.2	22.5	3.12	76.666	0.5300	0.3000	21/64 x 12 7/8	6	2	1	3	1	1	2	2		
S11	F,E	97.9084	23.0	60.90	16.2	8.2	-3.0	-5.8	2.5	6.5	2.88	79.206	0.7093	0.3958	21/64 x 12 7/8	6	2	1	3	1	1	2	2		
S8	F	37.8796	20.5	35.76	8.5	1.5	4.8	5.5	0.2	4.2	2.75	37.133	0.3885	0.2833	17/64 x 11 1/8	6	0	1	2	0	3	2	1		
S14	F,E	30.1024	12.5	35.76	43.2	49.5	10.2	12.8	5.0	20.0 ^a	2.75	57.928	0.4163	0.2636	17/64 x 11 1/8	6	0	1	2	0	3	2	1		

APPENDIX C-III (Continued)

Run No.	Comment Code	Energy Input In-Lb _f	Max Torque Lb _f -In	Theo Relative Contact Velocity Ft/Sec	X Disp				Y Disp				Positive Z Disp		Actual Ht. of Cut Above Base In	Per Cent Moisture Dry Basis %	Wet Linear Density Gm/In	Dry Linear Density Gm/In	Plant Size Dia X Ht. from End to C.G. In	Time in Chamber Hrs.	Coded Values of Independent Variable Pi Terms								
					C.G.		End		C.G.		End		C.G.								End		π ₂	π ₃	π ₄	π ₅	π ₆	π ₇	π ₉
S17	D,F,E	59.8528	39.0	35.76	4.5	11.5	6.0	6.0	7.2	11.5	1.12	14.595	0.3855	0.3364	21/64 x 9 3/8	2	0	1	0	0	0	0	0						
S3D	D,F	45.7441	20.5	35.76	-7.0	-3.5	5.0	2.0	4.0	4.0	1.12	15.069	0.2978	0.2588	21/64 x 9 3/8	2	0	1	0	0	0	0	0						
S18	D,F	127.8411	48.0	31.88	6.0	5.0	2.0	11.0	8.0 ^a	10.0 ^a	2.75	21.935	0.4675	0.3834	25/64 x 14 5/8	2	0	0	0	1	3	2	3						
S21	D,F	105.6543	37.0	31.88	11.0	7.0	13.0	3.5	0.8	3.0	2.62	16.658	0.4895	0.4196	25/64 x 14 5/8	2	0	0	0	1	3	2	3						
S19	F,E	87.3689	18.0	60.90	22.2	11.5	-3.0	-5.2	0.0	4.5	2.12	25.772	0.3255	0.2588	17/64 x 14 5/8	2	2	1	1	1	2	1	3						
S27	F,E	81.5906	20.0	60.90	28.5	18.2	2.0	-1.8	0.5	3.0	2.12	23.263	0.3354	0.2721	17/64 x 14 5/8	2	2	1	1	1	2	1	3						
S20	F	18.4836	5.0	66.59	47.0	43.0	-1.0	3.0	10.5	12.0 ^a	2.62	55.446	0.2226	0.1432	13/64 x 9 3/8	2	2	2	1	0	1	2	0						
S32	F	11.6404	2.2	66.59	18.0	13.5	-3.5	-5.5	2.5	9.0	2.75	19.047	0.2000	0.1680	13/64 x 9 3/8	2	2	2	1	0	1	2	0						
S22	O,F	76.6087	25.0	49.73	10.0	3.5	4.2	2.5	1.0	3.0	2.88	17.705	0.2360	0.2005	17/64 x 11 1/8	2	1	1	3	3	0	1	1						
S26	F	76.1970	42.0	49.73	6.0	7.0	38.0	46.0	34.0 ^a	36.0 ^a	1.88	35.316	0.3866	0.2857	17/64 x 11 1/8	2	1	1	3	3	0	1	1						
S23	D	30.4788	12.0	45.09	30.0	38.2	10.0	11.5	14.0 ^a	21.5 ^a	3.00	23.102	0.2595	0.2108	13/64 x 12 7/8	2	1	0	3	2	3	2	2						
S28	D,B	20.4291	11.5	45.09	22.0	13.5	8.5	6.8	85.0 ^a	85.0 ^a	2.62	25.763	0.1977	0.1572	13/64 x 12 7/8	2	1	0	3	2	3	2	2						
S24	D,F	134.5311	22.0	70.32	81.0 ^a	90.0 ^a	41.0 ^a	36.0 ^a	85.0 ^a	85.0 ^a	1.12	37.461	0.4418	0.3214	21/64 x 12 7/8	2	3	1	2	2	2	0	2						
S29	D,F	101.6329	19.5	70.32	56.5	66.2	10.2	9.0	60.0 ^a	70.0 ^a	1.12	25.741	0.3688	0.2933	21/64 x 12 7/8	2	3	1	2	2	2	0	2						
S25	F	120.4105	23.0	76.88	89.8	95.8	28.0	27.0	17.5	24.5	2.88	17.093	0.5117	0.4370	25/64 x 11 1/8	2	3	2	2	3	1	2	1						
S31	F,E	84.4056	13.0	76.88	72.5	66.0	5.0	4.0	9.0	19.0	2.88	17.060	0.3863	0.3300	25/64 x 11 1/8	2	3	2	2	3	1	2	1						

APPENDIX C-III (Continued)

Run No.	Comment Code	Input Energy In-Lb _f	Max Torque Lb _f -In	Theo Relative Contact Velocity Ft/Sec	X Disp In		Y Disp In		Positive Z Disp In		Actual Ht. of Cut Above Base In	Per Cent Moisture Dry Basis %	Wet Linear Density Gm/In	Dry Linear Density Gm/In	Plant Size Dia X Ht. from End to C.G. In	Time in Chamber Hrs.	Coded Values of Independent Variable Pi Terms							
					C.G.	End	C.G.	End	C.G.	End							π ₂	π ₃	π ₄	π ₅	π ₆	π ₇	π ₈	
					S33	F	59.2026	28.0	54.37	25.8							30.5	-4.5	-9.0	7.0	17.0	3.00	27.800	0.4450
S37	F	59.6284	25.0	54.37	24.2	18.8	1.0	-3.5	2.5	6.5	2.75	95.618	0.6340	0.3241	21/64 x 11 1/8	8	1	2	0	1	2	2	1	
S34	F,E	81.6778	18.5	49.73	23.0	14.0	0.0	-0.2	1.8	4.9	2.38	25.846	0.5132	0.4078	25/64 x 12 7/8	8	1	1	0	0	1	1	2	
S42	D,F	74.9611	28.0	49.73	18.0	8.5	9.5	10.8	2.5	3.0	1.88	33.325	0.5413	0.4060	25/64 x 12 7/8	8	1	1	0	0	1	1	2	
S35	F,E	19.8706	6.8	70.32	46.0	39.0	7.0	2.0	2.2	9.5	1.75	83.906	0.2514	0.1367	13/64 x 11 1/8	8	3	1	1	1	3	0	1	
S43	D,F	21.5005	11.0	70.32	32.8	37.8	0.0	-6.5	1.0	4.0	1.25	49.095	0.2636	0.1768	13/64 x 11 1/8	8	3	1	1	1	3	0	1	
S36	F,E	56.3396	10.0	63.76	10.2	1.8	4.8	3.2	1.5	1.8	2.62	114.057	0.4431	0.2070	17/64 x 12 7/8	8	3	0	1	0	0	2	2	
S46	F,E	32.7956	5.0	63.76	-5.7	-14.5	-2.5	-5.5	7.8	8.0 ^a	2.88	97.529	0.3358	0.1700	17/64 x 12 7/8	8	3	0	1	0	0	2	2	
S38	F	52.0565	11.0	55.22	34.5	25.2	10.5	6.8	11.5	11.5	3.00	42.593	0.4640	0.3254	21/64 x 14 5/8	8	2	0	2	3	0	2	3	
S44	F,E	63.3900	17.5	55.22	11.5	2.5	2.2	6.0	0.0	3.5	3.12	93.562	0.5743	0.2967	21/64 x 14 5/8	8	2	0	2	3	0	2	3	
S39	F,E	26.5992	7.0	35.76	25.5	14.2	19.2	17.2	10.0	10.0	1.62	82.673	0.2815	0.1541	13/64 x 14 5/8	8	0	1	3	3	1	0	3	
S47	F,E	9.6089	4.5	35.76	35.5	27.2	6.5	-2.5	27.5 ^a	34.0 ^a	1.25	47.966	0.1746	0.1180	13/64 x 14 5/8	8	0	1	3	3	1	0	3	
S40	F,E	36.5134	23.0	38.44	17.8	14.0	10.2	14.0	0.8	2.5	2.50	34.913	0.3103	0.2300	17/64 x 9 3/8	8	0	2	3	2	2	2	0	
S45	D,F	33.1225	12.5	38.44	8.2	3.0	7.2	6.0	2.5	3.0	2.50	75.925	0.3800	0.2160	17/64 x 9 3/8	8	0	2	3	2	2	2	0	
S41	F,E	66.4084	29.5	60.90	44.0	50.0	-6.0	-4.0	4.8	7.4	2.12	27.835	0.5557	0.4347	25/64 x 9 3/8	8	2	1	2	2	3	1	0	
S48	F,E	60.6832	15.0	60.90	41.0	35.0	-4.0	-3.0	3.8	8.0	1.88	47.043	0.6042	0.4109	25/64 x 9 3/8	8	2	1	2	2	3	1	0	

APPENDIX C-III (Continued)

Run No.	Comment Code	Energy Input In-Lb _f	Max Torque Lb _f -In	Theo Relative Contact Velocity Ft/Sec	X Disp		Y Disp		Positive Z Disp		Actual Ht. of Cut Above Base In	Per Cent Moisture Dry Basis %	Wet Linear Density Gm/In	Dry Linear Density Gm/In	Plant Size Dia X Ht. from End to C.G. In	Time in Chamber Hrs.	Coded Values of Independent Variable Pi Terms							
					C.G.	End	C.G.	End	C.G.	End							π ₂	π ₃	π ₄	π ₅	π ₆	π ₇	π ₈	
S49	D,F,E	85.5026	17.5	70.32	88.8	87.8	11.8	6.0	11.0 ^a	11.0 ^a	2.88	30.564	0.5045	0.3864	25/64 x 9 3/8	4	3	1	3	1	0	2	1	
S64	F,E	98.3871	28.0	70.32	38.0	41.8	-1.8	-5.5	1.5	4.0	2.88	21.230	0.5676	0.4682	25/64 x 9 3/8	4	3	1	3	1	0	2	0	
S50	F,E	11.0382	5.5	49.73	88.5	98.5	20.0	20.5	30.2 ^a	39.0 ^a	2.88	34.123	0.1867	0.1392	13/64 x 14 5/8	4	1	1	2	0	2	2	3	
S57	F,E	10.0497	2.5	49.73	23.2	15.2	0.8	-5.8	4.0	6.8	2.62	31.009	0.1973	0.1506	13/64 x 14 5/8	4	1	1	2	0	2	2	3	
S51	F	35.9569	18.8	66.59	75.8	69.5	19.2	11.5	42.0 ^a	64.0 ^a	1.12	64.044	0.3796	0.2314	17/64 x 12 7/8	4	2	2	0	3	3	0	2	
S55	F	22.2335	10.0	66.59	56.0	50.0	-2.5	-10.0	3.0	17.5 ^a	1.38	36.754	0.3758	0.2748	17/64 x 12 7/8	4	2	2	0	3	3	0	2	
S52	F,E	39.0457	14.0	45.09	6.8	1.0	3.0	2.5	0.0	1.0	2.25	60.320	0.2998	0.1870	17/64 x 9 3/8	4	1	0	2	1	1	0	0	
S59	F,E	30.4788	10.8	45.09	12.5	6.5	4.5	6.5	2.0	2.0	1.38	37.574	0.2768	0.2012	17/64 x 9 3/8	4	1	0	2	1	1	0	0	
S53	F,E	21.5335	12.0	60.90	23.5	22.5	-4.8	-11.0	0.5	7.0	3.12	45.148	0.1900	0.1309	13/64 x 11 1/8	4	2	1	0	2	0	2	1	
S60	F,E	23.0493	10.5	60.90	17.0	12.8	4.0	-0.8	0.2	1.5 ^a	2.62	45.769	0.2395	0.1643	13/64 x 11 1/8	4	2	1	0	2	0	2	1	
S54	D,F,E	142.6021	47.0	31.88	-10.8	-4.5	21.0	17.0	0.0	7.0 ^a	2.00	20.424	0.3862	0.3207	21/64 x 11 1/8	4	0	0	1	2	1	1	1	
S56	F,E	81.4539	35.0	31.88	0.0	-0.5	19.8	26.5	9.5	12.0	2.50	37.655	0.4465	0.3224	21/64 x 11 1/8	4	0	0	1	2	1	1	1	
S58	F,G	100.7290	35.5	76.88	42.0	31.0	2.5	6.0	77.0 ^a	85.0 ^a	1.75	15.416	0.5353	0.4638	21/64 x 14 5/8	4	3	2	3	0	3	1	3	
S62	F,G	86.6744	40.0	76.88	87.5	98.0	-9.0	-3.5	12.5 ^a	21.5 ^a	1.88	20.509	0.4924	0.4086	21/64 x 14 5/8	4	3	2	3	0	3	1	3	
S61	F,E	124.3547	85.5	35.76	13.8	6.8	14.8	9.5	3.2	3.8	2.62	54.560	0.7354	0.4785	25/64 x 12 7/8	4	0	1	1	3	2	2	2	
S63	D,F	137.1385	63.0	35.76	14.8	6.8	13.0	9.5	2.0	4.0	2.75	51.314	0.7192	0.4753	25/64 x 12 7/8	4	0	1	1	3	2	2	2	

^aEstimated Value; Exact Value Unobtainable Because the Vertical Trace Extended Out of the Camera Field or Stem Fell Outside Limits of Horizontal Grid Board

APPENDIX D

- D-I ANALYSIS OF VARIANCE AND TABLE OF MEAN VALUES FOR
DULL BLADE TEST SERIES
- D-II ANALYSIS OF VARIANCE AND TABLE OF MEAN VALUES FOR
SHARP BLADE TEST SERIES

APPENDIX D-I

ANALYSIS OF VARIANCE AND TABLE OF MEAN VALUES FOR DULL BLADE TEST SERIES

DULL BLADE SERIES ANALYSIS OF VARIANCE FOR ENERGY INPUT DATA					DULL BLADE SERIES TABLE OF MEAN VALUES FOR ENERGY INPUT DATA		
SOURCE OF VARIATION	DEGREES OF FREEDOM	SUM OF SQUARES	MEAN SQUARE	F RATIO	FACTOR	VALUE OF MEAN	STD ERROR OF MEAN
CORRECTED TOTAL	63	209464.56250			OVERALL MEAN	92.5147	3.2543
DIAMETER	3	149065.37500	49688.45703	73.3107	DIAMETER		
LINEAR EFFECT	1	147015.37500	147015.37500	216.9074	0 LEVEL	32.2607	6.5085
QUADRATIC EFFECT	1	1680.10205	1680.10205	2.4788	1 LEVEL	69.1824	6.5085
CUBIC EFFECT	1	369.90088	369.90088	0.5458	2 LEVEL	105.5993	6.5085
TIME IN CHAMBER	3	4424.10156	1474.70117	2.1758	3 LEVEL	163.0160	6.5085
LINEAR EFFECT	1	1068.14600	1068.14600	1.5759	TIME IN CHAMBER		
QUADRATIC EFFECT	1	495.41724	495.41724	0.7309	0 LEVEL	87.2413	6.5085
CUBIC EFFECT	1	2860.54004	2860.54004	4.2205	1 LEVEL	84.5004	6.5085
ROTOR SPEED INDEX	3	3434.63647	1144.87866	1.6892	2 LEVEL	106.0935	6.5085
LINEAR EFFECT	1	978.98364	978.98364	1.4444	3 LEVEL	92.2236	6.5085
QUADRATIC EFFECT	1	2412.52856	2412.52856	3.5595	ROTOR SPEED INDEX		
CUBIC EFFECT	1	43.12381	43.12381	0.0636	0 LEVEL	93.7742	6.5085
FEED RATE INDEX	2	5213.08984	2606.54517	3.8457	1 LEVEL	93.5246	6.5085
ROTOR ANGLE INDEX	3	2340.42334	780.14111	1.1510	2 LEVEL	99.2254	6.5085
LINEAR EFFECT	1	2182.16504	2182.16504	3.2196	3 LEVEL	103.5346	6.5085
QUADRATIC EFFECT	1	76.98965	76.98965	0.1136	FEED RATE INDEX		
CUBIC EFFECT	1	81.26859	81.26859	0.1199	0 LEVEL	101.5346	4.6022
LATERAL POSITION INDEX	3	8750.67578	2916.89233	4.3036	1 LEVEL	83.9330	6.5085
LINEAR EFFECT	1	5299.39844	5299.39844	7.8188	2 LEVEL	83.0566	6.5085
QUADRATIC EFFECT	1	1795.19995	1795.19995	2.6486	ROTOR ANGLE INDEX		
CUBIC EFFECT	1	1656.07715	1656.07715	2.4434	0 LEVEL	86.2813	6.5085
LEDGER ORIENTATION INDEX	3	567.05811	189.01942	0.2789	1 LEVEL	87.2947	6.5085
LINEAR EFFECT	1	24.08737	24.08737	0.0355	2 LEVEL	95.5411	6.5085
QUADRATIC EFFECT	1	299.55542	299.55542	0.4420	3 LEVEL	100.9417	6.5085
CUBIC EFFECT	1	243.41531	243.41531	0.3591	LATERAL POSITION INDEX		
CUTTING HEIGHT INDEX	2	1842.68213	921.34106	1.3594	0 LEVEL	72.7351	6.5085
C.G. HEIGHT INDEX	3	2280.56030	760.18677	1.1216	1 LEVEL	100.5662	6.5085
LINEAR EFFECT	1	147.46387	147.46387	0.2176	2 LEVEL	95.0557	6.5085
QUADRATIC EFFECT	1	1955.63599	1955.63599	2.8854	3 LEVEL	101.7018	6.5085
CUBIC EFFECT	1	177.46051	177.46051	0.2618	LEDGER ORIENTATION INDEX		
REMAINDER	5	9857.06250	1642.84375	2.4239	0 LEVEL	88.6560	6.5085
EXPERIMENTAL ERROR	32	21688.94141	677.77930		1 LEVEL	97.0203	6.5085
					2 LEVEL	92.3360	6.5085
					3 LEVEL	92.0465	6.5085
					CUTTING HEIGHT INDEX		
					0 LEVEL	101.0300	6.5085
					1 LEVEL	93.1869	6.5085
					2 LEVEL	87.9209	4.6022
					C.G. HEIGHT INDEX		
					0 LEVEL	85.5951	6.5085
					1 LEVEL	95.1296	6.5085
					2 LEVEL	100.9554	6.5085
					3 LEVEL	88.2787	6.5085

APPENDIX D-I (Continued)

DULL BLADE SERIES ANALYSIS OF VARIANCE FOR MAX TORQUE DATA					DULL BLADE SERIES TABLE OF MEAN VALUES FOR MAX TORQUE DATA		
SOURCE OF VARIATION	DEGREES OF FREEDOM	SUM OF SQUARES	MEAN SQUARE	F RATIO	FACTOR	VALUE OF MEAN	STD ERROR OF MEAN
CORRECTED TOTAL	63	21442.33594			OVERALL MEAN	29.6547	1.1159
DIAMETER	3	13316.91406	4438.96875	55.6972	DIAMETER		
LINEAR EFFECT	1	13221.36719	13221.36719	165.8927	0 LEVEL	11.4437	2.2318
QUADRATIC EFFECT	1	90.96390	90.96390	1.1414	1 LEVEL	22.3937	2.2318
CUBIC EFFECT	1	4.58403	4.58403	0.0575	2 LEVEL	34.5312	2.2318
					3 LEVEL	50.2500	2.2318
TIME IN CHAMBER	3	93.04047	31.01349	0.3891	TIME IN CHAMBER		
LINEAR EFFECT	1	7.90653	7.90653	0.0992	0 LEVEL	28.9063	2.2318
QUADRATIC EFFECT	1	83.03764	83.03764	1.0419	1 LEVEL	31.1937	2.2318
CUBIC EFFECT	1	2.09628	2.09628	0.0263	2 LEVEL	30.3937	2.2318
					3 LEVEL	28.1250	2.2318
ROTOR SPEED INDEX	3	2185.80273	728.60083	9.1420	ROTOR SPEED INDEX		
LINEAR EFFECT	1	1898.81323	1898.81323	23.8250	0 LEVEL	39.1312	2.2318
QUADRATIC EFFECT	1	286.03247	286.03247	3.5889	1 LEVEL	29.8125	2.2318
CUBIC EFFECT	1	0.95703	0.95703	0.0120	2 LEVEL	25.2687	2.2318
					3 LEVEL	24.4063	2.2318
FEED RATE INDEX	2	147.79796	73.89897	0.9272	FEED RATE INDEX		
					0 LEVEL	31.0812	1.5782
					1 LEVEL	27.4875	2.2318
					2 LEVEL	28.9688	2.2318
ROTOR ANGLE INDEX	3	1063.86914	354.62305	4.4496	ROTOR ANGLE INDEX		
LINEAR EFFECT	1	948.40869	948.40869	11.9000	0 LEVEL	25.1875	2.2318
QUADRATIC EFFECT	1	72.46265	72.46265	0.9092	1 LEVEL	27.9688	2.2318
CUBIC EFFECT	1	42.99777	42.99777	0.5395	2 LEVEL	29.2125	2.2318
					3 LEVEL	36.2500	2.2318
LATERAL POSITION INDEX	3	683.80908	227.93640	2.8600	LATERAL POSITION INDEX		
LINEAR EFFECT	1	516.89014	516.89014	6.4856	0 LEVEL	24.4250	2.2318
QUADRATIC EFFECT	1	39.53265	39.53265	0.4960	1 LEVEL	31.0625	2.2318
CUBIC EFFECT	1	127.38628	127.38628	1.5984	2 LEVEL	29.8187	2.2318
					3 LEVEL	33.3125	2.2318
LEDGER ORIENTATION INDEX	3	374.65283	124.88431	1.5670	LEDGER ORIENTATION INDEX		
LINEAR EFFECT	1	11.21253	11.21253	0.1407	0 LEVEL	26.6437	2.2318
QUADRATIC EFFECT	1	185.98140	185.98140	2.3336	1 LEVEL	33.4062	2.2318
CUBIC EFFECT	1	177.45903	177.45903	2.2266	2 LEVEL	29.3125	2.2318
					3 LEVEL	29.2562	2.2318
CUTTING HEIGHT INDEX	2	145.75046	72.87523	0.9144	CUTTING HEIGHT INDEX		
					0 LEVEL	31.4062	2.2318
					1 LEVEL	30.9000	2.2318
					2 LEVEL	28.1562	1.5782
C.G. HEIGHT INDEX	3	640.81543	213.60515	2.6802	C.G. HEIGHT INDEX		
LINEAR EFFECT	1	276.58179	276.58179	3.4704	0 LEVEL	28.2500	2.2318
QUADRATIC EFFECT	1	250.82640	250.82640	3.1472	1 LEVEL	28.5312	2.2318
CUBIC EFFECT	1	113.40703	113.40703	1.4230	2 LEVEL	26.8187	2.2318
					3 LEVEL	35.0187	2.2318
REMAINDER	6	239.53937	39.92322	0.5009			
EXPERIMENTAL ERROR	32	2550.34497	79.69827				

APPENDIX D-I (Continued)

DJLL BLADE SERIES ANALYSIS OF VARIANCE FOR ENERGY INPUT INDEX DATA					DULL BLADE SERIES TABLE OF MEAN VALUES FOR ENERGY INPUT INDEX DATA		
SOURCE OF VARIATION	DEGREES OF FREEDOM	SUM OF SQUARES	MEAN SQUARE	F RATIO	FACTOR	VALUE OF MEAN	STD ERROR OF MEAN
CORRECTED TOTAL	63	129578.75000			OVERALL MEAN	82.7694	3.6831
DIAMETER	3	14283.21094	4761.07031	5.4841	DIAMETER		
LINEAR EFFECT	1	11916.30469	11916.30469	13.7260	0 LEVEL	60.5037	7.3661
QUADRATIC EFFECT	1	108.51241	108.51241	0.1250	1 LEVEL	85.9390	7.3661
CUBIC EFFECT	1	2258.39478	2258.39478	2.6014	2 LEVEL	82.2041	7.3661
CUBIC EFFECT	1	2258.39478	2258.39478	2.6014	3 LEVEL	102.4309	7.3661
TIME IN CHAMBER	3	3496.82056	1165.60669	1.3426	TIME IN CHAMBER		
LINEAR EFFECT	1	0.92500	0.92500	0.0011	0 LEVEL	74.9179	7.3661
QUADRATIC EFFECT	1	3234.63184	3234.63184	3.7259	1 LEVEL	92.6431	7.3661
CUBIC EFFECT	1	261.26367	261.26367	0.3009	2 LEVEL	87.1142	7.3661
CUBIC EFFECT	1	261.26367	261.26367	0.3009	3 LEVEL	76.4025	7.3661
ROTOR SPEED INDEX	3	5649.30078	1883.10034	2.1691	ROTOR SPEED INDEX		
LINEAR EFFECT	1	1836.34375	1836.34375	2.1152	0 LEVEL	78.9097	7.3661
QUADRATIC EFFECT	1	2057.06128	2057.06128	2.3695	1 LEVEL	81.7319	7.3661
CUBIC EFFECT	1	1755.89600	1755.89600	2.0226	2 LEVEL	72.4682	7.3661
CUBIC EFFECT	1	1755.89600	1755.89600	2.0226	3 LEVEL	97.9678	7.3661
FEED RATE INDEX	2	9724.77344	4862.38672	5.6008	FEED RATE INDEX		
LINEAR EFFECT	1	9724.77344	9724.77344	11.2416	0 LEVEL	93.2133	5.2086
CUBIC EFFECT	1	0.00000	0.00000	0.0000	1 LEVEL	81.5857	7.3661
ROTOR ANGLE INDEX	3	1948.51099	649.50366	0.7481	2 LEVEL	63.0654	7.3661
LINEAR EFFECT	1	152.98819	152.98819	0.1762	ROTOR ANGLE INDEX		
QUADRATIC EFFECT	1	1681.53320	1681.53320	1.9369	0 LEVEL	76.1661	7.3661
CUBIC EFFECT	1	113.98944	113.98944	0.1313	1 LEVEL	85.4133	7.3661
LATERAL POSITION INDEX	3	11827.12500	3942.37524	4.5411	2 LEVEL	90.3772	7.3661
LINEAR EFFECT	1	11078.97656	11078.97656	12.7615	3 LEVEL	79.1211	7.3661
QUADRATIC EFFECT	1	593.62720	593.62720	0.6838	LATERAL POSITION INDEX		
CUBIC EFFECT	1	154.52193	154.52193	0.1780	0 LEVEL	61.3769	7.3661
CUBIC EFFECT	1	154.52193	154.52193	0.1780	1 LEVEL	82.0156	7.3661
LEDGER ORIENTATION INDEX	3	326.25830	108.75282	0.1253	2 LEVEL	89.6143	7.3661
LINEAR EFFECT	1	60.73064	60.73064	0.0700	3 LEVEL	98.0708	7.3661
QUADRATIC EFFECT	1	231.15129	231.15129	0.2663	LEDGER ORIENTATION INDEX		
CUBIC EFFECT	1	34.37653	34.37653	0.0396	0 LEVEL	82.5035	7.3661
CUBIC EFFECT	1	34.37653	34.37653	0.0396	1 LEVEL	84.1222	7.3661
CUTTING HEIGHT INDEX	2	747.61719	373.80859	0.4306	2 LEVEL	85.2175	7.3661
LINEAR EFFECT	1	747.61719	747.61719	8.6314	3 LEVEL	79.2343	7.3661
CUBIC EFFECT	1	0.00000	0.00000	0.0000	CUTTING HEIGHT INDEX		
C.G. HEIGHT INDEX	3	43324.83594	14441.60937	16.6349	0 LEVEL	78.2513	7.3661
LINEAR EFFECT	1	41831.96094	41831.96094	48.1850	1 LEVEL	80.6691	7.3661
QUADRATIC EFFECT	1	1126.83032	1126.83032	1.2980	2 LEVEL	86.0786	5.2086
CUBIC EFFECT	1	366.04468	366.04468	0.4216	3 LEVEL	77.2343	7.3661
CUBIC EFFECT	1	366.04468	366.04468	0.4216	C.G. HEIGHT INDEX		
REMAINDER	5	10469.42578	1744.90479	2.0099	0 LEVEL	122.3355	7.3661
LINEAR EFFECT	1	10469.42578	10469.42578	121.8426	1 LEVEL	86.7983	7.3661
CUBIC EFFECT	1	0.00000	0.00000	0.0000	2 LEVEL	70.3485	7.3661
CUBIC EFFECT	1	0.00000	0.00000	0.0000	3 LEVEL	51.5954	7.3661
EXPERIMENTAL ERROR	32	27780.91016	868.15332				

APPENDIX D-I (Continued)

DULL BLADE SERIES ANALYSIS OF VARIANCE FOR MAX TORQUE INDEX DATA					DULL BLADE SERIES TABLE OF MEAN VALUES FOR MAX TORQUE INDEX DATA		
SOURCE OF VARIATION	DEGREES OF FREEDOM	SUM OF SQUARES	MEAN SQUARE	F RATIO	FACTOR	VALUE OF MEAN	STD ERRJR OF MEAN
CORRECTED TOTAL	63	13200.23437			OVERALL MEAN	26.7171	1.4613
DIAMETER	3	873.48633	291.16211	2.1305	DIAMETER		
LINEAR EFFECT	1	734.21704	734.21704	5.3724	0 LEVEL	21.3519	2.9226
QUADRATIC EFFECT	1	1.75286	1.75286	0.0128	1 LEVEL	27.3345	2.9226
CUBIC EFFECT	1	137.51646	137.51646	1.0062	2 LEVEL	26.4307	2.9226
TIME IN CHAMBER	3	846.79492	282.26489	2.0654	3 LEVEL	31.7514	2.9226
LINEAR EFFECT	1	108.83723	108.83723	0.7964	TIME IN CHAMBER		
QUADRATIC EFFECT	1	301.07397	301.07397	2.2030	0 LEVEL	25.1293	2.9226
CUBIC EFFECT	1	436.88354	436.88354	3.1968	1 LEVEL	32.9746	2.9226
ROTOR SPEED INDEX	3	1403.75073	467.91675	3.4239	2 LEVEL	24.7975	2.9226
LINEAR EFFECT	1	1065.55322	1065.55322	7.7969	3 LEVEL	23.9670	2.9226
QUADRATIC EFFECT	1	304.22534	304.22534	2.2261	ROTOR SPEED INDEX		
CUBIC EFFECT	1	33.97205	33.97205	0.2486	0 LEVEL	34.0459	2.9226
FEED RATE INDEX	2	452.73120	226.36562	1.6564	1 LEVEL	27.3391	2.9226
ROTOR ANGLE INDEX	3	594.35449	198.11821	1.4497	2 LEVEL	21.7346	2.9226
LINEAR EFFECT	1	431.09595	431.09595	3.1544	3 LEVEL	23.7488	2.9226
QUADRATIC EFFECT	1	146.95004	146.95004	1.0753	FEED RATE INDEX		
CUBIC EFFECT	1	16.30856	16.30856	0.1193	0 LEVEL	28.8814	2.0666
LATERAL POSITION INDEX	3	486.99731	162.33249	1.1878	1 LEVEL	26.7390	2.9226
LINEAR EFFECT	1	453.46973	453.46973	3.3181	2 LEVEL	22.3666	2.9226
QUADRATIC EFFECT	1	0.00386	0.00386	0.0000	ROTOR ANGLE INDEX		
CUBIC EFFECT	1	33.52388	33.52388	0.2453	0 LEVEL	21.4940	2.9226
LEDGER ORIENTATION INDEX	3	212.94887	70.98296	0.5194	1 LEVEL	27.7490	2.9226
LINEAR EFFECT	1	2.31002	2.31002	0.0169	2 LEVEL	28.7158	2.9226
QUADRATIC EFFECT	1	121.12218	121.12218	0.8863	3 LEVEL	28.9096	2.9226
CUBIC EFFECT	1	89.51666	89.51666	0.6550	LATERAL POSITION INDEX		
CUTTING HEIGHT INDEX	2	100.67737	50.33868	0.3683	0 LEVEL	23.4773	2.9226
C.G. HEIGHT INDEX	3	3796.16602	1265.38867	9.2591	1 LEVEL	24.5479	2.9226
LINEAR EFFECT	1	3478.79712	3478.79712	25.4552	2 LEVEL	28.8708	2.9226
QUADRATIC EFFECT	1	310.77393	310.77393	2.2740	3 LEVEL	29.9725	2.9226
CUBIC EFFECT	1	6.59508	6.59508	0.0483	LEDGER ORIENTATION INDEX		
REMAINDER	6	59.09325	9.84888	0.0721	0 LEVEL	25.6154	2.9226
EXPERIMENTAL ERROR	32	4373.23437	136.66362		1 LEVEL	26.4211	2.9226
					2 LEVEL	29.7645	2.9226
					3 LEVEL	25.0674	2.9226
					CUTTING HEIGHT INDEX		
					0 LEVEL	25.4264	2.9226
					1 LEVEL	25.4999	2.9226
					2 LEVEL	27.9711	2.0666
					C.G. HEIGHT INDEX		
					0 LEVEL	38.6686	2.9226
					1 LEVEL	28.2413	2.9226
					2 LEVEL	20.7857	2.9226
					3 LEVEL	19.1728	2.9226

APPENDIX D-I (Continued)

DULL BLADE SERIES ANALYSIS OF VARIANCE FOR C.G. X DISP INDEX DATA					DULL BLADE SERIES TABLE OF MEAN VALUES FOR C.G. X DISP INDEX DATA		
SOURCE OF VARIATION	DEGREES OF FREEDOM	SUM OF SQUARES	MEAN SQUARE	F RATIO	FACTOR	VALUE OF MEAN	STD ERROR OF MEAN
CORRECTED TOTAL	63	3783.67407			OVERALL MEAN	5.5452	0.8269
DIAMETER	3	161.11523	53.70508	1.2273	DIAMETER		
LINEAR EFFECT	1	159.30190	159.30190	3.6404	0 LEVEL	7.4777	1.6538
QUADRATIC EFFECT	1	1.56518	1.56518	0.0358	1 LEVEL	6.4907	1.6538
CUBIC EFFECT	1	0.24817	0.24817	0.0057	2 LEVEL	4.9125	1.6538
TIME IN CHAMBER	3	58.76909	19.58969	0.4477	3 LEVEL	3.3000	1.6538
LINEAR EFFECT	1	44.72826	44.72826	1.0221	TIME IN CHAMBER		
QUADRATIC EFFECT	1	2.00728	2.00728	0.0459	0 LEVEL	4.7946	1.6538
CUBIC EFFECT	1	12.03354	12.03354	0.2750	1 LEVEL	4.4125	1.6538
ROTOR SPEED INDEX	3	737.78735	245.92912	5.6201	2 LEVEL	6.3237	1.6538
LINEAR EFFECT	1	691.63062	691.63062	15.8054	3 LEVEL	6.6500	1.6538
QUADRATIC EFFECT	1	13.40867	13.40867	0.3064	ROTOR SPEED INDEX		
CUBIC EFFECT	1	32.74788	32.74788	0.7484	0 LEVEL	0.3571	1.6538
FEED RATE INDEX	2	739.88428	369.94214	8.4540	1 LEVEL	5.4925	1.6538
ROTOR ANGLE INDEX	3	184.27249	61.42416	1.4037	2 LEVEL	6.5134	1.6538
LINEAR EFFECT	1	0.02317	0.02317	0.0005	3 LEVEL	9.8179	1.6538
QUADRATIC EFFECT	1	184.05766	184.05766	4.2061	FEED RATE INDEX		
CUBIC EFFECT	1	0.19166	0.19166	0.0044	0 LEVEL	2.2244	1.1694
LATERAL POSITION INDEX	3	119.57979	39.85992	0.9109	1 LEVEL	7.8339	1.6538
LINEAR EFFECT	1	63.39597	63.39597	1.4487	2 LEVEL	9.8982	1.6538
QUADRATIC EFFECT	1	6.49704	6.49704	0.1485	ROTOR ANGLE INDEX		
CUBIC EFFECT	1	49.68677	49.68677	1.1355	0 LEVEL	7.2911	1.6538
LEDGER ORIENTATION INDEX	3	68.93594	22.97864	0.5251	1 LEVEL	3.7845	1.6538
LINEAR EFFECT	1	20.42941	20.42941	0.4669	2 LEVEL	3.9143	1.6538
QUADRATIC EFFECT	1	38.01163	38.01163	0.8687	3 LEVEL	7.1911	1.6538
CUBIC EFFECT	1	10.49490	10.49490	0.2398	LATERAL POSITION INDEX		
CUTTING HEIGHT INDEX	2	50.29494	25.14746	0.5747	0 LEVEL	6.1679	1.6538
C.G. HEIGHT INDEX	3	97.05435	32.35144	0.7393	1 LEVEL	7.4911	1.6538
LINEAR EFFECT	1	94.83945	94.83945	2.1673	2 LEVEL	4.2366	1.6538
QUADRATIC EFFECT	1	1.80039	1.80039	0.0411	3 LEVEL	4.2854	1.6538
CUBIC EFFECT	1	0.41451	0.41451	0.0095	LEDGER ORIENTATION INDEX		
REMAINDER	6	165.68520	27.61420	0.6310	0 LEVEL	5.3768	1.6538
EXPERIMENTAL ERROR	32	1400.29517	43.75922		1 LEVEL	5.0652	1.6538
					2 LEVEL	4.4839	1.6538
					3 LEVEL	7.2550	1.6538
					CUTTING HEIGHT INDEX		
					0 LEVEL	6.5925	1.6538
					1 LEVEL	4.1375	1.6538
					2 LEVEL	5.7254	1.1694
					C.G. HEIGHT INDEX		
					0 LEVEL	4.0437	1.6538
					1 LEVEL	4.9411	1.6538
					2 LEVEL	5.8139	1.6538
					3 LEVEL	7.3821	1.6538

APPENDIX D-I (Continued)

DULL BLADE SERIES ANALYSIS OF VARIANCE FOR END X DISP INDEX DATA					DULL BLADE SERIES TABLE OF MEAN VALUES FOR END X DISP INDEX DATA		
SOURCE OF VARIATION	DEGREES OF FREEDOM	SUM OF SQUARES	MEAN SQUARE	F RATIO	FACTOR	VALUE OF MEAN	STD ERROR OF MEAN
CORRECTED TOTAL	63	4063.71631			OVERALL MEAN	4.8606	0.8820
DIAMETER	3	170.87759	56.95920	1.1441	DIAMETER		
LINEAR EFFECT	1	166.94705	166.94705	3.3534	0 LEVEL	7.1321	1.7640
QUADRATIC EFFECT	1	0.00239	0.00239	0.0000	1 LEVEL	5.2566	1.7640
CUBIC EFFECT	1	3.92814	3.92814	0.0789	2 LEVEL	4.4768	1.7640
TIME IN CHAMBER	3	49.12830	16.37610	0.3289	3 LEVEL	2.5768	1.7640
LINEAR EFFECT	1	41.08000	41.08000	0.8252	TIME IN CHAMBER		
QUADRATIC EFFECT	1	5.88582	5.88582	0.1182	0 LEVEL	3.5645	1.7640
CUBIC EFFECT	1	2.16247	2.16247	0.0434	1 LEVEL	4.5589	1.7640
ROTOR SPEED INDEX	3	641.37134	213.79047	4.2943	2 LEVEL	5.7687	1.7640
LINEAR EFFECT	1	581.09570	581.09570	11.6722	3 LEVEL	5.5500	1.7640
QUADRATIC EFFECT	1	2.67206	2.67206	0.0537	ROTOR SPEED INDEX		
CUBIC EFFECT	1	57.60344	57.60344	1.1571	0 LEVEL	0.1893	1.7640
FEED RATE INDEX	2	840.58936	420.29468	8.4423	1 LEVEL	4.9902	1.7640
ROTOR ANGLE INDEX	3	263.69678	87.89894	1.7656	2 LEVEL	5.1396	1.7640
LINEAR EFFECT	1	25.47507	25.47507	0.5117	3 LEVEL	9.1232	1.7640
QUADRATIC EFFECT	1	238.11795	238.11795	4.7830	FEED RATE INDEX		
CUBIC EFFECT	1	0.10378	0.10378	0.0021	0 LEVEL	1.3667	1.2473
LATERAL POSITION INDEX	3	86.00409	28.66803	0.5758	1 LEVEL	5.9929	1.7640
LINEAR EFFECT	1	32.79176	32.79176	0.6587	2 LEVEL	9.7161	1.7640
QUADRATIC EFFECT	1	11.14367	11.14367	0.2238	ROTOR ANGLE INDEX		
CUBIC EFFECT	1	42.06863	42.06863	0.8450	0 LEVEL	7.6539	1.7640
LEDGER ORIENTATION INDEX	3	98.16756	32.72252	0.6573	1 LEVEL	3.1598	1.7640
LINEAR EFFECT	1	15.80007	15.80007	0.3174	2 LEVEL	2.7036	1.7640
QUADRATIC EFFECT	1	36.31352	36.31352	0.7294	3 LEVEL	5.9250	1.7640
CUBIC EFFECT	1	46.05396	46.05396	0.9251	LATERAL POSITION INDEX		
CUTTING HEIGHT INDEX	2	37.93965	18.96982	0.3810	0 LEVEL	5.0411	1.7640
C.G. HEIGHT INDEX	3	75.82069	25.27356	0.5077	1 LEVEL	6.6857	1.7640
LINEAR EFFECT	1	63.42140	63.42140	1.2739	2 LEVEL	3.8700	1.7640
QUADRATIC EFFECT	1	12.01860	12.01860	0.2414	3 LEVEL	3.8455	1.7640
CUBIC EFFECT	1	0.38068	0.38068	0.0076	LEDGER ORIENTATION INDEX		
REMAINDER	6	207.01726	34.50287	0.6930	0 LEVEL	4.5579	1.7640
EXPERIMENTAL ERROR	32	1593.10352	49.78448		1 LEVEL	5.0232	1.7640
					2 LEVEL	3.1914	1.7640
					3 LEVEL	6.6598	1.7640
					CUTTING HEIGHT INDEX		
					0 LEVEL	6.1062	1.7640
					1 LEVEL	3.9964	1.7640
					2 LEVEL	4.6698	1.2473
					C.G. HEIGHT INDEX		
					0 LEVEL	3.9929	1.7640
					1 LEVEL	3.8786	1.7640
					2 LEVEL	4.4759	1.7640
					3 LEVEL	6.5950	1.7640

APPENDIX D-I (Continued)

DULL BLADE SERIES ANALYSIS OF VARIANCE FOR C.G. Y DISP INDEX DATA					DULL BLADE SERIES TABLE OF MEAN VALUES FOR C.G. Y DISP INDEX DATA		
SOURCE OF VARIATION	DEGREES OF FREEDOM	SUM OF SQUARES	MEAN SQUARE	F RATIO	FACTOR	VALUE OF MEAN	STD ERROR OF MEAN
CORRECTED TOTAL	63	1240.85937			OVERALL MEAN	2.5858	0.4133
DIAMETER	3	24.48351	8.16117	0.7466	DIAMETER		
LINEAR EFFECT	1	0.00370	0.00370	0.0003	0 LEVEL	2.1348	0.8265
QUADRATIC EFFECT	1	2.54516	2.54516	0.2328	1 LEVEL	3.5741	0.8265
CUBIC EFFECT	1	21.93465	21.93465	2.0067	2 LEVEL	1.9964	0.8265
					3 LEVEL	2.6380	0.8265
TIME IN CHAMBER	3	22.29950	7.43317	0.6800	TIME IN CHAMBER		
LINEAR EFFECT	1	11.88331	11.88331	1.0872	0 LEVEL	2.1571	0.8265
QUADRATIC EFFECT	1	0.05950	0.05950	0.0054	1 LEVEL	1.8839	0.8265
CUBIC EFFECT	1	10.35669	10.35669	0.9475	2 LEVEL	3.3437	0.8265
					3 LEVEL	2.9536	0.8265
ROTOR SPEED INDEX	3	19.71193	6.57064	0.6011	ROTOR SPEED INDEX		
LINEAR EFFECT	1	4.04422	4.04422	0.3700	0 LEVEL	3.4482	0.8265
QUADRATIC EFFECT	1	15.21836	15.21836	1.3923	1 LEVEL	2.0982	0.8265
CUBIC EFFECT	1	0.44936	0.44936	0.0411	2 LEVEL	2.0982	0.8265
					3 LEVEL	2.6987	0.8265
FEED RATE INDEX	2	65.02998	32.51498	2.9747	FEED RATE INDEX		
					0 LEVEL	3.0605	0.5844
					1 LEVEL	3.3687	0.8265
					2 LEVEL	0.8536	0.8265
ROTOR ANGLE INDEX	3	177.33066	59.11021	5.4078	ROTOR ANGLE INDEX		
LINEAR EFFECT	1	25.60422	25.60422	2.3424	0 LEVEL	2.3291	0.8265
QUADRATIC EFFECT	1	0.58250	0.58250	0.0533	1 LEVEL	0.3366	0.8265
CUBIC EFFECT	1	151.14394	151.14394	13.8277	2 LEVEL	5.0259	0.8265
					3 LEVEL	2.6518	0.8265
LATERAL POSITION INDEX	3	162.19574	54.06525	4.9463	LATERAL POSITION INDEX		
LINEAR EFFECT	1	151.21463	151.21463	13.8341	0 LEVEL	0.8871	0.8265
QUADRATIC EFFECT	1	10.45367	10.45367	0.9564	1 LEVEL	1.6161	0.8265
CUBIC EFFECT	1	0.52743	0.52743	0.0483	2 LEVEL	2.7473	0.8265
					3 LEVEL	5.0929	0.8265
LEDGER ORIENTATION INDEX	3	37.18565	12.39522	1.1340	LEDGER ORIENTATION INDEX		
LINEAR EFFECT	1	6.60675	6.60675	0.6044	0 LEVEL	2.9116	0.8265
QUADRATIC EFFECT	1	24.73996	24.73996	2.2634	1 LEVEL	1.4152	0.8265
CUBIC EFFECT	1	5.83894	5.83894	0.5342	2 LEVEL	2.5130	0.8265
					3 LEVEL	3.5036	0.8265
CUTTING HEIGHT INDEX	2	171.33702	85.66850	7.8375	CUTTING HEIGHT INDEX		
					0 LEVEL	2.0934	0.8265
					1 LEVEL	5.3812	0.8265
					2 LEVEL	1.4344	0.5844
C.G. HEIGHT INDEX	3	109.66359	36.55452	3.3443	C.G. HEIGHT INDEX		
LINEAR EFFECT	1	53.62109	53.62109	4.9056	0 LEVEL	4.8277	0.8265
QUADRATIC EFFECT	1	39.76653	39.76653	3.6381	1 LEVEL	1.5304	0.8265
CUBIC EFFECT	1	16.27594	16.27594	1.4890	2 LEVEL	2.0648	0.8265
					3 LEVEL	1.9205	0.8265
REMAINDER	6	101.84462	16.97409	1.5529			
EXPERIMENTAL ERROR	32	349.77710	10.93054				

APPENDIX D-I (Continued)

DJLL BLADE SERIES ANALYSIS OF VARIANCE FOR END Y DISP INDEX DATA					DJLL BLADE SERIES TABLE OF MEAN VALUES FOR END Y DISP INDEX DATA		
SOURCE OF VARIATION	DEGREES OF FREEDOM	SUM OF SQUARES	MEAN SQUARE	F RATIO	FACTOR	VALUE OF MEAN	STD ERROR OF MEAN
CORRECTED TOTAL	63	1408.57153			OVERALL MEAN	2.3379	0.4663
DIAMETER	3	32.32208	10.77403	0.7741	DIAMETER		
LINEAR EFFECT	1	1.69362	1.69362	0.1217	0 LEVEL	2.1732	0.9327
QUADRATIC EFFECT	1	0.36344	0.36344	0.0261	1 LEVEL	3.4086	0.9327
CUBIC EFFECT	1	30.26501	30.26501	2.1746	2 LEVEL	1.4179	0.9327
TIME IN CHAMBER	3	43.09578	14.36526	1.0322	3 LEVEL	2.3518	0.9327
LINEAR EFFECT	1	29.41351	29.41351	2.1134	TIME IN CHAMBER		
QUADRATIC EFFECT	1	0.99857	0.99857	0.0717	0 LEVEL	1.7523	0.9327
CUBIC EFFECT	1	12.68369	12.68369	0.9114	1 LEVEL	1.3125	0.9327
ROTOR SPEED INDEX	3	28.35445	9.45148	0.6791	2 LEVEL	3.1134	0.9327
LINEAR EFFECT	1	2.58789	2.58789	0.2516	3 LEVEL	3.1732	0.9327
QUADRATIC EFFECT	1	22.26491	22.26491	1.5998	ROTOR SPEED INDEX		
CUBIC EFFECT	1	3.50165	3.50165	0.2516	0 LEVEL	3.0929	0.9327
FEED RATE INDEX	2	42.11037	21.05518	1.5129	1 LEVEL	2.1518	0.9327
ROTOR ANGLE INDEX	3	178.91402	59.63800	4.2851	2 LEVEL	1.3443	0.9327
LINEAR EFFECT	1	24.16229	24.16229	1.7361	3 LEVEL	2.7625	0.9327
QUADRATIC EFFECT	1	0.11222	0.11222	0.0081	FEED RATE INDEX		
CUBIC EFFECT	1	154.63948	154.63948	11.1112	0 LEVEL	2.7967	0.6595
LATERAL POSITION INDEX	3	149.50461	49.83487	3.5808	1 LEVEL	2.8250	0.9327
LINEAR EFFECT	1	124.60031	124.60031	8.9528	2 LEVEL	0.9330	0.9327
QUADRATIC EFFECT	1	24.79327	24.79327	1.7815	ROTOR ANGLE INDEX		
CUBIC EFFECT	1	0.11100	0.11100	0.0080	0 LEVEL	2.2505	0.9327
LEDGER ORIENTATION INDEX	3	34.04762	11.34921	0.8155	1 LEVEL	-0.0643	0.9327
LINEAR EFFECT	1	0.47785	0.47785	0.0343	2 LEVEL	4.6562	0.9327
QUADRATIC EFFECT	1	20.38522	20.38522	1.4647	3 LEVEL	2.5089	0.9327
CUBIC EFFECT	1	13.18456	13.18456	0.9473	LATERAL POSITION INDEX		
CUTTING HEIGHT INDEX	2	180.54230	90.27115	6.4862	0 LEVEL	1.0696	0.9327
C.G. HEIGHT INDEX	3	190.75925	63.58641	4.5688	1 LEVEL	1.1473	0.9327
LINEAR EFFECT	1	109.16461	109.16461	7.8437	2 LEVEL	2.2836	0.9327
QUADRATIC EFFECT	1	39.18759	39.18759	2.8157	3 LEVEL	4.8509	0.9327
CUBIC EFFECT	1	42.40703	42.40703	3.0470	LEDGER ORIENTATION INDEX		
REMAINDER	6	83.56381	13.92730	1.0007	0 LEVEL	2.9893	0.9327
EXPERIMENTAL ERROR	32	445.35718	13.91742		1 LEVEL	1.1259	0.9327
					2 LEVEL	2.4211	0.9327
					3 LEVEL	2.8152	0.9327
					CUTTING HEIGHT INDEX		
					0 LEVEL	2.2312	0.9327
					1 LEVEL	5.1143	0.9327
					2 LEVEL	1.0029	0.6595
					C.G. HEIGHT INDEX		
					0 LEVEL	5.2366	0.9327
					1 LEVEL	1.0473	0.9327
					2 LEVEL	2.0634	0.9327
					3 LEVEL	1.0041	0.9327

APPENDIX D-I (Continued)

DULL BLADE SERIES ANALYSIS OF VARIANCE FOR C.G. Z DISP INDEX DATA					DULL BLADE SERIES TABLE OF MEAN VALUES FOR C.G. Z DISP INDEX DATA		
SOURCE OF VARIATION	DEGREES OF FREEDOM	SUM OF SQUARES	MEAN SQUARE	F RATIO	FACTOR	VALUE OF MEAN	STD ERROR OF MEAN
CORRECTED TOTAL	63	2672.93213			OVERALL MEAN	3.9741	0.6667
DIAMETER	3	170.15695	56.71898	1.9941	DIAMETER		
LINEAR EFFECT	1	142.76877	142.76877	5.0194	0 LEVEL	2.5357	1.3333
QUADRATIC EFFECT	1	6.03755	6.03755	0.2123	1 LEVEL	2.2241	1.3333
CUBIC EFFECT	1	21.35063	21.35063	0.7506	2 LEVEL	5.1098	1.3333
TIME IN CHAMBER	3	135.57706	45.19235	1.5889	3 LEVEL	6.0268	1.3333
LINEAR EFFECT	1	24.86449	24.86449	0.8742	TIME IN CHAMBER		
QUADRATIC EFFECT	1	105.28226	105.28226	3.7015	0 LEVEL	3.6580	1.3333
CUBIC EFFECT	1	5.43031	5.43031	0.1909	1 LEVEL	5.1446	1.3333
ROTOR SPEED INDEX	3	414.43750	138.14587	4.8569	2 LEVEL	5.3687	1.3333
LINEAR EFFECT	1	158.52470	158.52470	5.5734	3 LEVEL	1.7250	1.3333
QUADRATIC EFFECT	1	239.91797	239.91797	8.4350	ROTOR SPEED INDEX		
CUBIC EFFECT	1	15.99494	15.99494	0.5623	0 LEVEL	7.7982	1.3333
FEED RATE INDEX	2	70.47409	35.23705	1.2389	1 LEVEL	3.4125	1.3333
ROTOR ANGLE INDEX	3	190.15997	63.38666	2.2285	2 LEVEL	0.6634	1.3333
LINEAR EFFECT	1	120.85634	120.85634	4.2490	3 LEVEL	4.0223	1.3333
QUADRATIC EFFECT	1	47.11841	47.11841	1.6566	FEED RATE INDEX		
CUBIC EFFECT	1	22.18520	22.18520	0.7800	0 LEVEL	3.1558	0.9428
LATERAL POSITION INDEX	3	259.90186	86.63402	3.0459	1 LEVEL	3.8634	1.3333
LINEAR EFFECT	1	221.20750	221.20750	7.7771	2 LEVEL	5.7214	1.3333
QUADRATIC EFFECT	1	4.41000	4.41000	0.1550	ROTOR ANGLE INDEX		
CUBIC EFFECT	1	34.28458	34.28458	1.2054	0 LEVEL	3.2518	1.3333
LEDGER ORIENTATION INDEX	3	126.31700	42.10567	1.4803	1 LEVEL	1.7116	1.3333
LINEAR EFFECT	1	15.27502	15.27502	0.5370	2 LEVEL	4.5205	1.3333
QUADRATIC EFFECT	1	25.10725	25.10725	0.8827	3 LEVEL	6.4125	1.3333
CUBIC EFFECT	1	85.93472	85.93472	3.0213	LATERAL POSITION INDEX		
CUTTING HEIGHT INDEX	2	110.94138	55.47069	1.9502	0 LEVEL	2.0696	1.3333
C.G. HEIGHT INDEX	3	112.79741	37.59914	1.3219	1 LEVEL	1.8982	1.3333
LINEAR EFFECT	1	26.51575	26.51575	0.9322	2 LEVEL	5.5250	1.3333
QUADRATIC EFFECT	1	76.25031	76.25031	2.6808	3 LEVEL	6.4036	1.3333
CUBIC EFFECT	1	10.03135	10.03135	0.3527	LEDGER ORIENTATION INDEX		
REMAINDER	6	171.98344	28.66389	1.0078	0 LEVEL	2.1741	1.3333
EXPERIMENTAL ERROR	32	910.18506	28.44328		1 LEVEL	5.9366	1.3333
					2 LEVEL	3.2643	1.3333
					3 LEVEL	4.5214	1.3333
					CUTTING HEIGHT INDEX		
					0 LEVEL	4.4964	1.3333
					1 LEVEL	5.8929	1.3333
					2 LEVEL	2.7536	0.9428
					C.G. HEIGHT INDEX		
					0 LEVEL	4.0250	1.3333
					1 LEVEL	3.1259	1.3333
					2 LEVEL	2.6393	1.3333
					3 LEVEL	6.1062	1.3333

APPENDIX D-I (Continued)

DULL BLADE SERIES ANALYSIS OF VARIANCE FOR END Z DISP INDEX DATA					DULL BLADE SERIES TABLE OF MEAN VALUES FOR END Z DISP INDEX DATA		
SOURCE OF VARIATION	DEGREES OF FREEDOM	SUM OF SQUARES	MEAN SQUARE	F RATIO	FACTOR	VALUE OF MEAN	STD ERROR OF MEAN
CORRECTED TOTAL	63	2591.92065			OVERALL MEAN	5.1259	0.6638
DIAMETER	3	142.82634	47.60878	1.6883	DIAMETER		
LINEAR EFFECT	1	118.06328	118.06328	4.1868	0 LEVEL	3.8268	1.3276
QUADRATIC EFFECT	1	4.77735	4.77735	0.1694	1 LEVEL	3.4955	1.3276
CUBIC EFFECT	1	19.98570	19.98570	0.7087	2 LEVEL	6.2098	1.3276
TIME IN CHAMBER	3	115.83371	38.61124	1.3693	3 LEVEL	6.9714	1.3276
LINEAR EFFECT	1	24.89636	24.89636	0.8829	TIME IN CHAMBER		
QUADRATIC EFFECT	1	84.90306	84.90306	3.0109	0 LEVEL	4.9482	1.3276
CUBIC EFFECT	1	6.03430	6.03430	0.2140	1 LEVEL	6.1446	1.3276
ROTOR SPEED INDEX	3	362.40259	120.80090	4.2839	2 LEVEL	6.4107	1.3276
LINEAR EFFECT	1	98.21944	98.21944	3.4831	3 LEVEL	3.0000	1.3276
QUADRATIC EFFECT	1	247.72511	247.72511	8.7850	ROTOR SPEED INDEX		
CUBIC EFFECT	1	16.45816	16.45816	0.5837	0 LEVEL	8.5266	1.3276
FEED RATE INDEX	2	117.41472	58.70735	2.0819	1 LEVEL	4.3929	1.3276
ROTOR ANGLE INDEX	3	192.69711	64.23236	2.2779	2 LEVEL	1.9241	1.3276
LINEAR EFFECT	1	124.96428	124.96428	4.4316	3 LEVEL	5.6580	1.3276
QUADRATIC EFFECT	1	41.74081	41.74081	1.4802	FEED RATE INDEX		
CUBIC EFFECT	1	25.99199	25.99199	0.9217	0 LEVEL	3.9812	0.9387
LATERAL POSITION INDEX	3	249.61195	83.20398	2.9506	1 LEVEL	5.2464	1.3276
LINEAR EFFECT	1	227.42694	227.42694	8.0652	2 LEVEL	7.2946	1.3276
QUADRATIC EFFECT	1	0.12001	0.12001	0.0043	ROTOR ANGLE INDEX		
CUBIC EFFECT	1	22.06500	22.06500	0.7825	0 LEVEL	4.3437	1.3276
LEDGER ORIENTATION INDEX	3	89.51033	29.83678	1.0581	1 LEVEL	2.8384	1.3276
LINEAR EFFECT	1	8.29288	8.29288	0.2941	2 LEVEL	5.7982	1.3276
QUADRATIC EFFECT	1	6.25000	6.25000	0.2216	3 LEVEL	7.5232	1.3276
CUBIC EFFECT	1	74.96744	74.96744	2.6586	LATERAL POSITION INDEX		
CUTTING HEIGHT INDEX	2	92.56169	46.28084	1.6412	0 LEVEL	2.9027	1.3276
C.G. HEIGHT INDEX	3	127.33548	42.44516	1.5052	1 LEVEL	3.4518	1.3276
LINEAR EFFECT	1	34.47186	34.47186	1.2225	2 LEVEL	6.7134	1.3276
QUADRATIC EFFECT	1	82.48531	82.48531	2.9252	3 LEVEL	7.4357	1.3276
CUBIC EFFECT	1	10.37829	10.37829	0.3680	LEDGER ORIENTATION INDEX		
REMAINDER	6	199.37091	33.22849	1.1784	0 LEVEL	3.8464	1.3276
EXPERIMENTAL ERROR	32	902.35571	28.19861		1 LEVEL	6.7295	1.3276
					2 LEVEL	4.1473	1.3276
					3 LEVEL	5.7804	1.3276
					CUTTING HEIGHT INDEX		
					0 LEVEL	5.6393	1.3276
					1 LEVEL	6.8580	1.3276
					2 LEVEL	4.0031	0.9387
					C.G. HEIGHT INDEX		
					0 LEVEL	5.0964	1.3276
					1 LEVEL	4.2027	1.3276
					2 LEVEL	3.7786	1.3276
					3 LEVEL	7.4259	1.3276

APPENDIX D-II

ANALYSIS OF VARIANCE AND TABLE OF MEAN VALUES FOR SHARP BLADE TEST SERIES

SHARP BLADE SERIES ANALYSIS OF VARIANCE FOR ENERGY INPUT DATA					SHARP BLADE SERIES TABLE OF MEAN VALUES FOR ENERGY INPUT DATA		
SOURCE OF VARIATION	DEGREES OF FREEDOM	SUM OF SQUARES	MEAN SQUARE	F RATIO	FACTOR	VALUE OF MEAN	STD ERRJR OF MEAN
CORRECTED TOTAL	63	141719.25000			OVERALL MEAN	70.6307	2.2797
DIAMETER	3	82373.50000	27457.85156	82.5500	DIAMETER		
LINEAR EFFECT	1	82187.93750	82187.93750	247.0919	0 LEVEL	22.8777	4.5595
QUADRATIC EFFECT	1	10.93674	10.93674	0.0329	1 LEVEL	52.8015	4.5595
CUBIC EFFECT	1	174.67625	174.67625	0.5252	2 LEVEL	89.2867	4.5595
TIME IN CHAMBER	3	19537.65234	6512.55078	19.5795	3 LEVEL	117.5569	4.5595
LINEAR EFFECT	1	2014.27930	2014.27930	6.0558	TIME IN CHAMBER		
QUADRATIC EFFECT	1	6518.76172	6518.76172	19.5982	0 LEVEL	73.9293	4.5595
CUBIC EFFECT	1	11004.60937	11004.60937	33.0845	1 LEVEL	65.6392	4.5595
ROTOR SPEED INDEX	3	1272.33154	424.11035	1.2751	2 LEVEL	95.8069	4.5595
LINEAR EFFECT	1	138.14844	138.14844	0.4153	3 LEVEL	47.1474	4.5595
QUADRATIC EFFECT	1	4.60499	4.60499	0.0138	ROTOR SPEED INDEX		
CUBIC EFFECT	1	1129.57812	1129.57812	3.3960	0 LEVEL	66.5125	4.5595
FEED RATE INDEX	2	181.36656	90.68327	0.2726	1 LEVEL	75.8783	4.5595
ROTOR ANGLE INDEX	3	11864.72266	3954.90747	11.8901	2 LEVEL	65.9196	4.5595
LINEAR EFFECT	1	57.87772	57.87772	0.1740	3 LEVEL	74.2124	4.5595
QUADRATIC EFFECT	1	716.35181	716.35181	2.1537	FEED RATE INDEX		
CUBIC EFFECT	1	11090.49219	11090.49219	33.3427	0 LEVEL	73.2799	4.5595
LATERAL POSITION INDEX	3	4026.01855	1342.00610	4.0346	1 LEVEL	69.1735	3.2240
LINEAR EFFECT	1	1880.67871	1880.67871	5.6541	2 LEVEL	70.8960	4.5595
QUADRATIC EFFECT	1	1202.13867	1202.13867	3.6141	ROTOR ANGLE INDEX		
CUBIC EFFECT	1	943.20093	943.20093	2.8357	0 LEVEL	60.1222	4.5595
LEDGER ORIENTATION INDEX	3	2204.76294	734.92090	2.2095	1 LEVEL	91.2123	4.5595
LINEAR EFFECT	1	207.04065	207.04065	0.6225	2 LEVEL	56.7403	4.5595
QUADRATIC EFFECT	1	532.38623	532.38623	1.6006	3 LEVEL	74.4481	4.5595
CUBIC EFFECT	1	1465.33569	1465.33569	4.4054	LATERAL POSITION INDEX		
CUTTING HEIGHT INDEX	2	1905.56128	952.78052	2.8645	0 LEVEL	60.7407	4.5595
C.G. HEIGHT INDEX	3	5747.05859	1915.68652	5.7594	1 LEVEL	67.3899	4.5595
LINEAR EFFECT	1	4644.48437	4644.48437	13.9633	2 LEVEL	82.5395	4.5595
QUADRATIC EFFECT	1	32.61124	32.61124	0.0980	3 LEVEL	71.8527	4.5595
CUBIC EFFECT	1	1069.96411	1069.96411	3.2168	LEDGER ORIENTATION INDEX		
REMAINDER	6	1962.35352	327.05884	0.9833	0 LEVEL	72.2995	4.5595
EXPERIMENTAL ERROR	32	10643.86719	332.62085		1 LEVEL	67.8996	4.5595
					2 LEVEL	79.1302	4.5595
					3 LEVEL	63.1935	4.5595
					CUTTING HEIGHT INDEX		
					0 LEVEL	78.7838	4.5595
					1 LEVEL	72.4198	4.5595
					2 LEVEL	65.6595	3.2240
					C.G. HEIGHT INDEX		
					0 LEVEL	56.6591	4.5595
					1 LEVEL	73.0205	4.5595
					2 LEVEL	69.6686	4.5595
					3 LEVEL	83.1746	4.5595

APPENDIX D-II (Continued)

SHARP BLADE SERIES ANALYSIS OF VARIANCE FOR MAX TORQUE DATA					SHARP BLADE SERIES TABLE OF MEAN VALUES FOR MAX TORQUE DATA		
SOURCE OF VARIATION	DEGREES OF FREEDOM	SUM OF SQUARES	MEAN SQUARE	F RATIO	FACTOR	VALUE OF MEAN	STD ERROR OF MEAN
CORRECTED TOTAL	63	15290.88281			OVERALL MEAN	22.3266	0.8749
DIAMETER	3	6663.61328	2221.20508	45.3436	DIAMETER		
LINEAR EFFECT	1	6656.68750	6656.68750	135.8893	0 LEVEL	8.5500	1.7498
QUADRATIC EFFECT	1	2.76391	2.76391	0.0564	1 LEVEL	17.6312	1.7498
CUBIC EFFECT	1	4.16328	4.16328	0.0850	2 LEVEL	27.4375	1.7498
TIME IN CHAMBER	3	1114.50171	371.50049	7.5838	3 LEVEL	35.6875	1.7498
LINEAR EFFECT	1	424.35059	424.35059	8.6627	TIME IN CHAMBER		
QUADRATIC EFFECT	1	681.86255	681.86255	13.9195	0 LEVEL	22.3562	1.7498
CUBIC EFFECT	1	8.28828	8.28828	0.1692	1 LEVEL	27.2250	1.7498
ROTOR SPEED INDEX	3	1637.43408	545.81128	11.1422	2 LEVEL	23.9562	1.7498
LINEAR EFFECT	1	1407.42236	1407.42236	28.7310	3 LEVEL	15.7687	1.7498
QUADRATIC EFFECT	1	211.33890	211.33890	4.3143	ROTOR SPEED INDEX		
CUBIC EFFECT	1	18.67278	18.67278	0.3812	0 LEVEL	30.1937	1.7498
FEED RATE INDEX	2	6.40797	3.20398	0.0654	1 LEVEL	23.3312	1.7498
ROTOR ANGLE INDEX	3	1457.48779	485.82910	9.9177	2 LEVEL	17.6875	1.7498
LINEAR EFFECT	1	79.10252	79.10252	1.6148	3 LEVEL	18.0937	1.7498
QUADRATIC EFFECT	1	7.63141	7.63141	0.1558	FEED RATE INDEX		
CUBIC EFFECT	1	1370.75391	1370.75391	27.9825	0 LEVEL	21.8125	1.7498
LATERAL POSITION INDEX	3	271.12671	90.37556	1.8449	1 LEVEL	22.5875	1.2373
LINEAR EFFECT	1	256.86523	256.86523	5.2436	2 LEVEL	22.3187	1.7498
QUADRATIC EFFECT	1	0.19141	0.19141	0.0039	ROTOR ANGLE INDEX		
CUBIC EFFECT	1	14.07003	14.07003	0.2872	0 LEVEL	22.0937	1.7498
LEDGER ORIENTATION INDEX	3	497.73169	165.91057	3.3869	1 LEVEL	28.6875	1.7498
LINEAR EFFECT	1	65.43152	65.43152	1.3357	2 LEVEL	15.2750	1.7498
QUADRATIC EFFECT	1	6.56641	6.56641	0.1340	3 LEVEL	23.2500	1.7498
CUBIC EFFECT	1	425.73364	425.73364	8.6909	LATERAL POSITION INDEX		
CUTTING HEIGHT INDEX	2	154.27921	77.13960	1.5747	0 LEVEL	19.7937	1.7498
C.G. HEIGHT INDEX	3	350.07422	116.69141	2.3821	1 LEVEL	20.8562	1.7498
LINEAR EFFECT	1	196.09453	196.09453	4.0031	2 LEVEL	23.9062	1.7498
QUADRATIC EFFECT	1	111.56641	111.56641	2.2775	3 LEVEL	24.7500	1.7498
CUBIC EFFECT	1	42.41327	42.41327	0.8658	LEDGER ORIENTATION INDEX		
REMAINDER	6	1570.67041	261.77832	5.3439	0 LEVEL	22.4437	1.7498
EXPERIMENTAL ERROR	32	1567.55493	48.98608		1 LEVEL	18.0937	1.7498
					2 LEVEL	25.9187	1.7498
					3 LEVEL	22.8500	1.7498
					CUTTING HEIGHT INDEX		
					0 LEVEL	21.8062	1.7498
					1 LEVEL	24.9875	1.7498
					2 LEVEL	21.2562	1.2373
					C.G. HEIGHT INDEX		
					0 LEVEL	18.2937	1.7498
					1 LEVEL	23.9562	1.7498
					2 LEVEL	23.3375	1.7498
					3 LEVEL	23.7187	1.7498

APPENDIX D-II (Continued)

SHARP BLADE SERIES ANALYSIS OF VARIANCE FOR ENERGY INPUT INDEX DATA					SHARP BLADE SERIES TABLE OF MEAN VALUES FOR ENERGY INPUT INDEX DATA		
SOURCE OF VARIATION	DEGREES OF FREEDOM	SUM OF SQUARES	MEAN SQUARE	F RATIO	FACTOR	VALUE OF MEAN	STD ERROR OF MEAN
CORRECTED TOTAL	63	72149.87500			OVERALL MEAN	56.0741	2.4235
DIAMETER	3	11215.41016	3738.47070	9.9456	DIAMETER		
LINEAR EFFECT	1	9521.60547	9521.60547	25.3307	0 LEVEL	37.5647	4.8470
QUADRATIC EFFECT	1	890.25293	890.25293	2.3684	1 LEVEL	49.5950	4.8470
CUBIC EFFECT	1	803.55396	803.55396	2.1377	2 LEVEL	70.0125	4.8470
TIME IN CHAMBER	3	11926.65625	3975.55200	10.5763	3 LEVEL	67.1243	4.8470
LINEAR EFFECT	1	2947.81812	2947.81812	7.8422	TIME IN CHAMBER		
QUADRATIC EFFECT	1	2261.77417	2261.77417	6.0171	0 LEVEL	63.8163	4.8470
CUBIC EFFECT	1	6717.06250	6717.06250	17.8697	1 LEVEL	51.3092	4.8470
ROTOR SPEED INDEX	3	3358.83716	1119.61230	2.9786	2 LEVEL	72.7275	4.8470
LINEAR EFFECT	1	145.21033	145.21033	0.3863	3 LEVEL	36.4424	4.8470
QUADRATIC EFFECT	1	119.89839	119.89839	0.3190	ROTOR SPEED INDEX		
CUBIC EFFECT	1	3093.72852	3093.72852	8.2304	0 LEVEL	52.3126	4.8470
FEED RATE INDEX	2	1628.18408	814.09204	2.1658	1 LEVEL	63.3597	4.8470
ROTOR ANGLE INDEX	3	2714.12817	904.70923	2.4068	2 LEVEL	46.0510	4.8470
LINEAR EFFECT	1	16.09509	16.09509	0.0428	3 LEVEL	62.5730	4.8470
QUADRATIC EFFECT	1	45.72935	45.72935	0.1217	FEED RATE INDEX		
CUBIC EFFECT	1	2652.30371	2652.30371	7.0560	0 LEVEL	61.8535	4.8470
LATERAL POSITION INDEX	3	4688.89062	1562.96411	4.1580	1 LEVEL	57.2359	3.4273
LINEAR EFFECT	1	4657.68359	4657.68359	12.3910	2 LEVEL	47.9710	4.8470
QUADRATIC EFFECT	1	13.77764	13.77764	0.0367	ROTOR ANGLE INDEX		
CUBIC EFFECT	1	17.43079	17.43079	0.0464	0 LEVEL	53.0226	4.8470
LEDGER ORIENTATION INDEX	3	817.10278	272.36743	0.7246	1 LEVEL	65.7805	4.8470
LINEAR EFFECT	1	166.50314	166.50314	0.4430	2 LEVEL	48.0582	4.8470
QUADRATIC EFFECT	1	97.74205	97.74205	0.2600	3 LEVEL	57.4350	4.8470
CUBIC EFFECT	1	552.85742	552.85742	1.4708	LATERAL POSITION INDEX		
CUTTING HEIGHT INDEX	2	2338.88940	1169.44458	3.1111	0 LEVEL	45.3260	4.8470
C.G. HEIGHT INDEX	3	16892.84766	5630.94922	14.9803	1 LEVEL	51.0943	4.8470
LINEAR EFFECT	1	15569.12891	15569.12891	41.4192	2 LEVEL	60.1254	4.8470
QUADRATIC EFFECT	1	644.59448	644.59448	1.7148	3 LEVEL	67.7501	4.8470
CUBIC EFFECT	1	679.12329	679.12329	1.8067	LEDGER ORIENTATION INDEX		
REMAINDER	6	4540.39844	756.73340	2.0132	0 LEVEL	58.3167	4.8470
EXPERIMENTAL ERROR	32	12028.52344	375.89136		1 LEVEL	54.0880	4.8470
					2 LEVEL	50.5318	4.8470
					3 LEVEL	51.3599	4.8470
					CUTTING HEIGHT INDEX		
					0 LEVEL	56.7789	4.8470
					1 LEVEL	65.6886	4.8470
					2 LEVEL	50.9144	3.4273
					C.G. HEIGHT INDEX		
					0 LEVEL	78.7165	4.8470
					1 LEVEL	64.2461	4.8470
					2 LEVEL	41.5549	4.8470
					3 LEVEL	39.7759	4.8470

APPENDIX D-II (Continued)

SHARP BLADE SERIES ANALYSIS OF VARIANCE FOR MAX TORQUE INDEX DATA					SHARP BLADE SERIES TABLE OF MEAN VALUES FOR MAX TORQUE INDEX DATA		
SOURCE OF VARIATION	DEGREES OF FREEDOM	SUM OF SQUARES	MEAN SQUARE	F RATIO	FACTOR	VALUE OF MEAN	STD ERROR OF MEAN
CORRECTED TOTAL	63	7708.23437			OVERALL MEAN	18.2055	0.8297
DIAMETER	3	706.25879	235.41966	5.3436	DIAMETER		
LINEAR EFFECT	1	407.41650	407.41650	9.2475	0 LEVEL	13.2040	1.6594
QUADRATIC EFFECT	1	253.82611	253.82611	5.7613	1 LEVEL	17.9434	1.6594
CUBIC EFFECT	1	45.01622	45.01622	1.0218	2 LEVEL	22.4505	1.6594
TIME IN CHAMBER	3	515.89819	171.96608	3.9033	3 LEVEL	19.2240	1.6594
LINEAR EFFECT	1	415.00684	415.00684	9.4198	TIME IN CHAMBER		
QUADRATIC EFFECT	1	84.27240	84.27240	1.9128	0 LEVEL	20.7023	1.6594
CUBIC EFFECT	1	16.61897	16.61897	0.3772	1 LEVEL	19.8081	1.6594
ROTOR SPEED INDEX	3	1141.39307	380.46436	8.6358	2 LEVEL	18.8978	1.6594
LINEAR EFFECT	1	923.99072	923.99072	20.9727	3 LEVEL	13.4136	1.6594
QUADRATIC EFFECT	1	99.49507	99.49507	2.2583	ROTOR SPEED INDEX		
CUBIC EFFECT	1	117.90726	117.90726	2.6763	0 LEVEL	23.9431	1.6594
FEED RATE INDEX	2	97.01956	48.50978	1.1011	1 LEVEL	20.4789	1.6594
ROTOR ANGLE INDEX	3	377.75952	125.91989	2.8581	2 LEVEL	14.9616	1.6594
LINEAR EFFECT	1	43.38652	43.38652	0.9848	FEED RATE INDEX		
QUADRATIC EFFECT	1	134.23958	134.23958	3.0470	0 LEVEL	18.6277	1.6594
CUBIC EFFECT	1	200.13354	200.13354	4.5426	1 LEVEL	19.3501	1.1734
LATERAL POSITION INDEX	3	279.99463	93.33160	2.1184	2 LEVEL	16.0939	1.6594
LINEAR EFFECT	1	245.85417	245.85417	5.5804	ROTOR ANGLE INDEX		
QUADRATIC EFFECT	1	0.46725	0.46725	0.0106	0 LEVEL	19.9676	1.6594
CUBIC EFFECT	1	33.67342	33.67342	0.7643	1 LEVEL	19.4979	1.6594
LEDGER ORIENTATION INDEX	3	305.81250	101.93753	2.3138	2 LEVEL	14.0165	1.6594
LINEAR EFFECT	1	26.82413	26.82413	0.6089	3 LEVEL	19.3399	1.6594
QUADRATIC EFFECT	1	101.32231	101.32231	2.2998	LATERAL POSITION INDEX		
CUBIC EFFECT	1	177.66617	177.66617	4.0327	0 LEVEL	15.8149	1.6594
CUTTING HEIGHT INDEX	2	372.13867	186.06937	4.2234	1 LEVEL	16.4412	1.6594
C.G. HEIGHT INDEX	3	2200.41919	733.47290	16.6484	2 LEVEL	20.1406	1.6594
LINEAR EFFECT	1	2085.71704	2085.71704	47.3416	3 LEVEL	20.4252	1.6594
QUADRATIC EFFECT	1	4.22519	4.22519	0.0959	LEDGER ORIENTATION INDEX		
CUBIC EFFECT	1	110.47675	110.47675	2.5076	0 LEVEL	21.0774	1.6594
REMAINDER	5	301.72705	50.28784	1.1414	1 LEVEL	15.0014	1.6594
EXPERIMENTAL ERROR	32	1409.81567	44.05673		2 LEVEL	18.8931	1.6594
					3 LEVEL	17.8500	1.6594
					CUTTING HEIGHT INDEX		
					0 LEVEL	18.4032	1.6594
					1 LEVEL	22.0729	1.6594
					2 LEVEL	16.1729	1.1734
					C.G. HEIGHT INDEX		
					0 LEVEL	25.5339	1.6594
					1 LEVEL	22.2643	1.6594
					2 LEVEL	13.6328	1.6594
					3 LEVEL	11.3910	1.6594

APPENDIX D-II (Continued)

SHARP BLADE SERIES ANALYSIS OF VARIANCE FOR C.G. X DISP INDEX DATA					SHARP BLADE SERIES TABLE OF MEAN VALUES FOR C.G. X DISP INDEX DATA		
SOURCE OF VARIATION	DEGREES OF FREEDOM	SUM OF SQUARES	MEAN SQUARE	F RATIO	FACTOR	VALUE OF MEAN	STD ERROR OF MEAN
CORRECTED TOTAL	63	3439.25854			OVERALL MEAN	8.5482	0.6605
DIAMETER	3	103.06693	34.35564	1.2304	DIAMETER		
LINEAR EFFECT	1	0.75494	0.75494	0.0270	0 LEVEL	10.0732	1.3211
QUADRATIC EFFECT	1	91.61224	91.61224	3.2809	1 LEVEL	6.8518	1.3211
CUBIC EFFECT	1	10.69975	10.69975	0.3832	2 LEVEL	7.8518	1.3211
TIME IN CHAMBER	3	95.82376	31.94125	1.1439	3 LEVEL	9.4161	1.3211
LINEAR EFFECT	1	51.88800	51.88800	1.8582	TIME IN CHAMBER		
QUADRATIC EFFECT	1	24.22046	24.22046	0.8674	0 LEVEL	8.8929	1.3211
CUBIC EFFECT	1	19.71530	19.71530	0.7061	1 LEVEL	10.3107	1.3211
ROTOR SPEED INDEX	3	819.46558	273.15503	9.7824	2 LEVEL	8.0161	1.3211
LINEAR EFFECT	1	776.25781	776.25781	27.7997	3 LEVEL	6.9732	1.3211
QUADRATIC EFFECT	1	42.99611	42.99611	1.5398	ROTOR SPEED INDEX		
CUBIC EFFECT	1	0.21159	0.21159	0.0076	0 LEVEL	4.6696	1.3211
FEED RATE INDEX	2	647.78564	323.89282	11.5994	1 LEVEL	6.2482	1.3211
ROTOR ANGLE INDEX	3	488.43701	162.81233	5.8307	2 LEVEL	8.9491	0.9341
LINEAR EFFECT	1	114.31029	114.31029	4.0937	3 LEVEL	12.6107	1.3211
QUADRATIC EFFECT	1	2.35842	2.35842	0.0845	ROTOR ANGLE INDEX		
CUBIC EFFECT	1	371.76831	371.76831	13.3139	0 LEVEL	7.6411	1.3211
LATERAL POSITION INDEX	3	36.47928	12.15976	0.4355	1 LEVEL	4.9089	1.3211
LINEAR EFFECT	1	18.04999	18.04999	0.6464	2 LEVEL	12.5714	1.3211
QUADRATIC EFFECT	1	2.86576	2.86576	0.1026	3 LEVEL	9.0714	1.3211
CUBIC EFFECT	1	15.56352	15.56352	0.5574	LATERAL POSITION INDEX		
LEDGER ORIENTATION INDEX	3	92.03581	30.67860	1.0987	0 LEVEL	7.4036	1.3211
LINEAR EFFECT	1	71.82050	71.82050	2.5721	1 LEVEL	9.1839	1.3211
QUADRATIC EFFECT	1	5.12699	5.12699	0.1836	2 LEVEL	8.3357	1.3211
CUBIC EFFECT	1	15.08833	15.08833	0.5404	3 LEVEL	9.2696	1.3211
CUTTING HEIGHT INDEX	2	1.73755	0.86878	0.0311	LEDGER ORIENTATION INDEX		
C.G. HEIGHT INDEX	3	131.99275	43.99757	1.5757	0 LEVEL	6.6268	1.3211
LINEAR EFFECT	1	104.42450	104.42450	3.7397	1 LEVEL	9.0089	1.3211
QUADRATIC EFFECT	1	0.72250	0.72250	0.0259	2 LEVEL	8.6536	1.3211
CUBIC EFFECT	1	26.84575	26.84575	0.9614	3 LEVEL	9.9036	1.3211
REMAINDER	6	128.89023	21.48170	0.7693	CUTTING HEIGHT INDEX		
EXPERIMENTAL ERROR	32	893.54346	27.92323		0 LEVEL	8.7946	1.3211
					1 LEVEL	8.3304	1.3211
					2 LEVEL	8.5339	0.9341
					3 LEVEL	9.8661	1.3211

APPENDIX D-II (Continued)

SHARP BLADE SERIES
ANALYSIS OF VARIANCE
FOR
END X DISP INDEX DATA

SOURCE OF VARIATION	DEGREES OF FREEDOM	SUM OF SQUARES	MEAN SQUARE	F RATIO
CORRECTED TOTAL	63	4089.66504		
DIAMETER	3	124.30469	41.43489	1.0908
LINEAR EFFECT	1	1.03188	1.03188	0.0272
QUADRATIC EFFECT	1	78.95592	78.95592	2.0786
CUBIC EFFECT	1	44.31689	44.31689	1.1667
TIME IN CHAMBER	3	158.67122	52.89040	1.3924
LINEAR EFFECT	1	113.28799	113.28799	2.9825
QUADRATIC EFFECT	1	34.64163	34.64163	0.9120
CUBIC EFFECT	1	10.74159	10.74159	0.2828
ROTOR SPEED INDEX	3	1005.42358	335.14111	8.8232
LINEAR EFFECT	1	921.88794	921.88794	24.2703
QUADRATIC EFFECT	1	81.51509	81.51509	2.1460
CUBIC EFFECT	1	2.02066	2.02066	0.0532
FEED RATE INDEX	2	592.74609	296.37305	7.8025
ROTOR ANGLE INDEX	3	605.61914	201.87309	5.3147
LINEAR EFFECT	1	138.03758	138.03758	3.6341
QUADRATIC EFFECT	1	0.03719	0.03719	0.0010
CUBIC EFFECT	1	467.54443	467.54443	12.3089
LATERAL POSITION INDEX	3	14.92357	4.97452	0.1310
LINEAR EFFECT	1	4.88637	4.88637	0.1286
QUADRATIC EFFECT	1	10.01270	10.01270	0.2636
CUBIC EFFECT	1	0.02450	0.02450	0.0006
LEDGER ORIENTATION INDEX	3	127.89928	42.63309	1.1224
LINEAR EFFECT	1	113.15204	113.15204	2.9789
QUADRATIC EFFECT	1	8.61842	8.61842	0.2269
CUBIC EFFECT	1	6.12883	6.12883	0.1614
CUTTING HEIGHT INDEX	2	11.27224	5.63612	0.1484
C.G. HEIGHT INDEX	3	59.95764	19.98587	0.5262
LINEAR EFFECT	1	47.69637	47.69637	1.2557
QUADRATIC EFFECT	1	4.87148	4.87148	0.1283
CUBIC EFFECT	1	7.38981	7.38981	0.1945
REMAINDER	6	173.35162	28.89194	0.7606
EXPERIMENTAL ERROR	32	1215.49536	37.98422	

SHARP BLADE SERIES
TABLE OF MEAN VALUES
FOR
END X DISP INDEX DATA

FACTOR	VALUE OF MEAN	STD ERROR OF MEAN
OVERALL MEAN	7.8196	0.7704
DIAMETER		
0 LEVEL	9.1321	1.5408
1 LEVEL	5.5357	1.5408
2 LEVEL	7.8821	1.5408
3 LEVEL	8.7286	1.5408
TIME IN CHAMBER		
0 LEVEL	8.6857	1.5408
1 LEVEL	9.7000	1.5408
2 LEVEL	7.4107	1.5408
3 LEVEL	5.4821	1.5408
ROTOR SPEED INDEX		
0 LEVEL	3.7768	1.5408
1 LEVEL	5.2321	1.5408
2 LEVEL	8.1500	1.5408
3 LEVEL	14.1196	1.5408
FEED RATE INDEX		
0 LEVEL	3.0393	1.5408
1 LEVEL	8.3661	1.0895
2 LEVEL	11.5071	1.5408
ROTOR ANGLE INDEX		
0 LEVEL	7.0821	1.5408
1 LEVEL	3.5125	1.5408
2 LEVEL	12.0786	1.5408
3 LEVEL	8.6054	1.5408
LATERAL POSITION INDEX		
0 LEVEL	7.0446	1.5408
1 LEVEL	8.1179	1.5408
2 LEVEL	8.3125	1.5408
3 LEVEL	7.8036	1.5408
LEDGER ORIENTATION INDEX		
0 LEVEL	5.5304	1.5408
1 LEVEL	8.0071	1.5408
2 LEVEL	8.3661	1.5408
3 LEVEL	9.3750	1.5408
CUTTING HEIGHT INDEX		
0 LEVEL	8.4589	1.5408
1 LEVEL	7.2804	1.5408
2 LEVEL	7.7696	1.0895
C.G. HEIGHT INDEX		
0 LEVEL	6.5375	1.5408
1 LEVEL	7.2536	1.5408
2 LEVEL	8.9375	1.5408
3 LEVEL	8.5500	1.5408

APPENDIX D-II (Continued)

SHARP BLADE SERIES ANALYSIS OF VARIANCE FOR C.G. Y DISP INDEX DATA					SHARP BLADE SERIES TABLE OF MEAN VALUES FOR C.G. Y DISP INDEX DATA		
SOURCE OF VARIATION	DEGREES OF FREEDOM	SUM OF SQUARES	MEAN SQUARE	F RATIO	FACTOR	VALUE OF MEAN	STD ERROR OF MEAN
CORRECTED TOTAL	63	737.37915			OVERALL MEAN	1.7946	0.4072
DIAMETER	3	7.65275	2.55092	0.2404	DIAMETER		
LINEAR EFFECT	1	6.69490	6.69490	0.6309	0 LEVEL	2.2714	0.8144
QUADRATIC EFFECT	1	0.00862	0.00862	0.0008	1 LEVEL	1.7875	0.8144
CUBIC EFFECT	1	0.94923	0.94923	0.0895	2 LEVEL	1.8250	0.8144
TIME IN CHAMBER	3	39.38622	13.12874	1.2373	3 LEVEL	1.2946	0.8144
LINEAR EFFECT	1	34.92346	34.92346	3.2913	TIME IN CHAMBER		
QUADRATIC EFFECT	1	3.31760	3.31760	0.3127	0 LEVEL	2.9536	0.8144
CUBIC EFFECT	1	1.14515	1.14515	0.1079	1 LEVEL	2.0768	0.8144
ROTOR SPEED INDEX	3	136.88336	45.62778	4.3001	2 LEVEL	1.0571	0.8144
LINEAR EFFECT	1	45.04286	45.04286	4.2450	3 LEVEL	1.0911	0.8144
QUADRATIC EFFECT	1	60.84000	60.84000	5.7337	ROTOR SPEED INDEX		
CUBIC EFFECT	1	31.00049	31.00049	2.9216	0 LEVEL	3.5839	0.8144
FEED RATE INDEX	2	2.45069	1.22534	0.1155	1 LEVEL	2.1286	0.8144
ROTOR ANGLE INDEX	3	44.87857	14.95952	1.4098	2 LEVEL	-0.4893	0.8144
LINEAR EFFECT	1	2.59200	2.59200	0.2443	3 LEVEL	1.9554	0.8144
QUADRATIC EFFECT	1	27.78795	27.78795	2.6188	FEED RATE INDEX		
CUBIC EFFECT	1	14.49861	14.49861	1.3664	0 LEVEL	1.4875	0.8144
LATERAL POSITION INDEX	3	75.07376	25.02458	2.3584	1 LEVEL	1.8295	0.5758
LINEAR EFFECT	1	74.88449	74.88449	7.0573	2 LEVEL	2.0321	0.8144
QUADRATIC EFFECT	1	0.02469	0.02469	0.0023	ROTOR ANGLE INDEX		
CUBIC EFFECT	1	0.16458	0.16458	0.0155	0 LEVEL	1.0786	0.8144
LEDGER ORIENTATION INDEX	3	13.28949	4.42983	0.4175	1 LEVEL	1.7250	0.8144
LINEAR EFFECT	1	11.68265	11.68265	1.1010	2 LEVEL	3.1821	0.8144
QUADRATIC EFFECT	1	0.09434	0.09434	0.0089	3 LEVEL	1.1929	0.8144
CUBIC EFFECT	1	1.51250	1.51250	0.1425	LATERAL POSITION INDEX		
CUTTING HEIGHT INDEX	2	10.66816	5.33408	0.5027	0 LEVEL	0.3857	0.8144
C.G. HEIGHT INDEX	3	30.79877	10.26626	0.9675	1 LEVEL	1.2232	0.8144
LINEAR EFFECT	1	4.10159	4.10159	0.3865	2 LEVEL	2.3268	0.8144
QUADRATIC EFFECT	1	22.35937	22.35937	2.1072	3 LEVEL	3.2429	0.8144
CUBIC EFFECT	1	4.33780	4.33780	0.4088	LEDGER ORIENTATION INDEX		
REMAINDER	6	36.74982	6.12497	0.5772	0 LEVEL	2.4750	0.8144
EXPERIMENTAL ERROR	32	339.54761	10.61087		1 LEVEL	1.7411	0.8144
					2 LEVEL	1.7714	0.8144
					3 LEVEL	1.1911	0.8144
					CUTTING HEIGHT INDEX		
					0 LEVEL	1.8982	0.8144
					1 LEVEL	2.4196	0.8144
					2 LEVEL	1.4304	0.5758
					C.G. HEIGHT INDEX		
					0 LEVEL	0.9804	0.8144
					1 LEVEL	1.9232	0.8144
					2 LEVEL	2.8482	0.8144
					3 LEVEL	1.4268	0.8144

APPENDIX D-II (Continued)

SHARP BLADE SERIES ANALYSIS OF VARIANCE FOR END Y DISP INDEX DATA					SHARP BLADE SERIES TABLE OF MEAN VALUES FOR END Y DISP INDEX DATA		
SOURCE OF VARIATION	DEGREES OF FREEDOM	SUM OF SQUARES	MEAN SQUARE	F RATIO	FACTOR	VALUE OF MEAN	STD ERROR OF MEAN
CORRECTED TOTAL	63	894.56445			OVERALL MEAN	1.4054	0.4665
DIAMETER	3	11.94561	3.98187	0.2859	DIAMETER		
LINEAR EFFECT	1	6.66188	6.66188	0.4784	0 LEVEL	1.6625	0.9329
QUADRATIC EFFECT	1	3.80250	3.80250	0.2731	1 LEVEL	1.5893	0.9329
CUBIC EFFECT	1	1.48123	1.48123	0.1064	2 LEVEL	1.7089	0.9329
TIME IN CHAMBER	3	46.26642	15.42214	1.1075	3 LEVEL	0.6607	0.9329
LINEAR EFFECT	1	41.34865	41.34865	2.9692	TIME IN CHAMBER		
QUADRATIC EFFECT	1	4.65326	4.65326	0.3341	0 LEVEL	2.7821	0.9329
CUBIC EFFECT	1	0.26450	0.26450	0.0190	1 LEVEL	1.4089	0.9329
ROTOR SPEED INDEX	3	150.82744	50.27580	3.6103	2 LEVEL	0.8625	0.9329
LINEAR EFFECT	1	56.30408	56.30408	4.0432	3 LEVEL	0.5679	0.9329
QUADRATIC EFFECT	1	71.04080	71.04080	5.1014	ROTOR SPEED INDEX		
CUBIC EFFECT	1	23.48253	23.48253	1.6863	0 LEVEL	3.4464	0.9329
FEED RATE INDEX	2	0.89327	0.44663	0.0321	1 LEVEL	1.5839	0.9329
ROTOR ANGLE INDEX	3	74.22070	24.74023	1.7766	2 LEVEL	-0.8804	0.9329
LINEAR EFFECT	1	19.80049	19.80049	1.4219	3 LEVEL	1.4714	0.9329
QUADRATIC EFFECT	1	23.38412	23.38412	1.6792	FEED RATE INDEX		
CUBIC EFFECT	1	31.03607	31.03607	2.2287	0 LEVEL	1.4107	0.9329
LATERAL POSITION INDEX	3	45.03030	15.01010	1.0779	1 LEVEL	1.3071	0.6597
LINEAR EFFECT	1	43.93494	43.93494	3.1550	2 LEVEL	1.5964	0.9329
QUADRATIC EFFECT	1	0.35148	0.35148	0.0252	ROTOR ANGLE INDEX		
CUBIC EFFECT	1	0.74388	0.74388	0.0534	0 LEVEL	0.3661	0.9329
LEDGER ORIENTATION INDEX	3	11.22194	3.74065	0.2686	1 LEVEL	0.8268	0.9329
LINEAR EFFECT	1	10.51250	10.51250	0.7549	2 LEVEL	3.1929	0.9329
QUADRATIC EFFECT	1	0.04592	0.04592	0.0033	3 LEVEL	1.2357	0.9329
CUBIC EFFECT	1	0.66352	0.66352	0.0476	LATERAL POSITION INDEX		
CUTTING HEIGHT INDEX	2	40.85265	20.42632	1.4668	0 LEVEL	0.4161	0.9329
C.G. HEIGHT INDEX	3	29.60458	9.86820	0.7086	1 LEVEL	0.8161	0.9329
LINEAR EFFECT	1	1.09111	1.09111	0.0784	2 LEVEL	1.8464	0.9329
QUADRATIC EFFECT	1	22.83473	22.83473	1.6398	3 LEVEL	2.5429	0.9329
CUBIC EFFECT	1	5.67873	5.67873	0.4078	LEDGER ORIENTATION INDEX		
REMAINDER	6	38.07887	6.34648	0.4557	0 LEVEL	1.8768	0.9329
EXPERIMENTAL ERROR	32	445.62280	13.92571		1 LEVEL	1.7500	0.9329
					2 LEVEL	1.1143	0.9329
					3 LEVEL	0.8804	0.9329
					CUTTING HEIGHT INDEX		
					0 LEVEL	0.7518	0.9329
					1 LEVEL	2.7732	0.9329
					2 LEVEL	1.0482	0.6597
					C.G. HEIGHT INDEX		
					0 LEVEL	0.7661	0.9329
					1 LEVEL	1.5446	0.9329
					2 LEVEL	2.4607	0.9329
					3 LEVEL	0.8500	0.9329

APPENDIX D-II (Continued)

SHARP BLADE SERIES ANALYSIS OF VARIANCE FOR C.G. Z DISP INDEX DATA					SHARP BLADE SERIES TABLE OF MEAN VALUES FOR C.G. Z DISP INDEX DATA		
SOURCE OF VARIATION	DEGREES OF FREEDOM	SUM OF SQUARES	MEAN SQUARE	F RATIO	FACTOR	VALUE OF MEAN	STD ERROR OF MEAN
CORRECTED TOTAL	63	2137.53784			OVERALL MEAN	3.5571	0.6040
DIAMETER	3	150.26234	50.08745	2.1456	DIAMETER		
LINEAR EFFECT	1	24.32587	24.32587	1.0420	0 LEVEL	5.0018	1.2079
QUADRATIC EFFECT	1	0.00617	0.00617	0.0003	1 LEVEL	1.9607	1.2079
CUBIC EFFECT	1	125.93028	125.93028	5.3944	2 LEVEL	5.1732	1.2079
TIME IN CHAMBER	3	167.49101	55.83034	2.3916	3 LEVEL	2.0929	1.2079
LINEAR EFFECT	1	156.00101	156.00101	6.6825	TIME IN CHAMBER		
QUADRATIC EFFECT	1	3.94306	3.94306	0.1689	0 LEVEL	6.0536	1.2079
CUBIC EFFECT	1	7.54694	7.54694	0.3233	1 LEVEL	3.5464	1.2079
ROTOR SPEED INDEX	3	185.11806	61.70601	2.6433	2 LEVEL	3.0714	1.2079
LINEAR EFFECT	1	119.98000	119.98000	5.1395	3 LEVEL	1.5571	1.2079
QUADRATIC EFFECT	1	25.21474	25.21474	1.0801	ROTOR SPEED INDEX		
CUBIC EFFECT	1	39.92329	39.92329	1.7102	0 LEVEL	1.9946	1.2079
FEED RATE INDEX	2	29.36435	14.68218	0.6289	1 LEVEL	3.3768	1.2079
ROTOR ANGLE INDEX	3	249.76315	83.25438	3.5663	2 LEVEL	2.4821	1.2079
LINEAR EFFECT	1	153.69551	153.69551	6.5838	3 LEVEL	6.3750	1.2079
QUADRATIC EFFECT	1	40.05081	40.05081	1.7156	FEED RATE INDEX		
CUBIC EFFECT	1	56.01682	56.01682	2.3996	0 LEVEL	4.4929	1.2079
LATERAL POSITION INDEX	3	111.96826	37.32275	1.5988	1 LEVEL	2.9116	0.8541
LINEAR EFFECT	1	13.21473	13.21473	0.5661	2 LEVEL	3.9125	1.2079
QUADRATIC EFFECT	1	10.01270	10.01270	0.4289	ROTOR ANGLE INDEX		
CUBIC EFFECT	1	88.74081	88.74081	3.8014	0 LEVEL	2.6875	1.2079
LEDGER ORIENTATION INDEX	3	159.71397	53.23799	2.2805	1 LEVEL	0.8179	1.2079
LINEAR EFFECT	1	107.44923	107.44923	4.6028	2 LEVEL	4.7143	1.2079
QUADRATIC EFFECT	1	2.65224	2.65224	0.1136	3 LEVEL	6.0089	1.2079
CUBIC EFFECT	1	49.61249	49.61249	2.1252	LATERAL POSITION INDEX		
CUTTING HEIGHT INDEX	2	103.14252	51.57126	2.2091	0 LEVEL	3.8696	1.2079
C.G. HEIGHT INDEX	3	167.46173	55.82057	2.3912	1 LEVEL	1.3786	1.2079
LINEAR EFFECT	1	49.29799	49.29799	2.1118	2 LEVEL	4.9446	1.2079
QUADRATIC EFFECT	1	41.05147	41.05147	1.7585	3 LEVEL	4.0357	1.2079
CUBIC EFFECT	1	77.11224	77.11224	3.3032	LEDGER ORIENTATION INDEX		
REMAINDER	6	66.22719	11.03787	0.4728	0 LEVEL	2.0089	1.2079
EXPERIMENTAL ERROR	32	747.02515	23.34453		1 LEVEL	2.0000	1.2079
					2 LEVEL	5.5214	1.2079
					3 LEVEL	4.6982	1.2079
					CUTTING HEIGHT INDEX		
					0 LEVEL	5.2714	1.2079
					1 LEVEL	4.2839	1.2079
					2 LEVEL	2.3366	0.8541
					C.G. HEIGHT INDEX		
					0 LEVEL	2.0696	1.2079
					1 LEVEL	2.4929	1.2079
					2 LEVEL	6.2232	1.2079
					3 LEVEL	3.4429	1.2079

APPENDIX D-II (Continued)

SHARP BLADE SERIES
ANALYSIS OF VARIANCE
FOR
END Z DISP INDEX DATA

SOURCE OF VARIATION	DEGREES OF FREEDOM	SUM OF SQUARES	MEAN SQUARE	F RATIO
CORRECTED TOTAL	63	2319.05908		
DIAMETER	3	160.12096	53.37364	2.3480
LINEAR EFFECT	1	31.71600	31.71600	1.3952
QUADRATIC EFFECT	1	1.90046	1.90046	0.0836
CUBIC EFFECT	1	126.50449	126.50449	5.5651
TIME IN CHAMBER	3	182.65800	60.88600	2.6785
LINEAR EFFECT	1	172.20064	172.20064	7.5753
QUADRATIC EFFECT	1	0.33474	0.33474	0.0147
CUBIC EFFECT	1	10.12261	10.12261	0.4453
ROTOR SPEED INDEX	3	184.99208	61.66402	2.7127
LINEAR EFFECT	1	147.19186	147.19186	6.4752
QUADRATIC EFFECT	1	19.99367	19.99367	0.8795
CUBIC EFFECT	1	17.80653	17.80653	0.7833
FEED RATE INDEX	2	44.06737	22.03368	0.9693
ROTOR ANGLE INDEX	3	288.41504	96.13841	4.2293
LINEAR EFFECT	1	148.35681	148.35681	6.5264
QUADRATIC EFFECT	1	50.71474	50.71474	2.2310
CUBIC EFFECT	1	89.34367	89.34367	3.9304
LATERAL POSITION INDEX	3	106.30434	35.43477	1.5588
LINEAR EFFECT	1	12.25731	12.25731	0.5392
QUADRATIC EFFECT	1	12.15020	12.15020	0.5345
CUBIC EFFECT	1	81.89682	81.89682	3.6028
LEDGER ORIENTATION INDEX	3	192.38841	64.12947	2.8211
LINEAR EFFECT	1	162.69437	162.69437	7.1571
QUADRATIC EFFECT	1	1.44000	1.44000	0.0633
CUBIC EFFECT	1	28.25403	28.25403	1.2429
CUTTING HEIGHT INDEX	2	125.05206	62.52603	2.7506
C.G. HEIGHT INDEX	3	241.90126	80.63374	3.5472
LINEAR EFFECT	1	83.46530	83.46530	3.6718
QUADRATIC EFFECT	1	90.24998	90.24998	3.9702
CUBIC EFFECT	1	68.18596	68.18596	2.9996
REMAINDER	6	65.74382	10.95730	0.4820
EXPERIMENTAL ERROR	32	727.41528	22.73172	

SHARP BLADE SERIES
TABLE OF MEAN VALUES
FOR
END Z DISP INDEX DATA

FACTOR	VALUE OF MEAN	STD ERROR OF MEAN
OVERALL MEAN	4.8545	0.5960
DIAMETER		
0 LEVEL	6.2554	1.1919
1 LEVEL	3.4554	1.1919
2 LEVEL	6.5982	1.1919
3 LEVEL	3.1089	1.1919
TIME IN CHAMBER		
0 LEVEL	7.1607	1.1919
1 LEVEL	5.1268	1.1919
2 LEVEL	4.7268	1.1919
3 LEVEL	2.4036	1.1919
ROTOR SPEED INDEX		
0 LEVEL	3.1429	1.1919
1 LEVEL	4.3250	1.1919
2 LEVEL	4.2661	1.1919
3 LEVEL	7.6839	1.1919
FEED RATE INDEX		
0 LEVEL	5.2018	1.1919
1 LEVEL	4.0812	0.8428
2 LEVEL	6.0536	1.1919
ROTOR ANGLE INDEX		
0 LEVEL	4.2304	1.1919
1 LEVEL	1.6982	1.1919
2 LEVEL	6.2304	1.1919
3 LEVEL	7.2589	1.1919
LATERAL POSITION INDEX		
0 LEVEL	5.2089	1.1919
1 LEVEL	2.7054	1.1919
2 LEVEL	6.1321	1.1919
3 LEVEL	5.3714	1.1919
LEDGER ORIENTATION INDEX		
0 LEVEL	2.8625	1.1919
1 LEVEL	3.4000	1.1919
2 LEVEL	6.6089	1.1919
3 LEVEL	6.5464	1.1919
CUTTING HEIGHT INDEX		
0 LEVEL	6.8571	1.1919
1 LEVEL	5.4696	1.1919
2 LEVEL	3.5455	0.8428
C.G. HEIGHT INDEX		
0 LEVEL	2.5964	1.1919
1 LEVEL	4.1464	1.1919
2 LEVEL	7.9375	1.1919
3 LEVEL	4.7375	1.1919

APPENDIX E
STEM PHYSICAL PROPERTY TEST DATA

APPENDIX E

STEM PHYSICAL PROPERTY TEST DATA

Run No.	Nominal Size of Plant (In)	Average Dia at Cut (In)	Linear Density at Cut Wet Basis (Gm/In)	Linear Density at Cut Dry Basis (Gm/In)	Cutting Height (In)	X Percent Moisture Dry Basis	SE Shear Energy per Unit Dia (In-Lb/In)	BE Deflection Energy for 1 In Defl (In-Lb/In)	Y SE/BE	SE/G ² MM ² H	Y=A+BX+CX ² Curve No
S43	13/64 x 11 1/8	0.19175	0.22430	0.13510	1.25000	66.025	43.068	0.87100	49.447	7027.461	SP-1
S47	13/64 x 14 5/8	0.19750	0.24320	0.14040	1.25000	73.219	49.132	2.08072	23.613	6264.652	SP-1
D47	13/64 x 14 5/8	0.16225	0.26840	0.14790	1.37500	81.473	30.221	1.66135	18.191	3491.614	SP-1
D40	13/64 x 9 3/8	0.16775	0.16580	0.13840	1.50000	19.797	28.307	2.16137	13.097	8259.145	SP-1
D43	13/64 x 14 5/8	0.16750	0.10720	0.08350	1.50000	28.383	59.781	0.91939	65.022	17292.660	SP-1
S39	13/64 x 14 5/8	0.15725	0.23100	0.14000	1.62500	65.000	24.618	0.74196	33.179	3304.673	SP-1
D32	13/64 x 9 3/8	0.16925	0.20000	0.11910	1.75000	67.926	24.092	0.95165	25.316	5827.238	SP-1
S35	13/64 x 11 1/8	0.16625	0.25230	0.12830	1.75000	96.649	32.288	1.12907	28.597	5216.988	SP-1
S2	13/64 x 12 7/8	0.18625	0.23050	0.17000	2.37500	35.590	46.003	1.00004	46.001	7030.063	SP-2
S16	13/64 x 9 3/8	0.20625	0.21250	0.11670	2.12500	82.090	27.027	1.01617	26.597	6152.691	SP-2
S1	13/64 x 9 3/8	0.18350	0.33550	0.18210	2.00000	84.240	32.066	2.08072	15.411	4623.496	SP-2
S32	13/64 x 9 3/8	0.16550	0.15560	0.13000	2.75000	19.692	31.811	0.62906	50.569	9889.789	SP-2
S20	13/64 x 9 3/8	0.15625	0.14330	0.11730	2.62500	22.165	31.382	0.43550	72.059	10593.800	SP-2
D29	13/64 x 11 1/8	0.16250	0.14370	0.11620	2.87500	23.666	33.351	0.66131	50.432	9461.168	SP-2
S60 ^a	13/64 x 11 1/8	0.26350 ^a	0.18860	0.14720	2.62500	28.125 ^a	20.372	0.98391	20.705 ^a	4403.281	SP-2
D51	13/64 x 12 7/8	0.16975	0.17540	0.13580	2.87500	29.160	27.974	0.80648	34.686	5617.809	SP-2
D34	13/64 x 11 1/8	0.19000	0.15270	0.11570	2.75000	31.979	30.426	0.69357	43.868	8122.523	SP-2
S28	13/64 x 12 7/8	0.17375	0.20310	0.15280	2.62500	32.918	32.083	0.70970	45.206	5564.258	SP-2
D31	13/64 x 11 1/8	0.14300	0.16680	0.12410	2.62500	34.407	27.071	0.30646	88.333	6615.988	SP-2
S13	13/64 x 12 7/8	0.18675	0.21670	0.15530	2.62500	39.540	38.417	1.08068	35.549	4497.953	SP-2
D24 ^a	13/64 x 11 1/8	0.13875 ^a	0.13710	0.09650	2.87500	42.072 ^a	28.272	0.30646	92.252 ^a	8406.375	SP-2
S50	13/64 x 14 5/8	0.16350	0.16670	0.11720	2.87500	42.235	29.043	0.77422	37.513	5402.617	SP-2
S57	13/64 x 14 5/8	0.16775	0.20700	0.13720	2.62500	50.874	42.153	0.75809	55.605	6314.770	SP-2
D56	13/64 x 12 7/8	0.16750	0.27170	0.16180	2.87500	67.923	31.431	0.93552	33.598	4074.875	SP-2

APPENDIX E (Continued)

Run No.	Nominal Size of Plant (In)	Average Dia at Cut (In)	Linear Density at Cut Wet Basis (Gm/In)	Linear Density at Cut Dry Basis (Gm/In)	Cutting Height (In)	X Percent Moisture Dry Basis	SE Shear Energy per Unit Dia (In-Lb/In)	BE Deflection Energy for 1 In Defl (In-Lb/In)	Y SE/BE	SE/GxMxH	Y=A+BX+CX ² Curve No
D14	13/64 x 11 1/8	0.16725	0.16100	0.12180	3.12500	32.183	20.985	0.62906	33.360	5313.523	SP-3
D18	13/64 x 9 3/8	0.18525	0.15000	0.11310	3.12500	32.625	25.633	0.51615	49.663	8266.711	SP-3
S53 ^a	13/64 x 11 1/8	0.27650 ^a	0.21050	0.14270	3.12500	47.512 ^a	21.094	0.69357	30.413 ^a	4085.046	SP-3
D64	13/64 x 12 7/8	0.15225	0.18420	0.11860	3.25000	55.311	26.104	0.50808	51.377	4991.855	SP-3
D70	13/64 x 12 7/8	0.18775	0.20520	0.12130	3.25000	69.167	38.763	0.40324	96.128	6653.961	SP-3
S23	13/64 x 12 7/8	0.17950	0.29620	0.17190	3.00000	72.309	39.106	0.79035	49.480	4650.586	SP-3
D13	13/64 x 9 3/8	0.15400	0.18780	0.10800	3.00000	73.888	21.785	0.48389	45.022	5611.660	SP-3
08	13/64 x 11 1/8	0.15800	0.12430	0.09030	3.37500	37.652	49.001	0.77422	63.291	16070.470	SP-3
D23	13/64 x 9 3/8	0.15825	0.18250	0.11450	3.62500	59.388	33.268	0.54841	60.663	8818.363	SP-3
D72	13/64 x 14 5/8	0.17525	0.22070	0.13490	3.62500	63.602	29.452	0.41937	70.229	4138.180	SP-3
D66 ^a	13/64 x 14 5/8	0.15925	0.27950	0.14720	4.12500 ^a	89.877 ^a	38.893	0.32259	120.565 ^a	4315.090	SP-3
S55	17/64 x 12 7/8	0.24025	0.30110	0.23090	1.37500	30.402	47.264	3.83885	12.312	5529.258	SP-4
S51	17/64 x 12 7/8	0.20950	0.36470	0.25660	1.12500	42.127	55.680	4.43565	12.553	5377.828	SP-4
S59	17/64 x 9 3/8	0.17250	0.41580	0.22240	1.37500	86.960	73.607	3.82272	19.255	8563.590	SP-4
S26	17/64 x 11 1/8	0.21825	0.31380	0.23350	1.87500	21.675	53.921	3.37109	15.995	7004.762	SP-4
D12	17/64 x 14 5/8	0.21275	0.34210	0.27080	1.87500	26.329	64.048	2.79043	22.953	5805.652	SP-4
D71	17/64 x 11 1/8	0.18800	0.27270	0.19590	1.87500	39.203	43.927	2.19363	20.025	6566.633	SP-4
S27	17/64 x 14 5/8	0.21775	0.27450	0.23350	2.12500	17.558	61.156	3.33883	18.316	6908.582	SP-5
S19	17/64 x 14 5/8	0.23725	0.36100	0.29850	2.12500	20.938	66.137	2.67752	24.701	5681.066	SP-5
D68	17/64 x 11 1/8	0.22200	0.30330	0.24170	2.00000	25.486	68.587	1.93556	35.435	9218.543	SP-5
D16	17/64 x 12 7/8	0.21100	0.28670	0.21570	2.00000	32.916	51.859	2.59687	19.970	6371.535	SP-5
D7	17/64 x 14 5/8	0.20825	0.27960	0.20000	2.25000	39.800	47.587	1.70974	27.833	5277.750	SP-5
S52	17/64 x 9 3/8	0.20150	0.31710	0.20630	2.25000	53.709	71.723	2.03233	35.291	10941.600	SP-5
D15	17/64 x 14 5/8	0.20000	0.28970	0.18500	2.12500	56.594	48.002	1.59683	30.061	5138.121	SP-5

APPENDIX E (Continued)

Run No.	Nominal Size of Plant (in)	Average Dia at Cut (in)	Linear Density at Cut Wet Basis (Gm/in)	Linear Density at Cut Dry Basis (Gm/in)	Cutting Height (in)	X Percent Moisture Dry Basis	SE Shear Energy per Unit Dia (in-Lb/in)	BE Deflection Energy for 1 In Defl (in-Lb/in)	Y SE/BE	SE/GxMxH	Y=A+BX+CX ² Curve No
D69	17/64 x 9 3/8	0.21900	0.38200	0.23840	2.12500	60.234	62.692	2.77430	22.597	7939.051	SP-5
D11	17/64 x 12 7/8	0.19800	0.38400	0.23350	2.00000	64.453	62.563	2.30654	27.124	5738.961	SP-5
D67	17/64 x 9 3/8	0.22275	0.36100	0.20040	2.00000	80.139	36.611	1.69361	21.617	4905.988	SP-5
S22	17/64 x 11 1/8	0.24900	0.23130	0.18400	2.87500	25.706	51.822	2.06459	25.100	9133.363	SP-6
S45	17/64 x 9 3/8	0.21675	0.33580	0.24730	2.50000	35.786	54.770	1.95168	28.063	7890.098	SP-6
S36	17/64 x 12 7/8	0.23200	0.31180	0.22920	2.62500	36.038	57.844	2.14524	26.964	6534.730	SP-6
S8	17/64 x 11 1/8	0.23200	0.37540	0.26230	2.75000	43.120	62.294	2.30654	27.007	6764.590	SP-6
S15	17/64 x 14 5/8	0.20750	0.25780	0.17870	2.87500	44.264	41.789	1.46780	28.471	5026.641	SP-6
S40	17/64 x 9 3/8	0.19800	0.28350	0.19100	2.50000	48.429	43.794	1.88717	23.206	7472.836	SP-6
S46	17/64 x 12 7/8	0.20800	0.39340	0.23500	2.87500	67.404	72.459	1.53231	47.287	6487.891	SP-6
S14	17/64 x 11 1/8	0.20100	0.38920	0.22590	2.75000	72.288	52.385	1.67748	31.228	5486.898	SP-6
01	17/64 x 12 7/8	0.21300	0.41140	0.23100	2.50000	78.095	41.680	1.19359	34.919	3568.643	SP-6
S6	17/64 x 14 5/8	0.21500	0.38530	0.30250	3.12500	27.370	90.746	2.35493	38.535	7303.383	Not Plotted
D28	17/64 x 12 7/8	0.22750	0.29540	0.26050	3.37500	13.397	78.500	1.74200	45.063	9360.578	SP-7
D33	17/64 x 14 5/8	0.20670	0.23350	0.20170	3.37500	15.765	38.455	1.69361	22.706	5106.969	SP-7
027	17/64 x 14 5/8	0.21600	0.28800	0.24450	3.37500	17.791	71.209	2.03233	35.038	7667.254	SP-7
039	17/64 x 12 7/8	0.21950	0.32690	0.27100	3.37500	20.627	130.272	1.72587	75.482	14037.140	SP-7
D44	17/64 x 11 1/8	0.19950	0.24580	0.19410	3.62500	26.635	45.017	0.67744	66.452	7466.035	SP-7
D50	17/64 x 9 3/8	0.18875	0.18040	0.13800	3.50000	30.724	36.643	0.75809	48.336	9825.977	SP-7
D46	17/64 x 9 3/8	0.19250	0.27000	0.20510	3.37500	31.643	42.901	1.19359	35.942	7686.344	SP-7
049	17/64 x 11 1/8	0.18750	0.23370	0.16880	3.50000	38.447	54.505	0.96778	56.320	9507.598	SP-7

APPENDIX E (Continued)

Run No.	Nominal Size of Plant (In)	Average Dia at Cut (In)	Linear Density at Cut Wet Basis (Gm/In)	Linear Density at Cut Dry Basis (Gm/In)	Cutting Height (In)	X Percent Moisture Dry Basis	SE Shear Energy per Unit Dia (In-Lb/In)	BE Deflection Energy for 1 In Defl (In-Lb/In)	Y SE/BE	SE/G*MXH	Y=A+BX+CX ² Curve No
S30	21/64 x 9 3/8	0.24950	0.36870	0.31930	1.12500	15.471	77.784	14.32311	5.431	10205.600	SP-8
S17	21/64 x 9 3/8	0.26325	0.52840	0.44120	1.12500	19.760	137.247	13.61341	10.082	12564.960	SP-8
D48	21/64 x 14 5/8	0.25625	0.45630	0.36570	1.37500	24.774	79.764	7.80674	10.217	5420.641	SP-8
S29	21/64 x 12 7/8	0.28325	0.53530	0.42000	1.12500	27.452	110.792	12.50046	8.863	7290.457	SP-8
D53	21/64 x 14 5/8	0.23025	0.42100	0.32360	1.25000	30.098	86.977	7.90352	11.005	6406.484	SP-8
S24	21/64 x 12 7/8	0.27900	0.56610	0.33300	1.12500	70.000	91.020	8.83904	10.297	5663.516	SP-8
S62	21/64 x 14 5/8	0.23075	0.38650	0.32920	1.87500	17.405	97.526	5.22600	18.662	7824.652	Not Plotted
S58	21/64 x 14 5/8	0.27250	0.40330	0.33440	1.75000	20.604	90.918	4.96793	18.301	6990.629	Not Plotted
D25	21/64 x 11 1/8	0.25850	0.36690	0.31870	2.37500	15.123	111.815	5.03244	22.219	12423.540	SP-9
D26	21/64 x 9 3/8	0.25800	0.52450	0.43920	2.00000	19.421	108.031	5.74215	18.814	9963.754	SP-9
D54	21/64 x 12 5/8	0.22550	0.37600	0.29960	2.12500	25.500	67.752	4.24209	15.971	6347.105	SP-9
S54	21/64 x 11 1/8	0.19175	0.43250	0.34050	2.00000	27.019	124.898	5.32278	23.465	11772.320	SP-9
D41	21/64 x 11 1/8	0.24275	0.52450	0.38990	2.37500	34.521	133.529	5.06470	26.365	10378.160	SP-9
D73 ^a	21/64 x 14 5/8	0.21375	0.29870	0.24050 ^a	2.75000	24.199 ^a	54.331	1.82265	29.809 ^a	5640.414	SP-9
D21	21/64 x 9 3/8	0.22500	0.37270	0.29890	2.87500	24.690	69.737	1.58070	44.118	9051.613	SP-9
S4	21/64 x 9 3/8	0.24125	0.50830	0.39750	2.50000	27.870	92.425	5.03244	18.366	8796.109	SP-9
S56	21/64 x 11 1/8	0.20250	0.43980	0.33850	2.50000	29.926	130.503	3.98402	32.757	12096.370	SP-9
D42	21/64 x 12 3/8	0.25275	0.44870	0.33430	2.87500	34.220	93.938	2.83881	33.091	7672.398	SP-9
D5	21/64 x 9 3/8	0.23900	0.38840	0.28930	2.75000	34.255	90.272	1.69361	53.301	11243.290	SP-9
D60	21/64 x 12 7/8	0.25500	0.52630	0.37640	2.87500	39.824	93.919	3.04850	30.808	6285.832	SP-9
D35 ^a	21/64 x 9 3/8	0.28325	0.63870	0.45310 ^a	2.50000	40.962 ^a	147.965	4.70985	31.416 ^a	11206.850	SP-9
S11	21/64 x 12 7/8	0.23600	0.60720	0.42500	2.87500	42.870	76.110	3.32270	22.906	4415.234	SP-9
S37	21/64 x 11 1/8	0.26525	0.59850	0.39600	2.75000	51.136	96.516	3.09689	31.166	6573.969	SP-9

APPENDIX E (Continued)

Run No.	Nominal Size of Plant (In)	Average Dia at Cut (In)	Linear Density at Cut Wet Basis (Gm/In)	Linear Density at Cut Dry Basis (Gm/In)	Cutting Height (In)	X Percent Moisture Dry Basis	SE Shear Energy per Unit Dia (In-Lb/In)	BE Deflection Energy for 1 In Defl (In-Lb/In)	Y SE/BE	SE/GxMxH	Y=A+BX+CX ² Curve No
062	21/64 x 14 5/8	0.23300	0.40760	0.33290	3.25000	22.439	84.179	2.01620	41.751	6404.176	SP-10
S38	21/64 x 14 5/8	0.26175	0.42850	0.34230	3.00000	25.182	82.820	2.85494	29.009	5993.516	SP-10
D6	21/64 x 11 1/8	0.24375	0.35880	0.28090	3.25000	27.732	67.337	2.56461	26.256	7650.605	SP-10
S9	21/64 x 9 3/8	0.22675	0.37000	0.28520	3.00000	29.730	60.094	3.04850	19.713	7856.863	Not Plotted
S44	21/64 x 14 5/8	0.24925	0.42530	0.32320	3.12500	31.590	76.206	2.79043	27.310	5556.316	SP-10
S33	21/64 x 11 1/8	0.28100	0.43680	0.32170	3.00000	35.778	88.168	2.70978	32.537	8228.449	SP-10
D65	21/64 x 12 7/8	0.24075	0.58880	0.29300	3.12500	100.955	62.602	2.82268	22.178	3745.133	SP-10
S7	21/64 x 12 7/8	0.24750	0.59530	0.28810	3.12500	106.630	85.920	2.12911	40.355	5083.988	SP-10
D19	21/64 x 9 3/8	0.26250	0.31550	0.25970	3.37500	21.486	58.988	1.83878	32.080	9044.551	Not Plotted
017	21/64 x 11 1/8	0.26475	0.50960	0.40280	3.75000	26.514	95.139	1.50006	63.424	7610.621	Not Plotted
02	21/64 x 11 1/8	0.27200	0.52480	0.39110	3.37500	35.106	85.772	3.01624	28.437	6662.563	Not Plotted
S12	25/64 x 14 5/8	0.26700	0.59350	0.49060	1.00000	20.970	149.238	11.76818	12.682	7797.496	SP-11
S3	25/64 x 11 1/8	0.32650	0.65300	0.53780	1.37500	21.420	178.320	14.03278	12.707	11132.130	SP-11
D20	25/64 x 12 7/8	0.28250	0.64820	0.50830	1.37500	27.523	286.485	10.61330	26.993	15568.150	SP-11
061 ^a	25/64 x 11 1/8	0.32350	0.88270	0.66890 ^a	1.00000	31.962 ^a	181.888	18.38777	9.892 ^a	8400.074	SP-11
S10 ^a	25/64 x 11 1/8	0.28975	0.55000	0.39500 ^a	1.25000	39.240 ^a	135.027	12.48433	10.816 ^a	10008.030	SP-11
D58	25/64 x 11 1/8	0.30800	0.90060	0.50000	1.37500	80.120	106.581	8.71000	12.237	4824.363	SP-11
S5	25/64 x 14 5/8	0.28300	0.65800	0.52140	1.75000	24.090	140.801	9.29067	15.155	6635.516	SP-11
S42	25/64 x 12 7/8	0.31125	0.57290	0.45950	1.87500	24.678	181.087	10.29070	17.597	11134.040	SP-11
S48	25/64 x 9 3/8	0.31525	0.68340	0.51750	1.87500	32.057	138.840	9.38744	14.790	9827.887	SP-11
D4	25/64 x 12 7/8	0.26875	0.64000	0.45540	1.87500	40.535	88.345	5.79054	15.257	4862.367	SP-11
D9 ^a	25/64 x 12 7/8	0.30150	0.62100	0.36970 ^a	1.87500	67.974 ^a	127.368	7.88739	16.148 ^a	7224.578	SP-11

APPENDIX E (Continued)

Run No.	Nominal Size of Plant (In)	Average Dia at Cut (In)	Linear Density at Cut, Wet Basis (Gm/In)	Linear Density at Cut, Dry Basis (Gm/In)	Cutting Height (In)	X Percent Moisture Dry Basis	SE Shear Energy per Unit Dia (In-Lb/In)	BE Deflection Energy for 1 In Defl (In-Lb/In)	Y SE/BE	SE/GXM ² H	Y=A+BX+CX ² Curve No
D63	25/64 x 9 3/8	0.30975	0.42700	0.34770	2.37500	22.807	72.652	3.85498	18.846	8230.793	Not Plotted
S34	25/64 x 12 7/8	0.29800	0.47960	0.38980	2.37500	23.037	103.922	7.16156	14.511	7632.629	Not Plotted
D59	25/64 x 9 3/8	0.27525	0.51930	0.41170	2.25000	26.135	127.513	5.77441	22.083	11878.390	Not Plotted
S41	25/64 x 9 3/8	0.24625	0.44290	0.34730	2.12500	27.526	69.588	4.66146	14.928	7600.648	Not Plotted
S21	25/64 x 14 5/8	0.29200	0.53350	0.49120	2.62500	8.611	125.855	6.64541	18.939	7315.305	SP-12
S31 ^a	25/64 x 11 1/8	0.26125	0.36220	0.32390 ^a	2.87500	11.824 ^a	71.915	6.38733	11.259 ^a	8093.984	SP-12
S25 ^a	25/64 x 11 1/8	0.28150	0.72430	0.62140 ^a	2.87500	16.559 ^a	172.355	5.59698	30.794 ^a	9700.555	SP-12
S64	25/64 x 9 3/8	0.31800	0.68030	0.58280	2.87500	16.729	176.594	8.96807	19.691	12557.280	SP-12
S63	25/64 x 12 7/8	0.28950	0.69200	0.56490	2.75000	22.499	214.661	5.87118	36.562	10926.730	SP-12
D37	25/64 x 12 7/8	0.29950	0.53800	0.43500	2.50000	23.678	155.792	6.01635	25.895	10200.170	SP-12
D10	25/64 x 14 5/8	0.29025	0.72400	0.58180	2.87500	24.441	280.969	5.04857	55.653	12034.160	SP-12
S61 ^a	25/64 x 12 7/8	0.20000 ^a	0.58160	0.44660	2.62500	30.228 ^a	142.457	6.96800	20.444 ^a	8627.859	SP-12
D22	25/64 x 14 5/8	0.26625	0.60000	0.44300	2.75000	35.440	199.286	4.77437	41.741	10299.640	SP-12
S49 ^a	25/64 x 9 3/8	0.28350	0.65920	0.35130 ^a	2.87500	87.645 ^a	75.010	3.35496	22.358 ^a	5504.543	SP-12
D36	25/64 x 14 5/8	0.27275	0.54230	0.46170	3.25000	17.457	269.476	5.20987	51.724	15409.030	SP-13
O38	25/64 x 14 5/8	0.33125	0.52640	0.44420	3.12500	18.505	150.832	4.01628	37.555	8885.328	SP-13
D52	25/64 x 11 1/8	0.29825	0.64190	0.49560	3.25000	29.519	135.678	5.58085	24.311	8616.559	SP-13
D57	25/64 x 9 3/8	0.29000	0.45280	0.34770	3.12500	30.227	90.415	3.93563	22.973	9659.480	SP-13
D45	25/64 x 11 1/8	0.24475	0.48470	0.35330	3.25000	37.192	80.137	2.41944	33.122	6739.902	SP-13
S18	25/64 x 14 5/8	0.27975	0.45460	0.39670	3.62500	14.595	154.245	3.37109	45.755	10521.470	SP-13
D55	25/64 x 9 3/8	0.23325	0.43630	0.33800	3.75000	29.083	92.940	2.50009	37.175	10304.730	SP-13
D3	25/64 x 14 5/8	0.30150	0.63920	0.48880	4.00000	30.769	162.976	3.19367	51.031	7906.469	SP-13
D30	25/64 x 12 7/8	0.28175	0.75850	0.49140	4.00000	54.354	169.271	2.14524	78.905	7860.875	SP-13

^aDenotes values considered outliers because of wide variation of average diameter, dry linear density, or cutting height. In each instance a superscript marks the run number, the X and Y values and the particular parameter considered to widely vary, i.e., diameter, dry linear density, or cutting height.

VITA

Bobby Lynn Bledsoe 3

Candidate for the Degree of

Doctor of Philosophy

Thesis: THE DESIGN AND EXPERIMENTAL ANALYSIS OF A ROTARY
SICKLE FOR CUTTING AND TRAJECTING PLANT STEMS

Major Field: Agricultural Engineering

Biographical:

Personal Data: Born at Dyersburg, Tennessee, February
4, 1930, the son of Lynn H. and Gladys M. Bledsoe.

Education: Attended Burgies Chapel grade school in Dyer
County, Tennessee; graduated from Dyersburg High
School in 1948; received the Bachelor of Science
degree from the University of Tennessee in Decem-
ber, 1953, with a major in Agricultural Engineer-
ing, after completing eight work periods as a
cooperative engineering student; completed require-
ments for the Doctor of Philosophy degree from
Oklahoma State University in August, 1969.

Professional Experience: Cooperative student and layout
draftsman, Product Engineering Department, Inter-
national Harvester Co., Memphis, Tennessee, 1950-
1953; Served in U. S. Army, 1954-56; Design
Engineer, International Harvester Co., 1956-64;
Agricultural Engineer (part-time), ARS, USDA,
1964-65; Graduate Research Assistant, Oklahoma
State University, 1965-1969.

Professional and Honorary Organizations: Associate
Member, American Society of Agricultural Engineers;
Associate Member, Society of the Sigma Xi; Member,
Phi Kappa Phi, honorary society.